FLEET TECHNOLOGY LIMITED
A FLEET AEROSPACE COMPANY

CA1
DTC800-
89
M57
425512

41.D

FLEET TECHNOLOGY LIMITED

TP 9849E

MODIFICATION AND TESTING OF A SEGMENTED MODEL OF AN ICEBREAKER TO EVALUATE ICE RESISTANCE MATHEMATICAL MODELS

TP 9849E

Prepared for:
Transportation Development Centre
Policy & Coordination Group
Transport Canada

by

I.F. Glen
R. Abdelnour
M. Steele

31 March 1989

Prepared by

Fleet Technology Limited
311 Legget Drive
Kanata, Ontario
K2K 1Z8

425512

DDN 422617

90-01750/

DISCLAIMER

The contents of this report reflect the views of Fleet Technology Limited and not necessarily the official view or opinions of the Transportation Development Centre of Transport Canada.

LANGUAGE NOTICE

Un sommaire en français de ce rapport est inclus avant la Table des matières.

Transport Canada Transports Canada

PUBLICATION DATA FORM

1. Transport Canada Publication No. TP 9849E

2. Project No. 6994

3. Recipient's Catalogue No.

4. Title and Subtitle
Modification and Testing of a Segmented Model of an Icebreaker to Evaluate Ice Resistance Mathematical Models

5. Publication Date
March 31, 1989

6. Performing Organization Document No.
3108C

7. Author(s)
I.F. Glen, R. Abdelnour, M. Steele

8. Transport Canada File No.
D1460-194

9. Performing Organization Name and Address
Fleet Technology Limited
311 Legget Drive
Kanata, Ontario
K2K 1Z8

10. DSS File No.
11SD.T8200-7-7542

11. DSS or Transport Canada Contract No.
T8200-7-7542/01-SD

12. Sponsoring Agency Name and Address
Transportation Development Centre
200 René Lévesque Blvd. West
West Tower, Suite 601
Montreal, Quebec H2Z 1X4

13. Type of Publication and Period Covered
Final (Feb.'88 - Mar.'89)

14. Project Officer
J.E. Laframboise

15. Supplementary Notes (Funding programs, titles of related publications, etc.)
Funded by Energy, Mines and Resources Canada under the Energy R&D Program.

16. Abstract

The third phase of an experimental program designed to investigate the components of ice resistance on the hull of a vessel using a physically segmented model has been completed. The objective of the project was to compare the loads measured on portions of the hull of an icebreaker with those predicted by mathematical prediction models, with a view to obtaining a greater understanding of the ship/ice interaction process.

Further development and testing in ice of a segmented model of the R-Class icebreaker has been completed. The segmentation system comprises free floating panels of the hull on the port side bow, instrumented to measure load on the segment.

The data have been analyzed to investigate the local ship/ice interaction phenomena and to determine the contribution to resistance from each portion of the hull.

The results have been compared with two mathematical predictor models, RICE - a semi-empirical model and the analytical model of Dr. D. Carter.

The results indicate that the dynamic breaking pattern influences the mean load on areas aft of the stem. While the total resistance measured on the model appears to be lower than that predicted by the mathematical models, the relative contributors of resistance of the portions of the hull agree well with Carter's model. Recommendations for further analysis of the data are made.

17. Key Words
R-Class, Segmented Model, Ice Resistance, Mathematical Model

18. Distribution Statement
Limited number of copies available from the Transportation Development Centre

19. Security Classification (of this publication)
Unclassified

20. Security Classification (of this page)
Unclassified

21. Declassification (date)

22. No. of Pages
107

23. Price
N/A

Canada

Transports Canada Transport Canada

FORMULE DE DONNÉES POUR PUBLICATION

1. N° de la publication de Transports Canada
TP 9849E

2. N° de l'étude
6994

3. N° de catalogue du destinataire

4. Titre et sous-titre
Modification and Testing of a Segmented Model of an Icebreaker to Evaluate Ice Resistance Mathematical Models

5. Date de la publication
31 mars 1989

6. N° du document de l'organisme exécutant
3108C

7. Auteur(s)
I.F. Glen, R. Abdelnour, M. Steele

8. N° de dossier — Transports Canada
D1460-194

9. Nom et adresse de l'organisme exécutant
Fleet Technology Limited
311 Legget Drive
Kanata, Ontario
K2K 1Z8

10 N° de dossier — ASC
11SD.T8200-7-7542

11. N° de contrat — ASC ou Transports Canada
T8200-7-7542/01-SD

12. Nom et adresse de l'organisme parrain
Centre de développement des transports
200 ouest, boul. René-Lévesque
Tour ouest, suite 601
Montréal (Québec) H2Z 1X4

13. Genre de publication et période visée
Rapport final -
fév. 88 - mars 89

14. Agent de projet
J.E. Laframboise

15. Remarques additionnelles (Programmes de financement, titres de publications connexes, etc.)

Financé par Energie, mines et ressources Canada, programme de R et D énergétiques.

16. Résumé

Ce rapport rend compte de la phase 3 du programme d'expérimentation visant à déterminer la répartition des forces en jeu durant une opération de déglaçage, à l'aide d'une maquette de brise-glace dont la coque a été segmentée. Il s'agissait de mesurer les forces exercées sur chacun de ces segments et de les comparer aux résultats des modèles mathématiques de prévision, le tout débouchant sur une meilleure compréhension des interactions dynamiques glaces-coque.

Outre ces travaux, il y a eu les essais en bassin des glaces de la maquette d'un brise-glace de classe R, également segmentée. La partie segmentée de la coque, située à l'avant et à bâbord, comporte des panneaux en flottement libre dûment instrumentés, afin de permettre le mesurage des forces en jeu.

Les résultats, une fois analysés, ont permis de déterminer la nature des mécanismes de résistance et l'apport à la résistance totale de chacune des parties de la coque.

Ensuite, les résultats ont été comparés à ceux de deux modèles de prévision : le programme informatique RICE qui est semi-empirique et le modèle analytique mis au point par le docteur D. Carter.

L'étude a montré que la charge moyenne s'exerçant à l'arrière de l'étrave dépend du mode de rupture dynamique des glaces. D'autre part, bien que la résistance totale mesurée en bassin des glaces soit inférieure aux calculs théoriques, l'apport des diverses parties de la coque à la résistance totale concorde quand même avec les résultats tirés du modèle du Dr. Carter.

Le rapport se termine par des recommandations concernant une analyse plus approfondie des résultats.

17. Mots clés
Classe R, modèle à coque segmentée, résistance des glaces, modèle mathématique.

18. Diffusion
Le Centre de développement des transports dispose d'un nombre limité d'exemplaires.

19. Classification de sécurité (de cette publication)
Non classifiée

20 Classification de sécurité (de cette page)
Non classifiée

21. Déclassification (date)

22. Nombre de pages
107

23. Prix
Aucun

PROJECT TEAM

The project team included I.F. Glen, President of Fleet Technology and Project Advisor/Auditor; R. Abdelnour, Vice President and Project Manager; M. Steele, Research Engineer; A. Lemieux and D. Bourne, Technicians.

ACKNOWLEDGEMENTS

The assistance of Mr. Ian Bayly of the Transportation Development Centre (TDC) at the beginning of the project, of Dr. D. Carter, Consultant, and Mr. J. Laframboise of TDC for his support and understanding when problems arose is appreciated. We also acknowledge the contribution of Ms. Ann Godon, formerly Project Engineer.

The project was funded by Energy, Mines and Resources Canada under the Energy R&D Program.

SUMMARY

The third phase of an experimental program designed to investigate the components of ice resistance on the hull of a vessel using a physically segmented model has been completed. The work was sponsored by the Transportation Development Centre.

The objective of the project was to compare the loads measured on portions of the hull of an icebreaker with those predicted by mathematical prediction models, with a view to obtaining a greater understanding of the process leading to refinement of the math models.

In Phases I and II of this program, a 1:20 scale model of a Canadian Coast Guard R-Class Icebreaker had been constructed incorporating three bow 'segments' at the waterline. Force transducers were designed, built and installed in locations on the segments that allowed the data reduction procedures to determine the magnitude and location of the net normal force on each segment at any time, and the magnitude and direction of the friction force. Based on the calibration of this system and some preliminary ice testing, it was proposed to add a fourth segment to the model and execute a larger series of ice model tests and compare the results with the mathematical resistance predictor model by Dr. Donald Carter and reported in TP 3679 "Ship Resistance to Continuous Motion in Level Ice" and that known as RICE, as reported by I.F. Glen in TP 4377E "A Semi-Empirical Ice Resistance Model - Summary Report".

A total of 37 load transducers were fitted and extensive calibration of these was performed, including individual transducer calibrations, and in-situ segment calibrations. This included repeat calibrations for comparison with the work performed in the previous phase of the project. Transducer calibrations determined the load, strain, and voltage relationships and examined hysteresis performance and sensitivity to lateral loads. Transducers were found to perform satisfactorily. Segment calibrations consisted of applying known loads at known locations - using a specially constructed rig - and comparing the results with the calculated load and location using the data recording and reduction system. The results of this calibration effort were satisfactory, the errors being small.

In order to check the lines of the model, previously thought to be divergent from the lines plan, a photogrammetric specialist was contracted to measure the lines. This was also to evaluate that technique. The differences in lines and angles were considered to be within the accuracy of the experimental procedures, and since the results were obtained after the tests had started, no change was made to the data reduction algorithms to account for these minor hull form deviations. The technique of photogrammetry did, however, appear to be a cost-effective way of creating an accurate set of lines from a model or vessel.

Although the original plan was to execute three ice sheet tests at the National Research Council's Institute for Marine Dynamics' (IMD) Ice Tank in St. John's and thus permit longer test runs, budget and schedule problems arose during the preparation and calibration of the complex instrumentation system, and it was agreed with TDC and IMD that the tests should be carried out at Fleet Technology's laboratory. This resulted in short run lengths. Ten ice sheets were planned to provide the data points and the removal of the need to transport the somewhat delicate model was viewed as a risk-reducing factor. Table S.1 summarizes the test runs. Two channel widening tests followed each unbroken ice sheet test.

There were 39 channels of data recorded including vessel speed, carriage force (total resistance) and the 37 transducers.

During the tests a small number of sensor failures occurred - the most significant one being the 'x direction' compression cell (resistance direction) on Segment 4 which failed and was unable to be replaced for the tests. The resistance of Segment 4 could not therefore be recorded directly. Few other data points were lost. Video records of all tests were made.

Data reduction and quality checks took place after the testing period. All time series records were examined in detail. Data exhibiting unexpected or illogical response were isolated. An example of this is the occurrence on some occasions of a step shift in the mean force trace for Segment 1, due, it is thought, to re-alignment of the segment. Engineering calculations proceeded only on data exhibiting the necessary logical results and quality. The data reduction/analysis software permitted interactive selection of the record to be examined using a cursor technique, records being selected based on such factors as constant model velocity. All video records were reviewed in conjunction with data analysis. A typical time series plot with calculated engineering values is shown in Figure S.1.

Table 5.1

3108C - Segmented Model Tests

Test Matrix as Completed

					Mean Force / Unit Length			
Test	h (mm)	Sigma (kPa)	E/Sigma	V (m/s)	Seg1 (N/m)	Seg2 (N/m)	Seg3 (N/m)	Seg4 (N/m)
1S1	36.0	30.4	466	.17	44.3	29.9	27.3	15.1
1C1	35.5	(27.6)		.12	30.4	26.7	18.4	14.2
1C2	37.5	24.8		.58	48.3	54.5	33.2	46.8
1S2	31.7	48.2	(800)	.32	26.7	29.9	14.0	22.2
1C3	31.4	(37.5)		.26	20.5	21.5	12.2	10.1
1C4	34.7	26.9		.52	28.3	43.2	19.9	28.4
1S3	34.0	49.8	1161	.48	58.7	44.8	22.3	52.1
1C5	34.5	(32.5)		.32	40.8	31.7	22.7	29.4
1C6	36.8	15.3		.46	48.3	38.0	23.8	37.2
1S4	33.4	48.5	(2300)	.17	27.7	24.2	17.2	64.7
1C7	33.8	(39.6)		.63	38.4	62.7	27.7	60.1
1C8	35.2	29.5		.12	21.3	22.4	17.8	49.8
	***							
2S1	46.8	31.3	1271	.12	17.3	26.5	14.5	106.9
2C1	49.2	(27.4)		.15	40.3	35.7	14.4	81.0
2C2	51.9	23.4		.32	49.3	47.1	21.8	39.9
2S2	46.1	26.1	2916	.24	29.6	45.7	32.1	74.3
2C3	48.2	(30.0)		.12	46.7	54.5	31.4	88.5
2C4	50.0	33.9		.28	74.4	95.7	36.7	27.8
2S3	45.8	32.1	3270	.34	19.2	67.6	54.0	31.0
2C5	46.3	(33.3)		.29	67.2	62.4	60.5	26.4
2C6	48.5	34.5		.23	65.6	57.7	62.0	67.4
2S4	43.2	36.9	2716	.30	23.2	45.2	28.4	71.8
2C7	45.7	(41.2)		.14	41.6	46.3	19.7	19.3
2C8	47.2	45.4		.23	67.7	55.0	34.2	136.3
	***							
3S1	63.4	31.7	1511	.08	59.2	39.8	46.5	167.9
3C1	65.3	38.7		.11	83.5	77.8	54.7	52.1
3S2	54.1	30.9	2305	.19	47.7	89.3	59.7	167.0
3C2	56.3	42.4		.11	71.5	78.7	33.9	105.7

FIGURE S.1

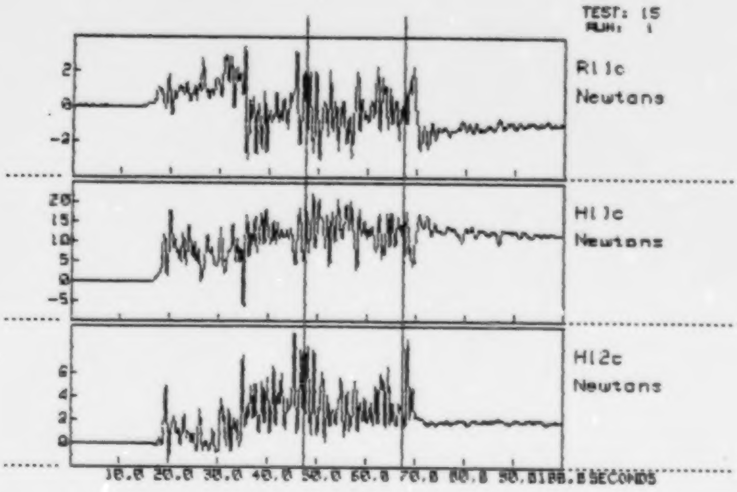

Test/Run: 1S1
Digitizing Rate: 10 Hz/Channel

Date Digitized: 10 Jan 1989
Filter Frequency: 1 Hz

Statistics For Int 47.30 to 67.40 Seconds

CHANNEL	MINIMUM	MAXIMUM	MEAN VALUE	STANDARD DEV
R11c	-2.97	2.34	-.29	1.16692
H11c	3.24	21.90	13.10	3.86379
H12c	.16	8.33	3.20	1.63874

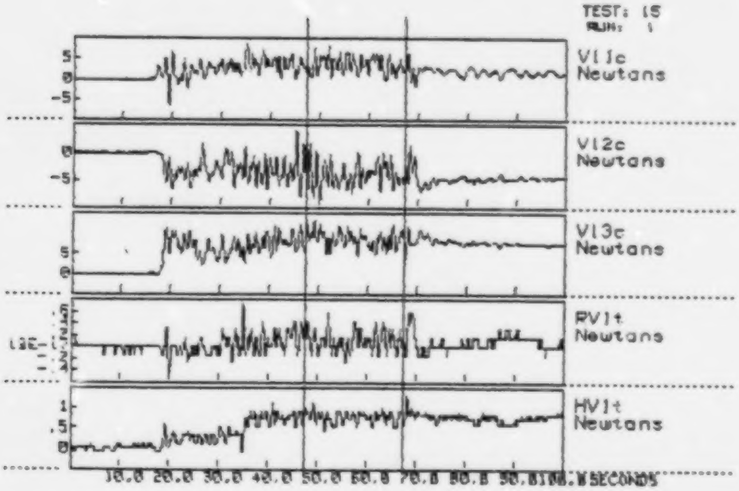

Test/Run: 1S1
Digitizing Rate: 10 Hz/Channel

Date Digitized: 10 Jan 1989
Filter Frequency: 1 Hz

Statistics For Int 47.30 to 67.40 Seconds

CHANNEL	MINIMUM	MAXIMUM	MEAN VALUE	STANDARD DEV
V11c	-.10	8.25	3.62	1.93897
V12c	-8.56	1.73	-4.01	2.09979
V13c	4.55	13.00	8.59	1.87263
RV1t	-.28	.60	.11	.16672
HV1t	.43	1.12	.78	.13604

Data analysis included investigation of the location and magnitude of normal loading on segments, friction force magnitude, direction and coefficient, resistance on segments and total resistance on the model. The resistance of Segment 4, unable to be directly measured due to transducer failure, was calculated from the normal force and average friction coefficient. The characteristics of the time histories were examined and frequency analysis was performed. As a consequence of unexpected results for friction direction in forward segments, sensitivity analysis of the effect of transducer error on friction direction was performed - an example of the post-test investigations that took place to investigate anomalies in results. Normal forces were examined as both peaks and means. Where appropriate data were compared with the results from the tests conducted in Phase II.

The results showed increased peak forces from Segment 1 (forward) to Segment 4, with decreasing peak frequency. Whereas Segment 1 experienced almost a continuous cyclic loading, Segment 4 saw only occasional peaks. Mean normal force on Segment 1 was higher than on Segment 4. Peak frequency increased with velocity. These tests showed some difference between unbroken ice and channel widening runs, the latter exhibiting higher loads. All forces increased with ice thickness, and normal forces on Segments 2 and 3 increased with speed.

As in previous tests, friction direction produced unexpected forward vectors on Segments 1 and 2 and high friction coefficients.

Regression analysis of the total model resistance was carried out, scaled to full scale and plotted against other R-Class model data, as shown in Figure S.2. The earlier data is extracted from TP 8828E "The Testing of the 1:8 Scale Model of the R-Class in Level Ice". The results from this test were generally in the middle of the previous data but exhibited a greater speed dependence. It is noted that unlike the earlier tests, the model was constrained against roll, yaw and pitch in the current tests.

Segments 1 to 3 were found to contribute about 40% of the total resistance (when multiplied for both sides) and Segments 1 to 4 about 55 - 60%. It appeared that much of the ice loading on the hull occurred below and/or aft of the segmented area.

The results were compared with the RICE semi-empirical prediction model and with Donald Carter's analytical model. The total resistance was comparable only in thick ice. The expectation that each segment would match one of the components of resistance of RICE was not achieved. The behaviour of the model ice in its flow around the model, and the application of RICE (a semi-empirical full scale math model that accounts for the dynamics of the vessel) at model scale with a fixed model are felt to be the cause of the discrepancies.

FIGURE S.2

Comparison of the Model Scale Results
at a strength of 800 kPa

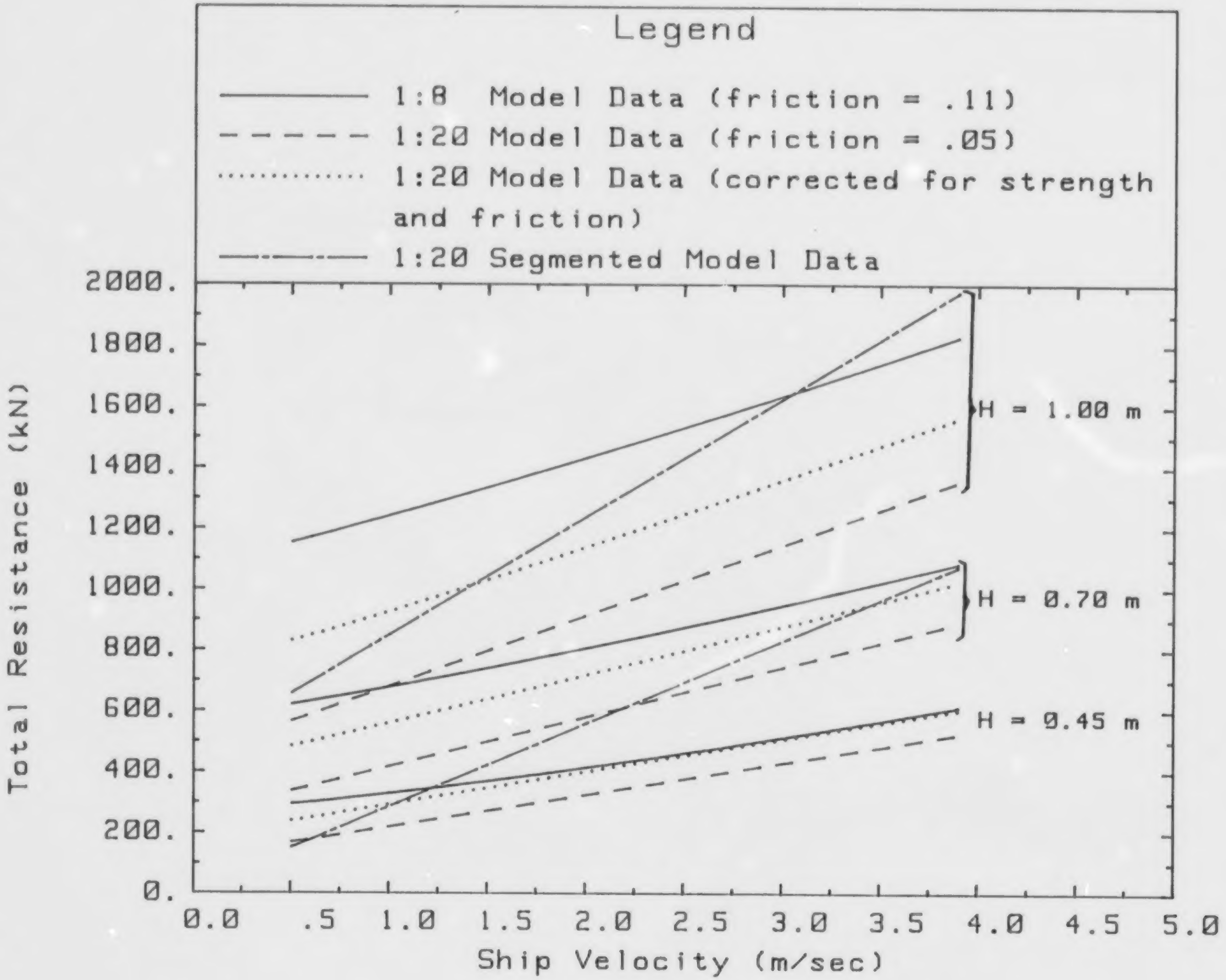

Appendix A to this report produces in full, Dr. Donald Carter's report on his model work. Total resistance predictions correlate well with full scale R-Class data and are twice that achieved from the model series. Figure S.3 shows how some of the data compares with Carter and RICE models.

The principle finding is that Carter's model and the segmented model's relative force distribution matched quite well in all segments. This is shown in Figure S.4 ('C' runs refer to channel widening runs, 'S' runs to unbroken ice sheet runs). For segment resistance contribution the best match shows a difference of 0.2% on Segment 2 and the worst match a difference of 6.8% on Segment 3. For mean normal force distribution, the best match shows a difference of 3% and the worst match a difference of 14% on Segment 2. These discrepancies are well within the normal range of error of physical modelling. It is the conclusion of this work that Carter's predictions of normal force and resistance contributions from the segments correlate with the mean relative distribution of force measured during the segmented model tests.

The report includes an assessment of the effect of the deficiencies in the ice modelling material on investigations of local interaction phenomena such as this.

The report concludes that the large amount of data acquired for this test series should be examined further. There should be a limited number of additional runs in another media (say MOD-ICE) and a long run at IMD to determine the effect of this. However, the complexity and limitations of the segment system are such that it is recommended that alternative methods of modelling be developed for future investigations of this type.

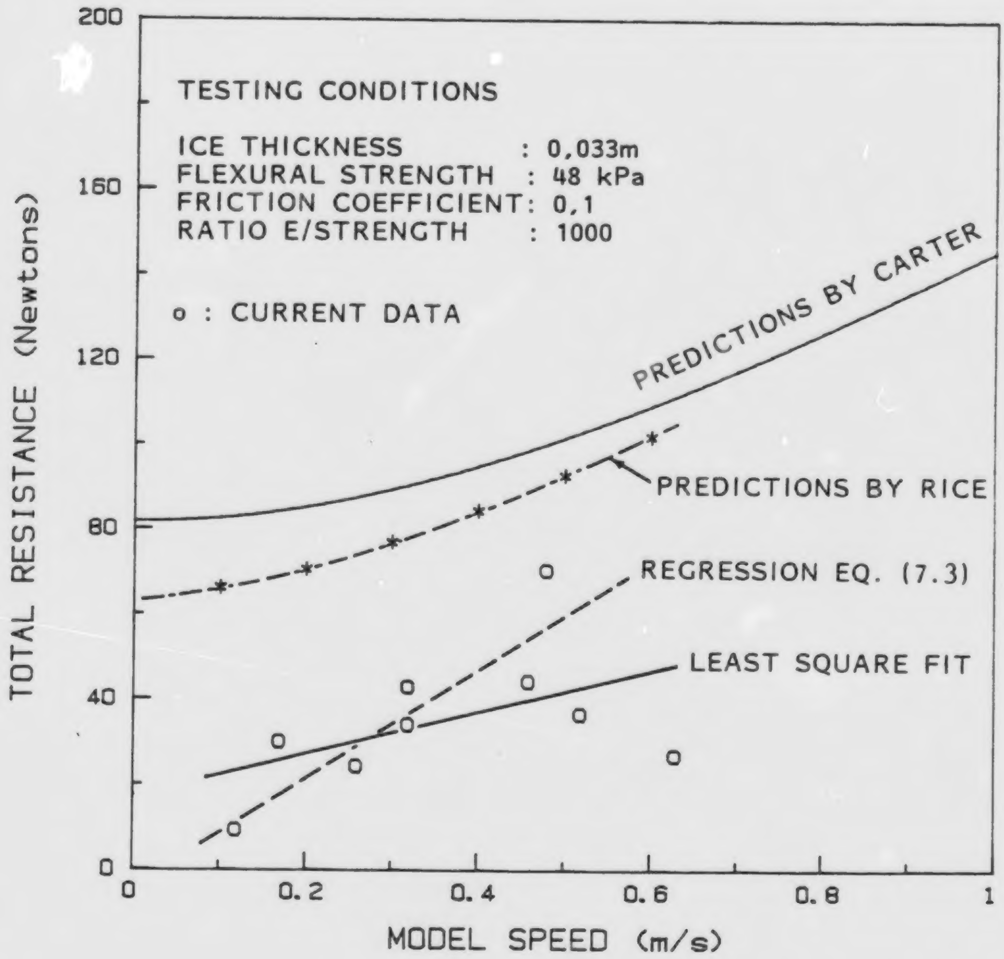

COMPARISON OF TOTAL RESISTANCE

FIGURE S.3

FIGURE S.4 — COMPARISON OF SEGMENT RESISTANCE PERCENTAGE WITH CARTER'S MATH MODEL PREDICTIONS

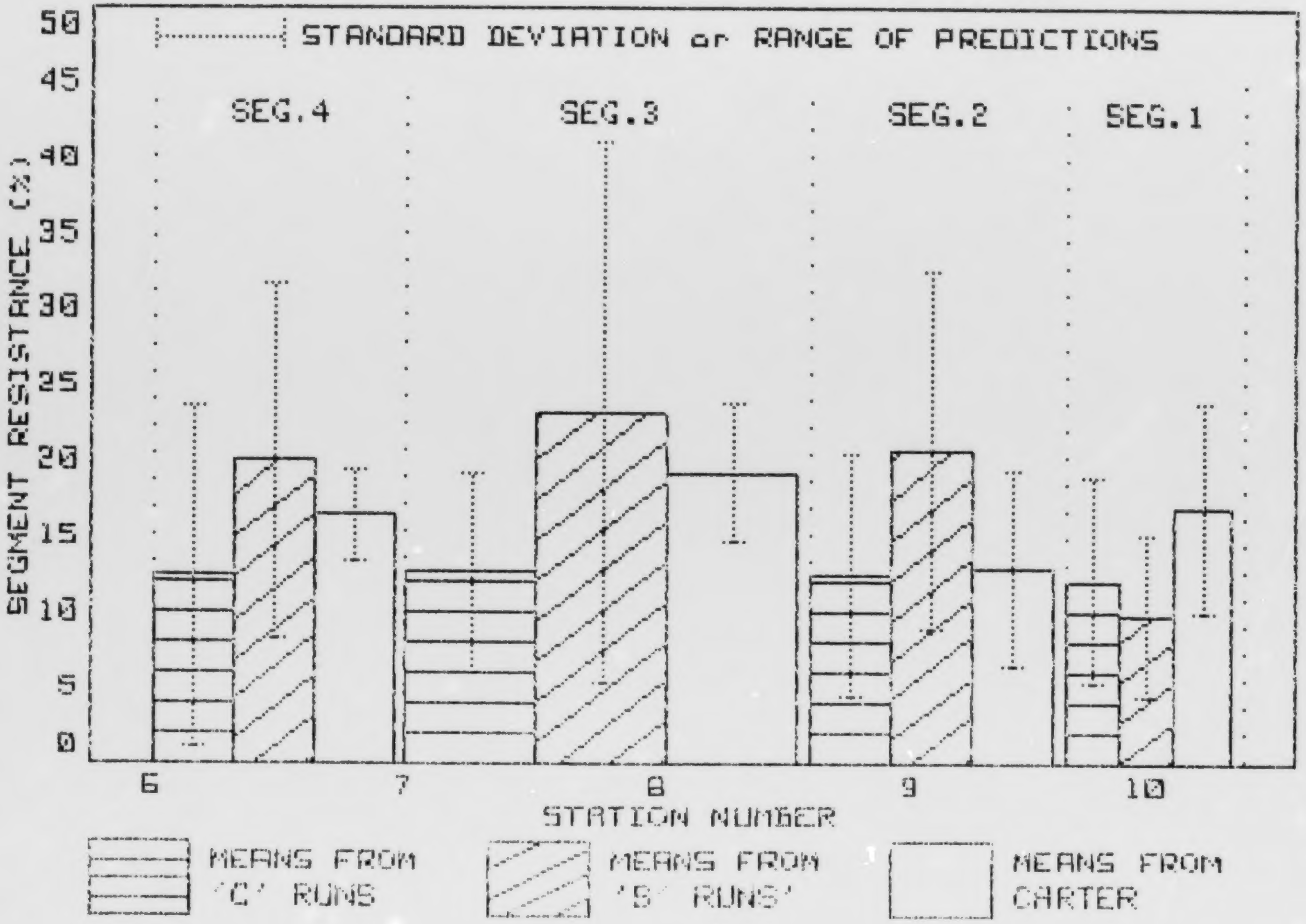

SOMMAIRE

Ce rapport rend compte de la phase III du programme d'expérimentation visant à approfondir la répartition des forces composant la résistance que la glace oppose à la coque d'un navire, et ce à l'aide d'une maquette de brise- glace dont la coque a été segmentée. La recherche a été financée par le Centre de développement des transports (CDT).

Il s'agissait de mesurer les forces exercées sur chacun des segments et de les comparer aux résultats des modèles de prévision, le tout débouchant sur une meilleure compréhension du phénomène en jeu et sur l'affinement des modèles utilisés.

Pour les besoins des phases I et II du programme, une maquette au 1/20 d'un brise-glace de classe R de la Garde côtière canadienne avait été réalisée; la partie avant de la coque avait été découpée en trois segments, au niveau de la ligne de flottaison. Des capteurs de forces conçus et réalisés exprès avaient été accolés aux segments, permettant ainsi, par la réduction des données obtenues, de déterminer l'amplitude et le point d'application des forces orthogonales nettes exercées sur chacun des segments à un moment donné, ainsi que l'amplitude et l'orientation des forces de frottement. L'étalonnage des segments et certains essais préliminaires dans le bassin des glaces ont amené les chercheurs à proposer l'adjonction d'un quatrième segment et d'entreprendre un programme d'essais sur maquette plus ambitieux, dans le but de comparer les résultats à ceux de deux modèles de prévision: le modèle analytique mis au point par le Dr Donald Carter (voir TP 3679E "Ship Resistance to Continuous Motion in Level Ice") et le programme informatique RICE (voir TP 4377E "A Semi-Empirical Ice Resistance Model, Summary Report, I.F. Glen).

La chaîne de mesure a comporté au total 37 capteurs de forces qui, une fois en place, ont été soumis à des étalonnages systématiques, comprenant des étalonnages individuels ainsi que des étalonnages de segments. Certains capteurs ont même été réétalonnés dans le but de procéder à des comparaisons aux résultats des essais antérieurs. Ces étalonnages ont permis de relier entre elles charges, déformations et tensions électriques et de caractériser l'hystérésis du système ainsi que sa sensibilité aux charges transversales. Le comportement des capteurs de forces a été jugé satisfaisant. Les étalonnages de segments ont consisté à appliquer une charge connue en certains endroits - grâce au montage d'essai réalisé exprès - et, après traitement ainsi que réduction des données, à comparer le résultat de ces étalonnages à ceux des modèles de prévision pour ce qui est de l'amplitude des interactions et des points d'application. Les travaux d'étalonnage ont donné des résultats jugés satisfaisants, les erreurs étant faibles.

Un photogrammètre a été engagé pour relever les formes de la coque de la maquette et afin de les vérifier par rapport au plan de formes dont on croyait qu'elles s'étaient écartées. Accessoirement, on en a profité pour évaluer le procédé de photogrammétrie dans cette application. Les écarts

linéaires et angulaires constatés ont été jugés conformes au degré d'exactitude exigé des expérimentations entreprises et aucun changement n'a été apporté aux algorithmes de réduction en vue de leur faire tenir compte des légers écarts constatés, d'autant plus que les essais sur maquettes avaient déjà commencé lorsqu'apparurent les résultats photogrammétriques. Néanmoins, la photogrammétrie s'est révélée comme un moyen économique et précis de levé des formes d'une maquette ou d'un navire.

Au départ, il était prévu de mener trois essais dans le bassin des glaces de l'Institut de dynamique marine de St-John's (IMD), qui appartient au Conseil national de recherches, afin de profiter des avantages offerts par la longueur des parcours d'essai. Des contraintes budgétaires et de temps découlant des travaux préparatoires et d'étalonnage plus compliqués que prévus ont cependant nécessité le transfert des essais, avec l'assentiment du CDT et de l'IMD, au laboratoire du contractant, où les parcours d'essais sont plus courts. Mais, le fait que la maquette plutôt fragile n'aurait plus à être transportée a quelque peu compensé ce désavantage. Pour les essais prévus, dix champs de glace ont dû être fabriqués. Le tableau S.1 récapitule les essais effectués. Deux essais d'élargissement de chenal suivaient chacun des essais de rupture de la glace.

Outre les 37 canaux d'enregistrement correspondant aux 37 capteurs de forces, il y en avait deux autres pour le mesurage de la vitesse d'avancement et de l'effort au chariot d'entraînement (résistance totale).

Un certain nombre de capteurs sont tombés en panne durant les essais, le plus important ayant été le capteur mesurant la force compressive dans l'axe des X (orientation de la résistance) exercée sur le segment 4 et qui n'a pu être remplacé. Ce paramètre n'a donc pu être mesuré directement. Par contre, les paramètres pour lesquels on a été incapables de mesurer les variations n'ont heureusement pas été nombreux. Des enregistrements vidéo de tous les essais ont été obtenus.

La réduction des données et la qualité des résultats étaient vérifiées après chaque période d'essai, et toutes les courbes de variations paramétriques dans le temps examinées attentivement. Tout résultat inattendu ou incohérent a été isolé. Par exemple, l'apparition occasionnelle d'un saut du signal de force moyenne venant du segment 1 et dû, semble-t-il, au changement opéré dans l'alignement de ce segment. Les calculs n'ont porté que sur les données ayant la qualité voulue et donnant le résultat logique prévu. Le logiciel de réduction et d'analyse des données permet le rappel sélectif de la partie utilisable de l'information, les mesures à vitesse constante, par exemple. Tous les renseignements vidéo ont été réexaminés en rapport avec le résultat de l'analyse des données. Une courbe type des variations paramétriques dans le temps est donnée à la figure S.1.

Les travaux analytiques ont porté sur l'amplitude des forces orthogonales et leur point d'application, l'amplitude et l'orientation des forces de frottement ainsi que les coefficients de frottement, la contribution de chaque segment au bilan total de la résistance à l'avancement et, enfin, la résistance totale opposée à la maquette. La contribution du segment 4 n'ayant pu être mesurée directement à cause de la panne du capteur correspondant, elle a

Tableau S.1

Essais sur maquette segmentée

Matrice des essais

Essai	h	Résistance	E/Résistance	V	Force moyenne par unité de longueur			
	(mm)	(kPa)		(m/s)	Seg.1 (N/m)	Seg.2 (N/m)	Seg.3 (N/m)	Seg.4 (N/M)
1S1	36.0	30.4	466	.17	44.3	29.9	27.3	15.1
1C1	35.5	(27.6)		.12	30.4	26.7	18.4	14.2
1C2	37.5	24.8		.58	48.3	54.5	33.2	46.8
1S2	31.7	48.2	(800)	.32	26.7	29.9	14.0	22.2
1C3	31.4	(37.5)		.26	20.5	21.5	12.2	10.1
1C4	34.7	26.9		.52	28.3	43.2	19.9	28.4
1S3	34.0	49.8	1161	.48	58.7	44.8	22.3	52.1
1C5	34.5	(32.5)		.32	40.8	31.7	22.7	29.4
1C6	36.8	15.3		.46	48.3	38.0	23.8	37.2
1S4	33.4	48.5	(2300)	.17	27.7	24.2	17.2	64.7
1C7	33.8	(33.6)		.63	38.4	62.7	27.7	60.1
1C8	35.2	29.5		.12	21.3	22.4	17.8	49.8

****

Essai	h (mm)	Résistance (kPa)	E/Résistance	V (m/s)	Seg.1 (N/m)	Seg.2 (N/m)	Seg.3 (N/m)	Seg.4 (N/M)
2S1	46.8	31.3	1271	.12	17.3	26.5	14.5	106.9
2C1	49.2	(27.4)		.15	40.3	35.7	14.4	81.0
2C2	51.9	23.4		.32	49.3	47.1	21.8	39.9
2S2	46.1	26.1	2916	.24	29.6	45.7	32.1	74.3
2C3	48.2	(30.0)		.12	46.7	54.5	31.4	88.5
2C4	50.0	33.9		.28	74.4	95.7	36.7	27.8
2S3	45.8	32.1	3270	.34	19.2	67.6	54.0	31.0
2C5	46.3	(33.3)		.29	67.2	62.4	60.5	28.4
2C6	48.5	34.5		.23	65.6	57.7	62.0	67.4
2S4	43.2	36.9	2716	.30	23.2	45.2	28.4	71.8
2C7	45.7	(41.2)		.14	41.6	46.3	19.7	19.3
2C8	47.2	45.4		.23	67.7	55.0	34.2	138.3

****

Essai	h (mm)	Résistance (kPa)	E/Résistance	V (m/s)	Seg.1 (N/m)	Seg.2 (N/m)	Seg.3 (N/m)	Seg.4 (N/M)
3S1	63.4	31.7	1511	.08	59.2	39.8	46.5	167.9
3C1	65.3	38.7		.11	83.5	77.8	54.7	52.1
3S2	54.1	30.9	2305	.19	47.7	89.3	59.7	167.0
3C2	56.3	42.4		.11	71.5	78.7	33.9	105.7

FIGURE S.1

Variations des paramètres au cours d'un essai

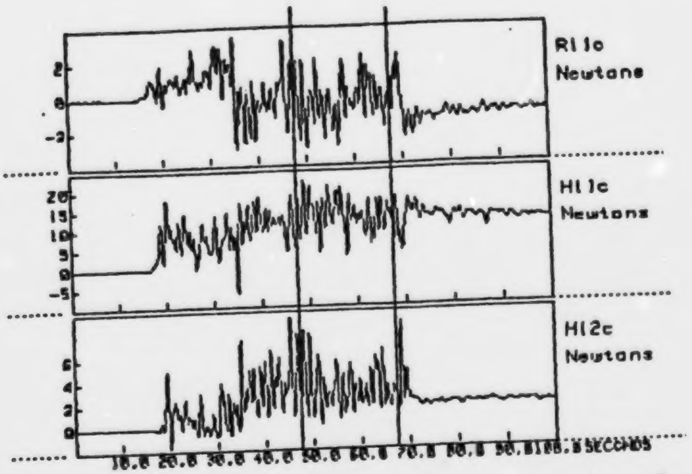

Essai/passage: 1S1
Fréquence de conversion
10 Hz/Canal

Fréquence de conversion
10 Hz/Canal

Date de la numérisation:
10 Jan. 1989
Fréquence passante 1 Hz

Statistique pour l'intervalle 47.30 à 67.40 secondes

CANAL	MINIMUM	MAXIMUM	VALEUR MOYENNE	ÉCART-TYPE
R11c	-2.97	2.34	-.24	1.16692
H11c	3.24	21.90	13.10	3.86379
H12c	.16	8.33	3.20	1.63874

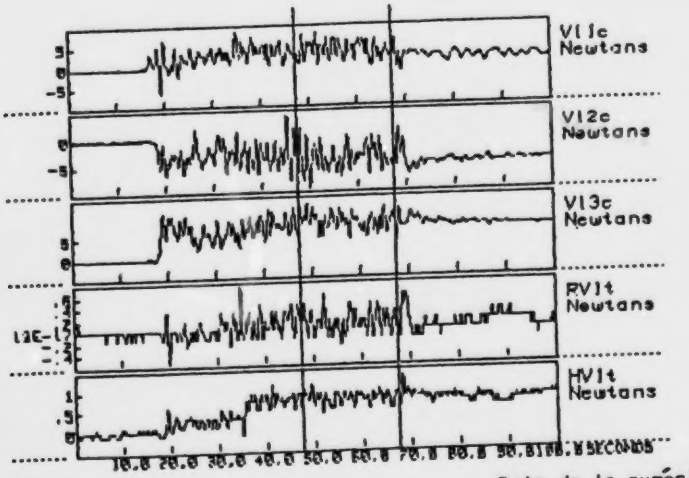

Essai/passage: 1S1
Fréquence de conversion
10 Hz/Canal

Fréquence de conversion
10 Hz/Canal

Date de la numérisation:
10 Jan. 1989
Fréquence passante 1 Hz

Statistique pour l'intervalle 47.30 à 67.40 secondes

CANAL	MINIMUM	MAXIMUM	VALEUR MOYENNE	ÉCART-TYPE
V11c	-.10	8.25	3.62	1.93897
V12c	-8.56	1.73	-4.01	2.09979
V13c	4.55	13.00	8.59	1.87263
RV1t	-.28	.50	.11	.16672
HV1t	.43	1.12	.78	.13604

pu être calculée selon la force orthogonale et le coefficient moyen correspondant. Les caractéristiques des courbes en fonction du temps ont été examinées et une analyse fréquentielle a été faite.

L'apparition de résultats inattendus relatifs à l'orientation des forces de frottement dans les segments antérieurs a mené à une analyse de la sensibilité de cette orientation aux erreurs de mesure. Il s'agit là d'un type d'investigations post-opératoires menées en vue d'approfondir les anomalies dans les résultats. Tant les valeurs maximales que moyennes des forces orthogonales ont été examinées et, là où c'était possible, comparées aux résultats des expérimentations exécutées au cours de la phase II du programme.

Les résultats montrent que la valeur des forces maximales va en augmentant de l'avant à l'arrière (segment 1 au segment 4) alors que leur fréquence, elle, va en diminuant. De même, les charges cycliques, fréquentes à l'avant, ne sont plus qu'occasionnelles à l'arrière. La force orthogonale moyenne est plus élevée à l'avant qu'à l'arrière. La fréquence des forces maximales augmente avec la vitesse. Des écarts ont été constatés dans les valeurs de charge, lorsque la glace est encore intacte et lorsqu'il s'agit d'élargir le chenal ouvert, les valeurs étant plus élevées dans ce dernier cas. Toutes les forces en jeu s'intensifient avec l'épaisseur de la glace et les forces orthogonales sur les segments 2 et 3 augmentent avec la vitesse.

A l'instar des essais antérieurs, les capteurs de forces de frottement ont produit, dans le cas des segments 1 et 2, des vecteurs de frottement dirigés vers l'avant, ce qui était inattendu, et des coefficients de frottement élevés.

Une analyse de la régression de la résistance totale opposée à la maquette a été faite; les résultats, mis à l'échelle, ont été tracés et comparés à ceux tirés d'essais sur d'autres maquettes d'un brise-glace de classe R, ces derniers provenant du rapport TP 8828E "The Testing of the 1:8 Scale Model of the R-Class in Level Ice" (voir la figure S.2). Les tracés obtenus se situent généralement entre ceux provenant des essais, mais l'influence de la vitesse y est plus marquée. A remarquer, cependant, que contrairement aux essais antérieurs, la maquette était, dans ce cas-ci, bridée contre le roulis, le lacet et le tangage.

La contribution des segments 1, 2, et 3 à la résistance totale a été de quelque 40 p. 100 (une fois les valeurs multipliées par deux pour tenir compte des deux côtés de la coque), et celle des segments 1 à 4 entre 55 et 60 p. 100. Apparemment, la charge des glaces sur la coque s'exerce dans une grande mesure au-dessous et/ou à l'arrière de la zone segmentée.

Les résultats de ces expérimentations ont été comparés à ceux obtenus à l'aide du modèle RICE et du modèle analytique mis au point par le Dr Donald Carter. Ils n'ont été comparables qu'à l'égard de la résistance totale dans une glace épaisse; l'espoir que chacun des segments traduise une étape particulière du processus de déglaçage tel que pris en compte dans le modèle RICE ne s'est donc pas réalisé. La cause de cet échec devrait être attribuée au comportement de la glace modèle, son écoulement autour de la maquette, et au fait que le programme RICE, qui est un modèle semi-empirique reproduisant le comportement dynamique d'un navire en vraie grandeur, ait été utilisé sur une maquette à l'échelle et à une seule liberté de mouvement.

FIGURE S.2

Résultats comparés: Essais en cours et essais antérieurs
Valeurs à l'échelle prototype
Résistance de la glace de 800 kPa

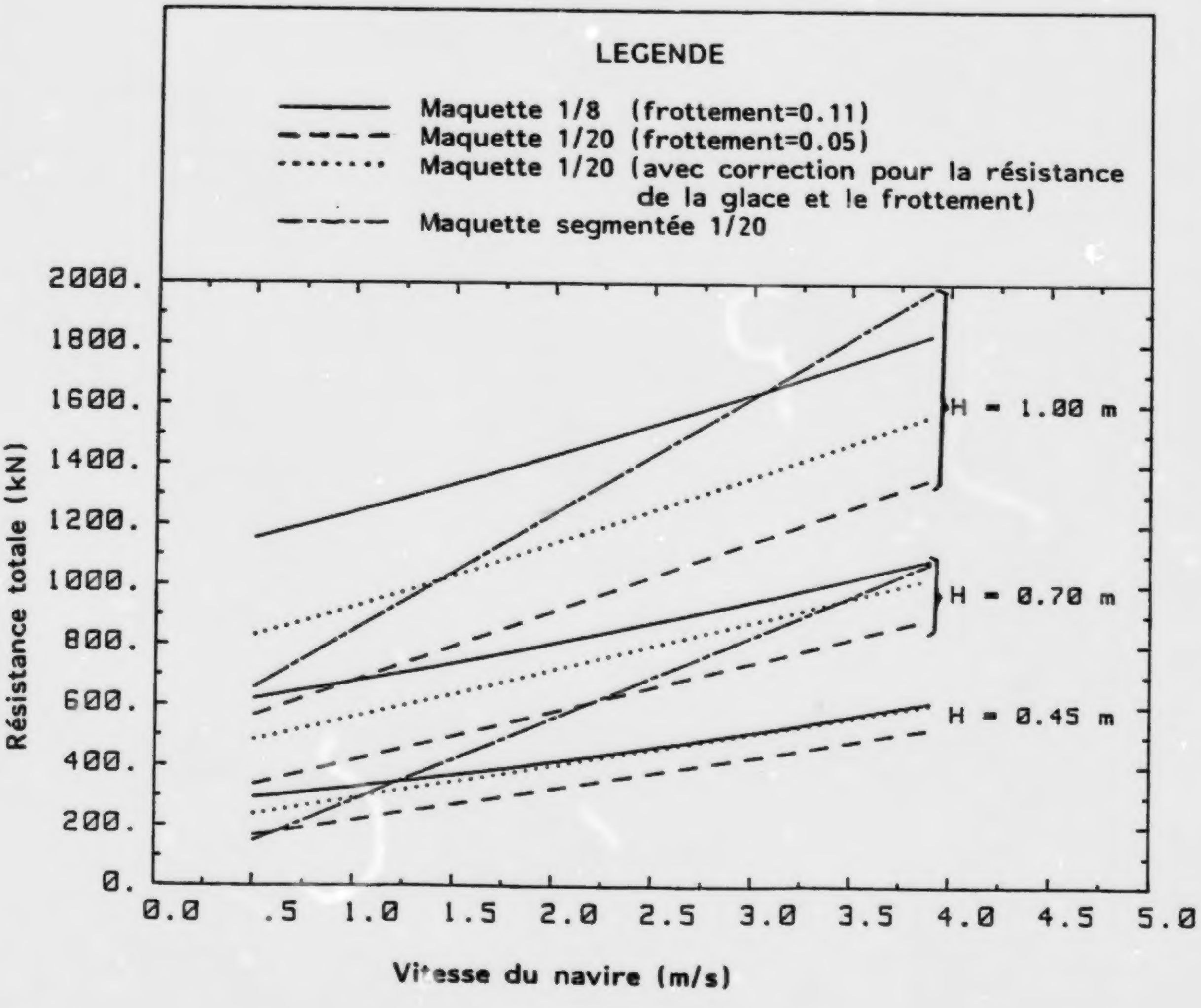

L'annexe A donne le rapport complet des prévisions obtenues à l'aide du modèle du Dr Carter. Les valeurs concernant la résistance totale concordent bien avec les expérimentations en vraie grandeur et elles sont le double de celles obtenues avec la maquette segmentée. La figure S.3 montre ces dernières comparées aux prévisions des modèles RICE et Carter.

La principale constatation est que les prévisions du modèle Carter s'harmonisent assez bien avec les expérimentations sur la maquette segmentée en ce qui concerne la réparation relative des forces en jeu, pour les quatre segments. Ceci est démontré à la figure S.4. Pour ce qui est de la contribution de chacun des segments à la résistance totale, l'ajustement le plus favorable fait ressortir un écart de 0,2 p.100 pour le segment 2, et le moins favorable un écart de 6,8 p.100 pour le segment 3. Quant à la répartition de la moyenne des forces orthogonales, les écarts le plus et le moins favorables pour le segment 2 ont été de 3 et de 14 p.100, respectivement. De tels écarts restent cependant à l'intérieur de l'étendue normale d'erreur admise en modélisation physique. Les résultats montrent que les prévisions fournies par le modèle du Dr Carter quant à la valeur des forces orthogonales et à la contribution de chacun des segments à la résistance totale concordent avec les expérimentations sur la maquette segmentée, c'est-à-dire la répartition relative de la moyenne des forces.

Le rapport traite également de la question des faiblesses présentées par la glace modèle utilisée et de l'influence qu'elles peuvent avoir sur des expérimentations comme celles qui ont été faites.

En conclusion, le rapport recommande que les données expérimentales, dont l'abondance est si grande, soient soumises à de plus amples analyses. Un petit nombre d'essais supplémentaires devraient avoir lieu dans une glace modèle d'un autre type, exemple MOD-ICE, de préférence à l'Institut de dynamique marine, pour tirer parti de la longueur du parcours d'essai. Mais, compte tenu des faiblesses et de la fragilité de la maquette segmentée, il serait indiqué de trouver et d'utiliser une autre méthode de modélisation.

FIGURE S.3

Résultats des expérimentations comparés aux prévisions
Valeurs à l'échelle de la maquette segmentée (1/20)

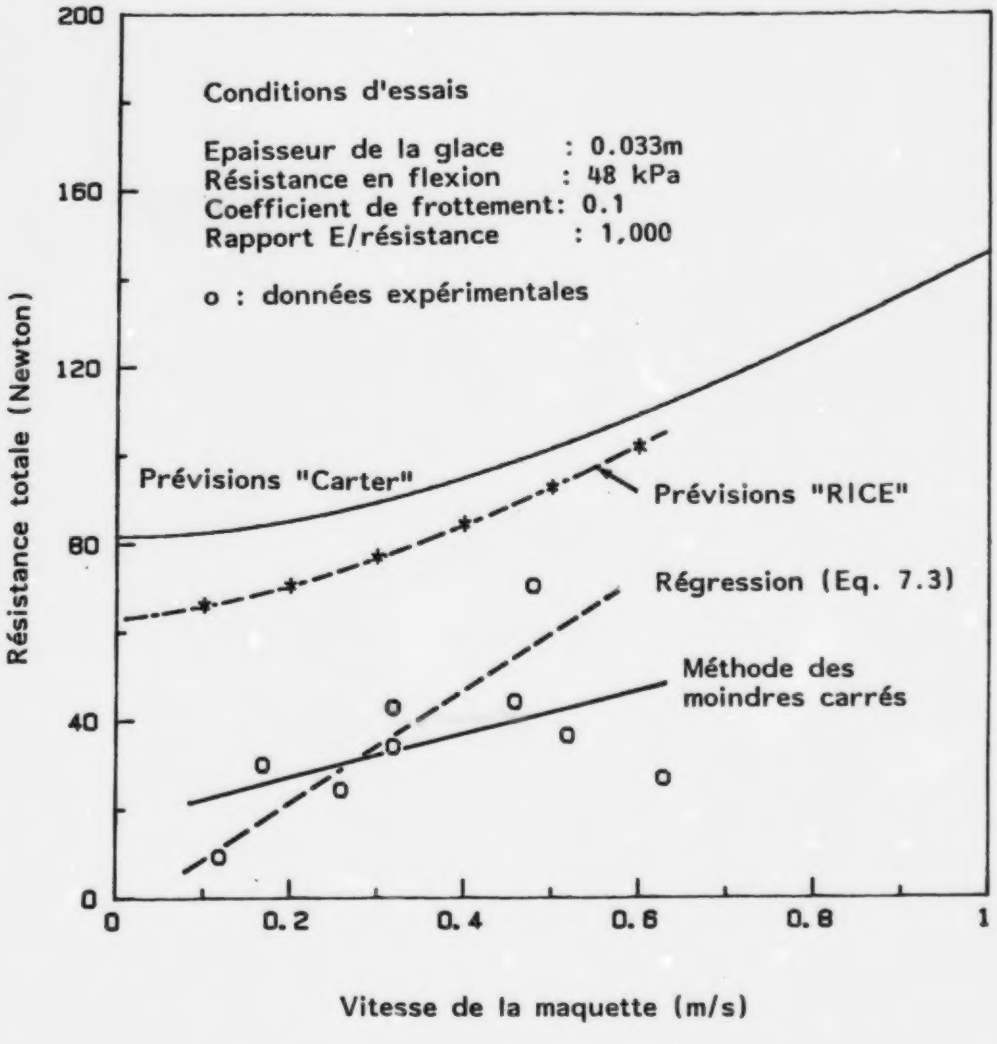

FIGURE S.4

Proportion de la résistance totale supportée par chaque segment

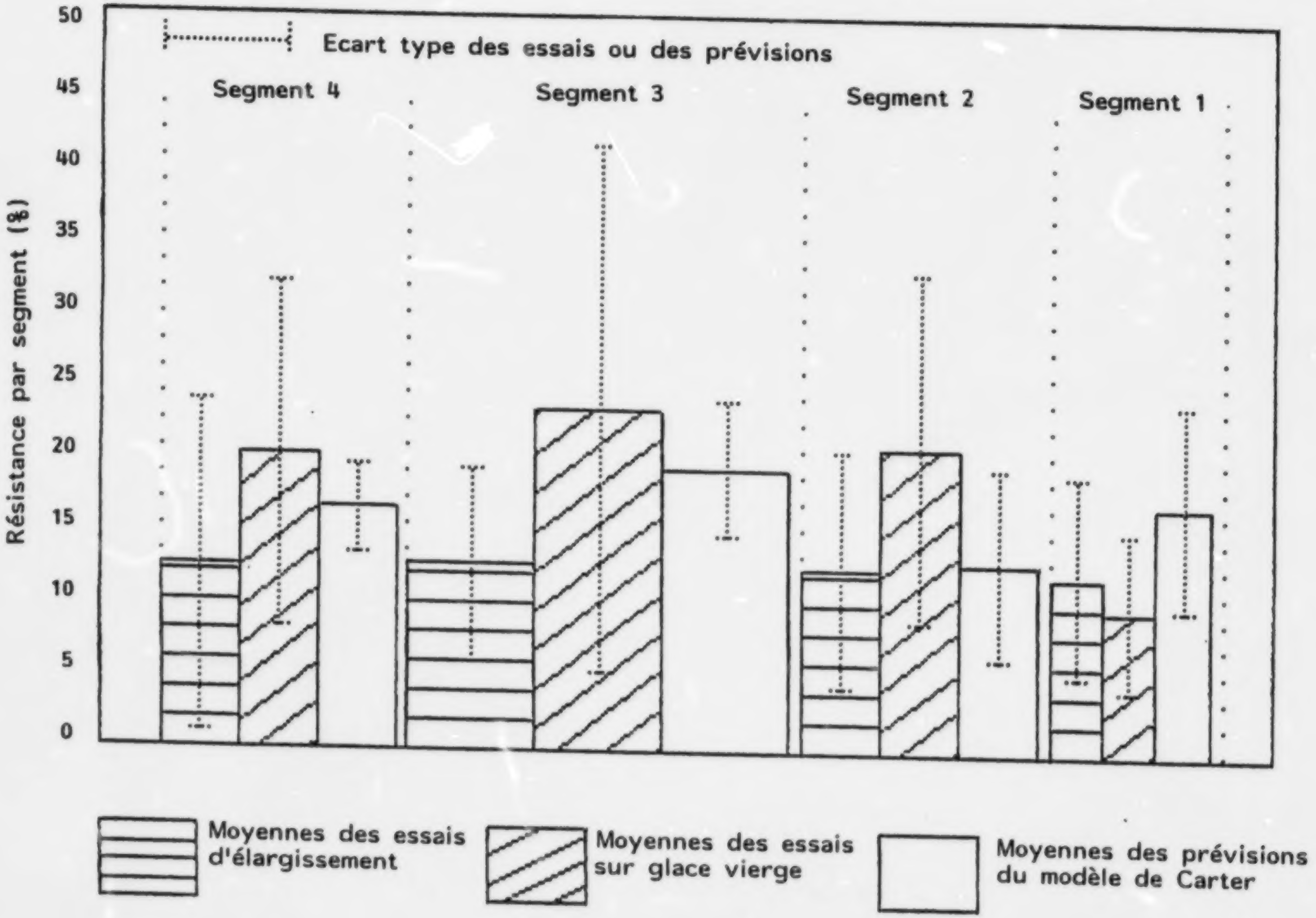

TABLE OF CONTENTS

1. INTRODUCTION..1

1.1 Background..1
1.2 Overview..2

2. SEGMENTATION SYSTEM DESCRIPTION..3

2.1 Segment System..3
2.2 Segment 4 Particulars...7

3. CALIBRATION...9

3.1 General...9
3.2 Transducer Calibrations...9
3.3 Segment Calibrations..11
3.4 Results...11

4. PHOTOGRAMMETRIC CHECK...22

4.1 Background..22
4.2 Mensuration by Photogrammetry.....................................22
4.3 Evaluation of Photogrammetry Technique............................27
4.4 Use of Data...27

5. TEST DESCRIPTION..28

5.1 Test Matrix...28
5.2 Test Procedures...34
5.3 Data Acquisition System...34
5.4 Quality of Measurements...36

6. PRESENTATION OF RESULTS...38

6.1 Approach..38
6.2 Transducer Time History Data......................................38
6.3 Data Reduction Techniques...40
6.4 Segment Normal Force..41
6.5 Segment Resistance..47
6.6 Load Position...50
6.7 Friction Coefficient and Direction................................57

TABLE OF CONTENTS CONTINUED

7. ANALYSIS AND DISCUSSION OF RESULTS....63

7.1 Approach....63
7.2 Time Histories....64
7.3 Normal Force....69
7.4 Friction Magnitude and Direction....76
7.5 Resistance....79
7.6 The RICE Model....87
7.7 Carter's Model....98
7.8 Ice Modelling Problems....110

8. CONCLUSIONS AND RECOMMENDATIONS....111

8.1 General....111
8.2 The Model Test Series....111
8.3 The Results....112
8.4 Comparison with Math Models....113
8.5 Recommendations....114

9. REFERENCES....115

APPENDIX A - VALIDATION OF CARTER'S MATH MODEL BY USE OF A SEGMENTED MODEL - COMPARISON OF PREDICTIONS WITH EXPERIMENTAL DATA

APPENDIX B - STATEMENT OF WORK

LIST OF FIGURES

FIGURE NO.	TITLE	PAGE NO.
S.1	TIME SERIES PLOT	x
S.2	COMPARISON OF THE MODEL SCALE RESULTS	xii
S.3	COMPARISON OF TOTAL RESISTANCE	xiv
S.4	COMPARISON OF SEGMENT RESISTANCE PERCENTAGE WITH CARTER'S MATH MODEL PREDICTIONS	xv
2.1	METHOD OF MODEL SEGMENTATION	4
2.2	SEGMENT LOCATIONS	4
2.3	SEGMENT SUPPORT SYSTEM	5
2.4	SEGMENT 4	8
2.5	MODEL CUT-OUT FOR SEGMENT 4	8
3.1	CALIBRATION RIG	12
3.2	THE CALIBRATION RIG APPLYING A LOAD TO SEGMENT 1	12
3.3	SEGMENT 1 CALIBRATION POINTS	14
3.4	SEGMENT 2 CALIBRATION POINTS	16
3.5	SEGMENT 3 CALIBRATION POINTS	18
3.6	SEGMENT 4 CALIBRATION POINTS	20
4.1	RADISSON BODY PLAN	23
4.2	HALF BREADTH PLAN	24
4.3	SHEAR PLAN	25
5.1	ICE SHEET UTILIZATION	29
5.2	ICE THICKNESS DATA FOR 1S3 SERIES	31
5.3	ICE THICKNESS DATA FOR 2S4 SERIES	32
5.4	FLEXURAL STRENGTHD ATA FOR S2S SERIES	33
5.5	FLEXURAL STRENGTH DATA FOR 2S4 SERIES	33
5.6	SEGMENTED MODEL INSTRUMENTATION	35
6.1	TYPICAL RAW DATA OUTPUT	39
6.2	CALCULATED SEGMENT NORMAL FORCES	42
6.3	NORMAL FORCE PEAKS	44
6.4	SEGMENT RESISTANCE VERSUS TIME	48
6.5(a-c)	CALCULATED LOAD POSITION VERSUS TIME	51
6.6	LOAD POSITION AT NORMAL FORCE MAXIMA VERSUS NORMAL FORCE	54
6.7	CALCULATED WATERPLANE AND FLARE ANGLES AT NORMAL FORCE MAXIMA VERSUS NORMAL FORCE	56
6.8(a-c)	CALCULATED FRICTION COEFFICIENT AND DIRECTION VERSUS TIME	58
6.9	FRICTION COEFFICIENT AND DIRECTION AT NORMAL FORCE MAXIMA VERSUS NORMAL FORCE	62

LIST OF FIGURES CONTINUED

7.1(a-f) EXAMPLE OF FREQUENCY SPECTRUM OF SEGMENT NORMAL FORCE 66
7.2 FREQUENCY OF PEAK TRANSDUCER LOADS VERSUS VELOCITY X THICKNESS 67
7.3 FREQUENCY OF PEAK LOADS VERSUS VELOCITY - SEGMENT 1 68
7.4 INTERVAL ANALYSIS - SEGMENTS 1 AND 2 71
7.5 EFFECT OF VELOCITY UPON MEAN NORMAL FORCE 74
7.6 AVERAGE FRICTION VECTORS 77
7.7 REGRESSION CURVES OF MODEL RESISTANCE 80
7.8 COMPARISON OF UNBROKEN ICE AND CHANNEL RUNS 81
7.9 COMPARISON OF THE MODEL SCALE RESULTS AT A STRENGTH OF 800 kPa 82
7.10 RATIO OF TOTAL SEGMENTS 1-3 RESISTANCE (x2) TO TOTAL RESISTANCE 86
7.11 RICE RUNS 89
7.12 RESISTANCE CORRELATION FACTORS FOR IMPORTANT PARAMETERS BY SEGMENT 92
7.13 RESULTS OF THE COMPONENTS OF RESISTANCE FROM RICE 93
7.14 RESULTS OF THE COMPONENTS OF RESISTANCE FROM RICE 94
7.15 RESULTS OF THE COMPONENTS OF RESISTANCE FROM RICE 95
7.16 COMPARISON BETWEEN FULL SCALE DATA, MODEL TEST RESULTS AND PREDICTIONS BY CARTER'S MATH MODEL 99
7.17 COMPARISON BETWEEN MODEL TEST RESULTS AND PREDICTIONS BY CARTER'S MATH MODEL 100
7.18 COMPARISON OF TOTAL RESISTANCE 101
7.19 NORMAL FORCE DISTRIBUTION ALONG WATERLINE FOR THREE DIFFERENT ELASTIC MODULI, E. 103
7.20 COMPARISON OF SEGMENT RESISTANCE PERCENTAGE WITH CARTER'S MATH MODEL PREDICTIONS 106
7.21 COMPARISON OF PERCENT MEAN NORMAL FORCES SEEN BY SEGMENTS WITH CARTER'S MATH MODEL PREDICTIONS 107

LIST OF TABLES

TABLE NO.	TITLE	PAGE NO.
S.1	SEGMENTED MODEL TESTS	ix
2.1	LOAD TRANSDUCER PARTICULARS	6
3.1	TRANSDUCER CALIBRATIONS	10
3.2	SEGMENT 1 - CALIBRATION ERRORS	15
3.3	SEGMENT 2 - CALIBRATION ERRORS	17
3.4	SEGMENT 3 - CALIBRATION ERRORS	19
3.5	SEGMENT 4 - CALIBRATION ERRORS	21
4.1	HULL ANGLE COMPARISON (23' WATERLINE)	26
5.1	TEST MATRIX	30
5.2	SUMMARY OF QUESTIONABLE TRANSDUCERS	37
6.1	MEAN NORMAL FORCE RESULTS	43
6.2	MEAN NORMAL FORCE PEAKS AND PEAK FREQUENCY	45
6.3	RATIO OF MEAN NORMAL FORCE/MEAN PEAK NORMAL FORCE	46
6.4	TOTAL SHIP RESISTANCE AND SEGMENT RESISTANCE	49
6.5	LOAD POSITION AT NORMAL FORCE MAXIMA	55
6.6	FRICTION COEFFICIENT AND DIRECTION	61
7.1	DIRECT COMPARISON OF SEGMENT MEAN NORMAL FORCES	70
7.2	REGRESSION ANALYSIS RESULTS	73
7.3	PARAMETERS SHOWING HIGHEST CORRELATION RELATIONSHIP WITH DATA	75
7.4	SENSITIVITY ANALYSIS OF TRANSDUCER ERROR - SEG.1&2	78
7.5	CONTRIBUTIONS TO RESISTANCE FROM SEGMENTS	84
7.6	RICE RESULTS FOR MODEL	90
7.7	COMPARISON OF RICE RESISTANCE COMPONENTS AND SEGMENT CONTRIBUTIONS	96
7.8	CALCULATED SHIP RESISTANCE AND SEGMENT RESISTANCE	104
7.9	CALCULATED MEAN NORMAL FORCE AND SEGMENT NORMAL FORCE	105
7.10	DISTRIBUTION ALONG THE HULL PERCENTAGE CONTRIBUTION TO TOTAL FORCE	108

NOMENCLATURE

Alpha	(or α) Waterplane angle (deg.)
Beta	(or β) Flare angle (deg.)
$F_{friction}$	Friction force (N)
F_{total}	Total force (N)
Fn	Normal force (N)
F_x, F_y, F_z	x, y and z direction force (N)
h	Ice thickness (mm) model scale
H	Ice thickness (m) full scale
Psi	Direction of friction force (deg.)
R_{OW}	Total resistance in ice free water
R_{RES}	Total model resistance - R_1, R_2, R_3 (N)
R_{Tfs}	Total resistance at full scale (N)
R_{Tms}	Total resistance at model scale (N)
S	(or σ_f) Sigma - bending strength of ice (kPa)
V	Ship model velocity (m/s)
x	Longitudinal load position (M) model scale
y	Transverse load position (M) model scale
z	Vertical load position (M) model scale
α	Waterplane angle (deg.)
β	Flare angle (deg.)
ε	Young's modulus of ice (MPa)
σ_c	Crushing strength of ice (kPa)
σ_f	Bending strength of ice (kPa)

1. INTRODUCTION

1.1 Background

The prediction of icebreaking resistance of ships has been the focus of much research for the past twenty years. Theories ranging from theoretical to purely empirical have been developed in an attempt to understand and describe the mechanisms involved. The use of segmented models to develop an understanding of icebreaking resistance from an experimental point of view has been supported by Transportation Development Centre (TDC) during the past five years. The objective of the segmented model is to provide experimental data on the resistance components along different zones of the hull to verify and improve the theories of icebreaking resistance of ships.

In 1983, Fleet Technology Limited, then known as Arctec Canada, with the support of TDC built a 1/20th model of the icebreaker, PIERRE RADISSON, which had three instrumented segments on the port side of the bow. Each segment was located so as to capture the icebreaking on a different zone of the hull. The rationale for the position of each segment was based upon the hull positions at which ice cusp breaking, turning and submergence would occur. The development of this technique was identified as Phase I and reported in [1].

A segment support system was designed [2, 3] which would measure the normal and frictional component of any force acting on the hull segments as well as the position of the force on the hull and the direction of the frictional component. The instrumentation system consisted of between 8 and 11 force transducers per segment.

From force and moment equilibrium equations and knowledge of the hull shape, an iterative data reduction algorithm was developed to determine the normal and frictional components of the load and its position and direction of action. This algorithm, along with interpolation routines to determine the hull offsets at any point on the segments, was incorporated into the in-house data collection and analysis software program. This software allows analysis of the ice forces on the hull at any data point collected during testing or at averaged data points.

In Phase II of the program, extensive calibrations were performed on the model and error estimates made which were such as to suggest that sufficient accuracy could be obtained to use the technique to validate current ice resistance models. Level ice resistance tests were performed in two ice sheets and results indicated that valuable information on the ship/ice interaction could be obtained. The results are reported in [2].

One surprising result was that the total resistance on the three segments, when doubled (to allow for both sides of the vessel) amounted to only 43 - 57% of the total resistance force. It was also noted that the magnitude of peak normal force increased from Segment 1 to Segment 3, and it was surmised that it might increase further aft.

The result of this work, and discussions with the sponsor - TDC - was a further phase to the project in which it was planned to add an additional hull segment, improve the calibrations, conduct a larger series of ice model tests, and compare results obtained with two numerical prediction techniques, that of Dr. Donald Carter [4] and the semi-empirical model known as RICE [5], [6].

This document reports on the results of this phase (Phase III).

1.2 Overview

The statement of work for the project is provided in Appendix B along with comments on the degree to which the work has complied with this statement. Indicated also is the percentage of the total budget allocated to each of the work items. This demonstrates quite clearly that the project had an overall emphasis on the experimental aspects. The intent was to identify the most useful data from the extensive data for further analysis, if desired, while continuing the comparison of the analysis herein with the mathematical prediction models.

The instrumentation of the fourth segment resulted in the model being outfitted with a total of 37 transducers. For accurate measurement of the small forces on each transducer, the especially designed and constructed sensors were extremely sensitive and required precision alignment. The model and instrumentation construction, outfit and calibration stages of the project consumed much time and effort, as the delicate and precision segmentation system was built and installed.

The original plan was to test the model at NRC's Institute for Marine Dynamics' (IMD) facility in St. John's to provide longer runs in order to provide higher quality data and a greater statistical data base. The IMD facility was heavily booked around the time that had been reserved for the model tests, and no slippage could be tolerated. In practice, the model was not ready for testing and in addition at that time it was clear that the preparation stages had absorbed more than their share of the budget. It was also felt that the model would suffer significantly from the shipping to IMD and would require considerable re-alignment and calibration for which there was neither time nor money. It was therefore agreed to test the model in ten ice sheets at Fleet Technology's Ice Basin in Kanata.

The test program was run in January and February, 1989. The budget and schedule were restored, and the instrumentation performed well with only a few failures noted later. The length of the runs were, of course, shorter, adding to the uncertainty in some of the data. This is examined briefly in the report.

The analysis of how the data fits with Dr. Donald Carter's model and RICE - the TDC semi-empirical model - is made, and the data is briefly examined. The potential for further analysis of the data is discussed.

2. SEGMENTATION SYSTEM DESCRIPTION

2.1 Segment System

The model segmentation system consists of four individual segments on one side (port) running from forward of midships at Station 6 to the bow. The top and bottom of each segment corresponds to the 7.54 m and 4.27 m waterlines respectively. The segments fit into box-like recesses in the model so that when in place, a 4 mm gap exists between the segment's outer face and the remaining hull surface on the model. Figures 2.1 and 2.2 illustrate the model segmentation.

Each segment is subjected to normal forces and their frictional components. At least six support points are needed on each segment to support these loads: three points in the x, y and z directions to support the normal load components and three points in the x-y, x-z, and y-z planes to provide support for the three moment components of load. At least five measurements are required to determine the position of the load, and its normal and frictional components. The segments each have either six or seven support points; two in the longitudinal (or x) direction, two or three in the transverse (or y) direction, and two, three or four in the vertical (or z) direction.

The load at each point is measured using unidirectional compressive load cells fitted to the main body of the model. Each load cell contacts with a hardened, polished surface on the segments, which have been machined to provide highly accurate surfaces in the three measurement planes. The load cells support and position each segment but do not actually hold them in place. Tension load rings in each measurement plane are used to maintain continuous compressive load on the load cells and to hold each segment in place. Negative reactions on certain load cells from the ice resistance forces necessitate the application of a sufficient preload to insure that the load cells are always in contact with the segment during testing. These load rings were designed to have less stiffness than the load cells in order to allow the load cells to carry the greatest part of the loads, ensuring that load positions could accurately be determined. Figure 2.3 shows the placement of each measurement transducer relative to the segments and Table 2.1 gives the position, load rating and preload range for each transducer.

For a complete discussion of the segment support system see [2].

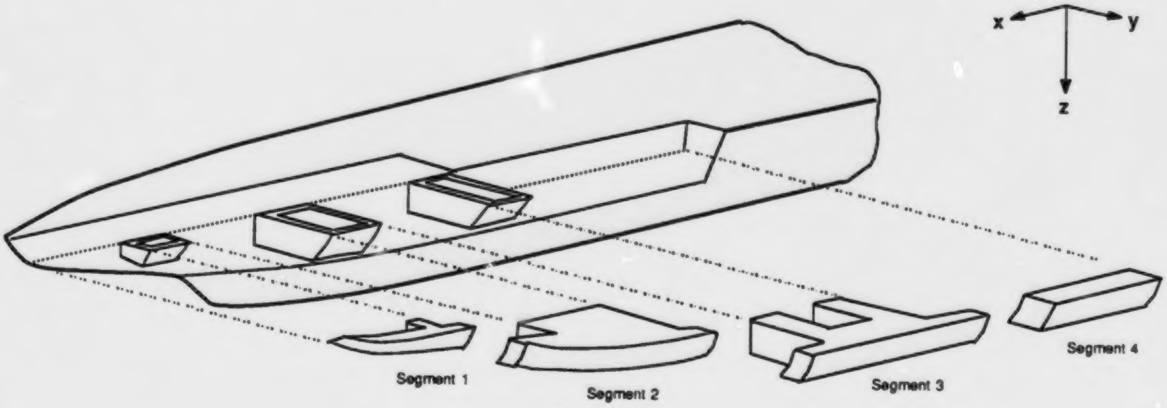

Main deck omitted for clarity.
Left hand coordinate system was used as illustrated .

Figure 2.1 Method of Model Segmentation

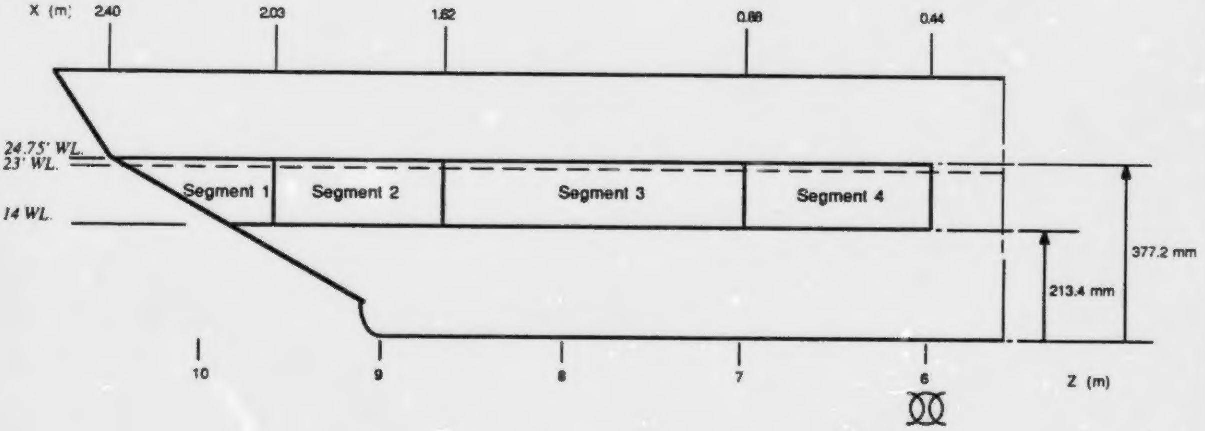

Figure 2.2 Segment Locations

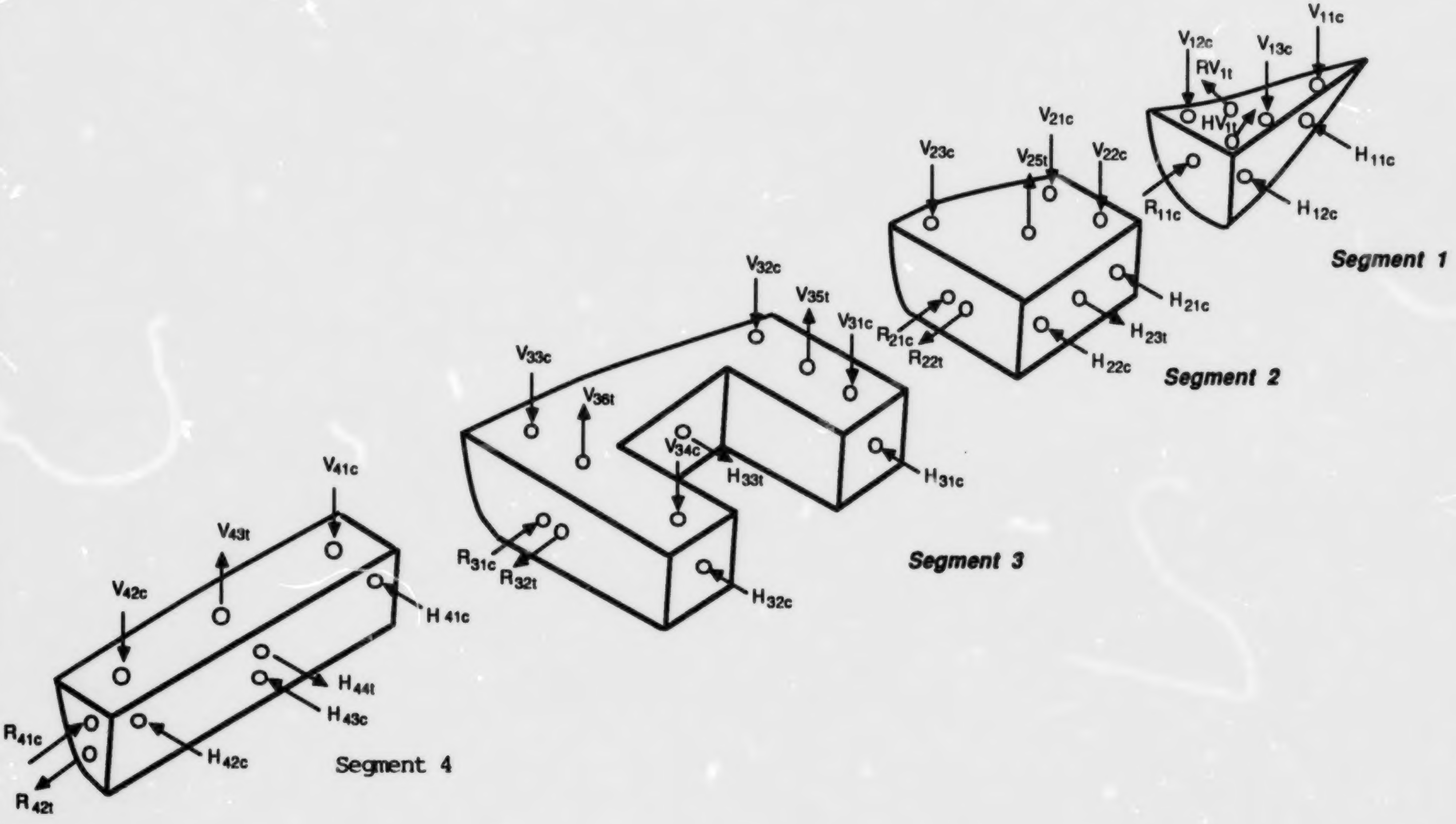

Figure 2.3 Segment Support System

TABLE 2.1

LOAD TRANSDUCER PARTICULARS

	[-------	POSITION	-------]		[- PRELOAD	-]
SEGMENT 1	X (m)	Y (m)	Z (m)	Rating (N)	MIN (N)	MAX
R11c	-	0.050	0.020	100	5	60
H11c	2.219	-	0.020	100	23	28
H12c	2.055	-	0.083	100	26	33
V11c	2.255	0.025	-	100	5	38
V12c	2.056	0.153	-	100	15	21
V13c	2.165	0.020	-	100	32	86
RV1t	2.160	0.050	0.020	140	5	125
HV1t	2.137	0.055	0.055	200	5	185
SEGMENT 2						
R21c	-	0.122	0.075	50	5	30
R22t	-	0.068	0.075	140	5	140
H21c	2.005	-	0.080	100	22	58
H22c	1.655	-	0.080	100	5	19
H23t	1.830	-	0.080	140	5	140
V21c	2.005	0.187	-	50	12	50
V22c	1.870	0.040	-	100	5	32
V23c	1.655	0.337	-	100	5	50
V25t	1.821	0.159	-	200	5	200
SEGMENT 3						
R31c	-	0.320	0.080	50	5	34
R32t	-	0.240	0.080	140	5	140
H31c	1.603	-	0.080	100	5	40
H32c	0.920	-	0.080	100	5	27
H33t	1.265	-	0.080	140	5	140
V31c	1.467	0.040	-	50	8	47
V32c	1.603	0.346	-	50	5	19
V33c	0.920	0.445	-	50	5	34
V34c	1.105	0.040	-	50	18	50
V35t	1.472	0.240	-	200	5	190
V36t	1.095	0.305	-	240	5	135
SEGMENT 4						
R41c	-	0.430	0.065	50	10	40
R42t	-	0.428	0.125	140	10	140
H41c	0.856	-	0.032	150	30	60
H42c	0.469	-	0.031	150	30	60
H43c	0.663	-	0.135	150	10	110
H44t	0.663	-	0.069	200	70	190
V41c	0.854	0.433	-	50	10	35
V42c	0.468	0.429	-	50	10	40
V43t	0.662	0.429	-	140	20	140

Origin of coordinate system at intersection of model centerline, midship plane and 7.54m waterline (the top of each segment).

R=resistance (x direction) H=horizontal (y direction) V=vertical (z direction)
c=compression transducer t=tension transducer

2.2 Segment 4 Particulars

The fourth segment was made by cutting out the existing model hull along the 7.54 m and 4.27 m waterlines between Stations 6 and 7. The cut-away hull surface was then bonded to a wood and aluminum framework forming a box with one face being the hull surface. Stainless steel bolts were bolted and cemented in place at each compression load cell contact point. The bolt heads were then machined in place on the segment to provide flat surfaces parallel to the three measurement planes. After machining, the surfaces were polished to a high finish giving a low friction plane for the load cells to bear against.

The physical constraints of the model and fourth segment were such that one tension link load ring was internal to the segment (R42t) and two were external to the segment (H44t and V43t). Attachment points for the load rings were then added at the appropriate positions. Finally, the entire segment was waterproofed. Figure 2.4 shows Segment 4 prior to final assembly (note the machined bolt heads, the opening for load ring R42t, and the attaching links for load rings H44t and V43t).

The opening in the model into which Segment 4 fits was boxed in and inserts were cemented in place for the mounting of the compression load cells and tension load rings. Figure 2.5 shows the aft portion of the segment opening before the installation of any load cells. Visible in the figure are the inserts for load cells R41c, H42c, H43c and V42c, access holes for load rings R42t and V43t, the housing for load ring H44t and the load ring itself.

The original model construction technique pre-stressed the outer hull surface so that, when cut away, the segment portion had a slight tendency to 'spring' out of shape. It was found that the best fit of the segment into its opening was one where each of the four corners was within 2 mm or closer to the original lines.

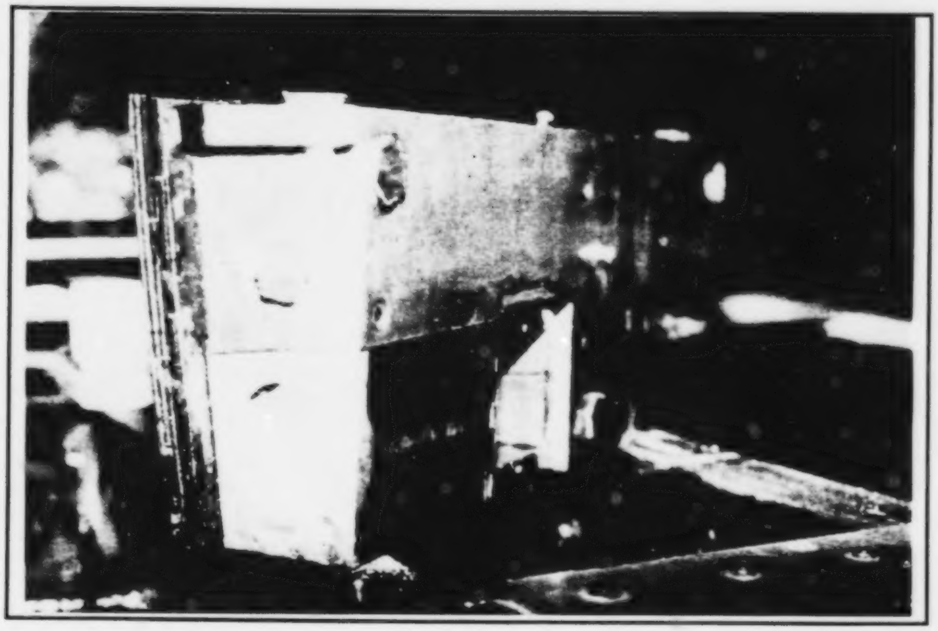

Figure 2.4 Segment 4

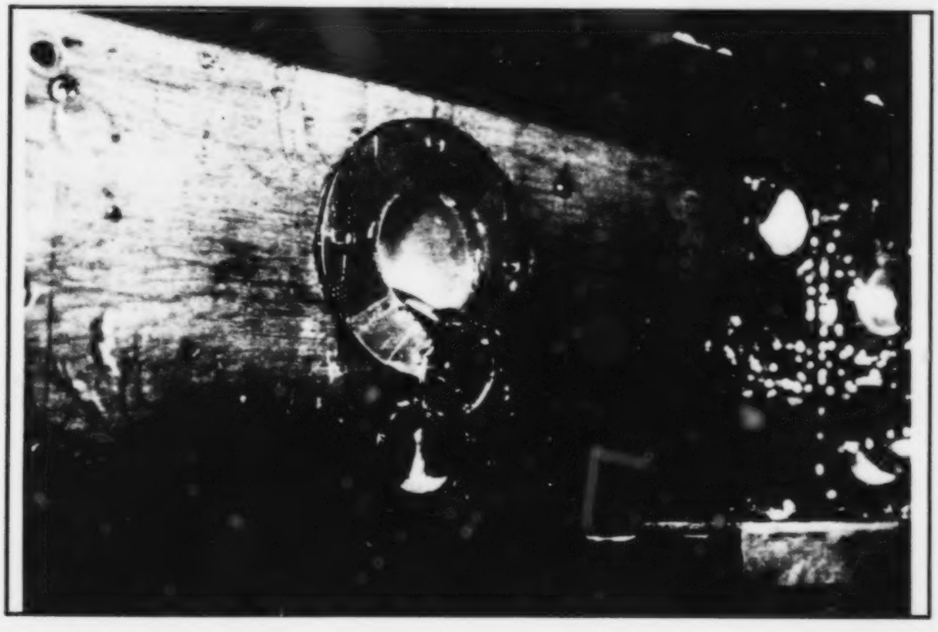

Figure 2.5 Model Cut-out for Segment 4

3. CALIBRATION

3.1 General

Two types of calibrations were performed: individual transducer calibrations and segment calibrations. All new transducers were calibrated and 25 transducers used in the earlier project (Phase II) were re-calibrated. Segment calibrations consisted of a complete series of calibrations for Segment 4 and a series of check calibrations for Segments 1 - 3 which had been thoroughly calibrated for Phase II.

3.2 Transducer Calibrations

All new load cells and load rings were calibrated individually. As well, 25 transducers from Phase II were re-calibrated. Three of the compression load cells were fixed somewhat permanently in the model and could not be removed for re-calibration. The calibration factors obtained in Phase II were used for these transducers.

The compression load cells were calibrated using a purpose-built hydraulic rig. The load on each transducer was increased and decreased in increments to check the response of the load cell for linearity and hysteresis. To ensure valid results, each transducer was calibrated through the same instrumentation channel (signal conditioning, etc.) as was used for the test series.

The tension load rings were calibrated in a similar, systematic manner, the load being applied by hanging a series of deadweights vertically from the load ring. Again, each transducer was calibrated through the same instrumentation channel as was used for the test series.

The results of the calibrations are summarized in Table 3.1. In all cases the transducers showed excellent linearity and hysteresis. As well, the re-calibrated transducers showed good repeatability of Phase II results given the fact that instrumentation channels and cable runs were different. This finding justified the use of the Phase II calibration results for the three fixed transducers in the model.

TABLE 3.1

TRANSDUCER CALIBRATIONS

	POSITION	S/N	CAL FACTOR	CORRELATION
SEGMENT 1	R11c	116	- 35.67	.999997
	H11c	114	39.00	*
	H12c	115	35.20	*
	V11c	110	40.22	.999995
	V12c	109	42.13	.999996
	V13c	108	38.04	.999996
	RV1t	209	59.96	.999992
	HV1t	208	40.32	.999995
SEGMENT 2	R21c	120	17.00	.999939
	R22t	201	41.28	.999993
	H21c	113	40.50	*
	H22c	111	39.88	.999997
	H23t	202	41.07	.999990
	V21c	101	38.31	.999998
	V22c	103	- 37.32	.999988
	V23c	104	39.23	.999997
	V25t	203	58.08	.999994
SEGMENT 3	R31c	118	17.30	.999987
	R32t	204	40.58	.999996
	H31c	112	- 42.01	.999996
	H32c	107	37.81	.999912
	H33t	205	40.57	.999994
	V31c	105	22.32	.999997
	V32c	102	21.03	.999996
	V33c	117	16.13	.999987
	V34c	106	- 14.49	.999996
	V35t	206	65.17	.999998
	V36t	207	123.70	.999965
SEGMENT 4	R41c	130	- 16.56	.999991
	R42t	210	36.34	.999995
	H41c	133	- 47.39	.999975
	H42c	134	- 56.52	.999974
	H43c	135	- 48.21	.999984
	H44t	212	104.1	.999992
	V41c	131	- 13.24	.999995
	V42c	132	- 18.48	.999914
	V43t	211	36.89	.999978

* Transducer in model, not recalibrated, Phase 2 cal factor used

R=resistance (x direction) H=horizontal (y direction) V=vertical (z direction)
c=compression transducer t=tension transducer
S/N = Serial Number

3.3 Segment Calibrations

The segment calibrations were carried out by applying a measured point load in the direction normal to the hull at a known location on the segment. The calibration procedure was to apply a nominal 10 - 15 Newton load at the desired load point which served as a starting reference load. The load was then increased to about 50 Newtons and another set of measurements was recorded. By using an initial preload, it could easily be verified that the desired load point was in fact where the load was actually applied.

Two other types of calibrations were undertaken for Segment 4. The first was similar to the above procedure except the load level was increased and decreased in steps, thus investigating the effect of load level upon measured forces. The second type of calibration consisted of applying a series of loads only in the x, y or z direction to see if any cross-coupling effects were found. The loading was accomplished by changing the tension on a desired load ring.

A special calibration rig, fabricated for Phase II tests, was used for the calibration where loads were applied normal to the hull surface. For a complete description of the calibration rig see [2]. Figure 3.1 shows the basic geometry of the calibration rig and Figure 3.2 shows the rig in use on Segment 1.

Some modifications to the calibration rig were made prior to calibrating. The length of travel along the model centreline had to be increased to allow access to Segment 4. Additionally, the rig was made sturdier so that the cantilevered loads on any arm caused less deflection thus ensuring more accurate positioning along the hull. Results from Phase II indicated that in-air calibrations were virtually identical to in-water calibrations, and so only in-air calibrations were performed.

3.4 Results

In the following pages, the calibration load locations are reported and the calibration results tabulated for each segment.

Segment 1: Seven positions on Segment 1 were calibrated (Figure 3.3). Typically the measured forces are very close to the resolved applied loads. Errors in frictional load are high on a percentage basis due to low loading in that direction. The calculated position of the applied load is typically within 5 mm of the actual point of application, the worst case being an error of 20 mm. The calibration results are similar, but slightly better, to those found in Phase II. Table 3.2 summarizes the errors in resolved and measured forces and calculated versus actual load position for the calibrations on Segment 1.

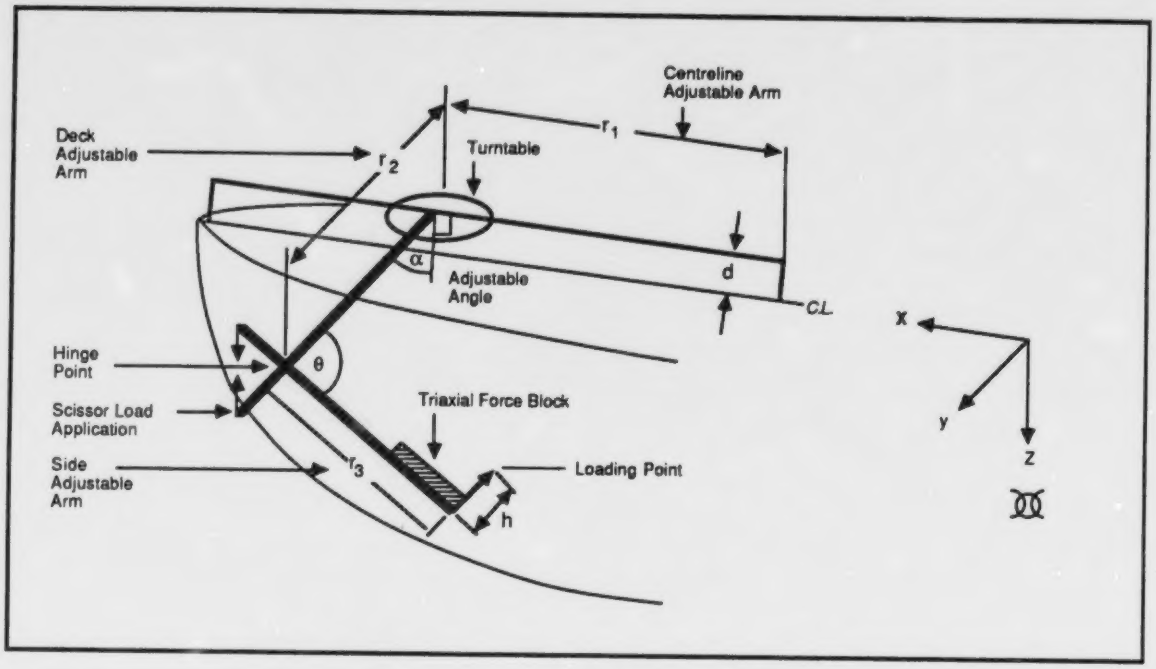

Figure 3.1 Calibration Rig

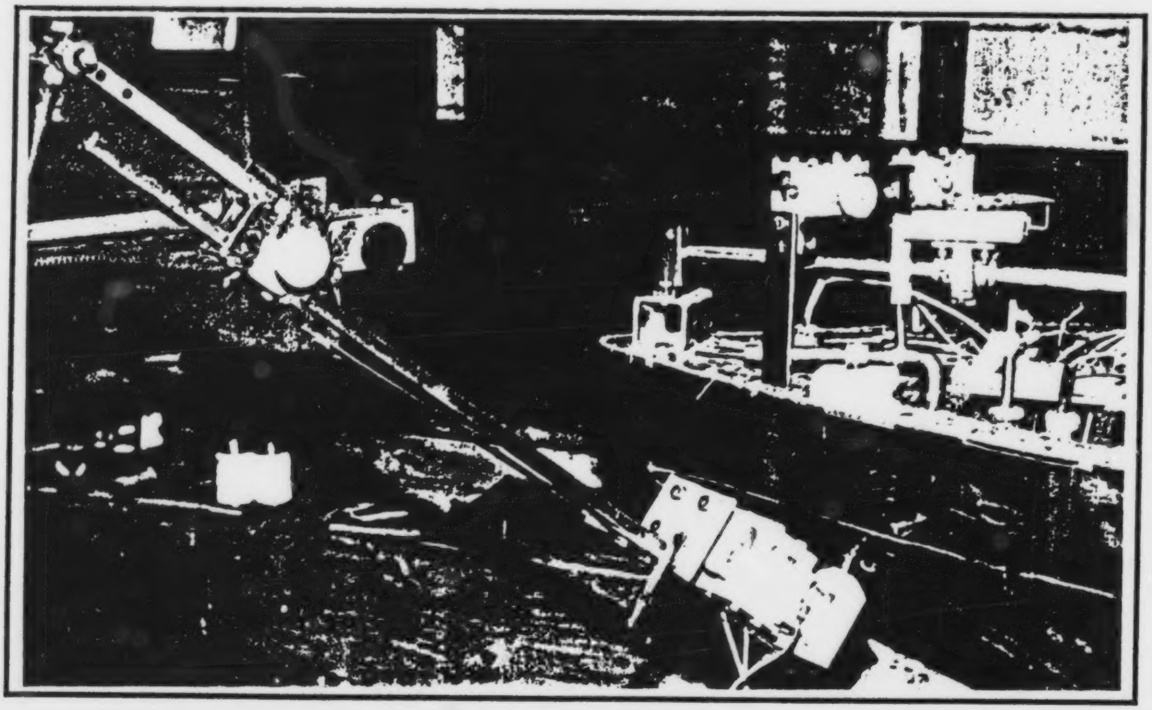

Figure 3.2 The Calibration Rig Applying a Load To Segment 1

Segment 2: Five positions were calibrated on Segment 2 (Figure 3.4). Calculation of normal force is within 2 or 3 Newtons (6-10%) of the applied normal force. This error is within the range found in Phase II. Resolved forces in x, y and z directions are within 2 - 3 Newtons of applied forces, again similar to Phase II results. These calibrations did show somewhat better results in the x direction and slightly worse results in the z directional forces. Position calculation errors ranged from 15 to 40 mm in the x direction and 0 to 23 mm in the z direction. Phase II results were comparable in x, but better in z. The results of Segment 2 calibrations are summarized in Table 3.3.

Segment 3: Six locations on Segment 3 were calibrated (Figure 3.5). The results of the calibrations on Segment 3 are not nearly as good as for the other segments. This was found as well in Phase II calibrations. Most errors between applied and measured forces are around 5 to 10 Newtons. The errors appeared to be much less for calibrations done on the aft portion of the segment. Errors in calculation of load position were also higher than for the other segments, again these results were found in Phase II calibrations. Table 3.4 lists the calibration errors for Segment 3.

Segment 4: A complete set of calibrations were performed on Segment 4. A total of twelve locations were calibrated (Figure 3.6) some more than once. As one might suspect, given the regular geometry of the segment (virtually flat), the errors found in the calibrations are very small. The only cases where the force errors are greater than 1 Newton are for friction and x directional force. This is understandable given the fact that both directions are perpendicular to the actual direction of loading.

The calibrations also show very good agreement in the calculated versus actual position of the load point. Typically the positional error is about 5 mm with the worst case being 16 mm. Table 3.5 shows a summary of the calibration errors for Segment 4.

Hysteresis calibrations were done at six locations on Segment 4. The purpose of these calibrations was to assess the effect of load range upon the measured errors. Seven different values of normal load were applied at a location and the resulting forces were measured. The results showed that the small errors in y and z forces did not substantially change over the load range. The typical error in x direction force was both greater and did change as a function of the applied load. The magnitude of the x directional force error is not alarming given the fact that the applied load was almost perpendicular.

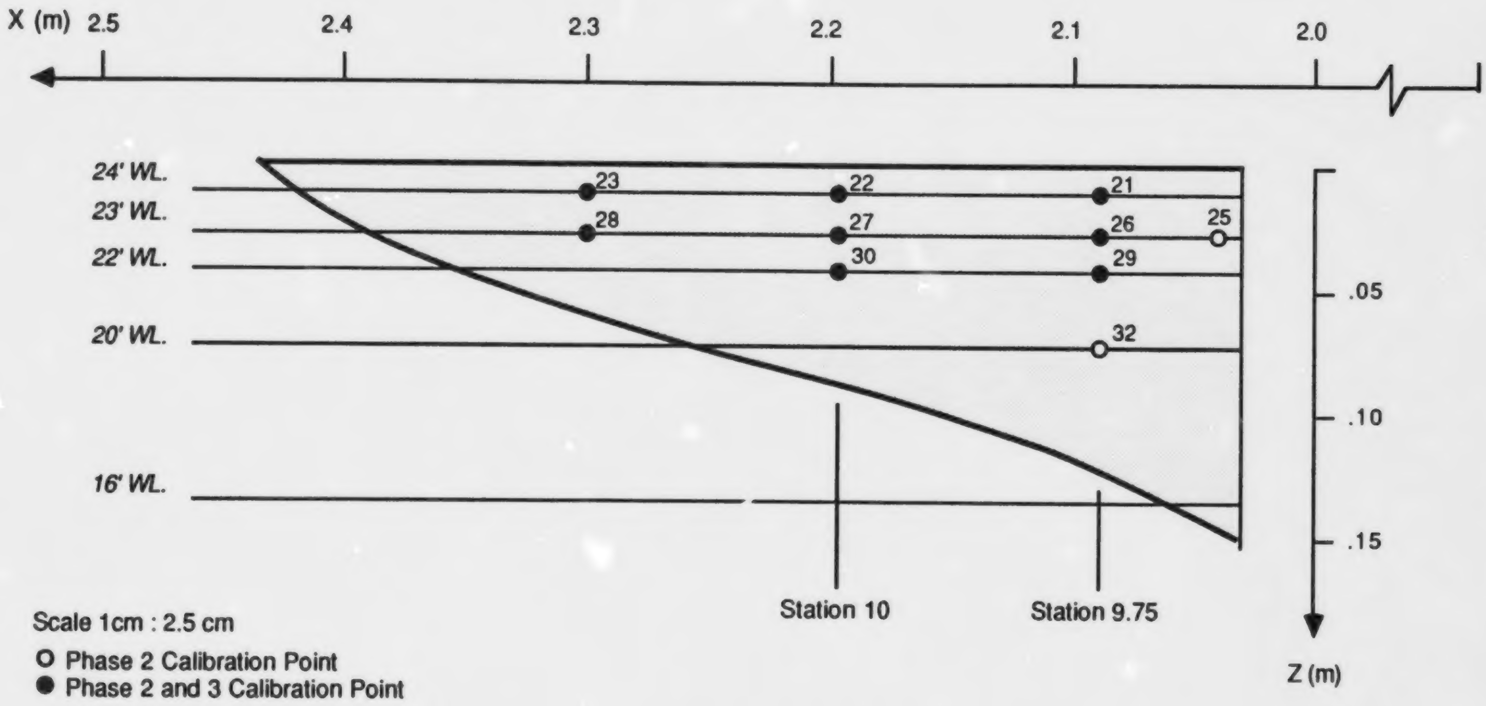

Figure 3.3 Segment 1 Calibration Points

TABLE 3.2

SEGMENT 1 - CALIBRATION ERRORS

	Error		Error		Error	
	Absolute	%	Absolute	%	Absolute	%
Parameter	Position 23		Position 22		Position 21	
Ftotal (N)	-0.3	-0.8	0.4	1.2	-0.5	-1.5
Fnormal (N)	-0.3	-0.8	0.4	1.5	-0.4	-1.4
Ffriction (N)	0.0	0.0	-0.5	-10.9	-0.5	-13.7
Fx (N)	0.1	1.0	0.8	9.0	-0.9	-9.0
Fy (N)	-0.7	-3	-1.3	-6	-5.9	-26
Fz (N)	0.3	2	1.5	8	5.3	29
Xposition (mm)	-14	-	-5	-	2	-
Zposition (mm)	4	-	9	-	20	-
Frict. dir. (deg)	1	-	17	-	241	-
Parameter	Position 28		Position 27		Position 26	
Ftotal (N)	0.4	1.3	1.0	3.3	0.0	0.0
Fnormal (N)	0.3	1.1	1.1	3.7	0.2	0.5
Ffriction (N)	0.3	4.1	-1.1	-25.8	-2.2	-33.0
Fx (N)	0.4	17	1.0	12	0.5	6
Fy (N)	0.4	2	-0.4	-2	-1.5	-7
Fz (N)	0.1	0	1.3	5	1.4	7
Xposition (mm)	-8	-	-5	-	0	-
Zposition (mm)	1	-	6	-	6	-
Frict. dir. (deg)	1	-	13	-	-4	-
Parameter			Position 30		Position 29	
Ftotal (N)			0.9	3.2	1.3	4.2
Fnormal (N)			1.1	3.5	1.4	4.6
Ffriction (N)			-0.7	-23.8	-0.8	-17.5
Fx (N)			1.0	15	1.5	15
Fy (N)			0.1	0	-0.2	-1
Fz (N)			0.9	4	1.4	7
Xposition (mm)			-4	-	3	-
Zposition (mm)			4	-	4	-
Frict. dir. (deg)			-6	-	14	-

Absolute Error = Measured Parameter - Applied Parameter
% Error = Absolute Error / Applied Parameter

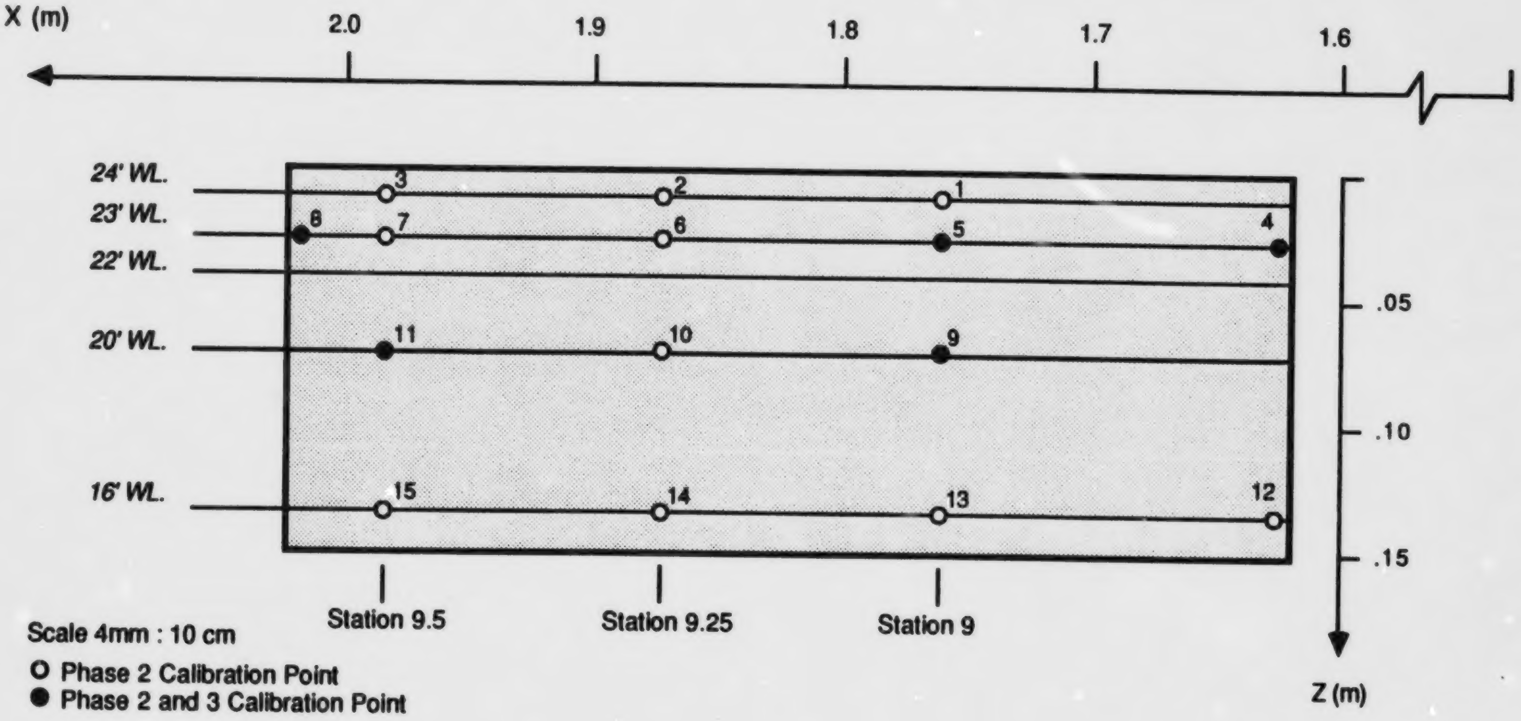

Figure 3.4 Segment 2 Calibration Points

TABLE 3.3

SEGMENT 2 - CALIBRATION ERRORS

		Error Absolute	%	Error Absolute	%	Error Absolute	%
Parameter		Position 8		Position 5		Position 4	
Ftotal	(N)	2.4	8.1	2.7	7.4	1.2	3.2
Fnormal	(N)	2.0	6.6	2.2	6.2	1.0	3.0
Ffriction	(N)	2.6	59.0	2.3	30.7	0.6	4.1
Fx	(N)	-1.2	-18.	0.2	4.	2.5	-227
Fy	(N)	-0.7	-4.	-2.6	-9.	-2.6	-9
Fz	(N)	4.2	20.	7.5	38.	4.6	20
Xposition	(mm)	-40	-	29	-	31	-
Zposition	(mm)	18	-	23	-	17	-
Frict. dir.	(deg)	-26	-	-33	-	-16	-

Parameter		Position 11		Position 9	
Ftotal	(N)	0.2	0.6	-3.0	-9.9
Fnormal	(N)	-0.2	-0.5	-3.1	-9.7
Ffriction	(N)	2.3	68.7	-0.8	-15.1
Fx	(N)	-2.5	-27.	-2.7	-32.
Fy	(N)	0.8	4.	-4.0	-16.
Fz	(N)	0.4	2.	1.7	12.
Xposition	(mm)	-15	-	35	-
Zposition	(mm)	0	-	-4	-
Frict. dir.	(deg)	340	-	-47	-

Absolute Error = Measured Parameter - Applied Parameter
% Error = Absolute Error / Applied Parameter

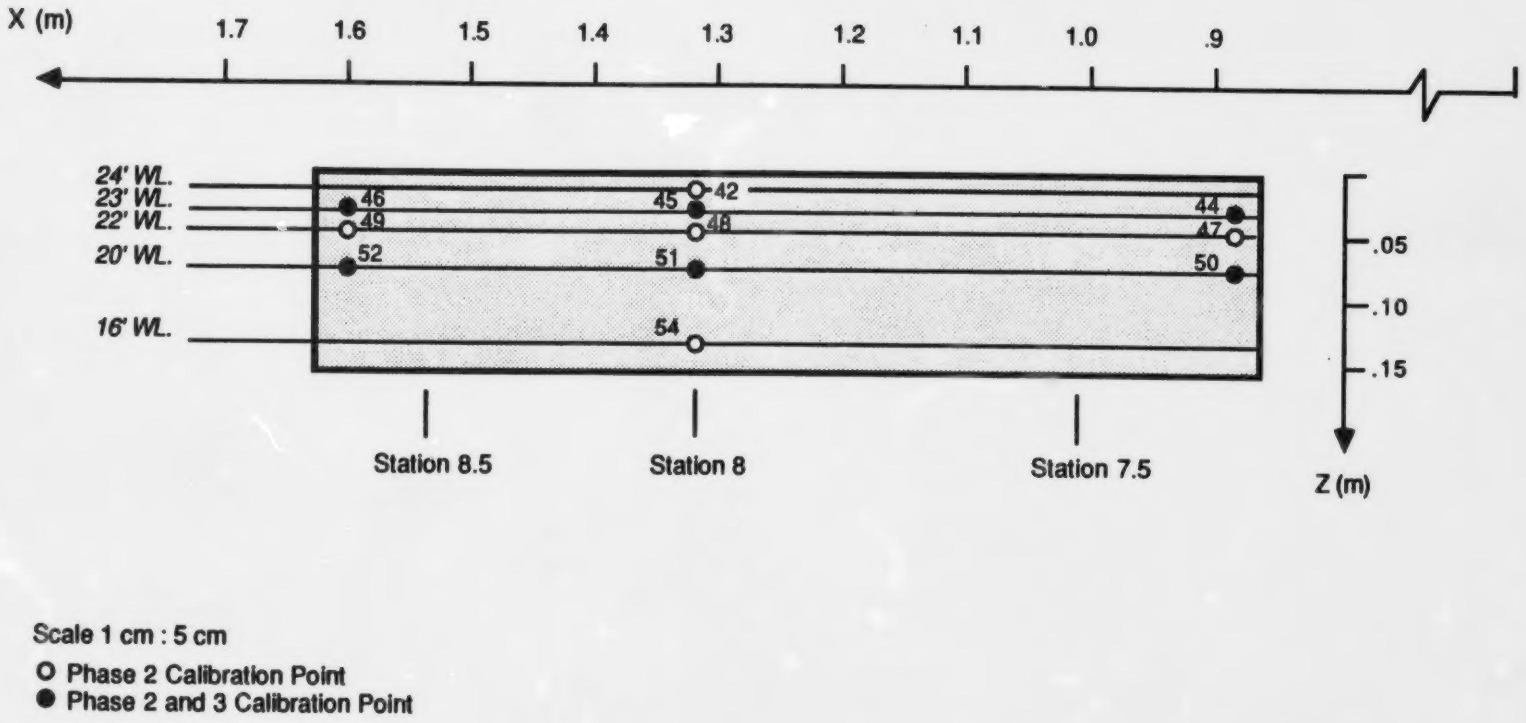

Figure 3.5 Segment 3 Calibration Points

TABLE 3.4

SEGMENT 3 - CALIBRATION ERRORS

		Error Absolute	%	Error Absolute	%	Error Absolute	%
Parameter		Position 46		Position 45		Position 44	
Ftotal	(N)	-9.2	-25.9	-7.8	-21.7	0.5	1.4
Fnormal	(N)	-11.4	-34.2	-9.4	-27.2	0.7	2.3
Ffriction	(N)	2.5	21.5	2.5	24.7	0.8	-8.7
Fx	(N)	0.7	-112.	9.6	-388.	3.6	-72
Fy	(N)	-13.1	-45.	-12.0	-97.	0.2	1
Fz	(N)	0.6	9.	2.8	19.	1.6	14
Xposition	(mm)	-7	-	-26	-	54	-
Zposition	(mm)	-28	-	5	-	24	-
Frict. dir.	(deg)	-38	-	-65	-	-20	-

		Error Absolute	%	Error Absolute	%	Error Absolute	%
Parameter		Position 52		Position 51		Position 50	
Ftotal	(N)	-8.7	-29.3	-8.9	-23.6	0.4	1.3
Fnormal	(N)	-9.1	-31.8	-9.7	-30.1	0.9	2.8
Ffriction	(N)	-0.4	-5.0	3.2	36.9	-1.6	-18.5
Fx	(N)	-0.5	-55.	8.5	-1079.	2.9	-55
Fy	(N)	-10.0	-40.	-13.0	-44.	0.5	2
Fz	(N)	-1.4	-9.	2.2	14.	0.8	7
Xposition	(mm)	8	-	-2	-	38	-
Zposition	(mm)	-28	-	12	-	18	-
Frict. dir.	(deg)	-40	-	-68	-	-14	-

Absolute Error = Measured Parameter - Applied Parameter
% Error = Absolute Error / Applied Parameter

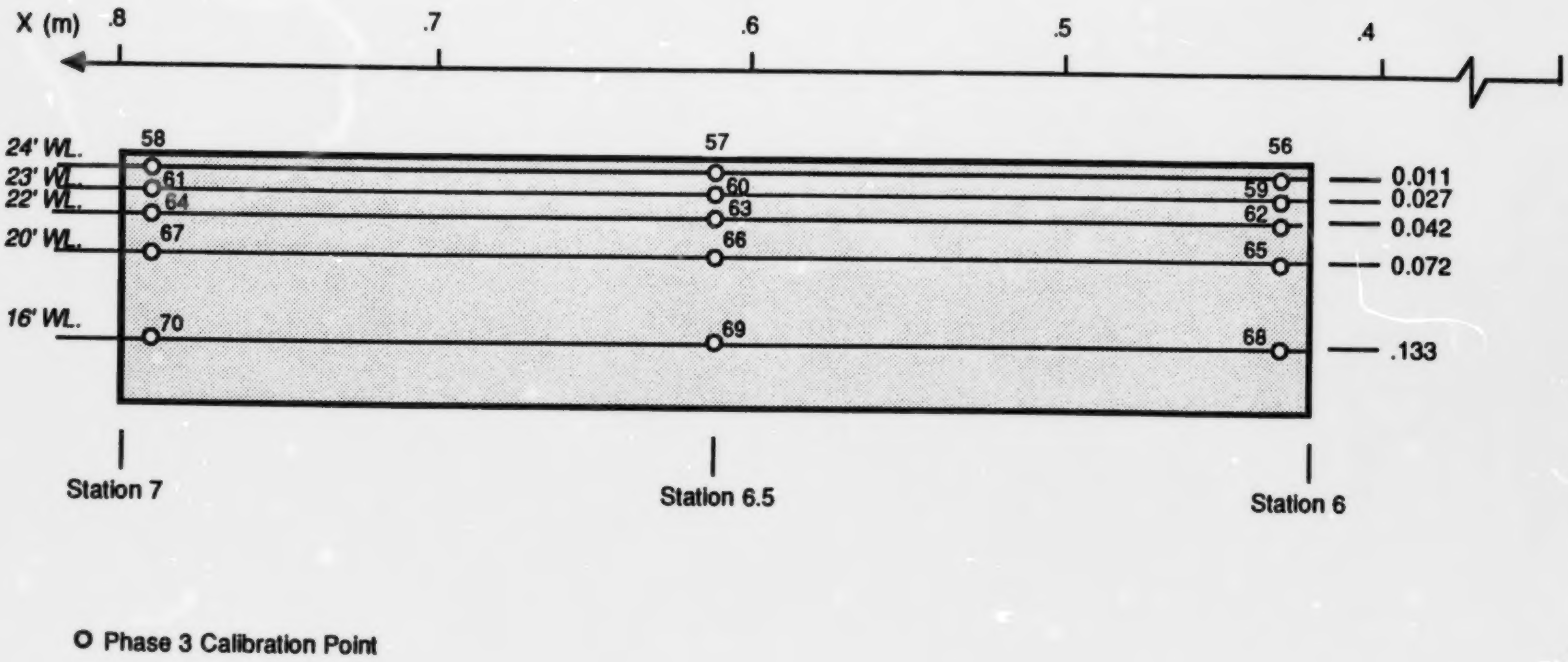

Figure 3.6 Segment 4 Calibration Points

TABLE 3.5

SEGMENT 4 - CALIBRATION ERRORS

		Error Absolute	%	Error Absolute	%	Error Absolute	%
Parameter		Position 58		Position 57		Position 56	
Ftotal	(N)	0.6	1.8	0.3	0.7	0.3	1.0
Fnormal	(N)	0.8	2.5	0.5	1.3	0.6	1.6
Ffriction	(N)	-1.0	-13.2	-1.0	-12.9	-1.2	-18.1
Fx	(N)	1.6	-30.	1.9	-35.	2.1	-51
Fy	(N)	0.8	2.	0.5	1.	0.6	2
Fz	(N)	0.2	2.	0.1	1.	-0.4	-4
Xposition	(mm)	-15	-	-8	-	0	-
Zposition	(mm)	7	-	9	-	6	-
Frict. dir.	(deg)	-9	-	-12	-	-16	-
Parameter		Position 61		Position 60		Position 59	
Ftotal	(N)	0.7	2.0	0.5	1.5	0.2	0.7
Fnormal	(N)	0.8	2.9	0.7	2.2	0.5	1.4
Ffriction	(N)	-0.6	-8.4	-1.1	-14.6	-1.4	-20.1
Fx	(N)	1.8	-71.	1.6	-29.	2.1	-48
Fy	(N)	0.7	2.	0.8	2.	0.5	1
Fz	(N)	0.4	4.	0.1	1.	-0.4	-4
Xposition	(mm)	-5	-	-5	-	-2	-
Zposition	(mm)	6	-	8	-	5	-
Frict. dir.	(deg)	-16	-	-9	-	-15	-
Parameter		Position 64		Position 63		Position 62	
Ftotal	(N)	0.4	1.0	0.4	1.2	0.2	0.4
Fnormal	(N)	0.7	1.8	0.5	1.6	0.4	1.1
Ffriction	(N)	-1.4	-17.4	-0.6	-7.7	-1.3	-14.4
Fx	(N)	1.7	-30.	1.5	-31.	2.2	-49
Fy	(N)	0.6	2.	0.5	2.	0.5	1
Fz	(N)	0.0	0.	0.4	4.	-0.4	-3
Xposition	(mm)	-8	-	-4	-	-1	-
Zposition	(mm)	5	-	7	-	4	-
Frict. dir.	(deg)	-7	-	-11	-	-13	-
Parameter		Position 67		Position 66		Position 65	
Ftotal	(N)	0.6	1.6	0.7	2.1	0.1	0.2
Fnormal	(N)	0.0	2.5	0.8	2.6	0.3	1.1
Ffriction	(N)	-1.1	-12.4	-0.8	-12.0	-1.0	-10.2
Fx	(N)	1.4	-28.	1.2	-25.	1.7	-47
Fy	(N)	0.9	3.	0.8	2.	0.4	1
Fz	(N)	-0.2	-2.	0.3	4.	-0.4	-3
Xposition	(mm)	-4	-	-2	-	1	-
Zposition	(mm)	5	-	7	-	4	-
Frict. dir.	(deg)	-5	-	-8	-	-9	-

Absolute Error = Measured Parameter - Applied Parameter
% Error = Absolute Error / Applied Parameter

4. PHOTOGRAMMETRIC CHECK

4.1 Background

An opportunity was taken during the contract to utilize a photogrammetric measuring technique to check the lines of the model against the lines plan.

The observation that the lines of the vessel in the area of the first and possibly second segments differed from the lines plan had been made in the earlier phases of the project. The coordinates of points on the surface of the segments are required for the calibration, and force and moment algorithms. These were taken from the lines plan.

A contract extension was negotiated to cover the measurement of the model lines at the fore end by photogrammetry. The work, contracted to Gary Robertson and Associates Inc. and reported in [8], provided an opportunity for TDC to evaluate the process.

4.2 Mensuration by Photogrammetry

The process comprised shooting ten stereoscopic images of the fore end of one half of the model only, using the frame station and waterline grids on the model as control references. After processing, two stereo models were produced. The drawings provided were a body plan, shear plan (profile), and a half breadth plan. These are reproduced from the report in Figures 4.1 to 4.3.

A comparison of the photogrammetrically measured hull angles with those read directly from the lines plan and those interpolated by the data acquisition program is shown in Table 4.1. This table shows the angles in degrees measured directly from the lines plan at the designated waterline. The angle at the same location as interpolated by the fairing routine in the data acquisition program using offsets lifted from the lines plan and the interpolated value using the same fairing program and the offsets measured by photogrammetry are also shown. There are three sources of error: measurement of angles from the lines plan, the offset values and the curve fitting (or fairing) routine.

As can be seen, difference 1 is a measure of the ability to measure the angle off the lines plan and the data acquisition system fairing routine. It shows that the biggest difference is 3.5° absolute. At a point of rapidly changing curvature, measurement of an angle from a reprinted lines plan is likely to have an error of ±2° or so. The biggest difference between the lines plan and the interpolated photogrammetric data (difference 2) was 6.7° at which point the data acquisition system and photogrammetric data using the same interpolation routine showed a 3° difference. Thus it is assumed that half of this difference is attributable to a difference in actual hull shape between the lines plan and the actual hull and half is attributable to lift-off errors or the interpolation program.

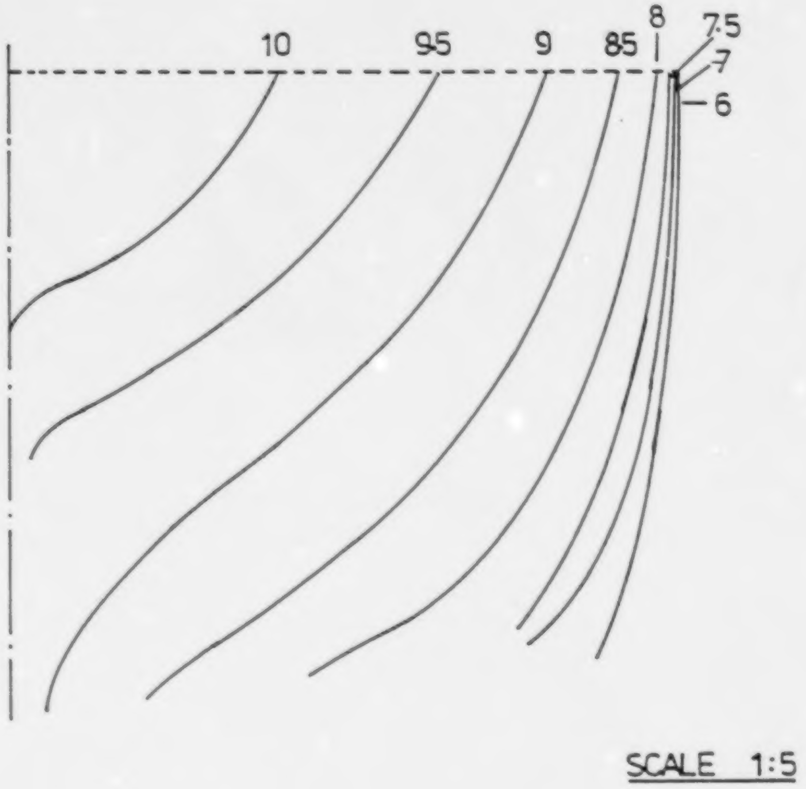

RADISSON BODY PLAN

FIGURE 4.1

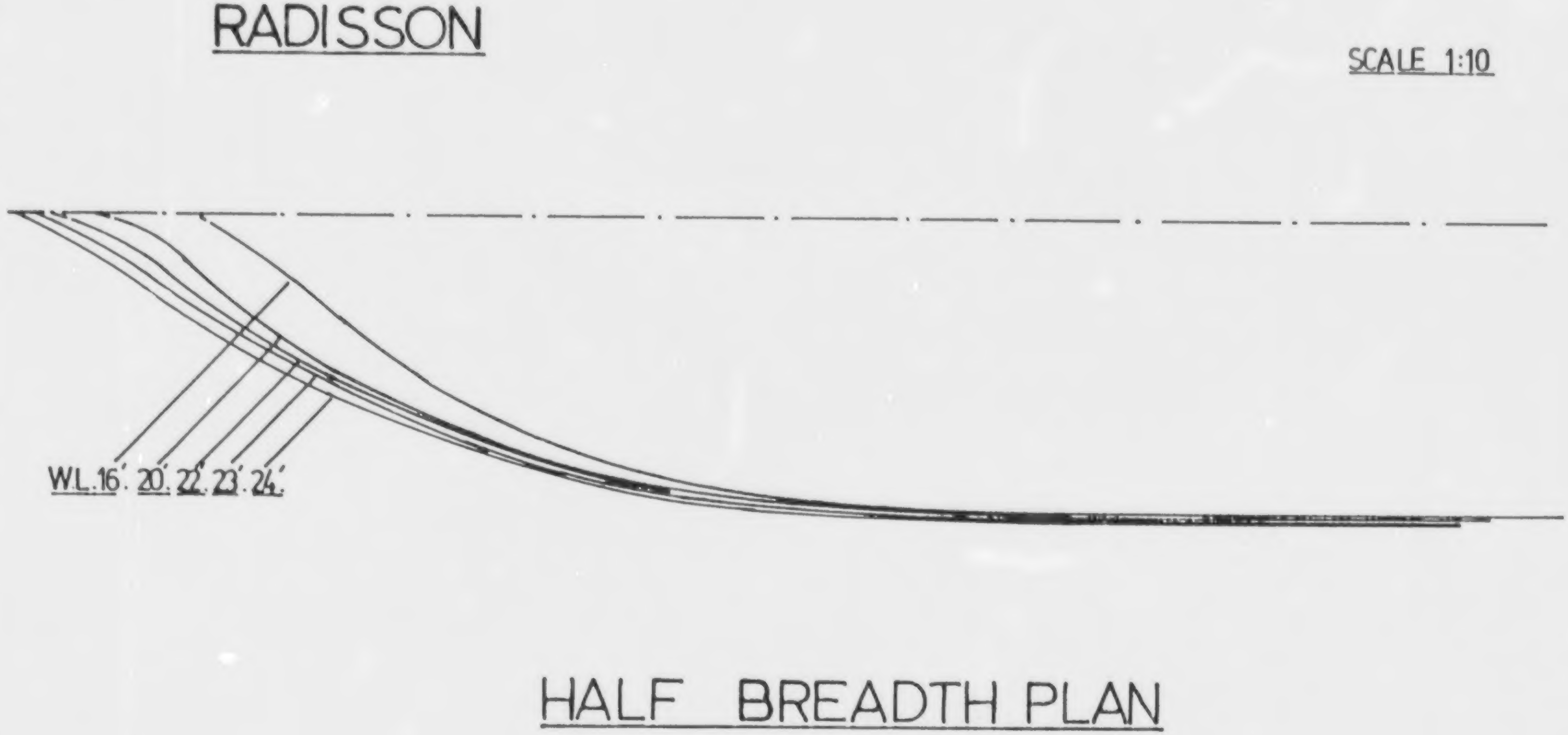

FIGURE 4.2

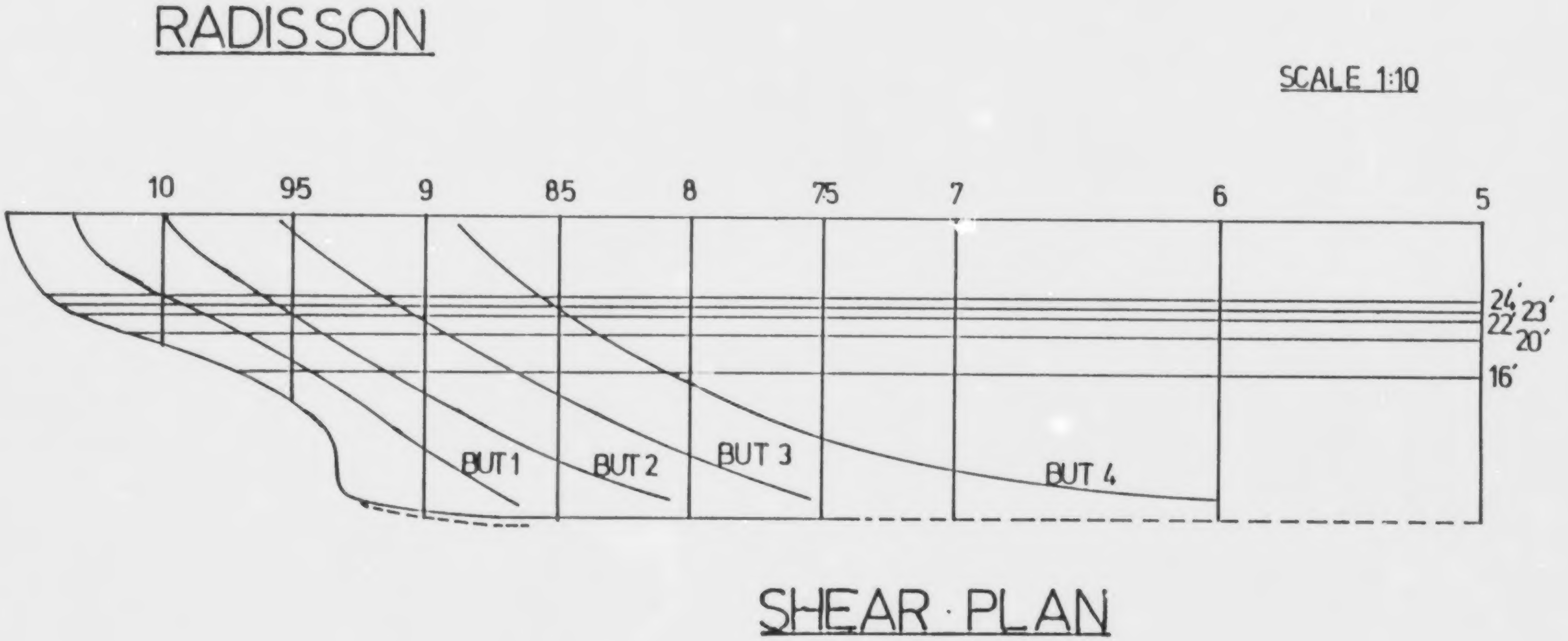
RADISSON
SCALE 1:10
BUT 1
BUT 2
BUT 3
BUT 4
SHEAR · PLAN

Figure 4.3

TABLE 4.1 HULL ANGLE COMPARISON (23' WATERLINE)

		WATERPLANE ANGLE (ALPHA)								
STN	X (m)	LINES PLAN	DA INTEF	ABS	DIFF (1)	PHOT	ABS 2	DIF (2)	ABS 3	DA/PH
6	0.44	0.0001	0.0001	0	0.0%	0.2	-0.19	0.00%	-0.199	0.00%
7	0.879	3.5	1.8	1.7	48.6%	1.8	1.7	48.6%	0	0.00%
7.5	1.099	5.5	4.7	0.8	14.5%	4.3	1.2	21.8%	0.4	8.51%
8	1.319	8.5	9	-0.5	-5.9%	8.2	0.299	3.5%	0.7999	8.89%
8.5	1.539	14.5	15.7	-1.2	-8.3%	16.6	-2.1	-14.5%	-0.9	-5.73%
9	1.759	23	22.8	0.19	0.9%	22.2	0.799	3.5%	0.6	2.63%
9.5	1.979	28	28.8	-0.8	-2.9%	29	-1	-3.6%	-0.199	-0.69%
10	2.198	29	31.8	-2.8	-9.7%	32.5	-3.5	-12.1%	-0.699	-2.20%
		FLARE ANGLE (BETA)								
ST/	X (m)	LINES PLAN	DA INTEF	ABS	DIFF (1)	PHOT	ABS 2	DIF (2)	ABS 3	DA/PH
6	0.44	2	5.2	-3.2	-160.0%	8.4	-6.4	-320.0%	-3.2	-61.54%
7	0.879	7	7.3	-0.3	-4.3%	9.9	-2.9	-41.4%	-2.6	-35.62%
7.5	1.099	10	10.6	-0.6	-6.0%	10.6	-0.6	-6.0%	0	0.00%
8	1.319	12.5	14	-1.5	-12.0%	11.3	1.2	9.6%	2.7	19.29%
8.5	1.539	22	23.2	-1.2	-5.5%	18.9	3.1	14.1%	4.3	18.53%
9	1.759	33	33.4	-0.4	-1.2%	29.8	3.2	9.7%	3.6	10.78%
9.5	1.979	43	44.4	-1.4	-3.3%	40.6	2.4	5.6%	3.8	8.56%
10	2.198	50	53.4	-3.4	-6.8%	55.4	-5.4	-10.8%	-2	-3.75%
KEY										
LINES PLAN		ANGLE MEASURED FROM DRAWING								
DA INTER		ANGLE INTERPOLATED USING OFFSETS AND FAIRING ROUTINE IN D A PROGRAM								
ABS		ANGLE DIFFERENCE BETWEEN LINES PLAN AND DA INTER								
DIFF 1		% DIFFERENCE BETWEEN ANGLES FROM LINES PLAN AND DA INTER								
PHOT		ANGLE FROM PHOTOGRAMMETRICALLY MEASURED OFFSETS & DA INTERPOLATOR								
ABS 2		ANGLE DIFFERENCE BETWEEN LINES PLAN AND PHOTGRAMMETRICALLY MEASURED ANGLE								
DIFF 2		% DIFFERENCE BETWEEN LINES PLAN AND PHOT								
ABS 3		ANGLE DIFFERENCE BETWEEN DA INTER AND PHOT								
DIFF 3		% DIFFERENCE IN ANGLE BETWEEN DA INTER AND PHOT								

4.3 Evaluation of Photogrammetry Technique

The photogrammetric process described in [8] occupied less than one day on site - required no special modifications to the model and was able to utilize the station and waterline markings as 'control' marks. The lines plans were delivered several weeks later but this was not due to the process so much as the availability of the expertise and the priority of the project.

The measurements are made to 1/1000th of a centimetre and are therefore more than sufficiently accurate for lines checking. In this case half of the model only was measured.

The drafted output in the referenced report is generally of poor quality. It is concluded that the use of the photogrammetric technique should endeavour to take the numeric output (or digital tapes) directly to the application.

In general, we believe the technique is very valuable and cost effective for 'lifting off' ship lines.

4.4 Use of Data

With only half of the model measured, any asymmetry in the actual model was not recorded.

The differences between the angles and dimensions that resulted from the measurement of the lines and those used in the algorithms were not as significant as the changes that might arise in aligning and balancing the segments in their recesses. Some of the time series records shown later clearly indicate small shifts in segment location after ice impact, with resulting changes in reduced parameters such as load location, friction direction.

The original intent was that the 'new' lines data would be used to modify the angles used in the algorithms that calculate normal and tangential forces and moments. In practice, the data arrived too late to change the data reduction algorithms, and in light of the comment in the previous paragraph, the new data was not used.

5. TEST DESCRIPTION

5.1 Test Matrix

The model was tested in ten ice sheets grown from water doped with 5 ppt concentration of urea. Four ice sheets had a target thickness of 30 mm, four had a target thickness of 45 mm, and two had a target thickness of 60 mm. Two types of tests were completed, icebreaking in a level unbroken ice sheet and channel widening of a broken ice channel. A total of 28 tests were performed, ten unbroken level ice sheet tests (or 'S') runs and one or two channel widening (or 'C') runs in each sheet (Figure 5.1).

A movable carriage was used to tow the model through the ice at a known constant velocity. The model was restrained from movement in all directions, with the restraint in the x direction (surge) being in the form of a force block capable of measuring total ship resistance.

The anticipated segment forces were the primary factors in determining the test matrix. The possibility of damage to some transducers from high loads restricted the testing range of ice thickness, ice strength and ship velocity. The initial test matrix targeted ice strength between 25 and 35 kPa for all runs. Upon completion of ice sheets 1 - 3 the target strength and thickness for the 1S4 ice sheet series was modified to better match the achieved values for ice sheets 2 and 3.

The actual and target values of ice properties are set out in Table 5.1 and Figures 5.2 to 5.5. Mean ice thickness was typically within 5 mm of the target, and had a standard deviation that varied from 3.3% at best to 10.4% (4.9 mm) in the worst case. Figures 5.2 and 5.3 show thickness data and distributions for a 'bad' and 'good' case respectively. The 'C' runs nearer the side of the tank show greater thickness scatter. The figures also show the thickness distribution along the tank.

Mean ice strength was typically within 5 kPa of the target at the beginning of the test. Figures 5.4 and 5.5 show the distribution of strength compared to the mean and at three locations along the tank for a 'good' and 'bad' set of data respectively. E/σ is related directly to σ in the model ice. Mean velocities were generally within .02 m/s of the target, limited only by the accuracy of the carriage control speed pre-setting device.

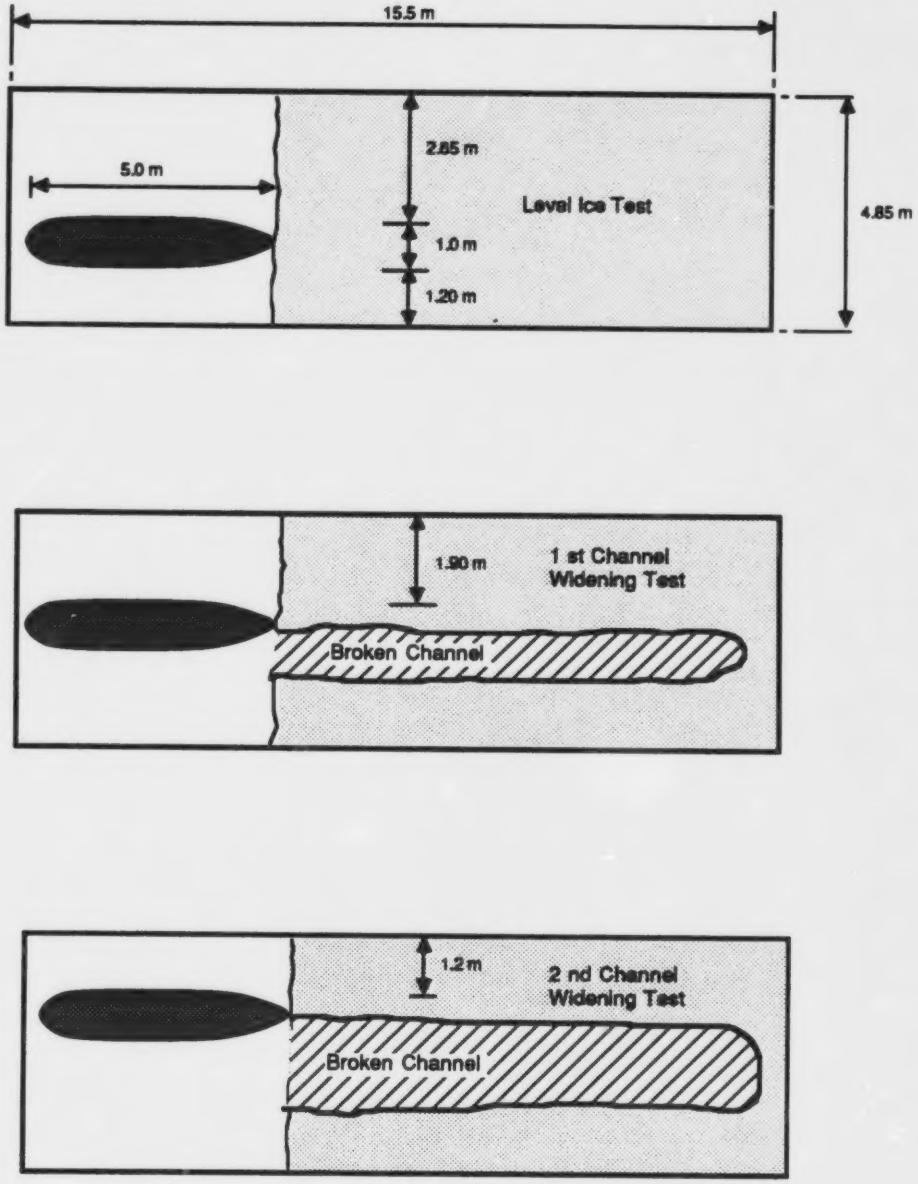

Figure 5.1 Ice Sheet Utilization

TABLE 5.1

TEST MATRIX

	Achieved					Target		
Test Number	Ice Thickness Av. (mm)	Ice Thickness S.D. (mm)	Ice Strength (kPa)	Velocity (m/s)	E/ Strength	Thickness (mm)	Strength (kPa)	Velocity (m/s)
1S1	36.0	1.5	30.4	.17	466	30	35	.15
1C1	35.5	2.6	(27.6)	.12			30	.10
1C2	37.5	2.6	24.8	.58			25	.60
1S2	31.7	2.5	48.2	.32	(800)	30	35	.30
1C3	31.4	2.5	(37.5)	.26			30	.20
1C4	34.7	2.9	26.9	.52			25	.50
1S3	34.0	1.3	49.8	.48	1161	30	35	.50
1C5	34.5	2.7	(32.5)	.32			30	.30
1C6	36.8	2.5	15.3	.46			25	.40
1S4	33.4	1.8	48.5	.17	(2300)	34	48	.15
1C7	33.8	2.3	(39.6)	.63			36	.60
1C8	35.2	3.2	29.5	.12			24	.10
2S1	46.8	2.0	31.3	.12	1271	45	35	.10
2C1	49.2	3.2	(27.4)	.15			30	.15
2C2	51.9	2.2	23.4	.32			25	.30
2S2	46.1	1.6	26.1	.24	2916	45	35	.20
2C3	48.2	3.6	(30.0)	.12			30	.10
2C4	50.0	3.2	33.9	.28			25	.25
2S3	45.8	2.2	32.1	.34	3270	45	35	.30
2C5	46.3	3.2	(33.3)	.29			30	.30
2C6	48.5	3.0	34.5	.23			25	.20
2S4	43.2	2.4	36.9	.30	2716	45	35	.30
2C7	45.7	3.9	(41.2)	.14			30	.10
2C8	47.2	4.9	45.4	.23			25	.20
3S1	63.4	3.0	31.7	.08	1511	60	35	.05
3C1	65.3	3.4	38.7	.11			30	.10
3S2	54.1	1.8	30.9	.19	2305	60	35	.15
3C2	56.3	2.4	42.4	.11			30	.08

Test Types : S = level ice Sheet C = Channel widening
( ) : Interpolated Data
S.D.: Standard Deviation

FIGURE 5.2
ICE THICKNESS DATA FOR 1S3 SERIES

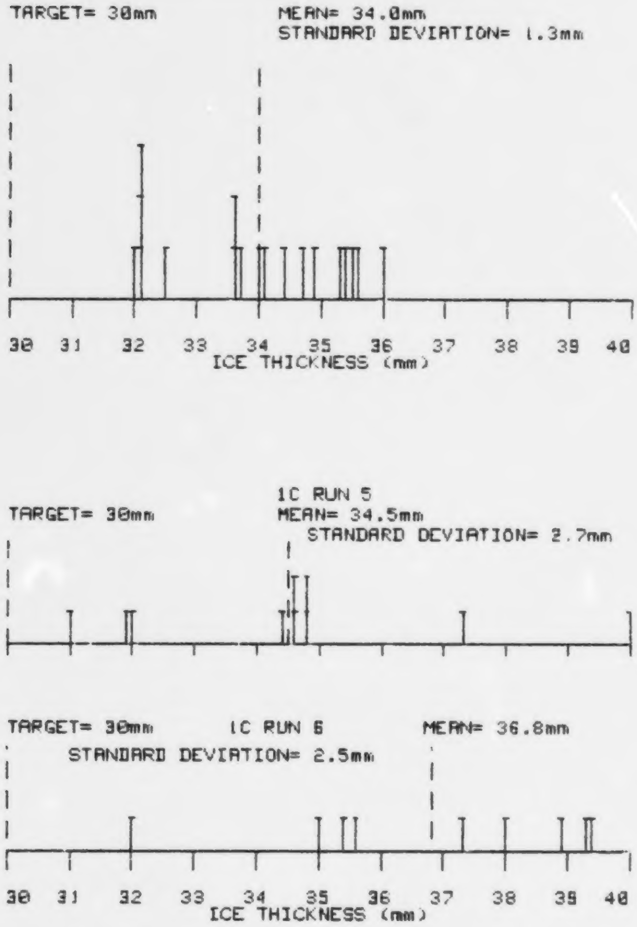

ICE THICKNESS VERSUS POSITION

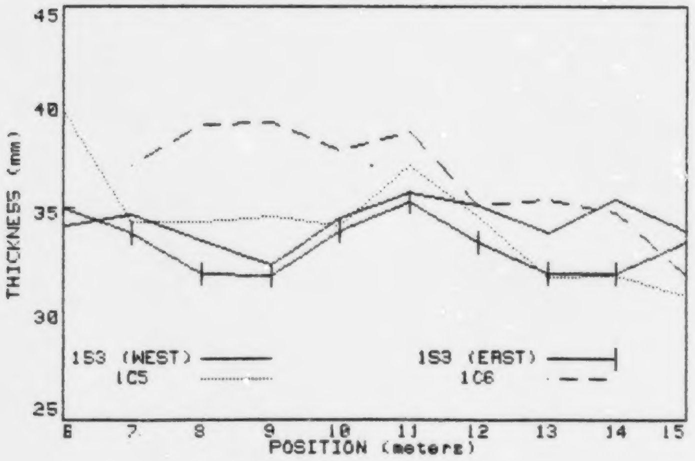

FIGURE 5.3
ICE THICKNESS DATA FOR 2S4 SERIES

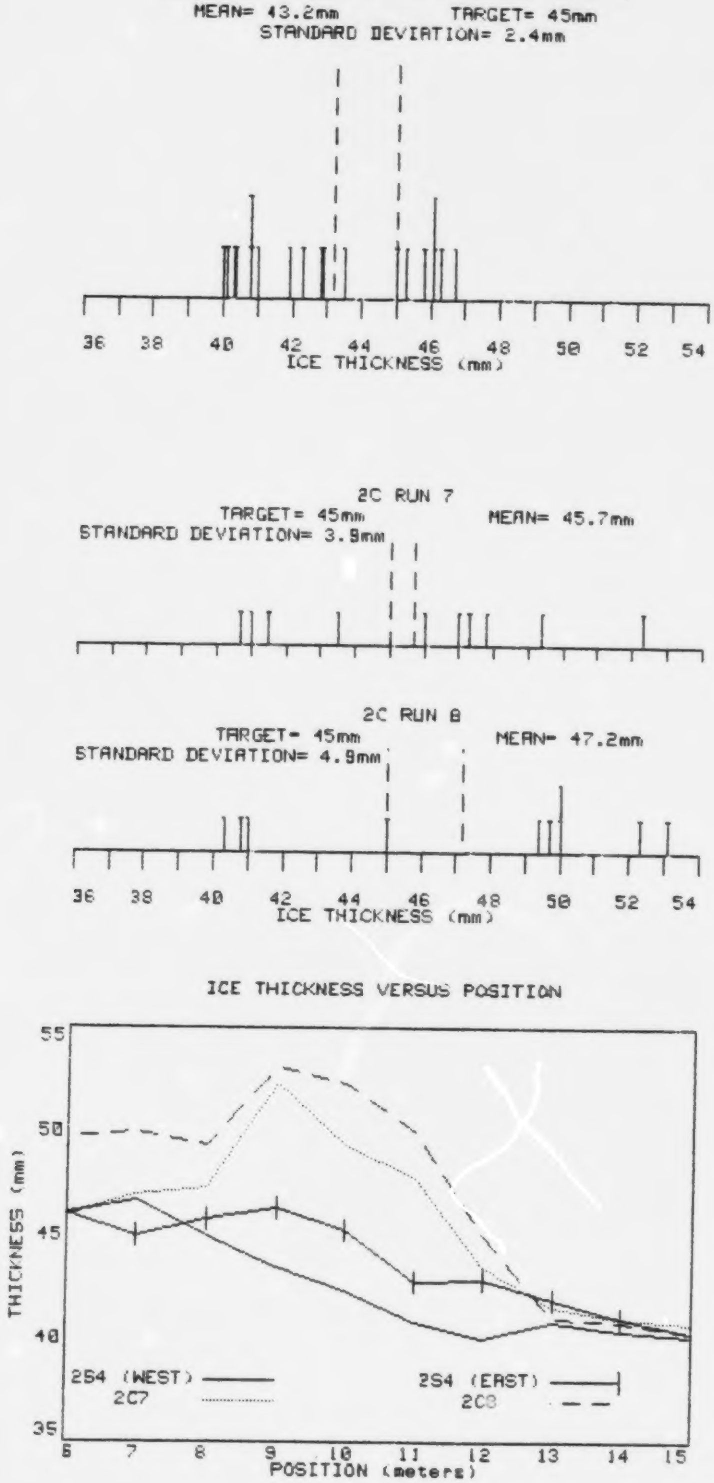

FIGURE 5.4

FLEXURAL STRENGTH DATA FOR S2S SERIES

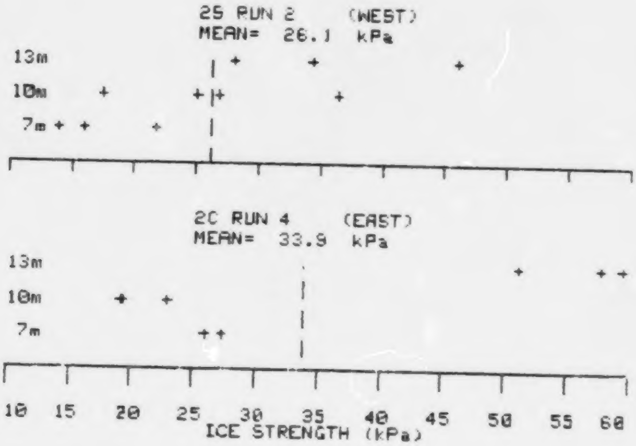

FIGURE 5.5

FLEXURAL STRENGTH DATA FOR 2S4 SERIES

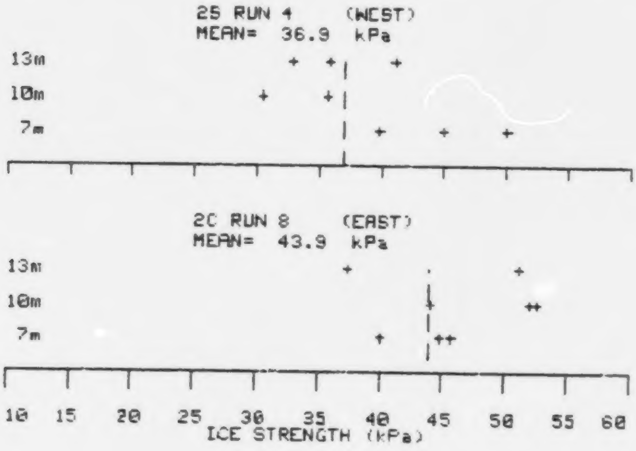

5.2 Test Procedures

Standard procedures at Fleet Technology were used to grow and perform ice properties tests. A complete description of these can be found in [2]. After growing an ice sheet to the desired thickness, the sheet was allowed to 'temper' by thawing at a temperature just above freezing. During this thaw period, flexural strength tests on the ice were performed once an hour to monitor the 'tempering' process by applying a load by hand to a small cantilever beam cut in the ice sheet. Preparations to the model prior to testing included attachment to the towing carriage, checking the model trim and position, and setting the desired preload on all segments. The segments were also checked for response to loads applied by hand.

When the ice sheet had attained a strength of between 50 and 70 kPa, a test of the elastic modulus was performed. Two ice sheets thawed quicker than anticipated and time did not permit the modulus test on these occasions.. When the ice reached the target flexural strength, the first 'S' run was completed. At the conclusion of the 'S' run, the model was backed up and repositioned for the next run. A comprehensive set of flexural strength measurements (typically 6 to 9) were taken along the side of the intact sheet closest to the ship track. Ice thickness measurements were taken at every meter of run length on both sides of the ship track.

After completing the above (about 15 to 30 minutes later), the first 'C' run was made. The model was again backed up and repositioned. Ice thickness measurements were taken along the intact side of the ship track at one meter intervals. A second 'C' run was possible in all cases except the two thickest ice sheets where an insufficient amount of intact ice remained. After the last run another comprehensive set of flexural strength measurements and ice thickness measurements were completed.

5.3 Data Acquisition System

The data acquisition system consisted of 38 channels of strain gauge load transducers and their associated signal conditioning, (37 segment load cells and one carriage load cell), one speed transducer, 39 channels of low pass filters, analogue to digital converters, and a Hewlett Packard computer with peripherals. Figure 5.6 illustrates the data acquisition system used. A digitizing rate of 10 Hz was used to acquire data with all frequencies above 1 Hz filtered out. Results from Phase II tests indicated these rates to be sufficient. For additional information regarding transducer design and specifications, and the acquisition system see [1].

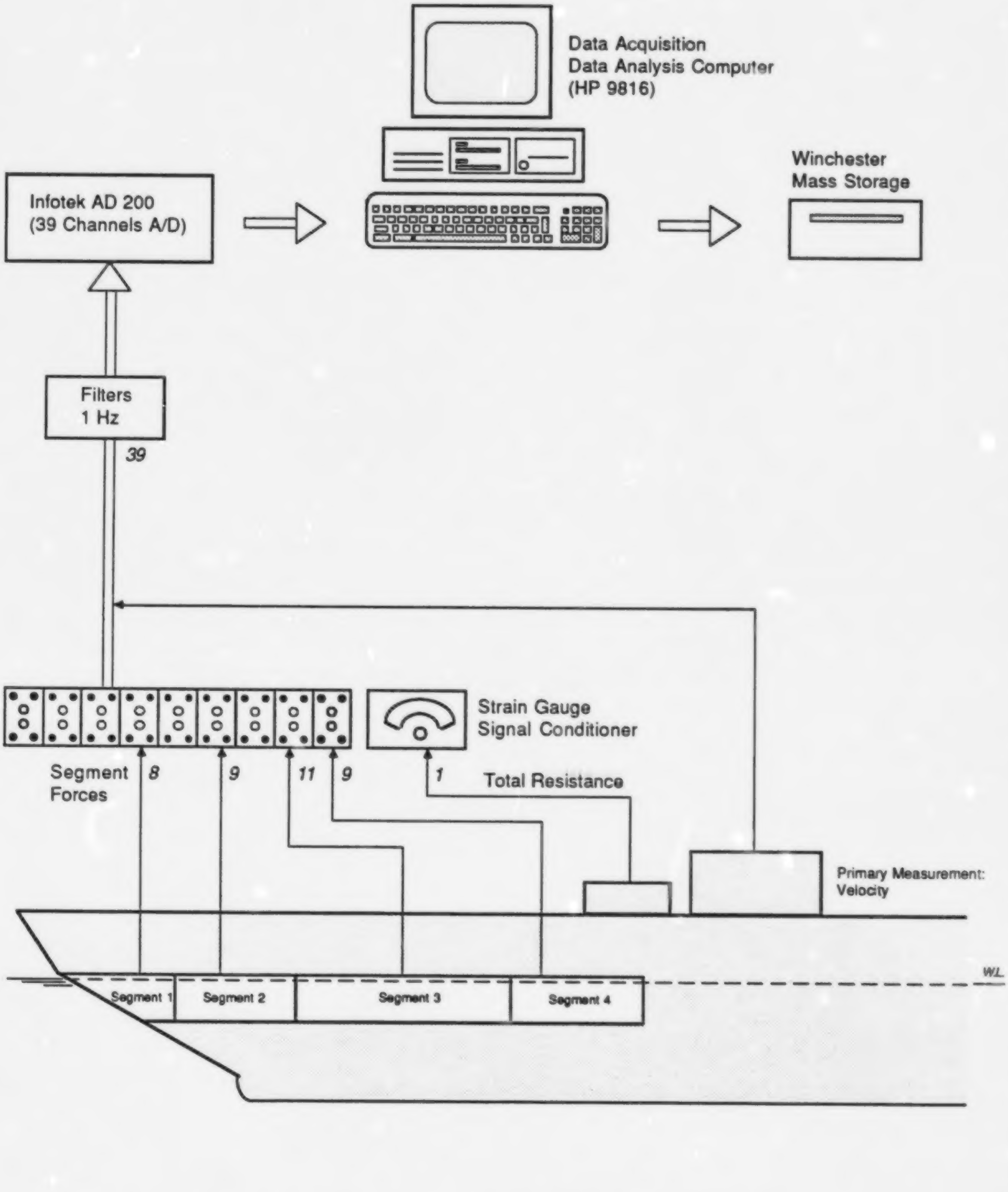

Figure 5.6 Segmented Model Instrumentation

5.4 Quality of Measurements

As might be expected with a complex set of 38 highly load sensitive instrumentation in a difficult and hostile environment, a number of transducer failures occurred. The low load range of some transducers, combined with a test matrix as wide in range as possible, produced some instances of invalid and/or questionable results. Unfortunately, the compression resistance transducer measuring force in the 'x direction' on Segment 4 sustained damage at the outset and was rendered inoperable. The effect of the loss of this channel on segment normal force is quite negligible as the segment's outer surface is flat and parallel to the x direction. Segment 4 friction force and resistance could not be measured directly, therefore but is estimated later using normal force and friction coefficient.

Two vertical transducers on Segment 4 failed after 70% of the tests were completed. Again, and for a similar reason, the effect upon measured segment normal forces is very slight. A sensitivity analysis on the effect of missing data upon the calculated normal forces for Segment 4 was run. A candidate test was selected where the forces seen on the transducers were similar to those seen when the two vertical transducers gave no data. The test (2S3) was analyzed, in the normal fashion using all transducers, and then with loads for the two vertical transducers set equal to zero. The effect of setting the loads for V41C and V42C to zero was to increase the calculated normal force by 1.5% and to decrease the calculated peak loads by 1.0%.

Two vertical pre-tensioning load rings (V25t and V35t) did not function for the first test series. The lack of data for these transducers has very little effect upon all the calculated results for Segments 2 and 3. This is due to the fact that the ring transducers carry much less load than the very stiff compression transducers. Examination of the results of tests 1S3, 1C5 and 1C6, which are comparable to the tests where V25t and V35t did not function (1S1, 1C1, 1C2), showed that these two transducers carry less than 5% of the vertical loads. In fact, the two transducers did not see even as much as 0.6 Newtons average load for tests 1S3, 1C5 or 1C6. It therefore seems reasonable to assume the loss of data for tests 1S1, 1C1 and 1C2 has had little effect upon the calculated results.

The combination of high loads coupled with a very limited range of preload that could be applied to Segment 1 caused some transducers to unload during testing. In these cases, the data is of questionable value without additional data manipulation. The likelihood is that reasonably reliable techniques could be formulated to calculate the degree of unloading if it were deemed to be cost effective. Table 5.2 summarizes questionable or missing data for the tests.

TABLE 5.2

Summary of Questionable Transducers

Test	Comments (see code below)	
1S1	X - V25t, V35t, FBx,	Q - R41c, R42t
1C1	X - V25t, V35t, FBx,	Q - R41c, R42t
1C2	X - V25t, V35t, FBx,	Q - R41c, R42t
1S2	X - R41c, R42t	
1C3	X - R41c, R42t	
1C4	X - R41c, R42t	
1S3	X - R41c, R42t	
1C5	X - R41c, R42t	Q - SEG4 (0 drift)
1C6	X - R41c, R42t	Q - SEG4 (0 drift), SEG1 (O - HV1t)
1S4	X - R41c, R42t, V41c, V42c	
1C7	X - R41c, R42t, V41c, V42c	Q - SEG1 (O - HV1t)
1C8	X - R41c, R42t, V41c, V42c	
2S1	X - R41c, R42t	
2C1	X - R41c, R42t	
2C2	X - R41c, R42t	
2S2	X - R41c, R42t, FBx	Q - SEG1 (L - V11c)
2C3	X - R41c, R42t	
2C4	X - R41c, R42t	
2S3	X - R41c, R42t	Q - SEG1 (L - V11c)
2C5	X - R41c, R42t	
2C6	X - R41c, R42t	
2S4	X - R41c, R42t, V41c, V42c	Q - SEG1 (O - H11c, L - V11c)
2C7	X - R41c, R42t, V41c, V42c	
2C8	X - R41c, R42t, V41c, V42c	
3S1	X - R41c, R42t	Q - SEG1 (L - V11c)
3C1	X - R41c, R42t	
3S2	X - R41c, R42t, V41c, V42c	Q - SEG1 (L - V11c)
3C2	X - R41c, R42t, V41c, V42c	

CODE :
X - Invalid data or did not function
O - Offset, possible segment shift
Q - Questionable data
L - Lift off (loading lost)

6. RESULTS PRESENTATION

6.1 Approach

Two types of data are presented: raw data from all transducers and calculated segment data from calculation algorithms. The results are presented in two forms:

(1) mean values over a selected time period.

(2) mean values occurring at normal force maxima (peaks) over a selected time period.

6.2 Transducer Time History Data

Time history data were obtained for all transducers. These data were stored on computer media in a 'raw' digitized form and served as a starting point for further data analysis. Figure 6.1 shows a typical output of transducer data from Segment 1. The 'zero' value on any transducer is defined as the mean value for the first ten seconds of digitized data. Statistics for a user selected interval are presented in the output as well. Mean values from this interval are only used for two data sets; velocity and total resistance. Mean values for all other transducers only serve as an indicator of load levels and data validity.

FIGURE 6.1

TYPICAL RAW DATA OUTPUT

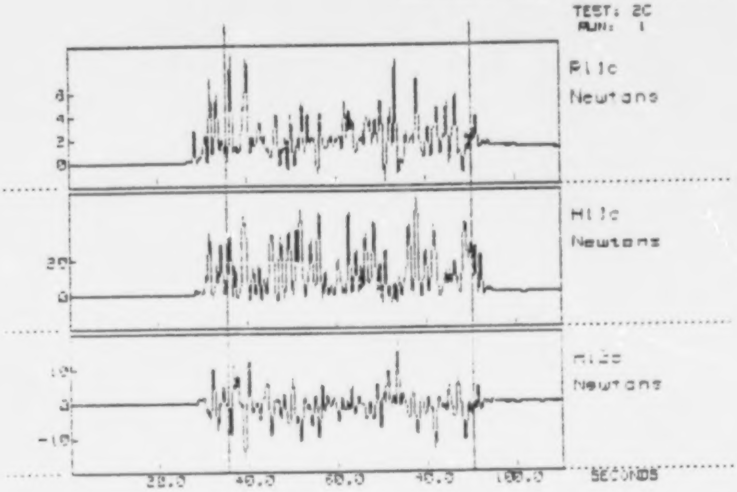

Test/Run: 2C1
Digitizing Rate: 10 Hz/Channel

Date Digitized: 18 Jan 1989
Filter Frequency: 1 Hz

Statistics For Interval from 35.30 to 89.90 Seconds

CHANNEL	MINIMUM	MAXIMUM	MEAN VALUE	STANDARD DEV
R11c	-1.74	9.32	2.16	1.76102
H11c	-5.22	57.62	13.76	13.58497
H12c	-16.41	17.62	-.84	4.59824

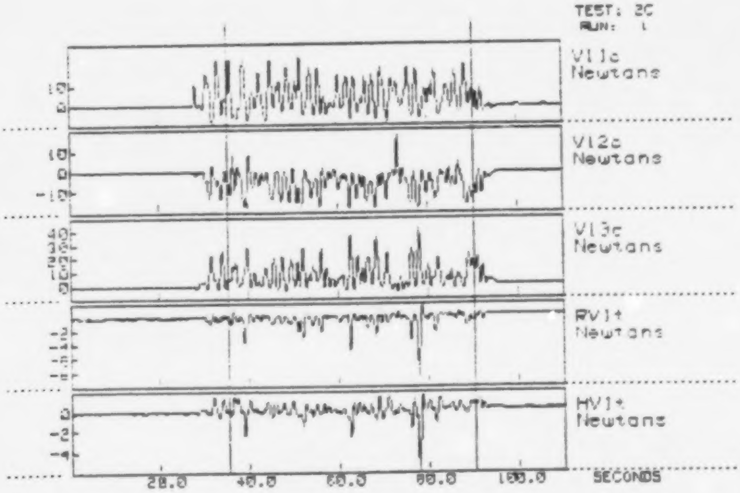

Test/Run: 2C1
Digitizing Rate: 10 Hz/Channel

Date Digitized: 18 Jan 1989
Filter Frequency: 1 Hz

Statistics For Interval from 35.30 to 89.90 Seconds

CHANNEL	MINIMUM	MAXIMUM	MEAN VALUE	STANDARD DEV
V11c	-8.74	24.74	4.73	7.58480
V12c	-18.30	17.39	-5.88	5.61349
V13c	-4.27	41.33	7.90	8.80931
RV1t	-8.55	1.69	-.32	1.08349
HV1t	-5.86	1.72	.13	.78737

6.3 Data Reduction Techniques

The following is a brief general description of the data reduction techniques employed. For a complete discussion of the algorithms used the reader is referred to [2]. Each segment is thought of as an individual transducer receiving a point load at some position on the surface of the segment. This is an over-simplification of the load distribution on the segment, but is valid for use in determining the total and normal force acting upon the segment.

Given the output from individual transducers, the sum of the forces in the x, y and z directions and the sum of the moments applied to the segment in those directions can be calculated. This information, combined with the transducer locations and knowledge of the hull lines allows one to iteratively calculate the applied normal force and the position of the load. The friction coefficient and friction vector can then be determined. At times in the iteration process the y coordinate on the hull and the hull angles at a given x, y and z point are required. A cubic spline algorithm was used to interpolate between measured x, y, z coordinates to find these values.

Given time history data from a segment's transducer, it is possible to calculate time history data of normal force, x position, z position, friction force and friction direction. It is not possible however to calculate these values for every point in time. Often when forces and moments are low and close to the resolution limits of the instrumentation, the calculated values are not valid. In order to limit erroneous results, calculations were performed only when the total force on a segment exceeded a threshold value. Also, at times even when the total force exceeded the threshold value, calculations placed the load position off the segment face, possibly due to cumulative errors, division by zero, etc. These results were also discarded.

6.4 Segment Normal Force

Using the approach described in Section 6.3, normal force time histories were created for each segment and each test. Figure 6.2 illustrates the normal force time histories obtained for a selected test. The time histories are characterized by high force peaks of relatively short duration corresponding to the loading and failure of ice cusps.

The mean normal force during a user selected interval was calculated for each segment as the arithmetic mean of all data points within the interval. Each data point is the instantaneous normal force at an instant of time, with components above the 1Hz cut-off frequency filtered out. For any test, the interval selected for each segment was identical so that data comparisons could be made. Typically the determining factors in setting an interval were the observance of steady-state ice loads on all four segments. Table 6.1 summarizes the mean normal force on each segment and the mean normal force per unit length on each segment.

The normal force plots show frequent peak loads followed by periods of very small forces. The force peaks occur immediately prior to ice cusp failure. As an aid for further analysis, a peak selection algorithm was written to automatically find the occurrence of normal force peaks. Peak values over a set time interval were found using the following peak definition criteria:

- minimum peak value
- minimum time interval between peaks
- hysteresis - minimum value from peak to trough

Figure 6.3 presents a summary output sheet of peaks selected for a representative test. Included on the summary sheet is a list of the peak definition criteria, the selected peaks, and statistics for the peaks and other calculated parameters occurring at the peaks.

A number of observations can be made regarding the peak normal forces. The magnitude of the peaks typically increases from Segments 1 to 4. The frequency of peaks typically decreases from Segments 1 to 4. Segments 1 and 2 often show very similar time history plots, while Segments 3 and 4 differ markedly from one another and from Segments 1 and 2. Table 6.2 summarizes the mean values of the normal force peaks and the mean peak frequency for all segments. Load position and friction data occurring during normal force peaks are discussed in Sections 6.6 and 6.7.

Table 6.3 shows the ratio of mean normal force to peak normal force for each segment for each test. The following can be observed:

- The ratio mean/peak drops significantly and consistently from Segment 1 to Segment 4, in the thinner ice, while in the thicker ice, this trend is less obvious.

- The thinner the ice, the higher the ratio.

- The average ratio is consistent for unbroken ice and channel runs, and the standard deviation is small.

FIGURE 6.2

CALCULATED SEGMENT NORMAL FORCES

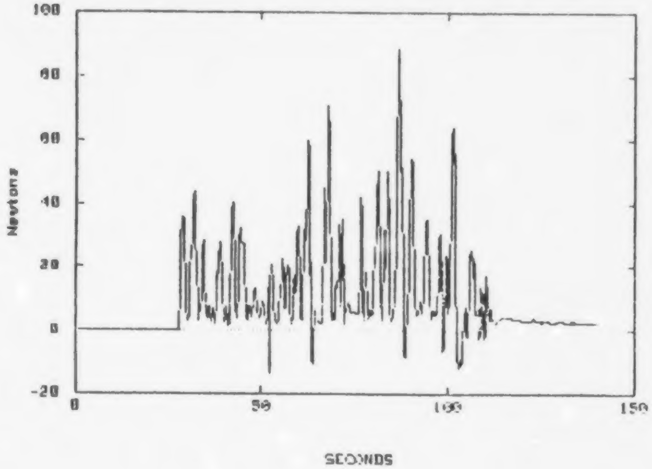
2C RUN 3 SEGMENT 1 20 Jan 1989
NORMAL FORCE

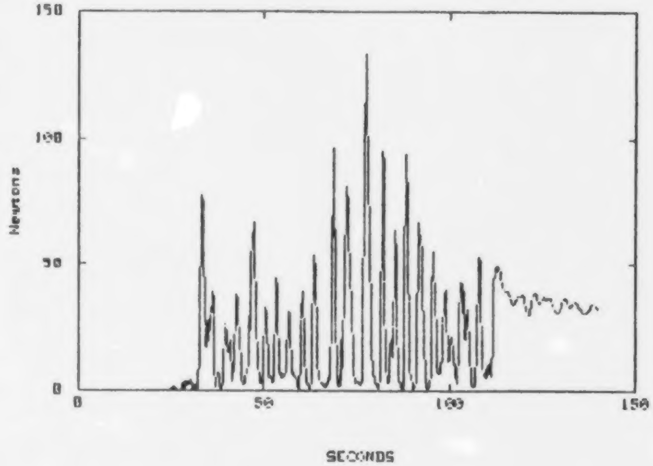
2C RUN 3 SEGMENT 2 20 Jan 1989
NORMAL FORCE

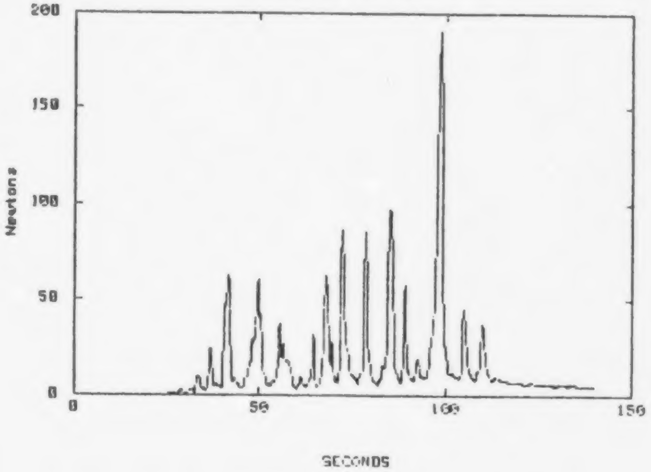
2C RUN 3 SEGMENT 3 20 Jan 1989
NORMAL FORCE

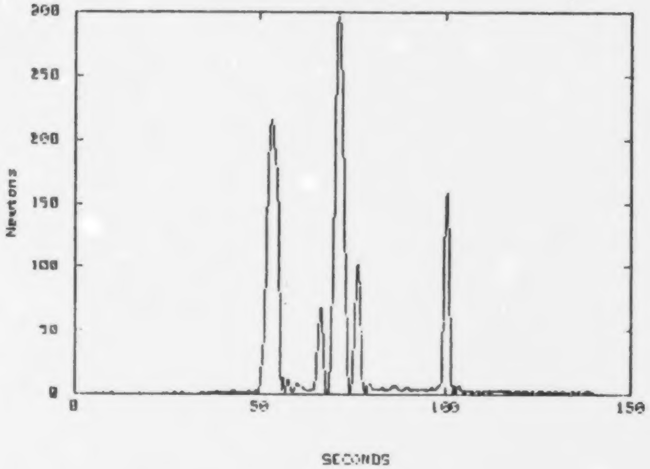
2C RUN 3 SEGMENT 4 20 Jan 1989
NORMAL FORCE

Table 6.1

Mean Normal Force Results

Test	[----Mean Normal Force-----]				[-Mean Force / Unit Length-]			
	Seg1 (N)	Seg2 (N)	Seg3 (N)	Seg4 (N)	Seg1 (N/m)	Seg2 (N/m)	Seg3 (N/m)	Seg4 (N/m)
1S1	16.6	13.2	20.7	6.6	44.3	29.9	27.3	15.1
1C1	11.4	11.8	13.9	6.2	30.4	26.7	18.4	14.2
1C2	18.1	24.1	25.1	20.4	48.3	54.5	33.2	46.8
1S2	10.0	13.2	10.6	9.7	26.7	29.9	14.0	22.2
1C3	7.7	9.5	9.2	4.4	20.5	21.5	12.2	10.1
1C4	10.6	19.1	15.1	12.4	28.3	43.2	19.9	28.4
1S3	22.0	19.8	16.9	22.7	58.7	44.8	22.3	52.1
1C5	15.3	14.0	17.2	12.8	40.8	31.7	22.7	29.4
1C6	*18.1	16.8	18.0	*16.2	*48.3	38.0	23.8	*37.2
1S4	10.4	10.7	13.0	28.2	27.7	24.2	17.2	64.7
1C7	*14.4	27.7	21.0	26.2	*38.4	62.7	27.7	60.1
1C8	8.0	9.9	13.5	21.7	21.3	22.4	17.8	49.8
2S1	6.5	11.7	11.0	46.6	17.3	26.5	14.5	106.9
2C1	15.1	15.8	10.9	35.3	40.3	35.7	14.4	81.0
2C2	18.5	20.8	16.5	17.4	49.3	47.1	21.8	39.9
2S2	*11.1	20.2	24.3	32.4	*29.6	45.7	32.1	74.3
2C3	17.5	24.1	23.8	38.6	46.7	54.5	31.4	88.5
2C4	27.9	42.3	27.8	12.1	74.4	95.7	36.7	27.8
2S3	* 7.2	29.9	40.9	13.5	*19.2	67.6	54.0	31.0
2C5	25.2	27.6	45.8	12.4	67.2	62.4	60.5	28.4
2C6	24.6	25.5	46.9	29.4	65.6	57.7	62.0	67.4
2S4	* 8.7	20.0	21.5	31.3	*23.2	45.2	28.4	71.8
2C7	15.6	20.5	14.9	8.4	41.6	46.3	19.7	19.3
2C8	25.4	24.3	25.9	60.3	67.7	55.0	34.2	138.3
3S1	*22.2	17.6	35.2	73.2	*59.2	39.8	46.5	167.9
3C1	31.3	34.4	41.4	22.7	83.5	77.8	54.7	52.1
3S2	*17.9	39.5	45.2	72.8	*47.7	89.3	59.7	167.0
3C2	26.8	34.8	25.7	46.1	71.5	78.7	33.9	105.7

* Questionable Data

FIGURE 6.3 - NORMAL FORCE PEAKS

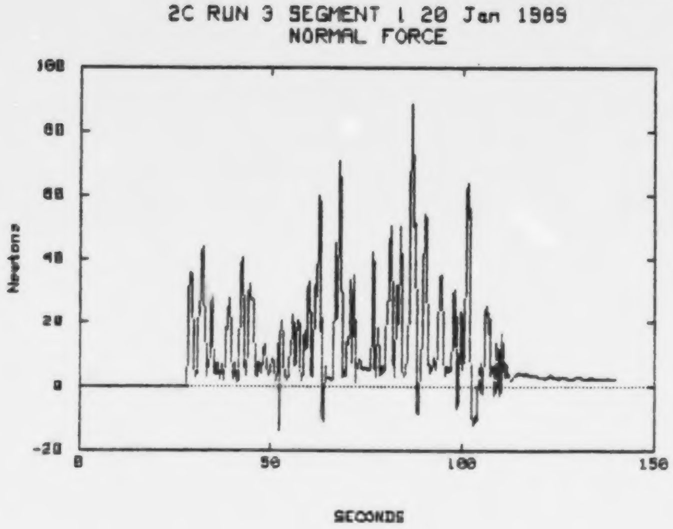

```
FILE NAME   2C3   Selected Peaks
Hysteresis: 5 N     Min. Peak Value: 15 N      Min. Delta t: 1 sec.

 TIME    NORMAL    LOCATION(M)          ANGLES        FRICT.   FRICT.    FRICT. ANGLE
         FORCE     X        Z       ALPHA      BETA   FORCE    COEFF.    PROJ
 42.40    40.4   2.214    .045      29.1      52.6    18.4      .46     -113.
 44.30    32.0   0.000   -.010    -180.0    -180.0     0.0     0.00     -180.
 52.70    20.8   2.315    .044      16.4      18.0     4.7      .23      156.
 55.70    22.7   2.110    .052      33.7      54.3     1.9      .08      -71.
 57.30    20.6   0.000   -.010    -180.0    -180.0     0.0     0.00     -180.
 59.80    33.0   2.289    .044      19.7      28.1     8.4      .25     -158.
 62.60    59.7   2.255    .056      28.8      34.3    23.4      .39     -145.
 67.90    70.4   2.123    .054      34.0      54.7     2.4      .03      -62.
 71.70    35.0   2.061    .051      31.5      52.1     2.2      .06      -26.
 76.80    42.1   2.254    .017      31.0      51.4    10.4      .25      -83.
 78.00    18.3   2.171    .055      33.4      55.7     5.1      .28      -76.
 81.30    49.9   2.272    .052      25.8      16.3    21.4      .43      150.
 84.00    49.8   2.107    .056      33.6      54.3     4.1      .08      -81.
 86.80    88.7   2.299    .039      18.4      35.0    33.7      .38     -130.
 90.40    54.1   2.257    .056      28.6      33.3    21.1      .39     -145.
 94.40    35.4   2.268    .053      26.4      20.1    13.2      .37      128.
 97.80    30.5   2.097    .067      33.5      54.1     7.9      .26     -110.
 99.70    23.5   0.000   -.010    -180.0    -180.0     0.0     0.00     -180.
101.20    63.6   2.259    .054      27.6      27.1    23.8      .37      155.
106.10    25.2   2.293    .048      21.2      16.8     9.7      .39      126.


PEAK Statistics for SEGMENT      1
STATISTICS FOR INTERVAL FROM    40.00 TO 110.00 Seconds
SAMPLES CALCULATED EVERY       .100 SECS
TEST: 2C      RUN: 3      DATE: 20 Jan 1989    TIME: 20:33:26

                               MEAN    STANDARD DEV.   NPTS
NORMAL FORCE                 40.768      18.552         20
X POSITION                    2.214        .078         17
Z POSITION                     .050        .010         17
Alpha                        27.806       5.360         17
Beta                         38.720      13.835         17
FRICTION COEFF                 .277        .130         17
PROJECTED FRICT. DIR.       -28.578      99.833         17
```

Table 6.2

Mean Normal Force Peaks and Peak Frequency

Test	[-Mean Normal	Force Peaks--]			[-------Peak	Frequency-----]		
	Seg1 (N)	Seg2 (N)	Seg3 (N)	Seg4 (N)	Seg1 (Hz)	Seg2 (Hz)	Seg3 (Hz)	Seg4 (Hz)
1S1	20.5	22.2	47.6	28.6*	.564	.581	.331	.195*
1C1	20.0	22.8	37.3	79.7*	.386	.392	.272	.185*
1C2	21.9*	32.9	49.2	37.0*	.690*	----	.500	.330*
1S2	12.8*	18.2	18.5	40.5*	.303*	.511	.394	.244*
1C3	11.6	14.1	21.4	34.1*	.340	.529	.429	.109*
1C4	15.4	27.2	28.3	39.4*	.495	.500	.506	.115*
1S3	25.4	27.2	28.5	46.8*	.541	----	.784	.455*
1C5	21.5	22.2	33.8	27.7*	.559	.495	.390	.282*
1C6	25.4	26.8	37.4	39.1*	.541	.481	.444	.357*
1S4	14.5	21.4	27.7	90.6*	.319	.534	.383	.185*
1C7	20.5*	34.9*	34.4*	54.7*	.556*	.741*	.385*	.588*
1C8	14.8	27.0	26.8*	36.6*	.301	.385	.385*	.133*
2S1	18.1	22.6	37.8	144.9	.244	.428	.209	.206
2C1	28.5	32.6	30.5	150.0*	.543	.426	.337	.075*
2C2	36.6	36.5	55.7	60.4*	.667	.509	.353	.130*
2S2	23.0	35.0	47.4	81.5*	.533	.750	.537	.224*
2C3	40.8	56.0	66.3	168.5*	.314	.324	.190	.085*
2C4	55.6	73.1	53.1	92.9*	.545	.564	.591	.122*
2S3	15.2	57.3	70.7	156.2	.492	.591	.611	.079*
2C5	51.4	50.3	96.0	61.1*	.494	.563	.479	.200*
2C6	50.6	56.1	90.9	158.9*	.556	.549	.456	----*
2S4	19.8*	34.2	39.1	286.9*	.588*	.575	.507	----*
2C7	26.5	47.2	30.0	29.1*	.438	.332	.289	.027*
2C8	47.5	47.2	57.6	252.0*	.520	.517	.410	.217*
3S1	58.5	50.2	86.6	266.9	.323	.207	.183	.080
3C1	51.8	80.4	83.1	129.7*	.511	.323	.342	.085*
3S2	33.1	72.9	93.1	206.5	.578	.601	.447	.222
3C2	41.9	81.5	63.0	103.3	.529	.370	.342	.233

* Values from 5 or fewer Peaks

Table 6.3

Ratio of Mean Normal Force / Mean Peak Normal Force

Test	Seg1	Seg2	Seg3	Seg4	Test	Seg1	Seg2	Seg3	Seg4
1S1	.810	.595	.435	.231	2S1	.359	.518	.291	.322
1S2	.781	.725	.573	.240	2S2	.483	.577	.513	.398
1S3	.866	.728	.593	.485	2S3	.474	.522	.579	.086
1S4	.717	.500	.469	.311	2S4	.439	.585	.550	.109
3S1	.379	.351	.406	.274					
3S2	.541	.542	.485	.353					
1C1	.570	.518	.373	.078	2C1	.530	.485	.357	.235
1C2	.826	.733	.510	.551	2C2	.505	.570	.296	.288
1C3	.664	.674	.430	.129	2C3	.429	.430	.359	.229
1C4	.688	.702	.534	.315	2C4	.502	.579	.524	.130
1C5	.712	.631	.509	.462	2C5	.490	.549	.477	.203
1C6	.713	.627	.481	.414	2C6	.486	.455	.516	.185
1C7	.702	.794	.610	.479	2C7	.589	.434	.497	.289
1C8	.541	.367	.504	.593	2C8	.535	.515	.450	.239
3C1	.604	.428	.498	.175					
3C2	.640	.427	.408	.446					

Statistics on Mean / Peak Normal Force Ratios

	Seg1		Seg2		Seg3		Seg4	
Data Set	Av	SD	Av	SD	Av	SD	Av	SD
All Runs	.592	.138	.556	.116	.472	.084	.295	.141
S Runs	.585	.190	.564	.110	.489	.094	.281	.122
C Runs	.596	.105	.551	.122	.463	.078	.302	.153
1S Runs	.794	.062	.637	.110	.518	.077	.317	.118
2S Runs	.439	.056	.551	.035	.483	.130	.229	.155
1C Runs	.677	.089	.631	.134	.494	.070	.378	.189
2C Runs	.508	.046	.502	.060	.435	.086	.225	.053

Av = Average SD = Standard Deviation

6.5 Segment Resistance

Total ship resistance was directly measured during the tests through the carriage force block. The resistance of each segment was calculated from the sum of the x directional forces. Figure 6.4 illustrates time history plots for Segments 1 to 3 for a selected test. The failure of the x-direction transducer on the fourth segment reported earlier prevented direct measurement of this force. However, the x-direction force may be estimated from the normal force and friction coefficient. For this calculation, a mean friction coefficient of 0.2 was assumed (see Section 6.7 later).

Table 6.4 summarizes the measured mean ship and segment resistance data for the test series as well as the calculated Segment 4. Analysis of this data is discussed in Section 7.7.2.

FIGURE 6.4
SEGMENT RESISTANCE VERSUS TIME

2C RUN 5 24 Jan 1989
SEGMENT 1 RESISTANCE vs. TIME

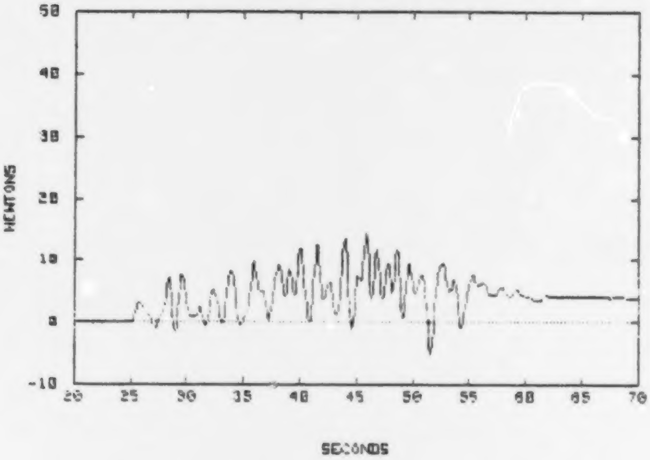

2C RUN 5 24 Jan 1989
SEGMENT 2 RESISTANCE vs. TIME

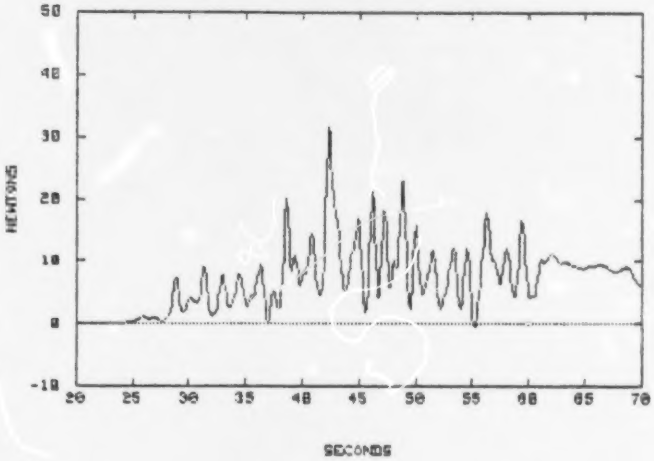

2C RUN 5 24 Jan 1989
SEGMENT 3 RESISTANCE vs. TIME

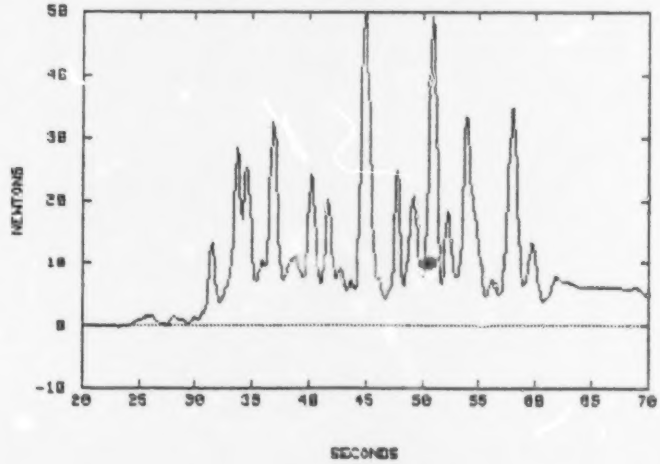

Table 6.4

Total Ship Resistance and Segment Resistance

	[----------- Resistance				------------]	[---- Percent of Total			----]
Test	Seg1 (N)	Seg2 (N)	Seg3 (N)	Seg4 (N) est	Tot. (N)	Seg1 (%)	Seg2 (%)	Seg3 (%)	Seg4 (%) est
1S1	----	3.9	8.6	1.3	----	----	----	----	----
1C1	1.9	2.4	6.3	1.2	----	----	----	----	----
1C2	3.9	5.4	7.6	4.1	----	----	----	----	----
1S2	3.5	4.1	2.6	1.9	42.9	8.3	9.5	6.0	4.5
1C3	1.9	1.8	2.2	0.9	24.3	7.6	7.5	9.2	3.6
1C4	3.0	3.4	3.4	2.5	36.6	8.2	9.1	9.3	6.8
1S3	4.9	5.1	5.2	4.5	70.4	7.0	7.2	7.4	6.4
1C5	5.1	3.1	3.9	2.6	34.1	15.0	9.1	11.3	7.5
1C6	6.4	3.6	4.1	3.2	44.2	14.4	8.1	9.2	7.3
1S4	1.5	3.7	3.5	5.6	30.0	5.0	12.4	11.8	18.8
1C7	8.6	7.4	4.3	5.2	26.9	31.8	27.7	16.2	19.5
1C8	1.4	2.7	2.4	4.3	9.3	14.7	28.9	25.7	46.6
2S1	2.7	1.6	3.6	9.3	64.5	4.1	2.5	5.6	14.4
2C1	1.9	1.3	2.4	7.1	41.4	4.7	3.1	5.9	17.1
2C2	4.8	3.6	3.4	3.5	45.4	10.6	7.9	7.5	7.7
2S2	1.8	4.7	5.6	6.5	----	----	----	----	----
2C3	3.6	2.8	5.1	7.7	55.3	6.5	5.1	9.1	14.0
2C4	5.3	4.2	7.2	2.4	78.0	6.8	5.3	9.2	3.1
2S3	----	11.0	13.4	2.7	101.1	----	10.9	13.2	2.7
2C5	5.8	10.4	16.1	2.5	67.3	8.7	15.5	23.9	3.7
2C6	4.9	7.9	15.9	5.9	61.1	8.0	12.9	26.0	9.6
2S4	3.7*	6.1	6.2	6.3	55.0	6.8*	11.2	11.2	11.4
2C7	5.8	4.3	4.0	1.7	42.3	13.7	10.2	9.5	4.0
2C8	8.9	4.5	5.5	12.1	51.2	17.3	8.8	10.8	23.6
3S1	----	8.6	11.3	14.6	155.2	----	5.6	7.3	9.2
3C1	6.5	15.9	6.8	4.5	95.6	6.8	16.6	7.1	4.7
3S2	----	17.5	8.3	14.6	76.2	----	23.0	10.9	19.1
3C2	8.2	10.6	5.4	9.2	44.1	18.7	24.0	12.2	20.9

* Questionable Data

NOTE : Segment 4 results are estimates based upon R4= 0.2 * Fn4
where R4=estimated resistance, 0.2=assumed friction factor
and Fn4=Segment 4 Mean normal force from Table 6.1

6.6 Load Position

As explained earlier, if the load on a segment is idealized as a simple point load, the point of load application can be determined using the load algorithm. It is then possible to construct load position time history data for the tests. There are occasions when the calculated position data should be discarded, however; when small loads occur the resolution of the instrumentation is insufficient to accurately calculate position, and when the calculated position falls outside a segment's boundaries. Position time history plots therefore, comprise a series of partially continuous time records. Figures 6.5 (a) to (c) show time history plots of load location in x and z directions.

The position time histories primarily fall into two categories:

(1) When the segment loads are low or moderate and are close to static, the position data (in both x and z) shows little variability.

(2) When segment loads are high and dynamic, the position data is quite variable. Often the load position moves longitudinally and/or vertically over the face of a segment.

The common occurrence of Type 2 behaviour makes mean values of position data over an entire test somewhat less useful.

Of interest, is position data during normal force maxima (immediately prior to ice failure). Using the peak selection criteria outlined in Section 6.4, the x and z position data were extracted. Figure 6.6 shows the x and z position data for Segment 2 during a test as a function of normal force. The mean values of these data are summarized in Table 6.5.

The load position on Segment 1 is quite constant in the x direction, and varies as a function of ice thickness in the z (vertical) direction. The vertical position is typically deeper in the water for 'S' runs than for 'C' runs, suggesting a difference in breaking pattern to be expected at the extreme fore end of the vessel. Segment 2 shows similar behaviour as Segment 1, but with higher variability in both directions. Segment 3 has very high variability of position and seems to not exhibit consistent differences between 'S' and 'C' runs. This would indicate that there is more ice sheet bending and ice piece turning occurring on this segment, producing more position variability but that at this point on the hull the breaking pattern is relatively consistent for unbroken ice and channel widening. The relative infrequency of peaks on Segment 4 produces a limited data set, however some generalizations can be made. x position variability is roughly comparable to that shown on Segment 3, while the z position shows relatively little variability. This is likely because most forces on Segment 4 are from ice pieces that have turned on end hence, the ice thickness has little effect upon vertical position of the load.

Given a calculated x and z position of loading, the corresponding hull angles can be found. The waterplane and flare angles during normal force maxima were thus plotted as a function of normal force. Figure 6.7 shows a plot of angles versus normal force maxima for all segments.

FIGURE 6.5a
CALCULATED LOAD POSITION VERSUS TIME

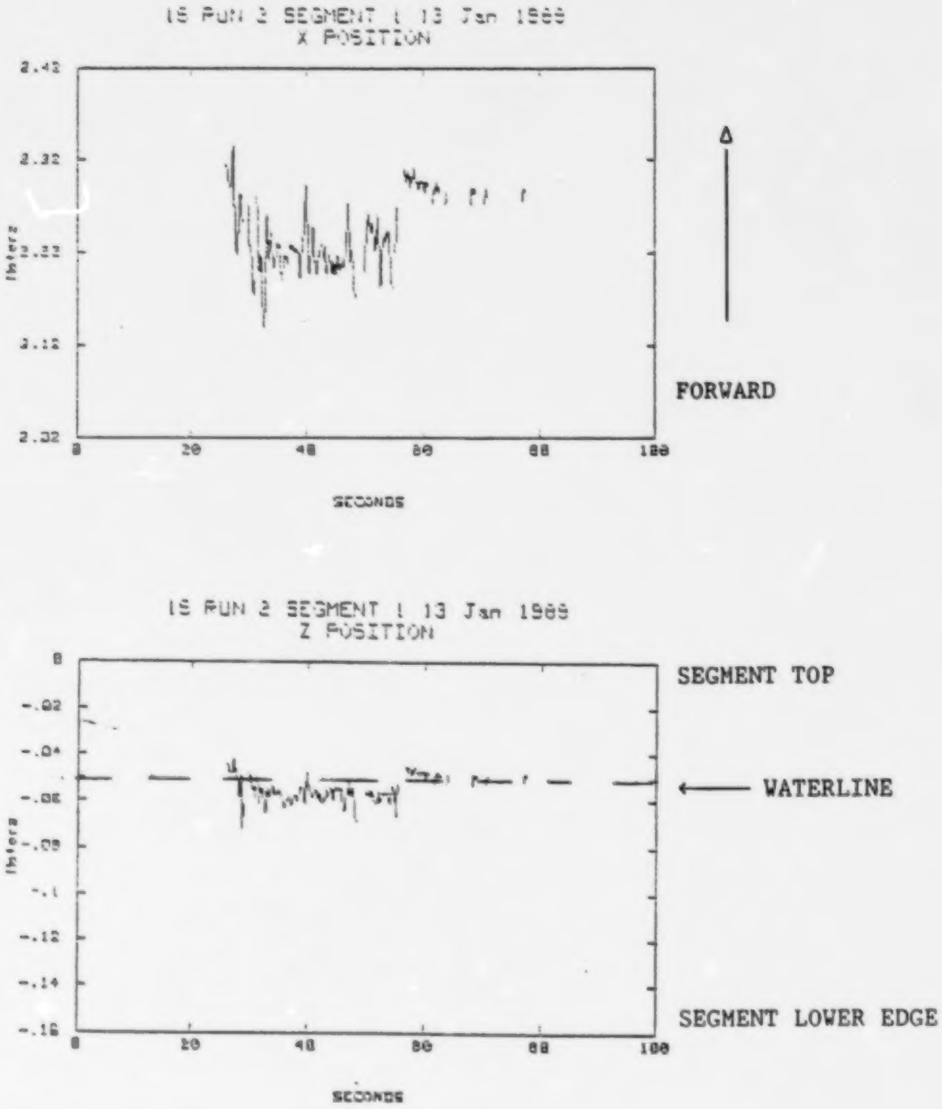

X position scale has origin at amidships
Z position scale has origin at top segment

FIGURE 6.5b
CALCULATED LOAD POSITION VERSUS TIME

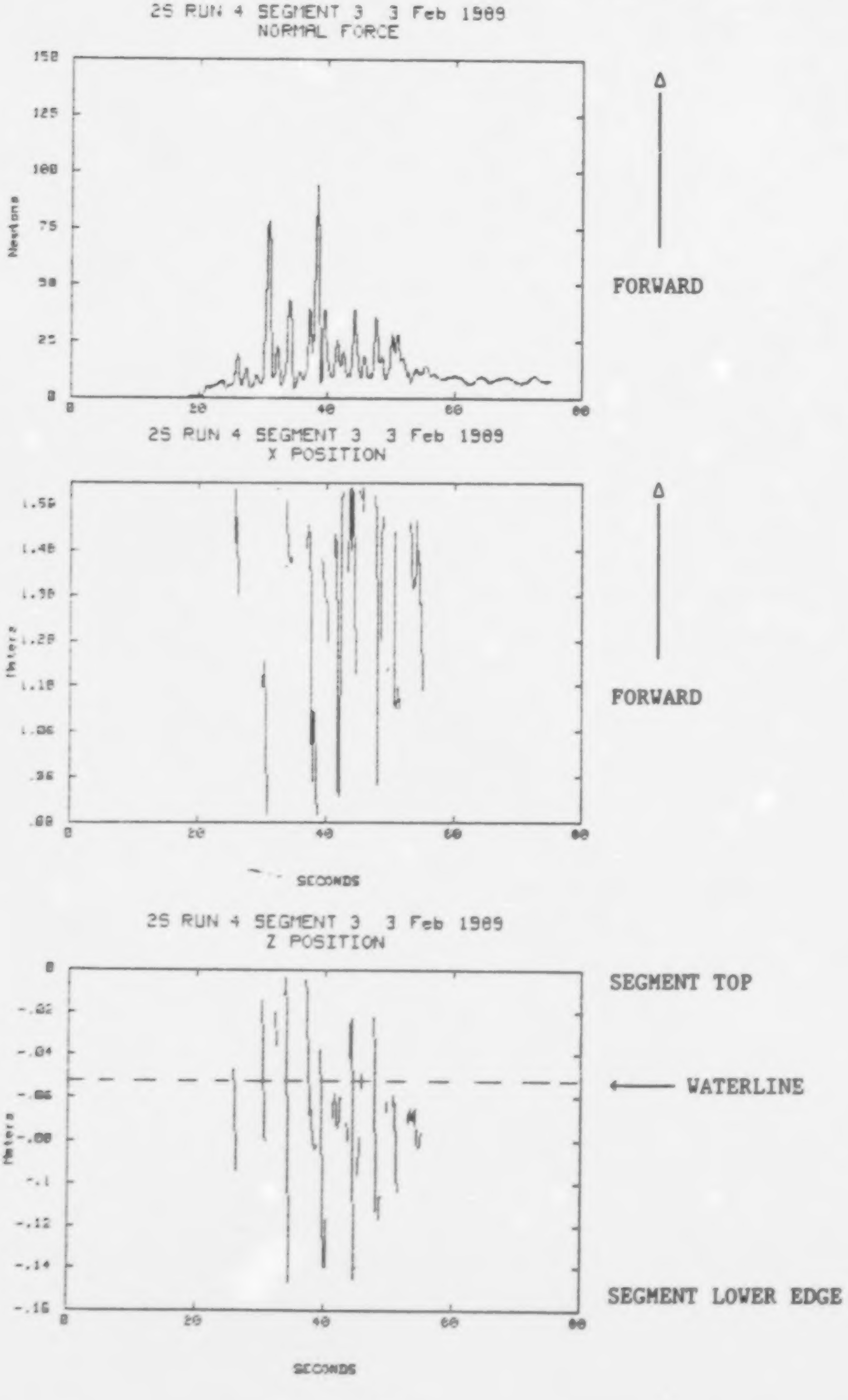

FIGURE 6.5c
CALCULATED LOAD POSITION VERSUS TIME

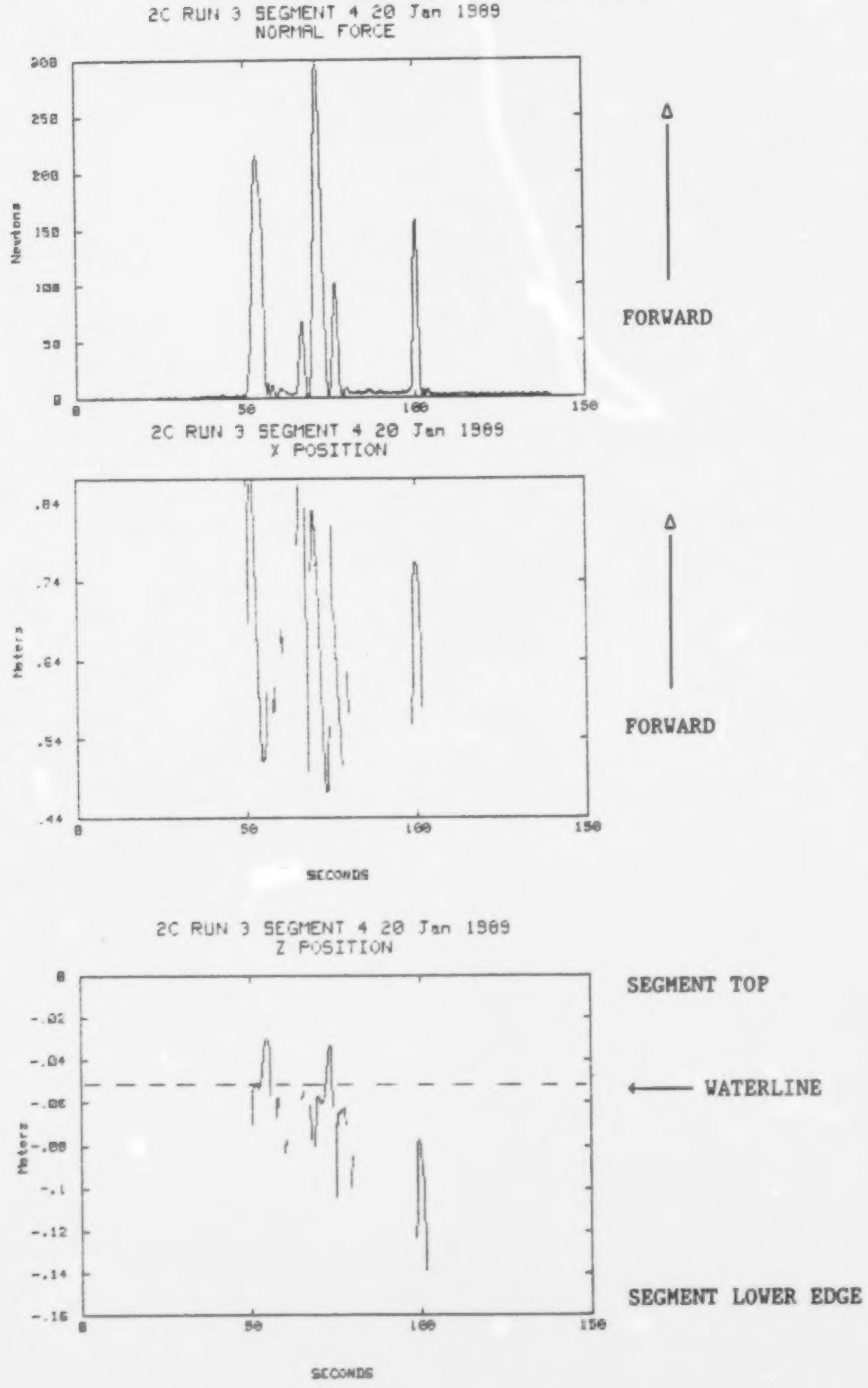

FIGURE 6.6

LOAD POSITION AT NORMAL FORCE MAXIMA VERSUS NORMAL FORCE

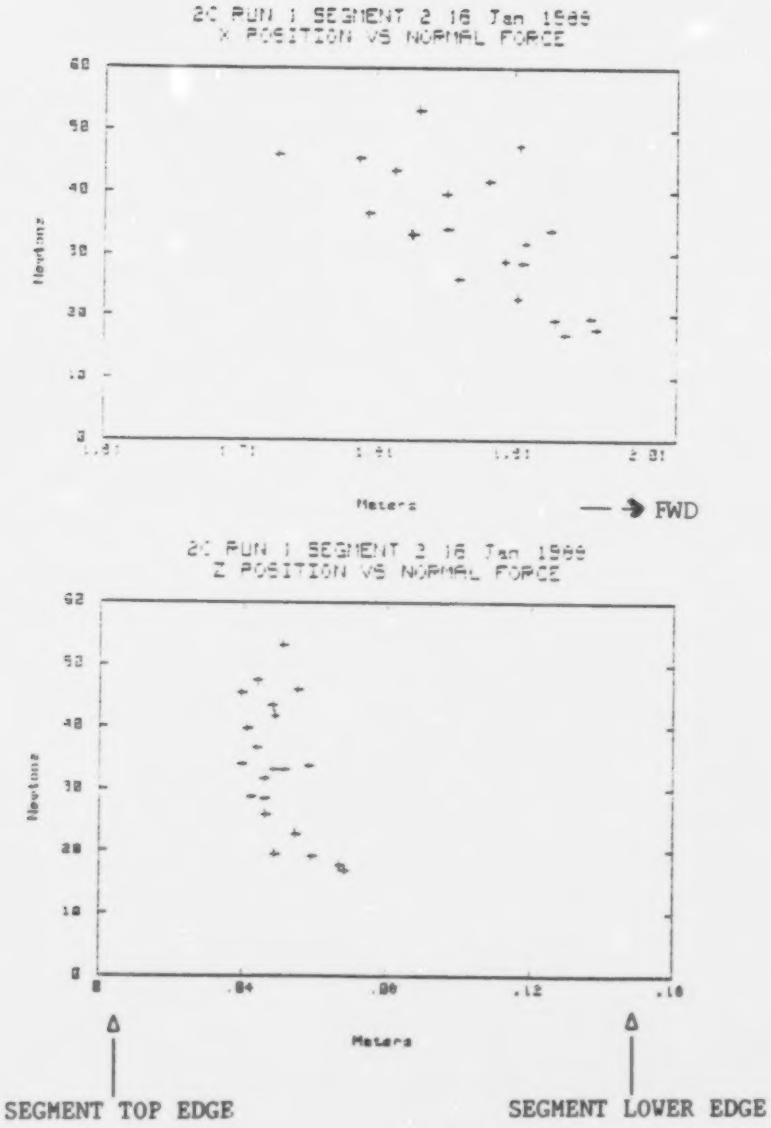

TABLE 6.5

LOAD POSITION AT NORMAL FORCE MAXIMA

Test	[------- X Position			-------]	[--------- Z Position			-----]
	Seg1 (m)	Seg2 (m)	Seg3 (m)	Seg4 (m)	Seg1 (m)	Seg2 (m)	Seg3 (m)	Seg4 (m)
1S1	2.246	1.871	1.183	0.568*	.052	.065	.043	.067*
1C1	2.276	1.872	1.142	0.581*	.044	.058	.034	.054*
1C2	2.254	1.745	1.089	0.532*	.037	.063	.034	.066*
1S2	2.221	1.857	-----	0.587*	.055	.061	----	.057*
1C3	2.212	1.786	1.291	0.563*	.047	.059	.060	.051*
1C4	2.193	1.756	1.188	0.600*	.046	.064	.054	.077*
1S3	2.248	1.763	-----	0.625*	.043	.051	----	.056*
1C5	2.239	1.788	-----	0.614	.036	.048	----	.072*
1C6	2.246	1.745	-----	-----	.032	.050	----	----
1S4	2.286	1.810	1.347	0.653	.043	.047	.065	.052
1C7	2.231*	1.827*	1.346*	0.659*	.017*	.048*	.084*	.049*
1C8	2.267	1.806	1.177	0.670*	.035	.046	.064	.047*
2S1	2.229	1.847	0.955*	0.728*	.067	.056	.041*	.050
2C1	2.314	1.880	1.333	0.738*	.044	.050	.024	.050*
2C2	2.249	1.865	1.348	0.771*	.041	.048	.030	.068*
2S2	-----	1.896	1.287*	0.571	----	.073	.062*	.068
2C3	2.214	1.846	1.442	0.681*	.050	.060	.058	.064*
2C4	2.262	1.873	1.466	0.593*	.042	.059	.085	.045*
2S3	2.300*	1.810	1.324	0.556*	.051*	.074	.048	.059*
2C5	2.269	1.842	1.412	0.639*	.046	.072	.056	.079*
2C6	2.236	1.819	1.514	-----	.049	.066	.052	----
2S4	2.252*	1.761	1.423	0.658*	.058*	.059	.054	.052*
2C7	2.249	1.789	1.386	0.670*	.051	.052	.044	.056*
2C8	2.261	1.823	1.343	0.668*	.046	.054	.078	.052*
3S1	-----	1.738	1.364	0.644	----	.102	.113	.069
3C1	2.218	1.800	1.370	0.662*	.060	.092	.106	.066*
3S2	2.243	1.791	1.340	0.664	.062	.085	.069	.063
3C2	2.222	1.837	1.366	0.682	.059	.081	.075	.070

* Values from less than 5 data points

FIGURE 6.7

CALCULATED WATERPLANE AND FLARE ANGLES AT NORMAL FORCE MAXIMA VERSUS NORMAL FORCE

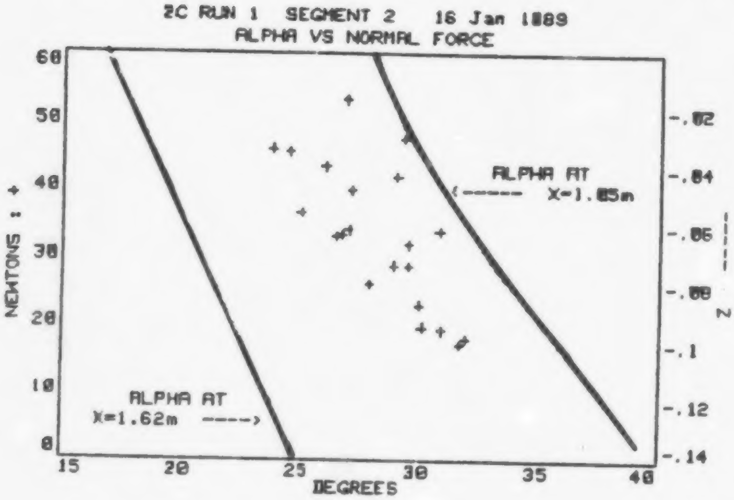

KEY:

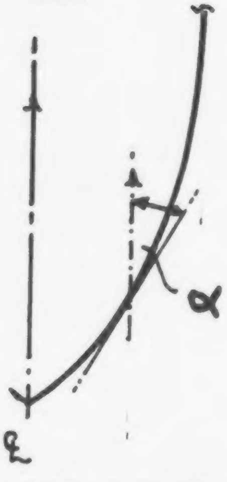

PLAN OF WATERLINE

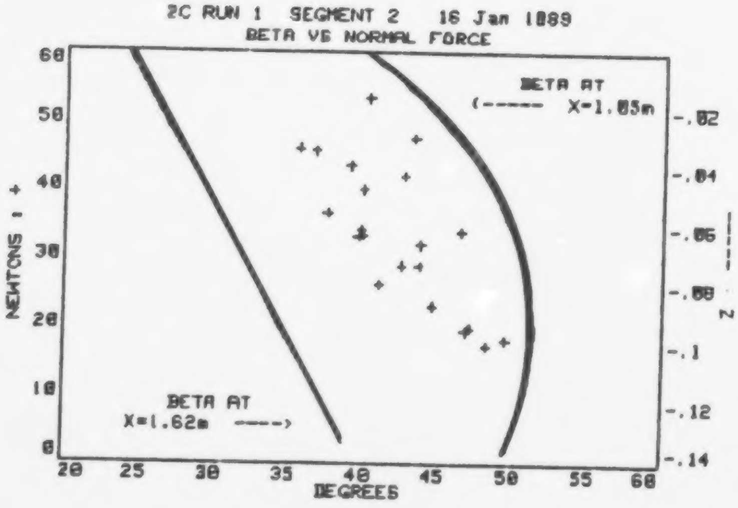

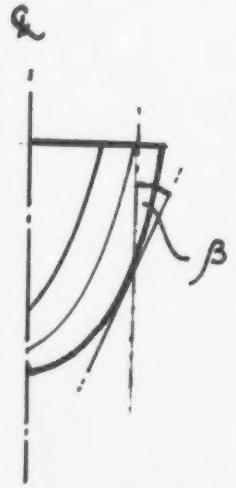

ELEVATION OF SECTION

6.7 Friction Coefficient and Direction

As was described earlier, the loading algorithm allowed the calculation of frictional force and direction. The derivation of these parameters is explained in detail in the Phase 1 report [2]. Time history plots of friction coefficient and friction direction were constructed using the same data limitation criteria as discussed in Section 6.5. The defined coordinate system for friction vector was: 0° directed aft, + 90° directed vertically up, - 90° directed vertically down, and ± 180° directed forward.

Typical time history plots of friction coefficient and direction are shown in Figures 6.8 (a) to (c). Friction direction continually reverses between upward and downward vectors throughout the test. For the sake of clarity, individual data points are plotted therefore, rather than a continuous line. In the case of Figure 6.8 (a), the friction direction oscillates between ±135° and -90° with the downward direction predominating. This is discussed further in Section 7. Additionally, calculations of mean values for both parameters were made for upward and downward cases. Table 6.6 summarizes the mean values for both parameters. The friction coefficient was virtually identical in the upward and downward directions when a sufficient number of data points were observed for each case. Therefore, Table 6.6 presents an average value for friction coefficient rather than one for each direction.

Values of friction coefficient and direction occurring during normal force maxima were also calculated. Both were found to be relatively independent of normal force magnitude. Figure 6.9 shows typical plots of these parameters as a function of normal force.

FIGURE 6.8(a)

CALCULATED FRICTION COEFFICIENT
AND DIRECTION VERSUS TIME

1S RUN 2 SEGMENT 1 13 Jan 1989
FRICTION COEFF

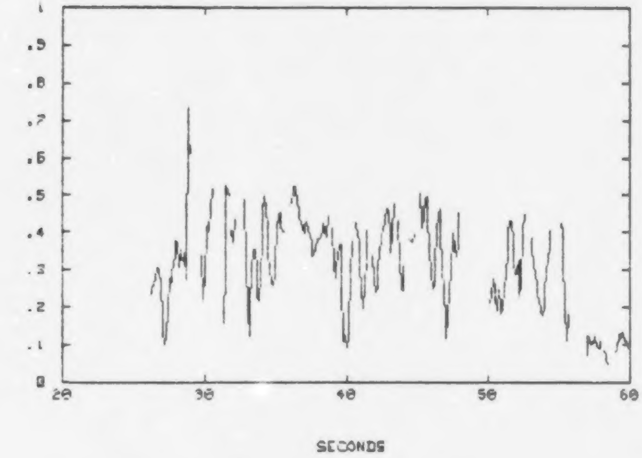

1S RUN 2 SEGMENT 1 13 Jan 1989
FRICTION DIRECTION

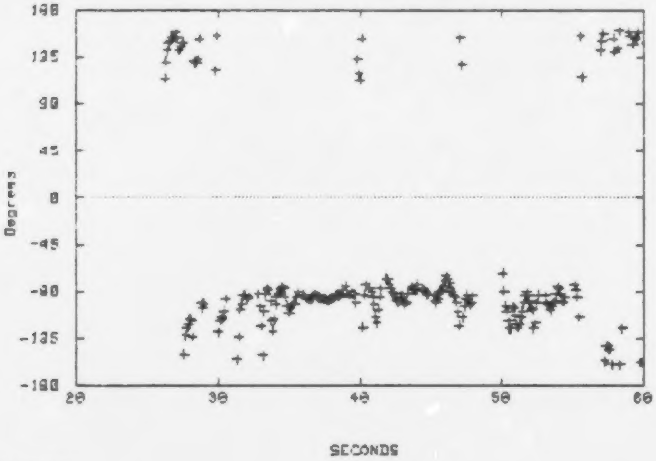

```
SEGMENT    1
STATISTICS FOR INTERVAL FROM   40.00 TO  50.00 Seconds
SAMPLES CALCULATED EVERY       .100 SECS
TEST: 1S     RUN: 2      DATE: 13 Jan 1989    TIME: 22:33:37

                               MEAN   STANDARD DEV.   NPTS
NORMAL FORCE           N       9.96       2.444         99
FRICTION FORCE         N       4.00       1.237         83

X POSITION             m       2.21        .018         83
Z POSITION             m        .06        .003         83

FRICTION COEFF  -UP-            .14        .026          3
PROJECTED FRICT. DIR. deg    144.83      11.986          3

FRICT. COEFF  -DOWN-            .36        .083         64
PROJECTED FRICT. DIR. deg    -94.52      10.239         64
```

FIGURE 6.8(b)

CALCULATED FRICTION COEFFICIENT AND DIRECTION VERSUS TIME

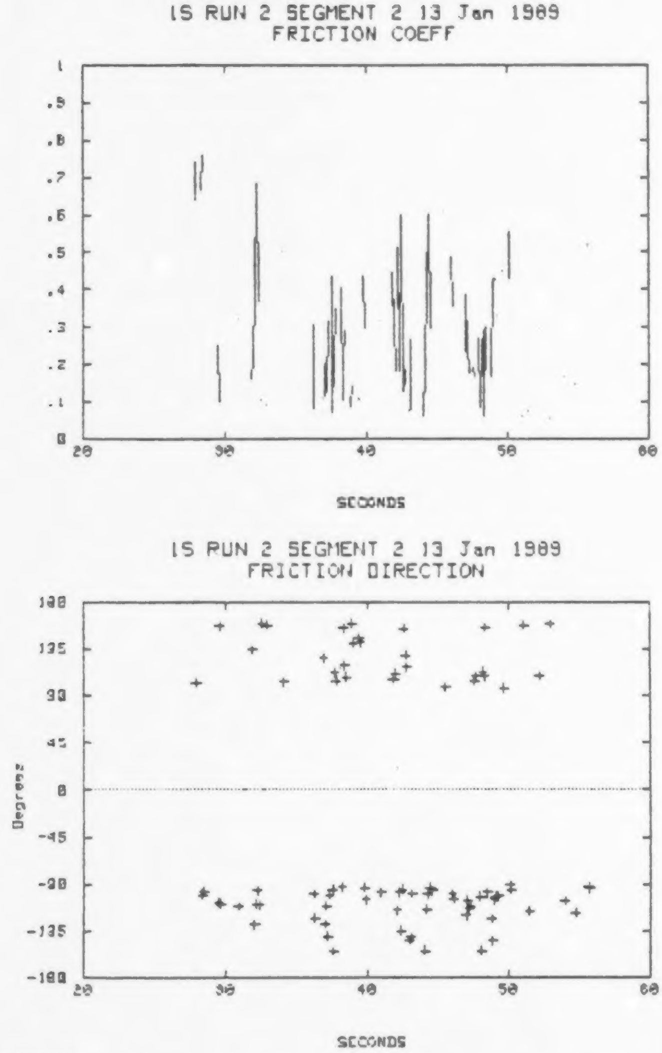

```
SEGMENT   2
STATISTICS FOR INTERVAL FROM    40.00 TO   50.00 Seconds
SAMPLES CALCULATED EVERY       .100 SECS
TEST: 1S      RUN: 2      DATE: 13 Jan 1989    TIME: 22:33:37

                                  MEAN    STANDARD DEV.   NPTS
NORMAL FORCE             N        13.24       3.667         99
FRICTION FORCE           N         4.15       2.319         81

X POSITION               m         1.82        .093         81
Z POSITION               m          .06        .004         81

FRICTION COEFF  -UP-                .28        .147         13
PROJECTED FRICT. DIR. deg        116.28      18.304         13

FRICT. COEFF   -DOWN-               .30        .156         28
PROJECTED FRICT. DIR. deg       -112.55      18.725         28
```

FIGURE 6.8(c)

CALCULATED FRICTION COEFFICIENT AND DIRECTION VERSUS TIME

1S RUN 2 SEGMENT 3 13 Jan 1989
FRICTION COEFF

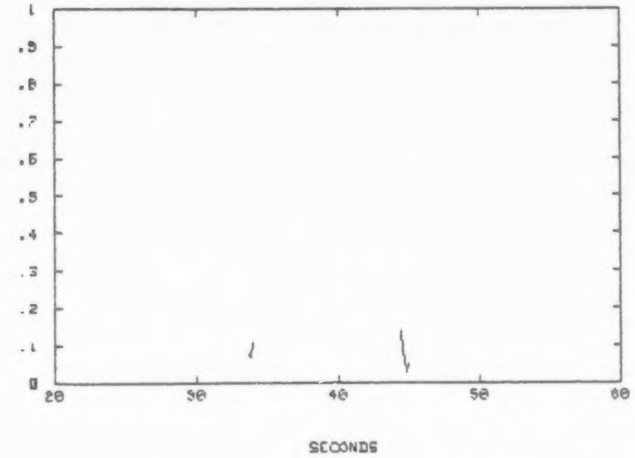

1S RUN 2 SEGMENT 3 13 Jan 1989
FRICTION DIRECTION

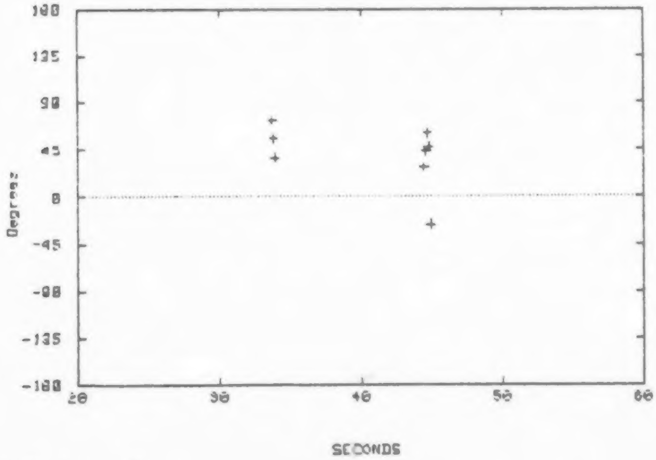

```
SEGMENT     3
STATISTICS FOR INTERVAL FROM    40.00 TO   50.00 Seconds
SAMPLES CALCULATED EVERY        .100 SECS
TEST: 1S      RUN: 2       DATE: 13 Jan 1989     TIME: 22:33:37

                                     MEAN    STANDARD DEV.   NPTS
NORMAL FORCE             N          10.55        5.276          99
FRICTION FORCE           N           1.67         .888           5

X POSITION               m           1.14         .123           5
Z POSITION               m            .02         .005           5

FRICTION COEFF   -UP-                 .08         .041           4
PROJECTED FRICT. DIR. deg           45.08       11.555           4

FRICT. COEFF   -DOWN-                 .05        0.000           1
PROJECTED FRICT. DIR. deg          -25.96        0.000           1
```

TABLE 6.6

FRICTION COEFFICIENT AND DIRECTION

Test	Seg1 mu	up psi (deg)	dn psi (deg)	Seg2 mu	up psi (deg)	dn psi (deg)	Seg3 mu	up psi (deg)	dn psi (deg)
1S1	.50	155.6	-133.0	.32	124.1	-112.2	.34	33.5	-43.2
1C1	.26	125.1	-119.5	.29	139.1	-126.4	.41	42.9	----
1C2	.34	-----	-106.6	.35	129.4	-113.3	.26	29.3	----
1S2	.35	144.8*	-94.5	.29	116.3	-112.6	---	----	----
1C3	.30	157.1	-117.8	.37	132.1	-126.3	.40	84.9	----
1C4	.26	149.3	-106.2	.32	135.1	-123.9	.34	70.9	-56.1
1S3	.22	147.8	-115.7	.30	120.8	-112.3	---	----	----
1C5	.17	86.7	-86.9	.35	129.5	-121.7	---	----	----
1C6	.22	96.2	-88.9	.36	125.8	-117.1	---	----	----
1S4	.23	120.4	-135.5	.12	145.0	-124.4	.43	77.3	----
1C7	.35	55.2	-----	.10	149.4	-123.9	.38	77.0	----
1C8	.24	116.7	-146.2	.16	149.9	-132.4	.38	85.1	----
2S1	.54	125.0	-94.9	.43	137.9	-119.3	.15	113.2	----
2C1	.34	121.0	-124.6	.47	132.4	-124.7	.30	97.0	-128.7
2C2	.34	101.2	-101.4	.43	125.9	-116.7	.33	88.3	----
2S2	.28*	-----	-78.5	.66	140.1	-101.7	.22	70.2	-96.4
2C3	.48	98.1	-113.6	.48	135.8	-128.1	.22	108.8	-110.2
2C4	.51	90.6	-110.8	.56	124.3	-120.7	.18	107.8	-75.5
2S3	.48	91.3*	-127.7	.29	-----	-87.6	.33	38.4	-49.2
2C5	.35	109.8	-109.8	.16	151.8	-96.7	.25	41.5	-42.4
2C6	..55	90.1	-118.7	.21	156.9	-111.5	.17	31.0	-47.9
2S4	1.24	84.9	-118.4*	.36	157.0	-106.8	.22	78.0	-56.0
2C7	.82	74.9	-98.3	.29	152.6	-119.7	.16	51.2	-83.7
2C8	.52	65.7	-90.8	.27	149.1	-120.0	.19	87.8	-91.7
3S1	---	-----	-----	.12	136.3	-80.1	.37	90.4	-95.7
3C1	.72	86.9	-105.5	.14	120.1	-72.4	.40	102.6	-103.2
3S2	.44	78.0	-92.4	.34	-----	-80.2	.26	78.5	-40.3
3C2	.72	78.7	-107.9	.19	148.6	-100.5	.20	108.6	-58.8

* Values from less than 5 data points

FIGURE 6.9

FRICTION COEFFICIENT AND DIRECTION AT NORMAL FORCE MAXIMA VERSUS NORMAL FORCE

2C RUN 1 SEGMENT 2 08 Jan 1989
Friction Coeff VS NORMAL FORCE

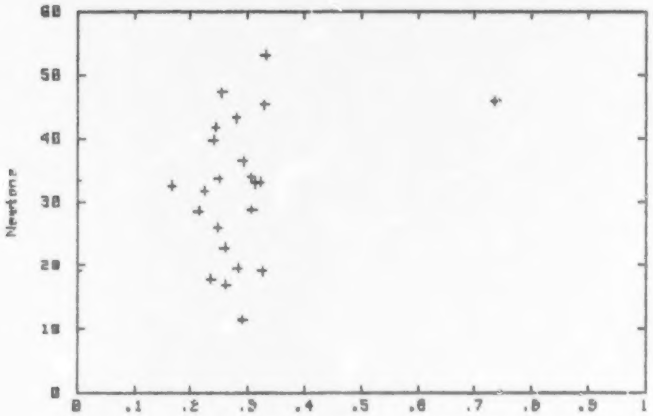

2C RUN 1 SEGMENT 2 10 Jan 1989
Friction Dir VS NORMAL FORCE

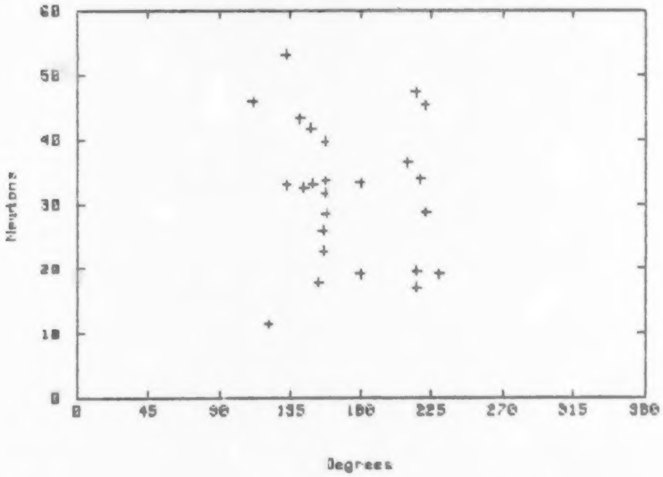

7. ANALYSIS AND DISCUSSION OF RESULTS

7.1 Approach

The principal objective was to compare the results of normal force and resistance calculations on the segments with the numerical process of Dr. Carter and also with the RICE model.

The discussion of results reported in this section are limited to a comparison of the data with previous data from Phase II, comparison with the numerical models and a brief discussion of the general results in sufficient detail to see if further analysis is worth pursuing.

In analyzing the results the following factors had significant effect:

(a) The run lengths were generally about one to two ship lengths and were therefore shorter than originally hoped.

(b) There was both time and fiscal constraint on the analysis phase.

7.2 Time Histories

7.2.1 Time Series Plots of Individual Transducers

The significant features of the individual transducer plots that help us to understand the ice/ship interaction are:

- frequency of loading
- force characteristics compared to physical behaviour of the ice
- force direction

Typically Segment 1 is subject to high frequency forces in all planes associated with the crushing, failing process. This frequency increased with speed and decreased with strength as would be expected. A similar pattern is seen for Segment 2. Segment 3 experiences lower frequency loading at each transducer with generally larger amplitude forces. Segment 4 exhibits very low frequency, large magnitude peaks with very little loading in between the peaks.

In most cases there is a large peak as the segment enters the ice sheet which is rarely repeated - this perhaps reflects that the initial breaking pattern is quite different from that once the vessel is fully in the ice sheet.

Force characteristics on individual segments exhibit features that are supported by a continuous crush-fail sequence in Segments 1 and 2 (Cusp Rows 1 and 2). For Segment 4 the characteristic of the forces is that of a fairly constant low mean, with occasional peaks that are much greater than the mean. Segment 3 force characteristics are between these extremes. Table 6.3 indicated that peak/mean force ratios in Segment 1 averaged approximately 2:1, increasing through Segments 2 and 3 to approximately 4:1 in Segment 4.

Some individual transducers exhibit 'negative' forces (i.e. unloading of the preloading condition due to tilting of the segment during ice interaction. The net force on the segment is, of course, always positive.

The analysis of the time series data confirms that the nature of the loading is different in the forward section (Segments 1 and 2), from those further aft (Segments 3 and 4).

The time series plots thus clearly indicate that not all segments (hull locations) experience the same loading conditions, nor can the relationship between the mean force and the peak forces be considered the same at all locations.

Frequency analysis of the time series normal force data was performed using an FFT program. An example of the output for each segment and the total carriage force is shown in Figures 7.1 (a) to (f). The analysis of the full data set showed:

- **Segment 1:** energy at several frequencies that appeared to be 'harmonic' at slow speed in thick ice, changing to one dominant frequency (.465 Hz) at higher speed, and to (.625 Hz) at even higher speeds.

- **Segment 2:** a peak at about .290 Hz rising to two peaks about .375 Hz and .6 Hz and then dropping to lower frequency and lower energy levels at higher speeds (.32 Hz).

- **Segment 3:** a 'decaying' frequency distribution with several peaks, and most energy at lower frequencies at low speeds, becoming more evenly spread across the frequency band at higher speeds.

- **Segment 4:** a 'decaying' frequency distribution at all speeds, with most activity at low frequencies.

Examples of the relationship between peak frequencies, velocity and thickness. by segment are shown in Figures 7.2 and 7.3 for different ice thicknesses. These clearly show increasing peak frequency with velocity.

The significance of this relates to the manner in which a predictive model deals with determining a mean force in what is a dynamic situation. Clearly, as the peak frequency drops, the process can not be approximated by a steady force.

There appears to be no significant relationship between the frequencies of the total resistance force on the carriage and those on the measured segments. This is, of course, expected as the segments represented only a portion of the loaded hull, all of which is responding at different frequencies.

FIGURE 7.1 (a) to (f)
EXAMPLE OF FREQUENCY SPECTRUM OF SEGMENT NORMAL FORCE

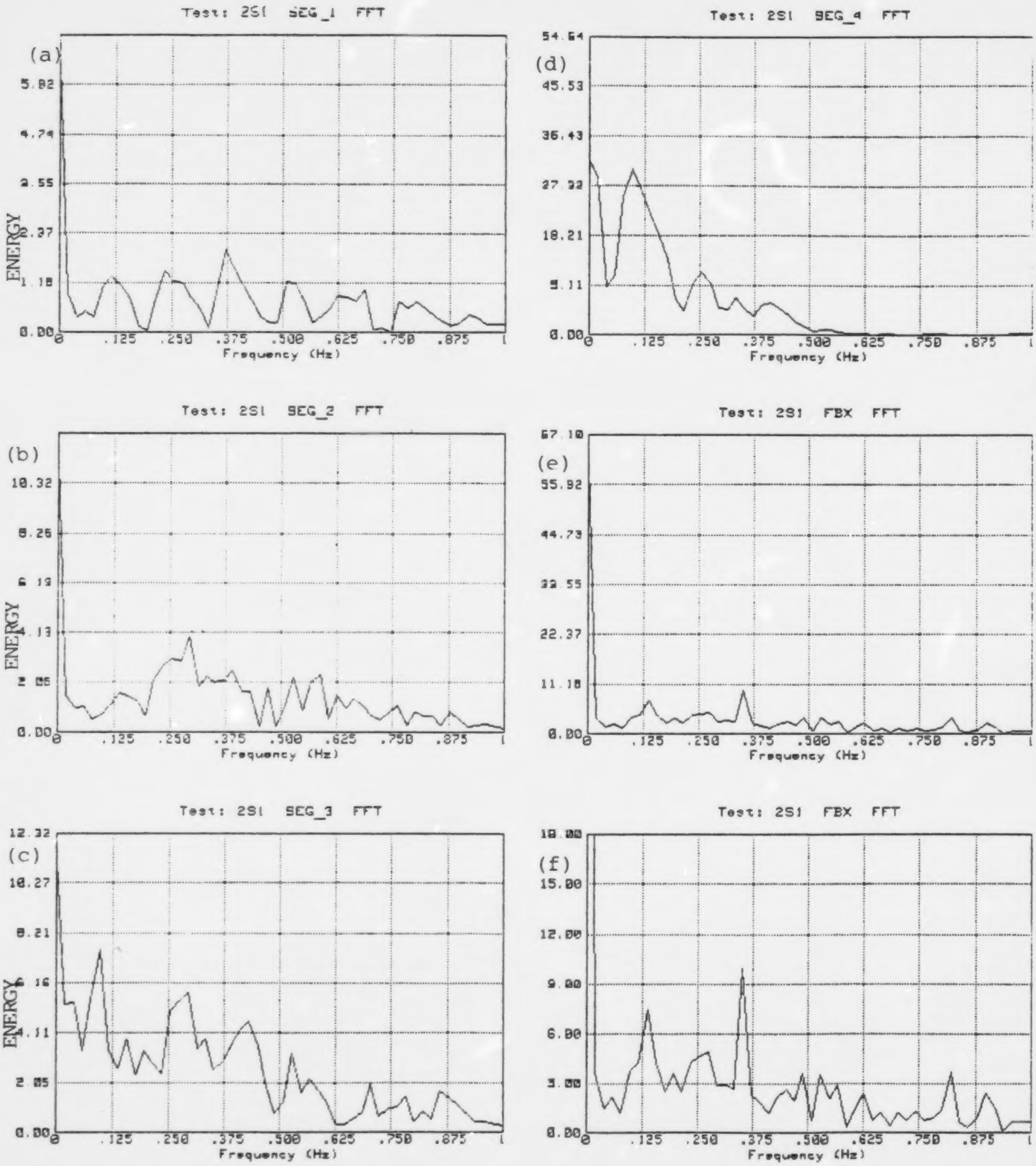

FIGURE 7.2

FREQUENCY OF PEAK TRANSDUCER LOADS
VERSUS VELOCITY X THICKNESS

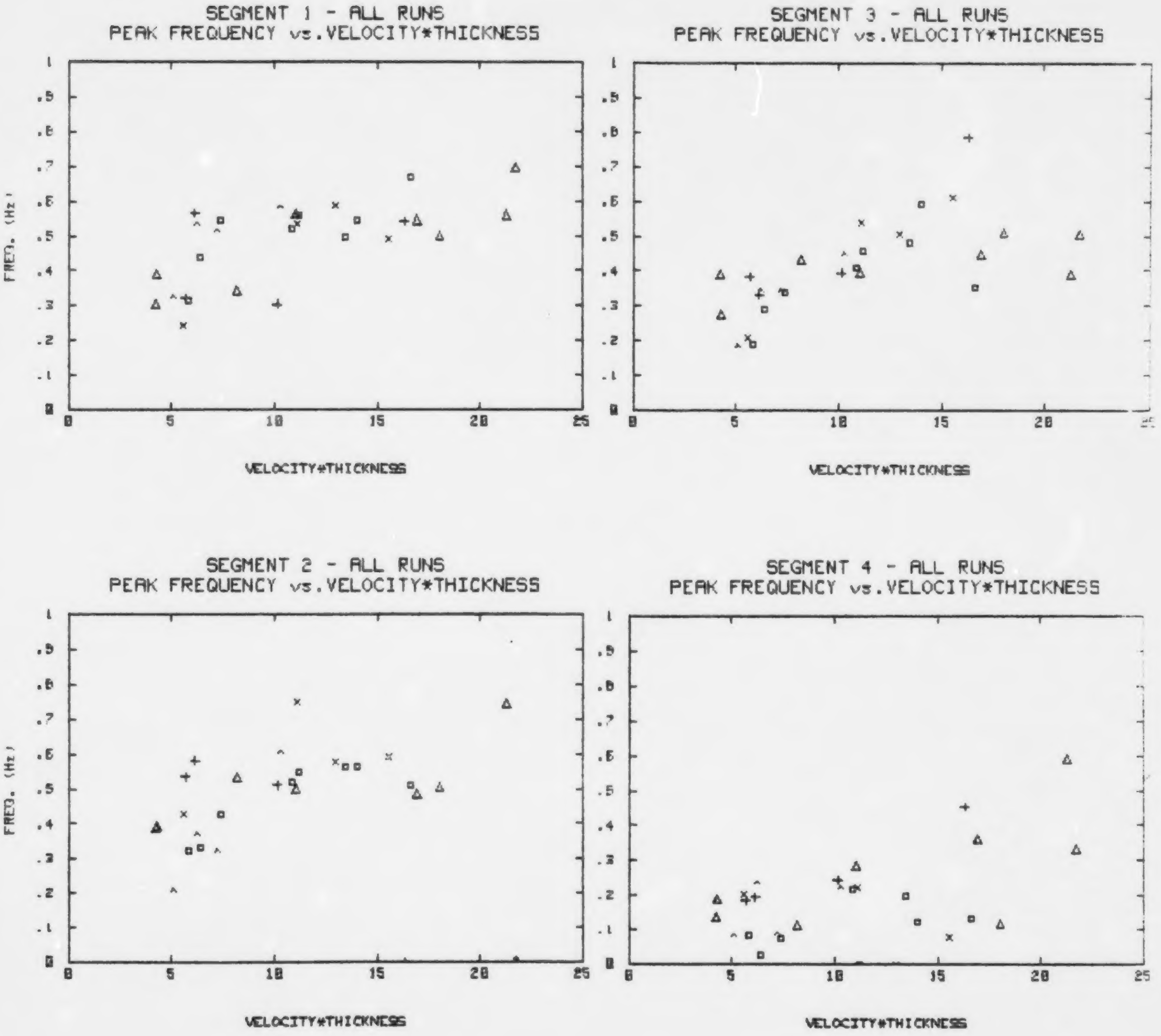

FIGURE 7.3
FREQUENCY OF PEAK LOADS VERSUS VELOCITY - SEGMENT 1

SEGMENT 1 - h=35 mm.
PEAK FREQUENCY vs.VELOCITY

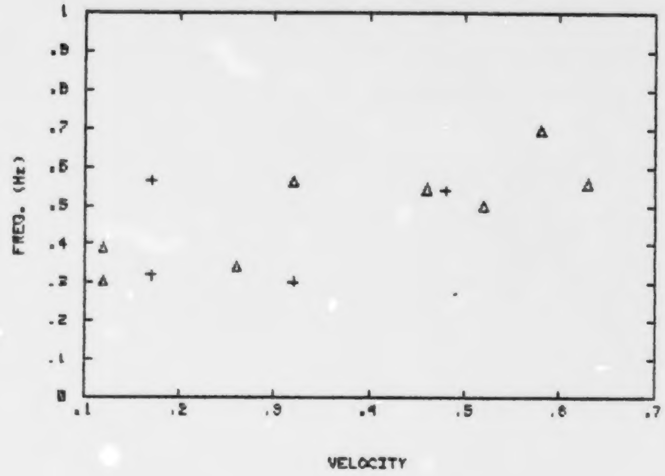

SEGMENT 1 - h=45 mm.
PEAK FREQUENCY vs.VELOCITY

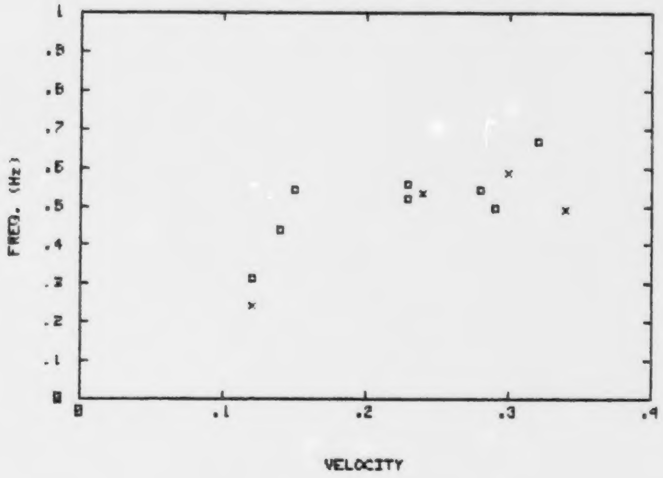

SEGMENT 1 - h=35 & 45 mm.
PEAK FREQUENCY vs.VELOCITY

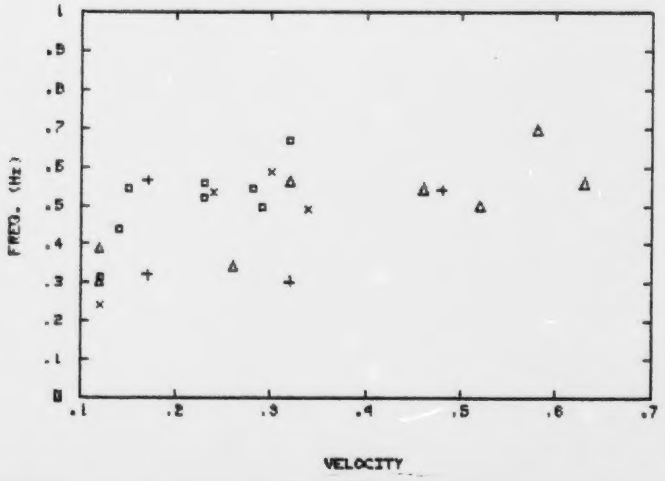

7.3 Normal Force

7.3.1 Variation of Mean Force Per Unit Segment Length with Test Parameters

In Table 7.1, the mean normal force per unit length is compared for a number of test runs, investigating repeatability, unbroken ice and channel width effects, thickness and speed effects.

Repeatability: Two of the three data sets used show good repeatability on Segments 1 and 2, poorer on Segments 3 and 4. This is due to the lower frequency of high force impacts on Segments 3 and 4 and it is expected that longer run lengths would reduce the difference in these forces. The third run shows a poor repetition, thought due to possible slight yaw angle on the model.

The effect of using a broken channel versus unbroken ice confirms the earlier comment that, while the results are comparable, they do not match very well, the channel data apparently exhibiting higher loads.

The effect of thickness is to show increased force on all segments, although in the example chosen Segment 1 shows only a small increase.

The effect of speed is directly compared and shows significant increase in Segments 2 and 3 where the majority of turning is taking place, while the loss of normal force in Segment 4 is attributed to the altered flow of cusps along the hull.

7.3.2 Sensitivity to Sampling Interval

It was noted in Section 6 that the intervals over which mean values were calculated were selected primarily upon the appearance of steady-state forces on all segments. The irregular force frequency on Segments 3 and 4, combined with short run times (relative to that frequency) has made the sampling interval for data calculation fairly critical. To illustrate this point, a sensitivity analysis of interval selection was performed on a selected test.

Figure 7.4 shows the calculated normal forces on the four segments as a function of selected data interval. Segments 1 and 2 are relatively insensitive to the selected interval, particularly when the beginning point is chosen well into the run. Segments 3 and 4 show very high sensitivity to interval selection, with differences as great as 150% observed. As the interval increases however, the results tend towards a specific value.

TABLE 7.1

DIRECT COMPARISON OF SEGMENT MEAN NORMAL FORCES

				CORRECTED VALUES OF Fn/UNIT LENGTH (N/m) SEGMENT NUMBER			
TEST	h mm	σ kPa	V m/sec	1	2	3	4
TO SHOW REPEATABILITY							
2C6	48.5	34.0	0.23	65.6	57.7	62.0	67.4
2C8	47.2	45.0	0.23	67.7	55.0	34.2	138.3
3C1	65.3	38.7	0.11	83.5	77.8	54.7	52.1
3C2	56.3	47.4	0.11	71.5	78.7	33.9	105.7
2S1	40.8	31.3	0.12	17.3	26.5	14.5	106.9
2C3	48.2	30.0	0.12	46.7	54.5	31.4	88.5
TO SHOW EFFECT OF UNBROKEN ICE AND CHANNEL WIDTH							
1S2	31.7	48.2	0.32	26.7	29.9	14	22.2
1C5	34.5	36.0	0.32	40.8	31.7	22.7	29.4
THICKNESS EFFECT							
1S1	36.0	30.4	0.17	44.3	29.9	27.3	15.1
3S2	54.1	30.9	0.19	47.7	89.3	59.7	167.0
SPEED EFFECT							
2S1	46.8	31.3	0.12	17.3	26.5	14.5	106.9
2S3	45.8	32.1	0.34	19.2	67.6	54	31.0

FIGURE 7.4

INTERVAL ANALYSIS - SEGMENTS 1, 2, 3, AND 4

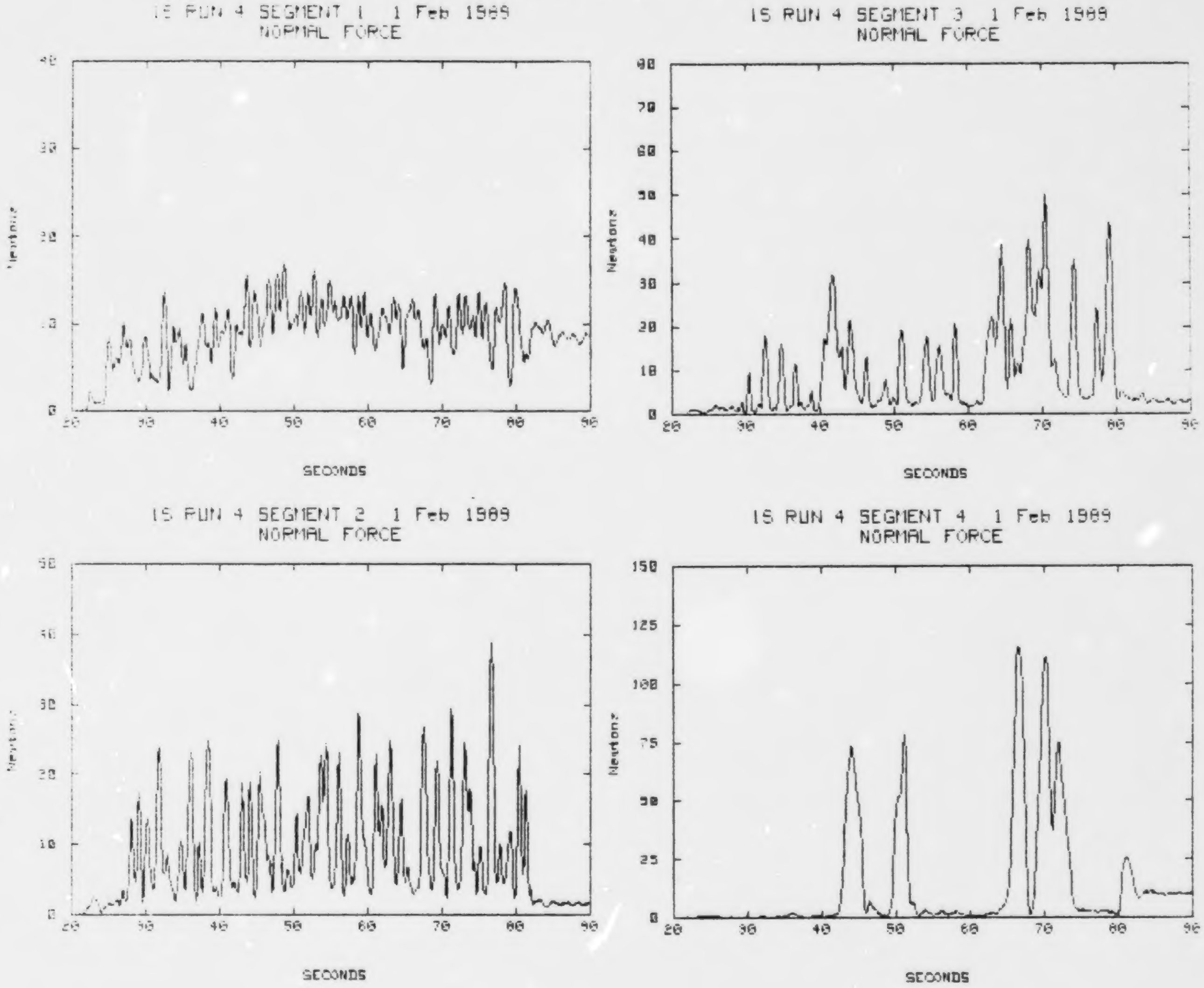

INTERVAL ANALYSIS for RUN 1S4

INTERVAL (sec)	SEG1 (n)	SEG2 (n)	SEG3 (n)	SEG4 (n)
30 - 80	9.7	10.4	12.3	27.9
40 - 80	10.4	10.7	13.0	28.2
30 - 40	6.9	9.4	7.3	2.1
40 - 50	10.8	9.5	11.2	26.8
50 - 60	11.5	11.8	7.7	18.5
60 - 70	9.6	10.8	17.0	42.0
70 - 80	9.8	11.0	16.0	24.9

7.3.3 Regression Analysis

Regression analysis was done for the mean normal forces and peak normal forces on all segments, with both cases being divided into 'S' and 'C' runs. The form of all regression equations was:

$$Fn = C1 + C2 \cdot h + C3 \cdot v + C4 \cdot s \tag{7.1}$$

where Fn = mean unit normal force (or mean peak) in Newtons
h = ice thickness in metres
v = model velocity in metres/sec.
s = ice flexural strength in kPa
and C1 to C4 are the regression coefficients.

Table 7.2 lists the values of the regression coefficients along with the correlation coefficient and standard error of estimate for these equations. The correlation values reflect the scatter in the data, but in most cases, they indicate reasonable predictive ability. One should keep in mind that there are about twice as many 'C' runs as 'S' runs and therefore, the predictive ability on 'C' runs is somewhat better.

Figure 7.5 shows examples of the plots in which the effect of varying a single parameter upon predicted force is demonstrated.

Table 7.3 lists the 'best' regression fits for all segments against a number of parameter and parameter combinations - to explore the possibility of a 'better' curve fit than that of Equation 7.1. The lack of any significant influence of velocity on the data is notable.

Table 7.2

Regression Analysis Results

Mean Segment Normal Force - 'S' Runs

	C1	C2	C3	C4	R^2	Error
Segment 1	-42.6	1015.9	16.3	0.82	.213	17.1
Segment 2	-20.2	1332.5	116.9	-0.60	.536	17.0
Segment 3	-21.1	1267.2	59.4	-0.46	.639	12.1
Segment 4	-244.5	5606.4	-106.2	2.84	.836	27.2

Mean Segment Normal Force - 'C' Runs

	C1	C2	C3	C4	R^2	Error
Segment 1	-58.6	1920.3	39.6	0.39	.768	9.9
Segment 2	-79.0	1936.6	72.1	0.79	.734	11.5
Segment 3	-37.0	1100.3	30.2	0.33	.401	12.9
Segment 4	-55.2	1398.8	15.5	1.26	.256	32.3

Mean Peak Segment Normal Force - 'S' Runs

	C1	C2	C3	C4	R^2	Error
Segment 1	-164.6	3861.8	-20.5	1.82	.753	22.1
Segment 2	-97.9	3669.3	148.5	-0.43	.673	28.5
Segment 3	-67.9	3396.0	43.0	-0.54	.624	33.3
Segment 4	-907.5	21645.6	-285.4	8.17	.732	145.0

Mean Peak Segment Normal Force - 'C' Runs

	C1	C2	C3	C4	R^2	Error
Segment 1	-113.0	3830.3	31.3	0.76	.737	23.2
Segment 2	-159.6	4411.4	37.2	1.67	.793	24.5
Segment 3	-65.6	2633.2	31.8	0.26	.529	23.7
Segment 4	0.7	5594.5	-147.7	-2.05	.263	118.8

FIGURE 7.5
EFFECT OF VELOCITY UPON MEAN NORMAL FORCE

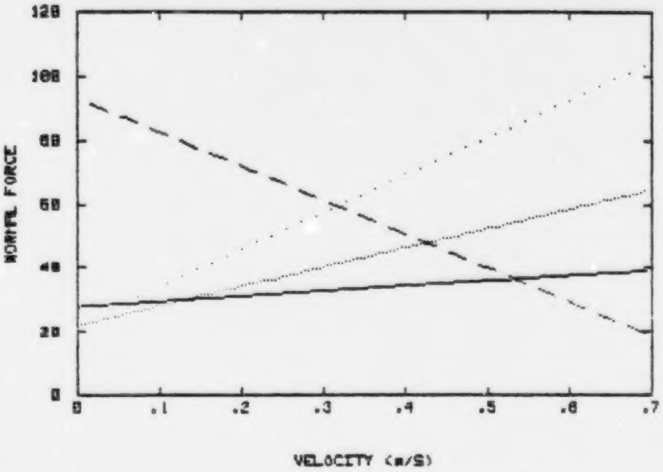
Predicted UNIT NORMAL FORCE from 'S' RUNS
h - .045 m   Sigma - 30 kPa

			'S'	'C'
SEGMENT 1	———————	R^2 =	.213	.788
SEGMENT 2	··············	R^2 =	.536	.734
SEGMENT 3	┈┈┈┈┈┈┈	R^2 =	.639	.401
SEGMENT 4	– – – – – –	R^2 =	.836	.256

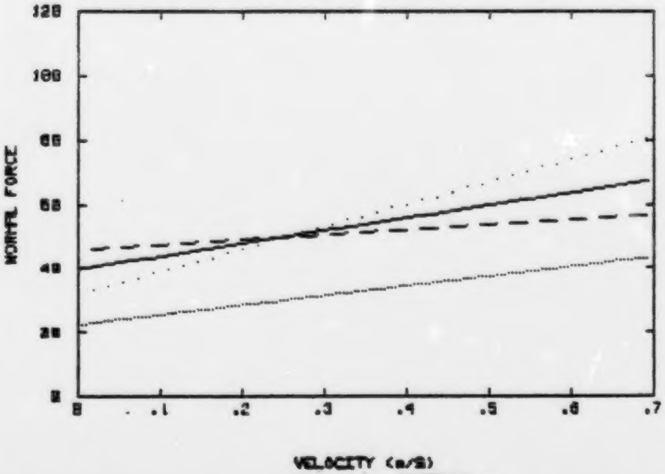
Predicted UNIT NORMAL FORCE from 'C' RUNS
h - .045 m   Sigma - 30 kPa

TABLE 7.3

PARAMETERS SHOWING HIGHEST CORRELATION RELATIONSHIP WITH DATA

ALL RUNS				UNBROKEN ICE				CHANNEL			
SEGMENT				SEGMENT				SEGMENT			
1	2	3	4	1	2	3	4	1	2	3	4
HIGHEST CORRELATION											
σh^2	h	h	h	σh	$Vh^{1.5}$	h	σh^2	h	σh^2	E/σ	σh^2

7.4 Friction Magnitude and Direction

As noted in Section 6.7 the direction of the friction forces typically oscillates about the waterline. Analysis of friction results was conducted upon two sets of data, upward and downward occurring events. The calculated value of friction coefficient was unaffected by direction of friction for all segments.

The range of coefficient of friction values varies as a function of segment longitudinal position. Segment 1 shows the most variance in range with mean values between .17 and 1.24 measured. Segment 2 shows a range from .10 to .66, and Segment 3 values lie between .15 and .43. This is perhaps not surprising given the increase in normal loads from Segment 1 to 3. As the load decreases the resolution error associated with transducer accuracy increases.

The direction of the friction force (friction vector) was symmetrical about the waterline in thin ice and became somewhat more asymmetrical in thicker ice. This is possibly due to the lower data sample size in thicker ice. Segments 1 and 2 show friction vectors that point forward while Segment 3 points aft (Figure 7.6). The finding of forward friction vectors is consistent with [2], but does not agree with intuition or theory. To determine if this result was due to transducer error, an error analysis for Segments 1 and 2 was performed. The load measured on any transducer was varied by ± 25% and new friction calculations made using the friction algorithm. Table 7.4 presents these results. Segment 1 friction direction shows sensitivity to transducer error particularly in the upward cases. Segment 2 with the most forward friction vectors, shows less sensitivity to transducer error. The forward friction vectors do not seem to be caused by transducer error and remain unexplained. This is an area where further investigation is warranted, as it was hoped that the technique could lead to a greater understanding of friction effects.

FIGURE 7.6

AVERAGE FRICTION VECTORS

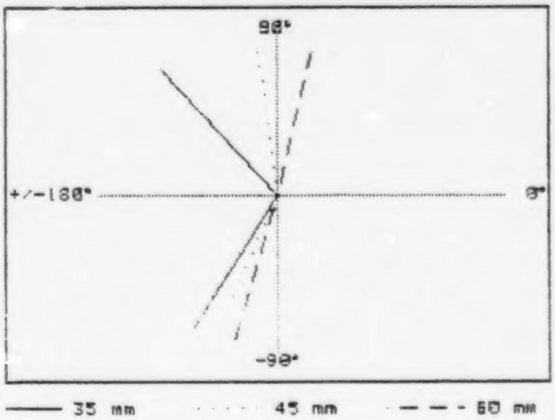
Friction Vector - SEGMENT 1

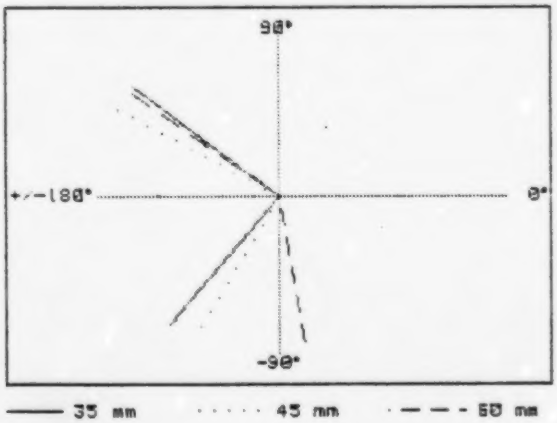
Friction Vector - SEGMENT 2

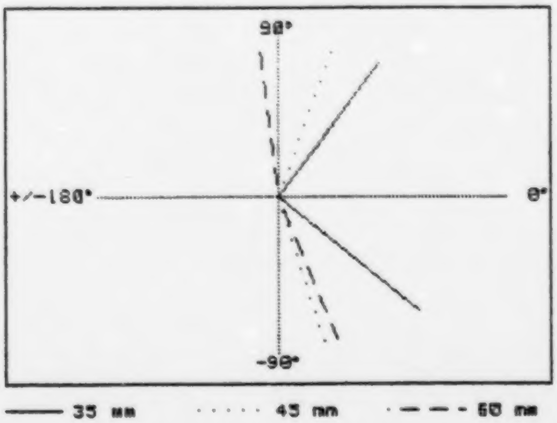
Friction Vector - SEGMENT 3

TABLE 7.4

SENSITIVITY ANALYSIS OF TRANSDUCER ERROR - SEGMENTS 1 AND 2

Segment 1 - Test 1S3

	Mu up	Mu dn	Psi up	Psi dn
Original Data	.17	.23	147.8	-115.6

	Mu up		Mu dn		Psi up		Psi dn	
	+25%	-25%	+25%	-25%	+25%	-25%	+25%	-25%
R11c	.13	.21	.20	.27	132.9	152.8	-102.4	-125.6
H11c	.20	.14	.34	.14	160.7	124.6	-112.0	-114.4
H12c	.16	.17	.23	.23	147.2	148.6	-115.9	-114.8
V11c	.18	.15	.20	.27	147.0	147.1	-121.2	-111.0
V12c	.12	---	.20	.28	109.8	-----	-113.7	-112.9
V13c	.22	.09	.23	.22	150.0	70.1	-115.5	-115.8
RV1t	.17	.17	.23	.23	147.5	147.7	-115.7	-115.8
HV1t	.17	.16	.23	.23	148.5	147.3	-115.7	-115.2

Segment 2 - Test 1S3

	Mu up	Mu dn	Psi up	Psi dn
Original Data	.33	.27	120.8	-112.3

	Mu up		Mu dn		Psi up		Psi dn	
	+25%	-25%	+25%	-25%	+25%	-25%	+25%	-25%
R21c	.32	.35	.25	.30	110.4	126.9	-104.0	-121.0
R22t	.32	.34	.27	.28	119.2	122.2	-120.0	-115.3
H21c	.32	.35	.30	.23	124.0	118.2	-114.9	-110.9
H22c	.31	.36	.32	.20	126.5	114.2	-113.7	-110.9
H23t	.33	.33	.28	.27	121.3	120.3	-113.2	-111.4
V21c	.33	.32	.23	.32	123.9	119.5	-120.5	-106.9
V22c	.34	.33	.27	.27	118.2	122.2	-112.4	-114.1
V23t	.39	.28	.25	.28	118.2	123.3	-116.6	-111.6

7.5 Resistance

7.5.1 Trends in Total Resistance

The total resistance data was subjected to regression analysis using a number of variables. The generally accepted resistance formulation:

$$R = C_o + C_1h^2 + C_2Vh \qquad (7.2)$$

as discussed in [5] and [6], based on a review of a large data base, correlated well with a correlation coefficient of .8186 on the unbroken ice sheet and .685 on the channel runs. This results in the following equation for model scale:

$$R_{Tms} = -33.85 + 32384 \times h^2 + 4199\ vh \qquad (7.3)$$

and at full scale:

$$R_{Tfs} = -270.8 + 647.69 \times H^2 + 375.69\ VH \qquad (7.4)$$

Figure 7.7 shows the plot of total resistance (model) versus speed for the unbroken ice sheets. The equation is really only applicable over the range of speeds (and thicknesses) experienced. The data is also plotted. The negative intercept at zero speed can be ignored as this is outside the range of applicability, and at near zero speed the resistance tends to a constant value.

Figure 7.8 shows the regression of the unbroken ice sheet with that for twice the resistance measured in the channel corrected for open water resistance. The different speed dependence is noted and is perhaps a suitable subject for further investigation. Another form of regression equation, incorporating strength effects, was examined and resulted in the following equation:

$$R_{Tms} = -138.4 + 3726.8\ h + 4344.15\ vh + .00602\sigma^2 \qquad (7.5)$$

This equation was plotted in full scale units against other 1/20th scale data from model tests reported in [7] in Figure 7.9. Again the near zero speed negative resistance can be ignored. It must be recognized also that, in the current tests, the model was fully constrained. In the IMD tests reported in [7] the model was constrained only in surge, sway and yaw. Note also that, in model ice E/σ is directly determined by σ and h and thus is not an independent variable.

The results of this analysis show that the current test series produces total resistance data somewhat below that previously measured, and with greater velocity dependence. Fully restraining the model may have contributed to this result. The effect of restraint should be investigated further.

FIGURE 7.7

REGRESSION CURVES OF MODEL RESISTANCE

(NOTE: Figures next to data points are thickness, h, in mm)

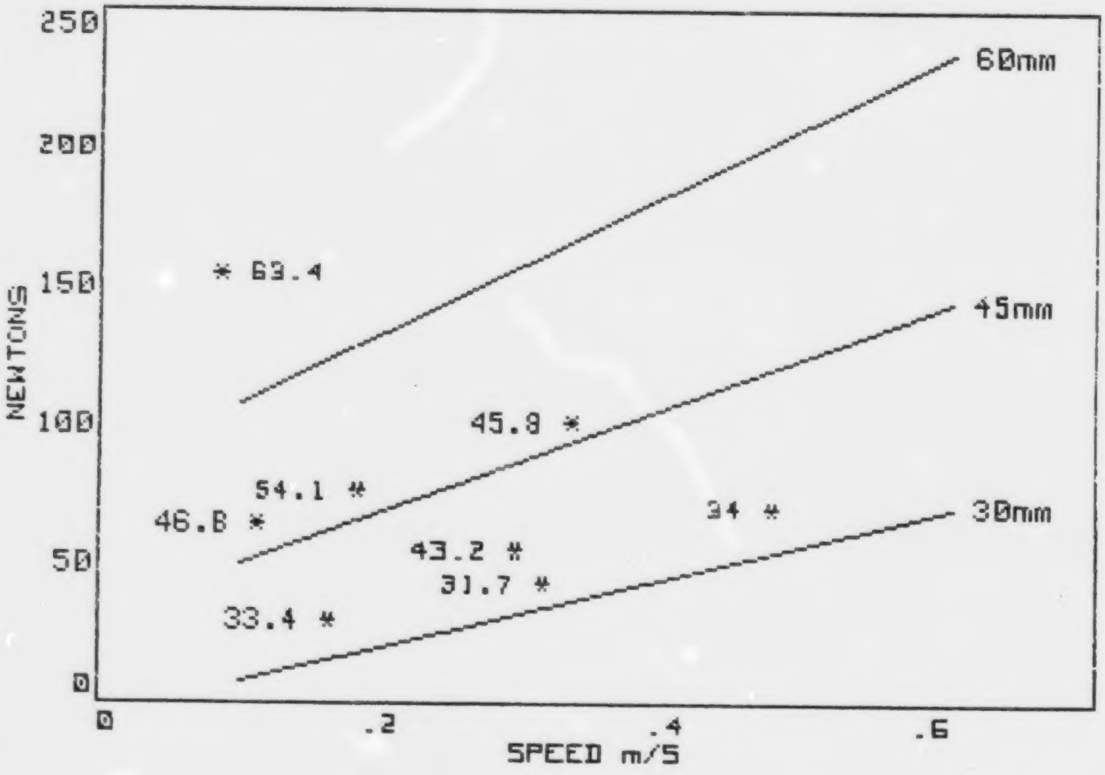

FIGURE 7.8

COMPARISON OF UNBROKEN ICE AND CHANNEL RUNS

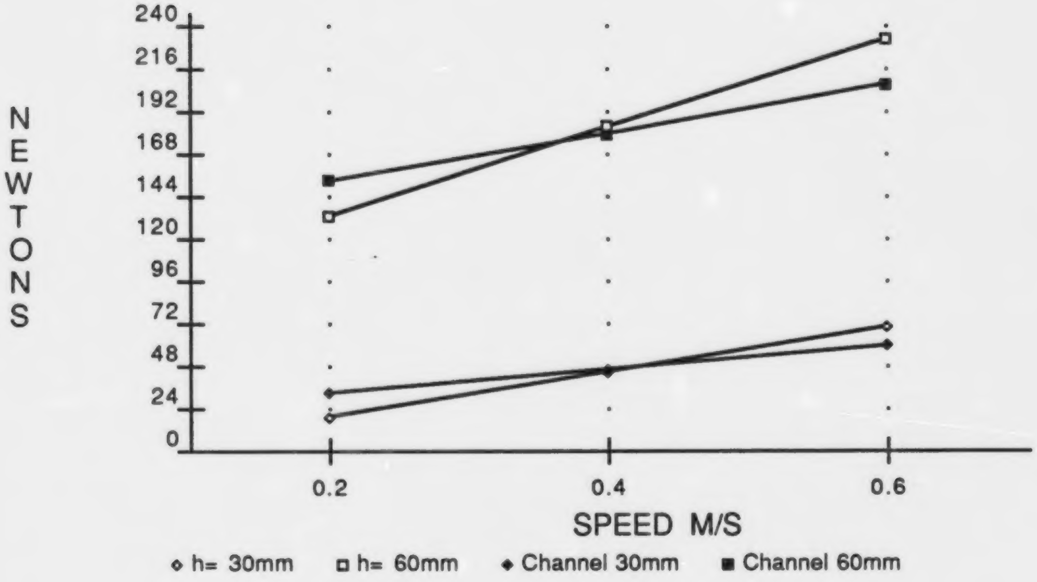

FIGURE 7.9

COMPARISON OF THE MODEL SCALE RESULTS AT A STRENGTH OF 800 kPa

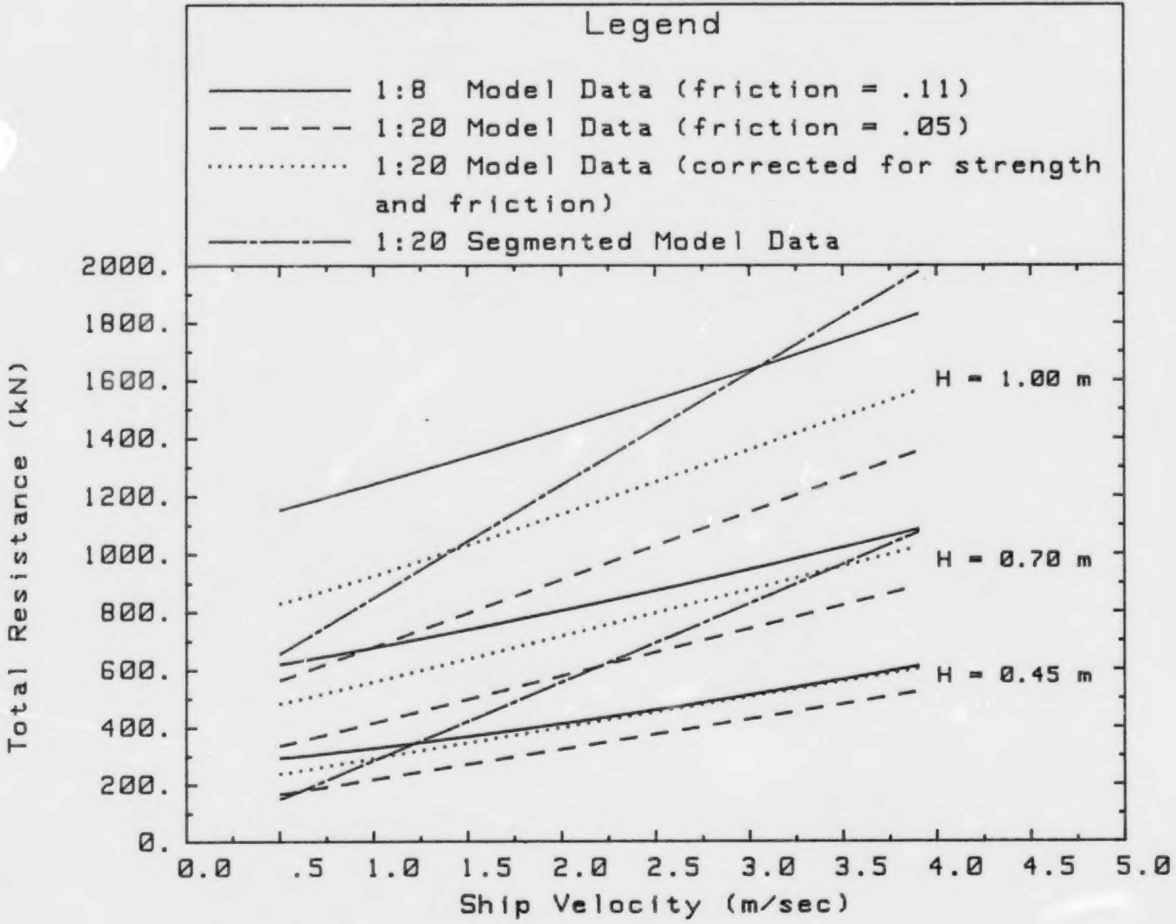

7.5.2 Contribution to Resistance from Segments

The analysis separated the continuous icebreaking runs from those in the channel. The full data set is presented in Table 7.5. Note that total resistance for the run 2S2 in which the force block failed, has been calculated from the regression equation (7.3) described in the previous section. There were six good data points for the unbroken ice runs. In the other (four) cases, calculated Segment 1 resistance was negative. As noted before the resistance component of Segment 4 was not recorded, but the value calculated from normal force and an assumed friction coefficient is given. The results show the following contributions to resistance on average.

	SEGMENT 1	2	3	TOTAL 1-3	4	TOTAL 1-4	REMAINING
MEAN	9.17%	16.09%	16.97%	42.2%	18.19%	60.4%	39.6%
STD. DEV.	5.5%	7.3%	6.4%		12.39%		17.7%

In the channels there were fifteen good points when only the measured segment data was used with the following results:

	SEGMENT 1	2	3	TOTAL 1-3	4	TOTAL 1-4	REMAINING
MEAN	11.92%	11.39%	11.77%	35%	10.21%	45.2%	54.7%
STD. DEV.	6.79%	8.01%	6.66%		11.21%		

We assume that the total resistance on the carriage in unbroken ice is given by:

$$R_{Tms} = R_{ow} + 2 \times [R_1 + R_2 + R_3 + R_4] + 2 \times R_{RES} \qquad (7.6)$$

where R_{ow} = ice free water resistance

R_{RES} = resistance for all other parts of half of the hull

In the channel runs:

$$R_{TC} \simeq R_{ow} + R_1 + R_2 + R_3 + R_4 + R_{RES} \qquad (7.7)$$

[ignoring the channel wavemaking resistance.]

Then on average we have $R_{RES} + R_{ow}$ = 39.6% of R_{Tms} in unbroken ice and 54.7% of R_{Tms} in broken ice.

TABLE 7.5

CONTRIBUTIONS TO RESISTANCE FROM SEGMENTS

RUN	TOTAL RES	SEG 1	% 1	SEG 2	% 2	SEG 3	% 3	SEG 4 CALC	%4	REMAIN	R%
1S1 *	23.87	-0.23		3.87	32.43%	8.57	71.81%	1.3	10.89%	-3.15	
1S2	42.91	3.54	16.50%	4.08	19.02%	2.59	12.07%	1.9	8.86%	18.69	43.56%
1S3	70.36	4.91	13.96%	5.07	14.41%	5.22	14.84%	4.5	12.79%	30.96	44.00%
1S4	29.98	1.48	9.87%	3.72	24.82%	3.53	23.55%	5.6	37.36%	1.32	4.40%
2S1	64.47	2.65	8.22%	1.61	4.99%	3.64	11.29%	9.3	28.85%	30.07	46.64%
2S2 **	81.43	1.83	4.49%	4.69	11.52%	5.56	13.66%	6.5	15.96%	44.27	54.37%
2S3	101.1	0.99	1.96%	11.02	21.79%	13.37	26.44%	2.7	5.34%	44.98	44.47%
2S4 *	54.99	3.74	13.60%	6.13	22.29%	6.16	22.40%	6.3	22.91%	10.33	18.79%
3S1 *	155.2	-7.57		8.63	11.12%	11.27	14.52%	14.6	18.81%	101.3	65.30%
3S2 *	76.2	-1.17		17.49	45.91%	8.31	21.81%	14.6	38.32%	26.94	35.35%
MEAN OF	6	RUNS	9.17%		16.09%		16.97%		18.19%		39.57%
STD DEVIATION			5.51%		7.27%		6.40%		12.39%		17.69%
CHANNEL RUNS											
1C3	24.3	1.85	7.61%	1.82	7.49%	2.23	9.18%	0.9	3.70%	17.5	72.02%
1C4	36.62	2.99	8.16%	3.35	9.15%	3.41	9.31%	2.5	6.83%	24.37	66.55%
1C5	34.08	5.12	15.02%	3.09	9.07%	3.86	11.33%	2.6	7.63%	19.41	56.95%
1C6	44.22	6.37	14.41%	3.58	8.10%	4.06	9.18%	3.2	7.24%	27.01	61.08%
1C7	26.88	8.55	31.81%	7.44	27.68%	4.34	16.15%	5.2	19.35%	1.35	5.02%
1C8 *	9.32	1.37	14.70%	2.7	28.97%	2.4	25.75%	4.3	46.14%	-1.45	
2C1	41.43	1.94	4.68%	1.28	3.09%	2.44	5.89%	7.1	17.14%	28.67	69.20%
2C2	45.39	4.8	10.58%	3.59	7.91%	3.43	7.56%	3.5	7.71%	30.07	66.25%
2C3	55.33	3.61	6.52%	2.8	5.06%	5.05	9.13%	7.7	13.92%	36.17	65.37%
2C4	77.99	5.28	6.77%	4.16	5.33%	7.17	9.19%	2.4	3.08%	58.98	75.63%
2C5	67.29	5.82	8.65%	10.4	15.46%	16.08	23.90%	2.5	3.72%	32.49	48.28%
2C6	61.1	4.9	8.02%	7.85	12.85%	15.89	26.01%	5.9	9.66%	26.56	43.47%
2C7	42.29	5.8	13.71%	4.32	10.22%	4.04	9.55%	1.7	4.02%	26.43	62.50%
2C8	51.23	8.88	17.33%	4.49	8.76%	5.53	10.79%	12.1	23.62%	20.23	39.49%
3C1	95.56	6.48	6.78%	15.9	16.64%	6.81	7.13%	4.5	4.71%	61.87	64.74%
3C2	44.08	8.24	18.69%	10.58	24.00%	5.39	12.23%	9.2	20.87%	10.67	24.21%
MEAN OF	15	RUNS	11.92%		11.39%		11.77%		10.21%		54.72%
STD DEVIATION			6.79%		8.01%		6.66%		11.21%		19.53%
*	NOT USED IN DATA BASE										
**	TOTAL RESISTANCE ESTIMATED FROM REGRESSION EQUATION										

From the RICE runs, the open water resistance represents the following percentage of the total resistance: 0.13% at 0.1 m/s to 2.5% at 0.6 m/s and may be neglected in the above cases.

Clearly there is a significant resistance force arising around the rest of the hull. In particular, from the video it is clear that broken ice cusps that are pushed down around the bow would impart forces on the hull below the segments at the shoulders.

We draw the following conclusions:

- As before, the resistance of Segments 1-3 (both sides) accounts for about 40% of the total resistance, in unbroken ice, slightly less in the broken channel, since in this latter case the total resistance includes all the open water resistance and only half the ice resistance. The current data is compared with that previously reported in Figure 7.10.

- The 4th segment area resistance, while not directly measured, appears to contribute a further 18% on average for a total of about 60% over the forward waterline area. Thus a significant contribution (≈ 40%) to resistance is generated elsewhere on the hull.

- It appears that the contribution of Segment 1 increases relative to the others in the channel - this is difficult to believe since the breaking component is surely reduced, and throws additional suspicion on the results from Segment 1 in the unbroken ice.

- The drop in contribution to resistance at the shoulders, perhaps reflects a difference in breaking pattern in the channel side runs.

- As can be seen from Figure 7.10 there is no evidence of a trend in change in contribution from the segments with velocity. However at specific different velocities, the relative contribution from each segment varied, thought due to the change in breaking pattern and broken ice behaviour. The significance of this on a mathematical model relates to the need to recognize the change in breaking pattern with speed (and thickness) in order to model the appropriate contribution from each hull area.

  Once more, the data collected may be worthy of further investigation.

FIGURE 7.10

RATIO OF TOTAL SEGMENTS 1-3 RESISTANCE (x 2) TO TOTAL RESISTANCE

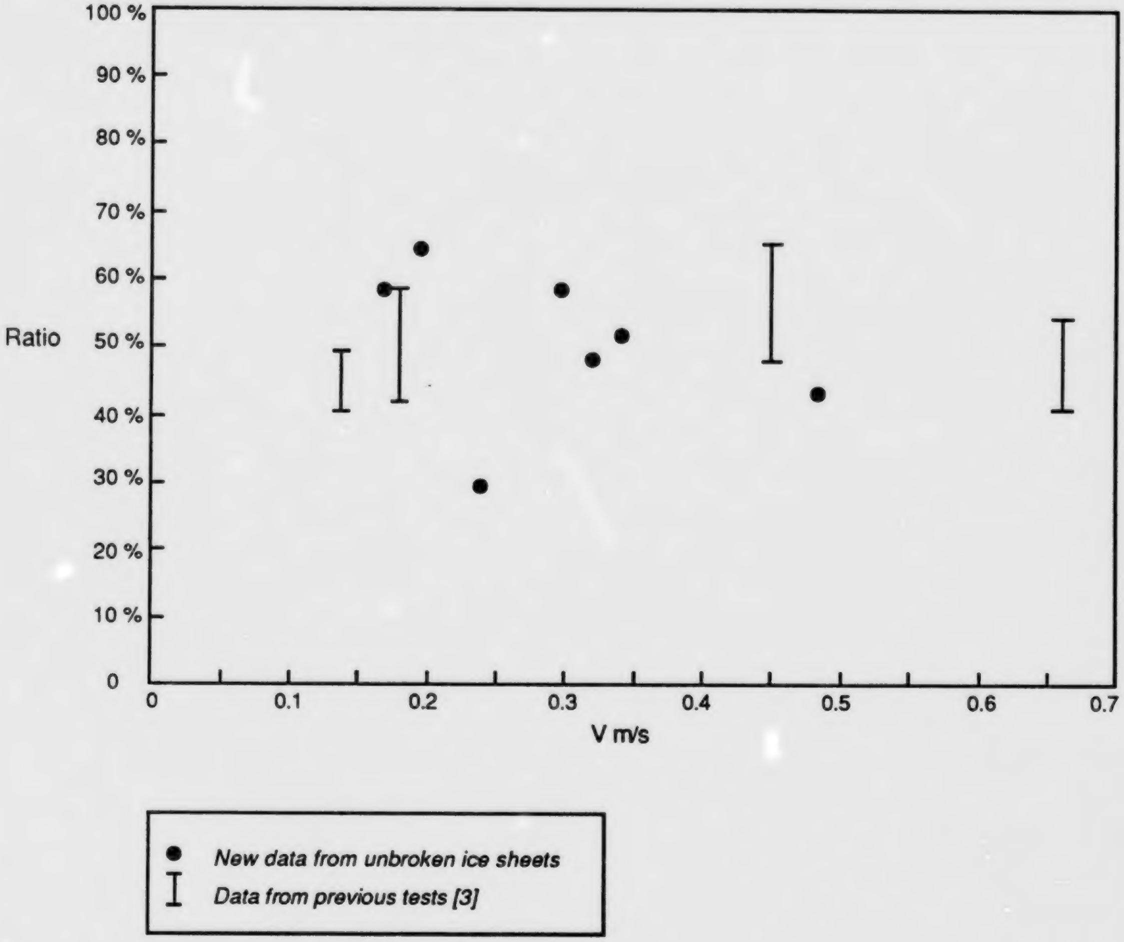

7.6 The RICE Model

7.6.1 The Principal of the Model

The RICE model [5,6] based on Naegle's thesis [9] follows an approach in which the motions of the ship and their effect on the breaking pattern are accounted for. The basic principle of the Naegle model involves a solution of the equations of motion for the surge components of the forces associated with icebreaking. These forces are written as functions of displacement, velocities and accelerations and the rigid body motion of the icebreaker. The ice force model developed breaks total ice forces on the ship into three components: one associated with breaking of the ice, a component associated with overturning the broken ice, and a component associated with the submergence of the ice. Each of these three components is further subdivided into two sub-components: one due to the normal forces perpendicular to the hull, and one due to frictional forces tangential to the hull. It is assumed that the ice breaks in a consistent and predictable manner called the icebreaking pattern. This pattern is generally accepted as the one in which the ice breaks in a series of cusps. The key to the icebreaking pattern and therefore to the icebreaking forces is associated with determining the geometric parameters of these cusps. In determining the breaking forces, the individual floes are assumed to behave as an edge loaded semi-infinite elastic plate resting upon an elastic foundation. The free edge is crushed when interacting with the hull until the stresses in the ice sheet exceed the ultimate strength of the ice in bending. This, of course, generates a normal force on the hull as well as a frictional force. Also included in the breaking force is the energy lost while accelerating the floe during breaking, expressed as an average resistance. The turning forces caused by the flared sides of the ship include an element for ventilation and the forces associated with submergence assume that the submerged floes remain in contact with the hull and slide under its entire length.

It will be noted that the rigid body motions of the model were restricted in this test series at the request of the Scientific Authority. We must therefore confine our discussion to a form of comparison of the icebreaking forces only, as the non-ice related forces (hydrodynamics, hydrostatic restoring forces and propulsion forces are not present in the model tests - other than water resistance).

The comparisons that can be made therefore, are based on the assumption that the load on each segment originates predominantly from one only of the components of resistance.

7.6.2 Total Resistance

RICE runs were made for two sets of measured conditions:

- Runs 1S2 - 1S4 - mean thickness 33 mm and σ_f = 48 kPa
- Runs 2S1 - 2S3 - mean thickness 46 mm and σ_f = 30 kPa

and at two friction coefficients.

The results are shown in Figure 7.11 along with two sets of measured data and are tabulated in Table 7.6.

The previously discussed over-influence of velocity on total resistance is the only factor that detracts from a favourable comparison of measured and calculated data in the 46 mm ice sheet. In the thinner, stronger ice sheet, however, the results are not good. The low E/σ ratio for these sheets may be part of the explanation. In addition, the use of RICE at model scale is suspect, as all the assumptions and coefficients pertain to full scale vessels, and such factors as buoyancy are incorporated.

However, it has been shown elsewhere that RICE predicts full scale resistance well, and so there was little to be gained from further analysis of the total resistance data.

7.6.3 Resistance Components

The principal attraction for comparing the RICE model and the segmented model results is that the former examines various components of resistance discretely, and associates these components with the physical interaction between the ship and the ice and therefore the location on the hull.

To begin with it was assumed that:

- Segment 1 force is associated with breaking,
- Segment 2 breaking and turning,
- Segment 3 with overturning, and
- Segment 4 with submergence.

In fact, third row cusp breaking occurs in Segment 3 and 4, but as discussed elsewhere, this is at a low frequency and contributes less to the mean resistance. By observation, Segment 2's contribution varies between both breaking and turning, depending on speed and thickness. We will assume, based on observation of all video footage that Segment 2 is similar to Segment 1.

FIGURE 7.11

RICE RUNS

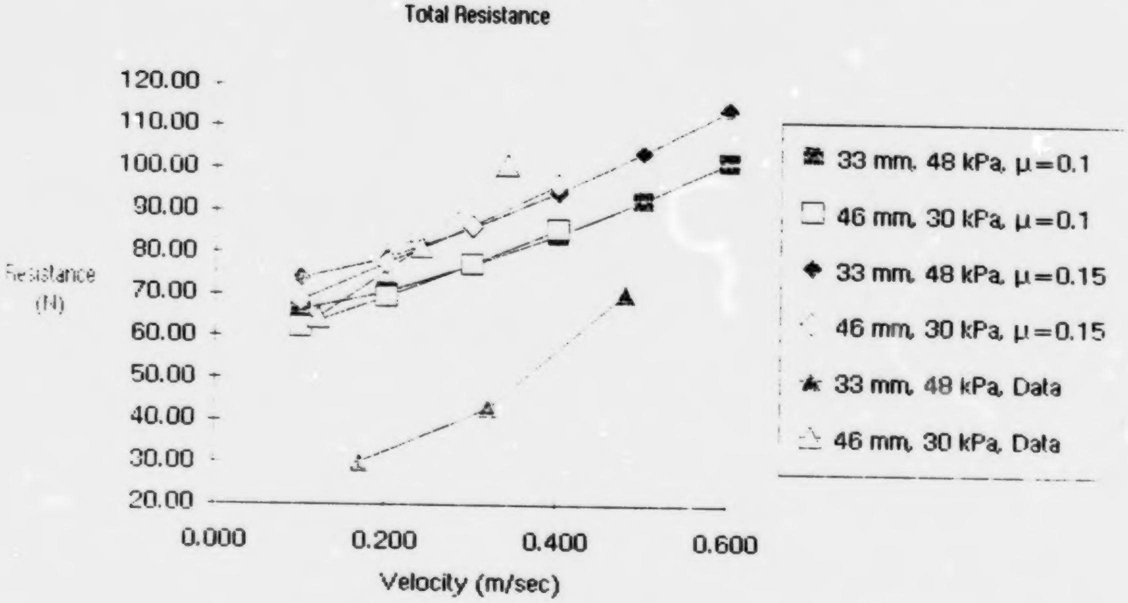

TABLE 7.6

RICE RESULTS FOR MODEL

Ice Thickness (m)	Velocity (m/sec)	Flexural Strength (kPa)	Hull Friction	Total Resistance (N)	Water Resistance (N)	Breaking Resistance (N)	Breaking Friction (N)	Turning Resistance (N)	Turning Friction (N)	Sliding Resistance (N)	Sliding Friction (N)
0.033	0.100	48	0.10	66.16	0.09	37.16	10.85	4.79	1.62	9.27	2.46
0.033	0.200	48	0.10	70.56	0.32	37.16	10.97	8.20	2.50	9.27	2.46
0.033	0.300	48	0.10	76.98	0.69	37.16	11.51	12.52	4.06	9.27	2.46
0.033	0.400	48	0.10	84.39	1.19	37.16	11.83	17.73	5.94	9.27	2.46
0.033	0.500	48	0.10	92.71	1.81	37.16	12.04	23.85	7.93	9.27	2.46
0.033	0.600	48	0.10	101.98	2.55	37.16	12.24	30.86	9.99	9.27	2.46
0.046	0.100	30	0.10	62.15	0.09	36.33	8.65	6.79	1.47	6.39	2.52
0.046	0.200	30	0.10	69.46	0.32	36.33	9.79	10.78	3.64	6.39	2.52
0.046	0.300	30	0.10	77.22	0.69	36.33	10.16	15.89	5.93	6.39	2.52
0.046	0.400	30	0.10	85.86	1.19	36.33	10.40	22.09	8.13	6.39	2.52
0.033	0.100	48	0.15	73.78	0.09	37.16	16.39	4.79	2.49	9.27	3.69
0.033	0.200	48	0.15	78.61	0.32	37.16	16.50	8.20	3.79	9.27	3.69
0.033	0.300	48	0.15	86.05	0.69	37.16	17.30	12.52	6.12	9.27	3.69
0.033	0.400	48	0.15	94.56	1.19	37.16	17.76	17.73	8.94	9.27	3.69
0.033	0.500	48	0.15	103.96	1.81	37.16	18.08	23.85	11.92	9.27	3.69
0.033	0.600	48	0.15	114.35	2.55	37.16	18.36	30.86	15.00	9.27	3.69
0.046	0.100	30	0.15	68.51	0.09	36.33	12.99	6.79	2.23	6.39	3.78
0.046	0.200	30	0.15	77.47	0.32	36.33	14.70	10.78	5.48	6.39	3.78
0.046	0.300	30	0.15	86.55	0.69	36.33	15.25	15.89	8.91	6.39	3.78
0.046	0.400	30	0.15	96.39	1.19	36.33	15.60	22.09	12.20	6.39	3.78

Each of these three contributions has a normal friction force. According to RICE:

- Breaking Forces $\alpha\ h^2$ and σ_c, or $\sigma_f h^2$
- Turning Forces $\alpha\ h\ v^2$
- Submergence $\alpha\ h$

Table 7.3 showed the top correlation for normal force for each segment, for all runs, unbroken ice and channel runs.

The correlation of resistance forces with the parameters identified above are shown in Figure 7.12.

The results are not conclusive, particularly for Segment 1, where there is a speed dependency on resistance that is not expected. However, the correlation of resistance force with thickness for Segment 3 and with strength and thickness for Segment 2 is encouraging. Segment 4 resistance was not measured due to the failure of one transducer.

Figures 7.13 to 7.15 show the results of the components of resistance from RICE, onto which have been plotted typical values for the appropriate segment (which is numbered), multiplied by two for both sides of the vessel.

There is no correlation, based on the assumption that the segments contribute as described earlier. For example, if we assume the resistance of Segments 1 and 2 is predominantly due to breaking we see a speed dependence not confirmed in Figure 7.13 by RICE. There appears to be better matching with the turning component and Segment 3 (Figure 7.14). A major difference relates to the sliding resistance and friction, which in RICE totals between 9 N and 13 N, while, if we assume all residual resistance to be a sliding type, totals between 12 and 40 N (33 mm) and 48 N and 61 N (46 mm).

The final comparison, for two cases, compares the percentage contribution from RICE components with the segments and is shown in Table 7.7.

FIGURE 7.12

RESISTANCE CORRELATION FACTORS FOR IMPORTANT PARAMETERS BY SEGMENT

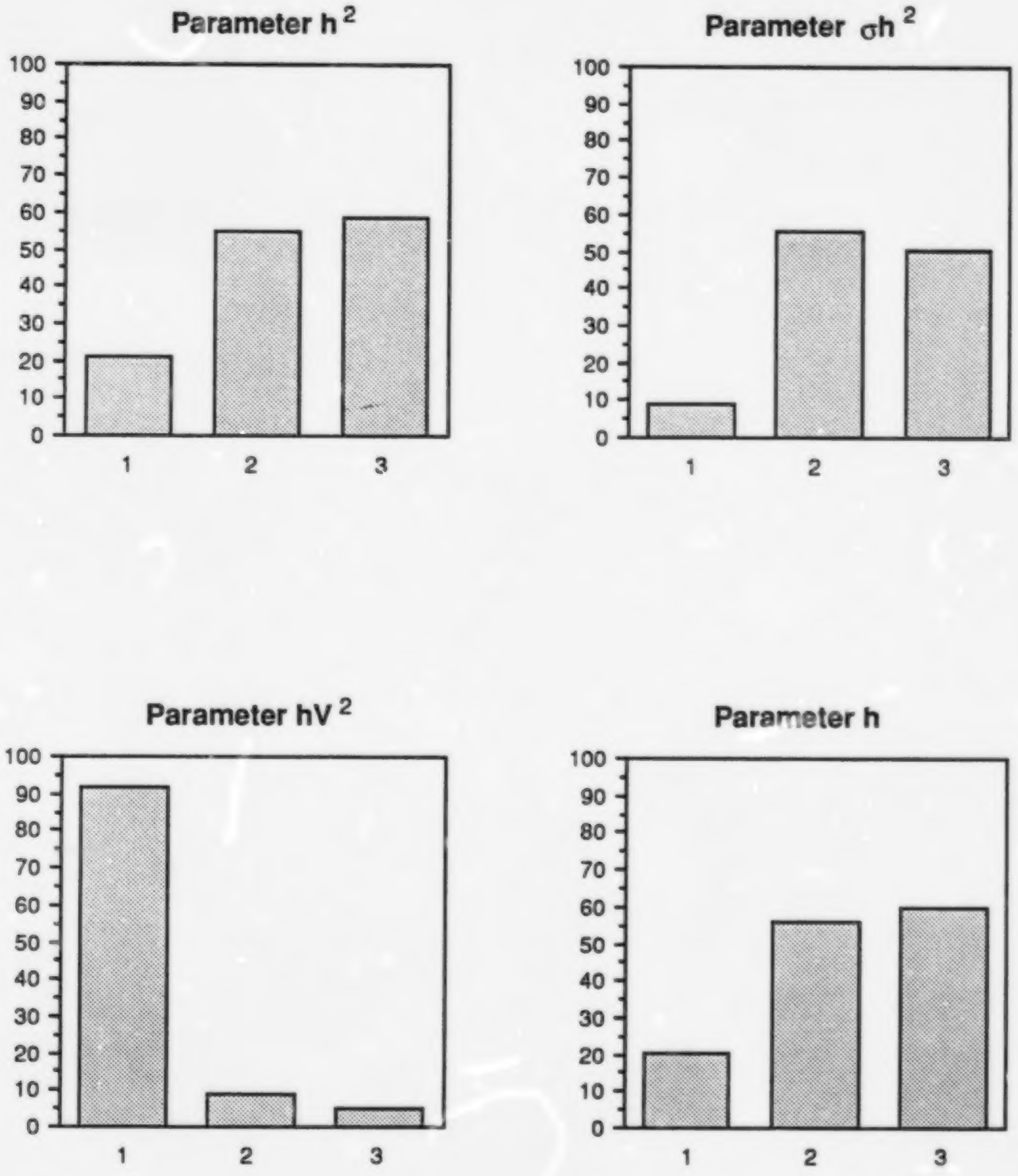

FIGURE 7.13

RESULTS OF THE COMPONENTS OF RESISTANCE FROM RICE

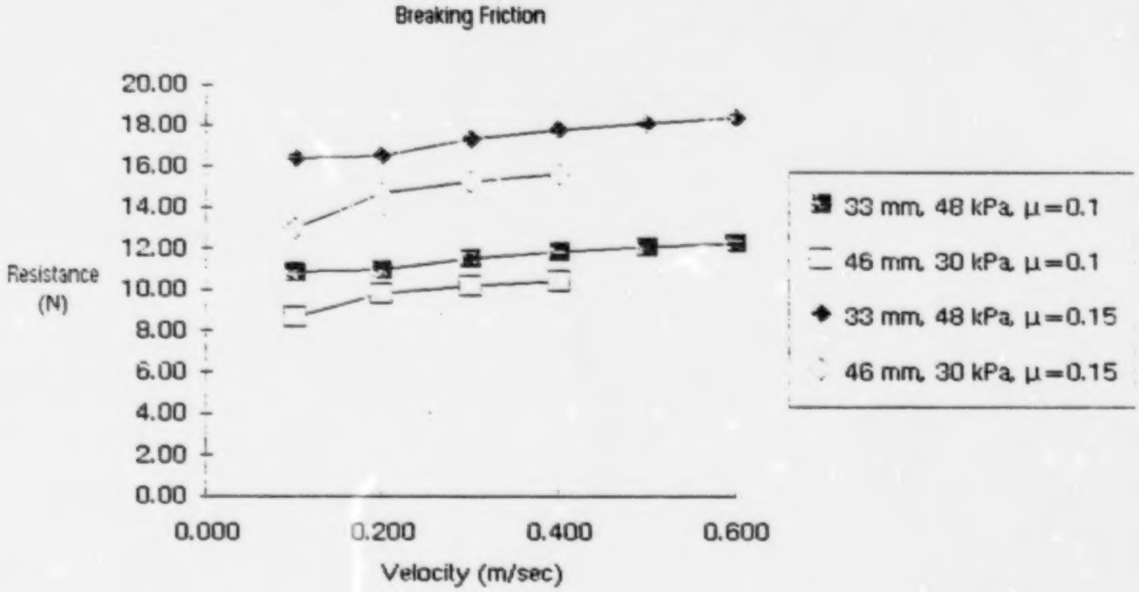

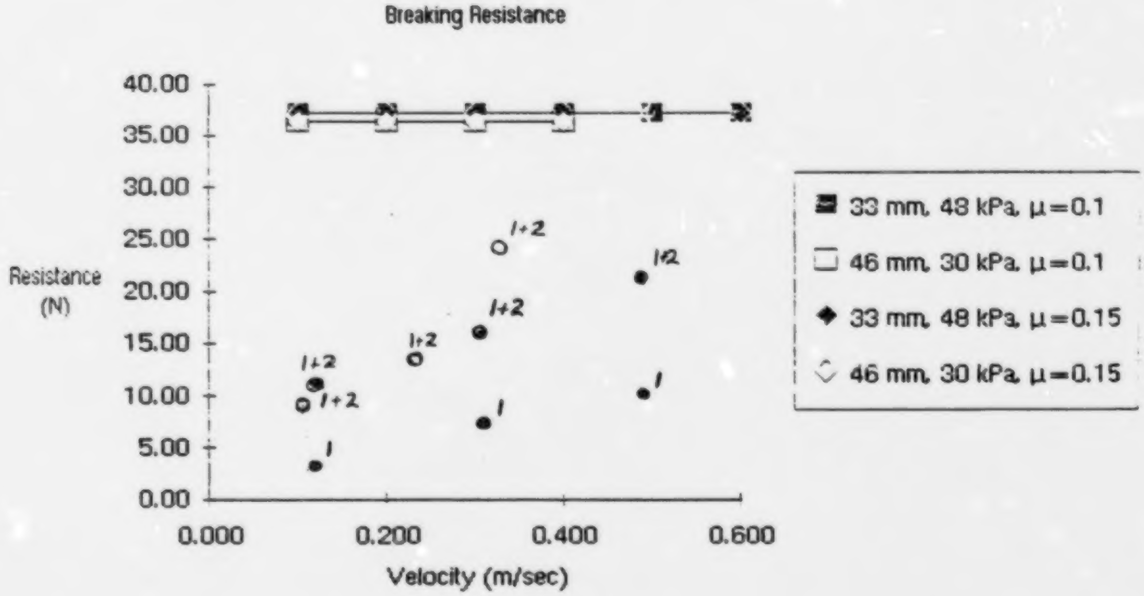

FIGURE 7.14

RESULTS OF THE COMPONENTS OF RESISTANCE FROM RICE

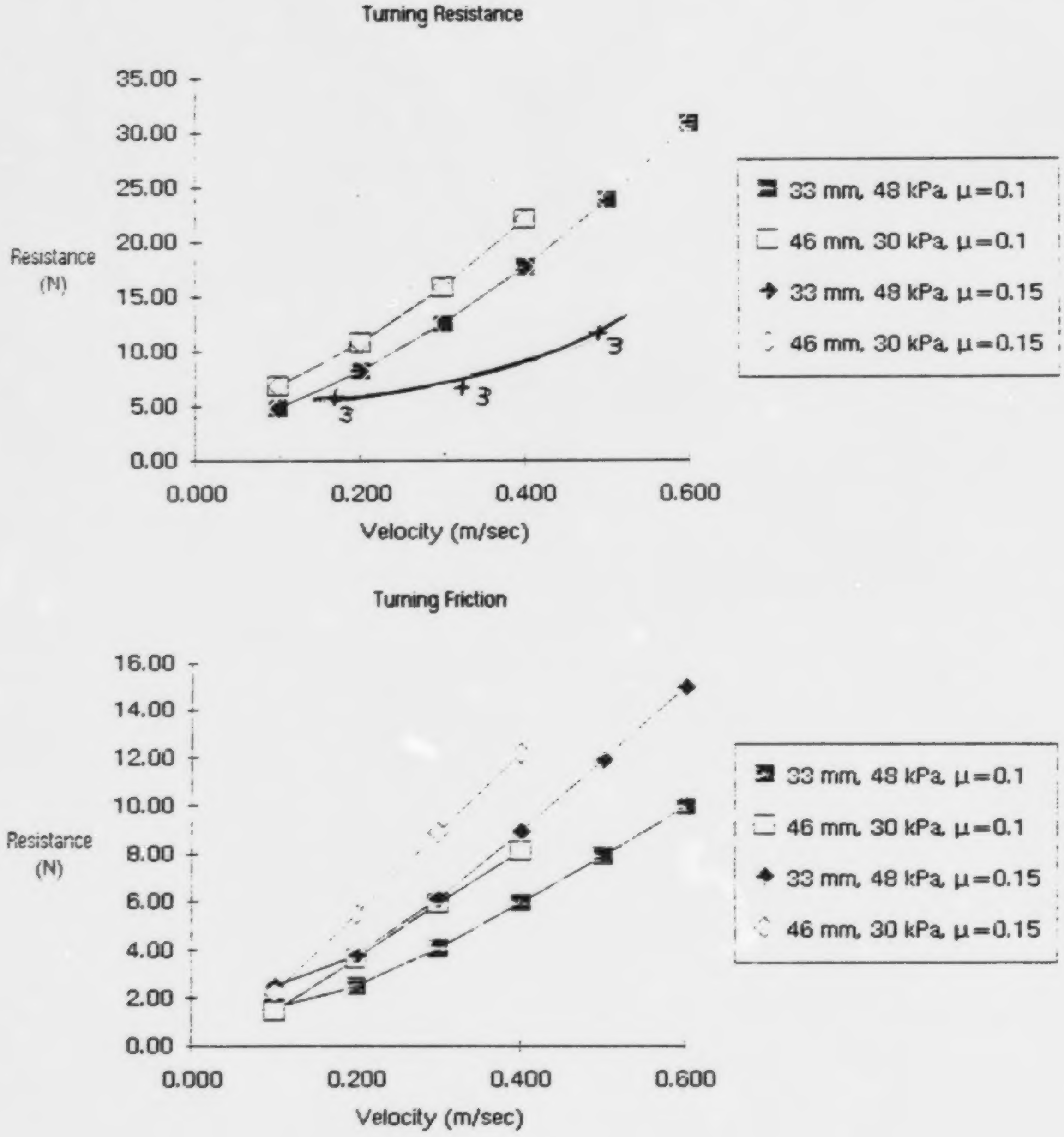

FIGURE 7.15

RESULTS OF THE COMPONENTS OF RESISTANCE FROM RICE

Sliding Resistance

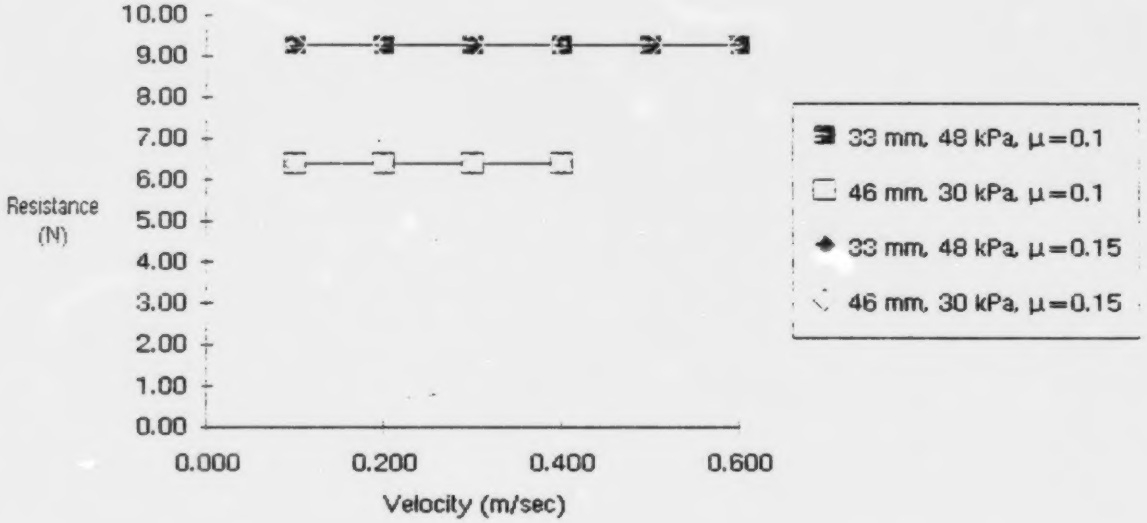

Sliding Friction

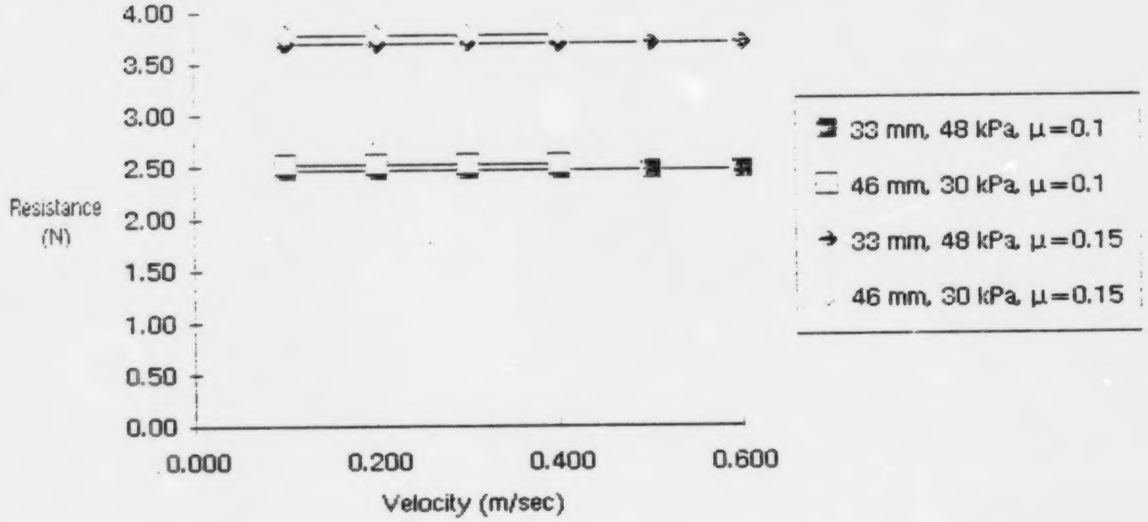

TABLE 7.7

COMPARISON OF RICE RESISTANCE COMPONENTS AND SEGMENT CONTRIBUTIONS

RUN 1S3				RUN 2S1			
SEG 1 & 2	SEG 3	SEG 4	REM	SEG 1 & 2	SEG 3	SEG 4	REM
28.37%	14.84%	12.79%	44%	13.12%	11.29%	28.85%	46.64%

RICE RUNS					
Breaking & Friction	Turning & Friction	Water Sliding & Friction	Breaking & Friction	Turning & Friction	Sliding & Friction & Open Water
53%	34%	14.6%	72%	13.2%	14.8%

Clearly, the assignation of segments to specific icebreaking components does not correlate well. More significantly, the RICE model attributes much more of the resistance to breaking than appears to be the case from the observed (measured) data.

Much of this discrepancy is due to the behaviour of the model ice, and the application of the full scale RICE model at model scale. Nevertheless, further manipulation of this data may be of value in assisting with understanding how the various components contribute and how the modelling material may affect the results. In addition, subsequent work to investigate the measured friction forces on the segments may be appropriate.

7.7 Carter's Model

7.7.1 General

An objective of this project was to compare the segmented model data with results predicted using the analytical prediction model developed by Dr. D. Carter - 'Carter's Model'. Carter's report on this is reproduced in full as received in Appendix A. Prior to testing, the model was exercised to predict the results for the target test conditions, and these were reported in the Interim Report [10].

The measured data from the test results was forwarded to Dr. Carter in order to report the comparison with measured data.

7.7.2 Total Resistance

Dr. Carter's report compares the full scale total resistance of the vessel as predicted and measured in the well reported trials of 'RADISSON' and 'FRANKLIN'. Figure 7.16 is reproduced from Figure 2.2 of the appendix. It is observed from this, and Figure 2.3 and 2.4 in the appendix that:

(1) The segmented model results show a relatively high scatter in ice force measurements.

(2) The speed dependency of the data appears to be too high and does not coincide with that of the full scale tests.

Figure 7.17 reproduced from Figure 2.5 of the appendix shows that the Carter model predictions for total resistance are twice that measured on the carriage.

Figure 7.18 shows measured total resistance for a number of the test cases from the current test series and the predictions by RICE and CARTER for the model testing conditions. This clearly shows that the model data are only about 50% of the predictions by both math models which, as shown previously, correlate with the full scale data.

FIGURE 7.16

COMPARISON BETWEEN FULL SCALE DATA, MODEL TEST RESULTS AND PREDICTIONS BY CARTER'S MATH MODEL

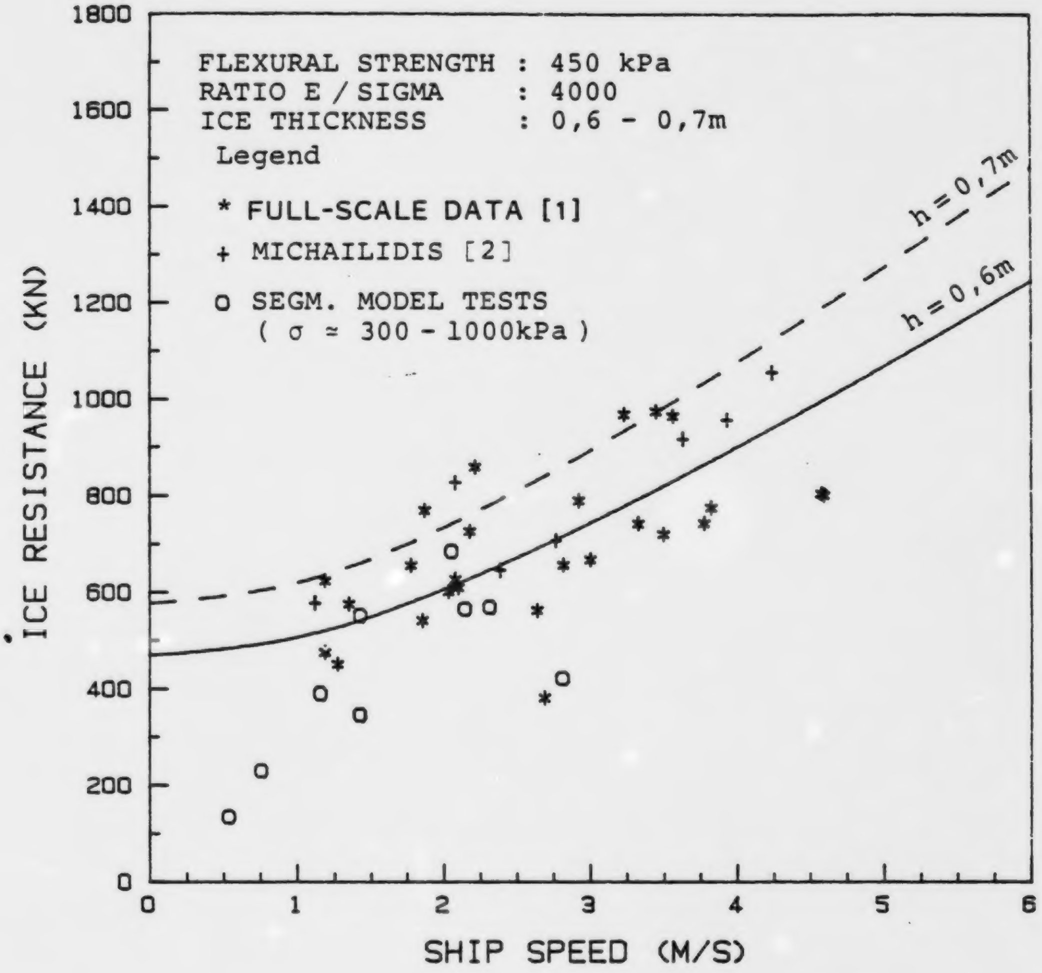

FIGURE 7.17

COMPARISON BETWEEN MODEL TEST RESULTS AND PREDICTIONS BY CARTER'S MATH MODEL

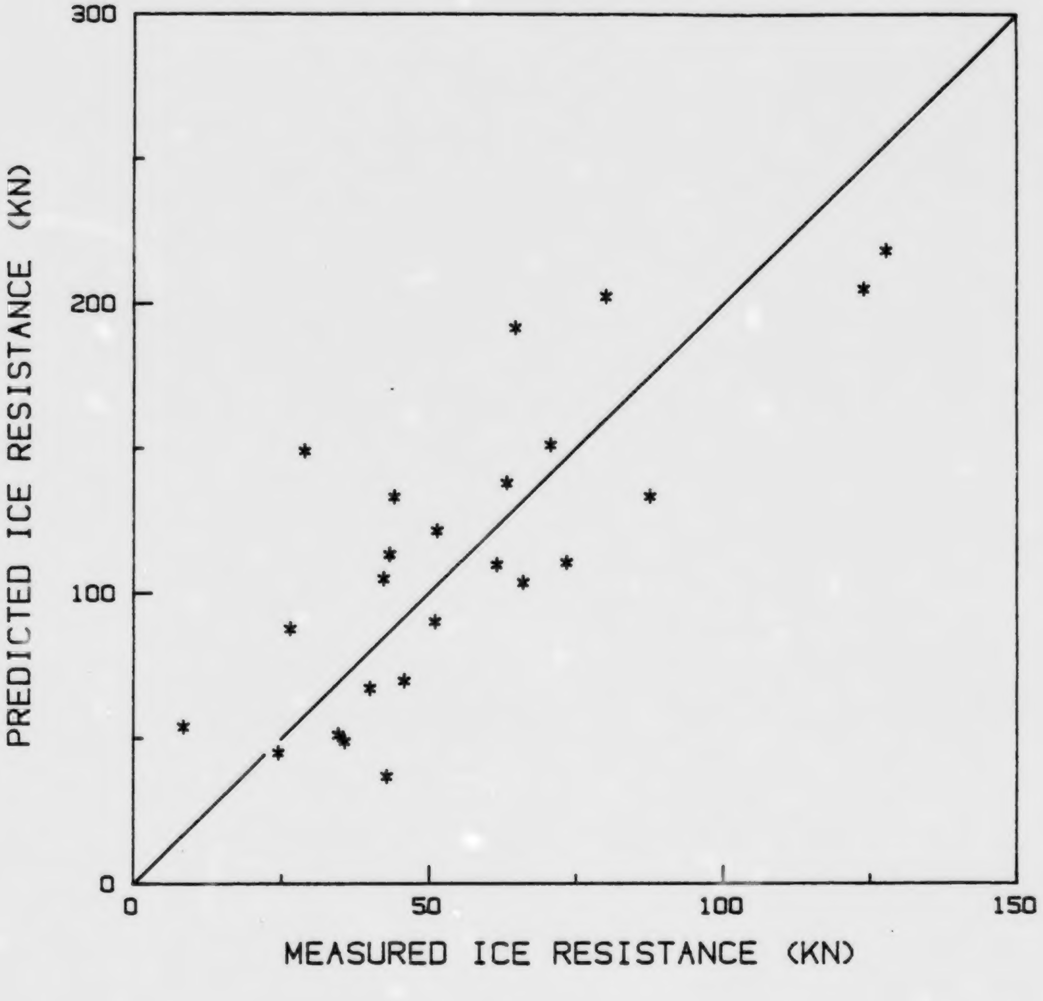

FIGURE 7.18

COMPARISON OF TOTAL RESISTANCE

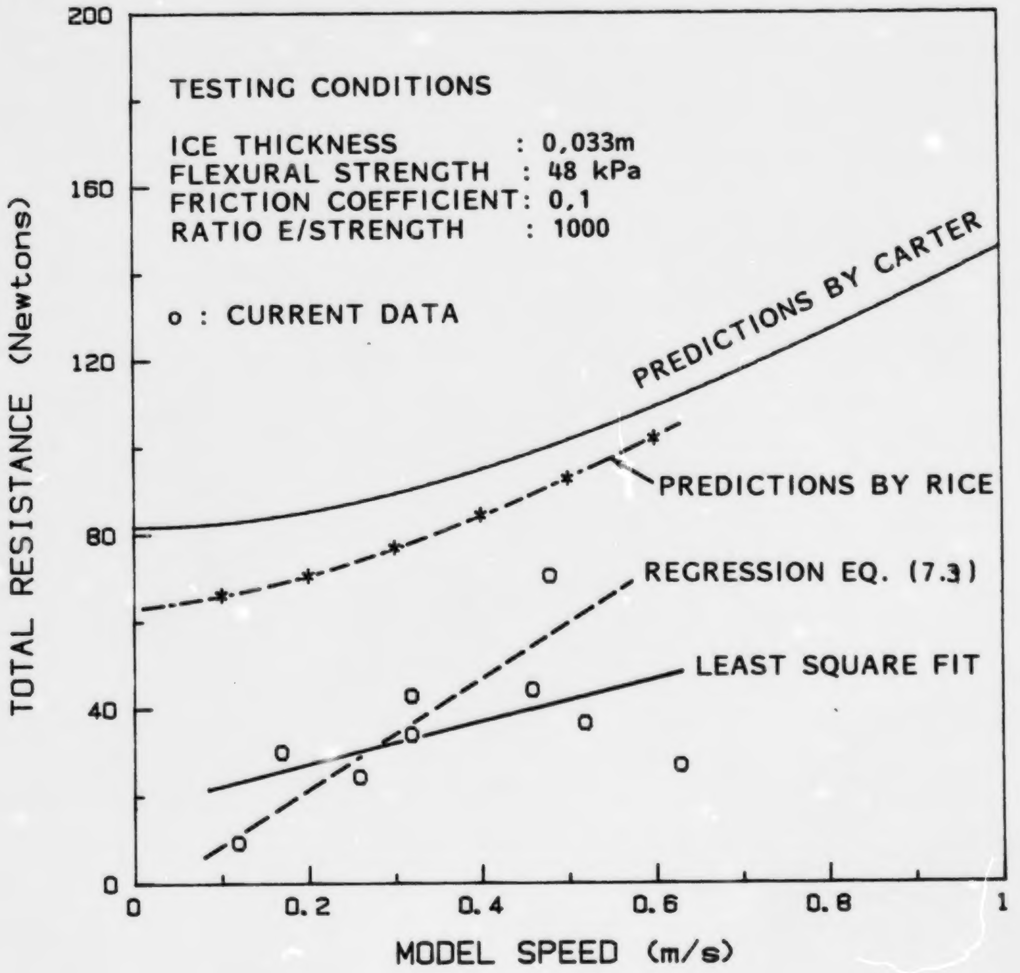

7.7.3 Distribution of Force Along the Hull

From the foregoing it is evident that the examination of the force components on each segment may best be made on a relative basis, i.e. as percentage contribution to total force.

The first comment in this area is made with respect to Figure 7.19 (reproduced from Figure 3.1 of Appendix A). This clearly indicates that, in the Carter model, the distribution of force along the hull is very sensitive to the ratio E/σ. In order to properly reflect the ice conditions as tested, the program was rerun for all particular testing conditions and the results, presented in Table 2.1 of the appendix are reproduced in Table 7.8 and 7.9.

Figure 7.20 compares the measured (Table 6.2) and calculated (Table 7.8) percentage contribution of each segment to total resistance. The Segment 4 resistance contribution is based on the calculated value. Means from data sets and predictions are shown in chart form.

A comparison of percentage contribution to mean normal force (Table 7.9 versus Table 6.1) is graphically shown on Figure 7.21.

Finally, a comparison of mean percentage segment contributions to total force is made in Table 7.10. In the Carter model, Segments 1, 2 and 3 contribute about 51% to the total resistance, while the model tests average 35% - 42%. For Segments 1-4 the Carter model gives 67%, the test results average 45 - 60% (channel and unbroken ice). The best match shows a difference of 1.44% on Segment 4 and the worst match a difference of 13.97% on Segment 3.

On the average, the Carter model predicts 34%, 22%, 42% and 35% contributions to mean normal force from Segments 1 to 4, which compares with the 29%, 36%, 39% and 40% from the physical model. Considering the large scatter in the model test results, the agreement between means from data sets and predictions for relative distribution of force along the hull appears good.

FIGURE 7.19

NORMAL FORCE DISTRIBUTION ALONG WATERLINE
FOR THREE DIFFERENT ELASTIC MODULI, E.

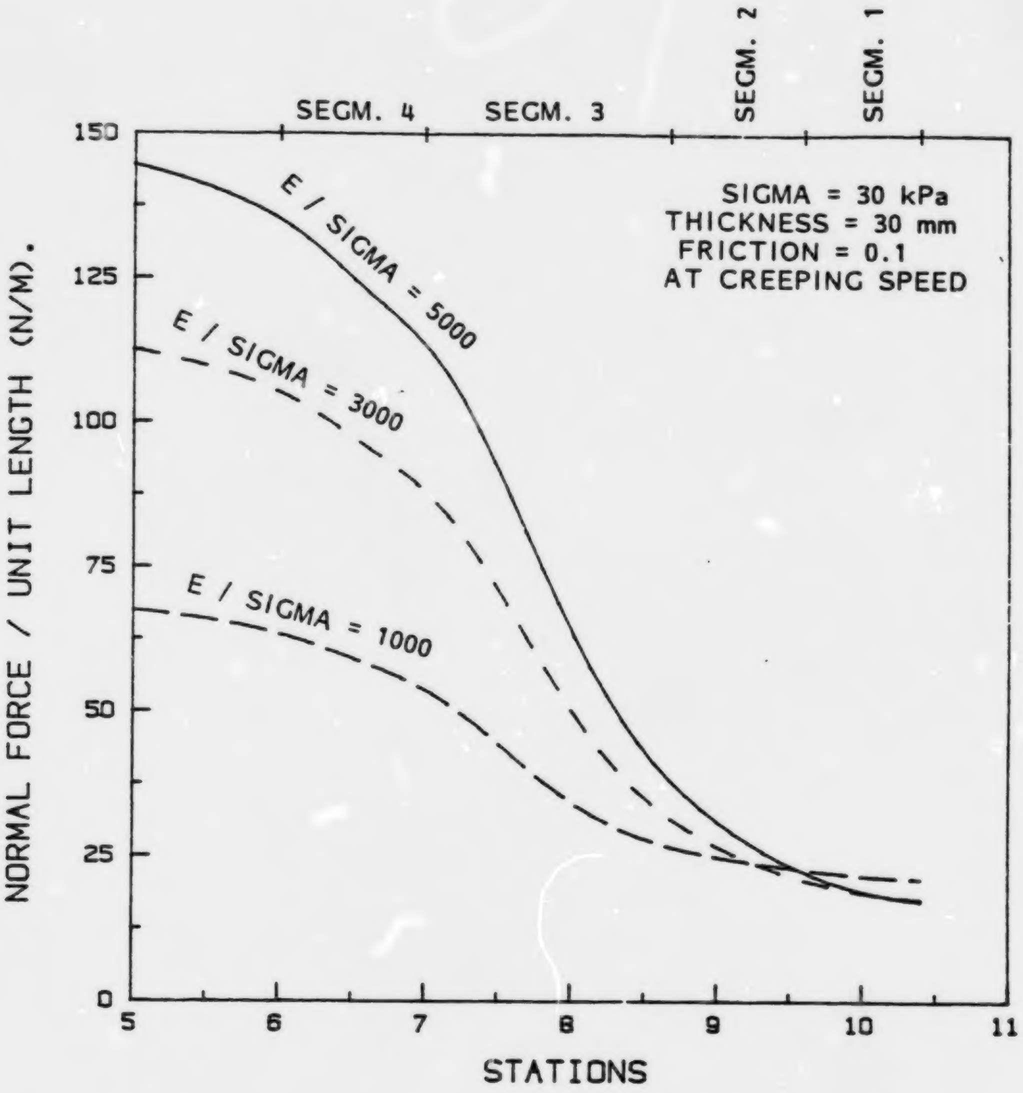

TABLE 7.8

CALCULATED SHIP RESISTANCE AND SEGMENT RESISTANCE

	PERCENT OF TOTAL (%)				REMAINING	TOTAL RESISTANCE (N)
TEST	SEG. 1	SEG. 2	SEG. 3	SEG. 4		
1S1	23.62	19.01	20.17	14.04	23.17	83.27
1C1	23.78	19.37	20.57	14.34	21.94	37.27
1C2	17.39	14.09	14.97	10.44	43.11	50.67
1S2	19.67	15.53	19.29	14.77	30.75	113.43
1C3	19.67	15.94	19.83	15.25	29.30	45.04
1S3	16.30	12.69	17.93	14.41	38.66	151.26
1C5	17.05	13.79	19.53	15.80	33.83	51.16
1C6	13.70	11.67	16.60	13.56	44.47	36.91
1S4	14.95	12.69	22.61	19.10	30.65	149.16
1C7	10.86	9.38	16.74	14.19	48.83	87.66
1C8	14.59	12.81	22.90	19.51	30.19	53.94
2S1	19.80	14.73	21.49	17.37	26.61	138.18
2C1	19.62	14.57	21.26	17.20	27.34	67.30
2C2	17.97	13.34	19.47	15.76	33.46	69.84
2S2	13.53	11.63	22.17	18.81	33.86	160.71
2C3	14.66	12.24	23.29	19.65	30.15	90.26
2C4	14.15	11.52	21.90	18.38	34.05	110.73
2S3	12.58	10.89	21.32	18.03	37.18	205.11
2C5	13.07	11.23	21.99	18.56	35.15	103.79
2C6	13.75	11.59	22.68	19.08	32.90	109.94
2S4	13.85	11.53	21.53	18.17	34.92	191.77
2C7	15.30	12.36	23.05	19.34	29.95	104.99
2C8	15.20	12.01	22.38	18.69	31.72	121.61
3S1	20.68	14.07	21.72	17.56	25.97	218.40
3C1	21.24	13.97	21.53	17.29	25.97	133.60
3S2	16.35	12.48	22.20	18.51	30.46	202.54
3C2	17.62	12.79	22.69	18.72	28.18	133.27
MEAN	16.67	13.24	20.64	16.75	32.69	109.67

TABLE 7.9

CALCULATED MEAN NORMAL FORCE AND SEGMENT NORMAL FORCE

	PERCENT OF TOTAL (%)				NORMAL FORCE (N)	TOTAL RESISTANCE (N)
TEST	SEG. 1	SEG. 2	SEG. 3	SEG. 4		
1S1	41.04	30.61	38.74	28.47	80.40	83.27
1C1	40.04	30.61	38.67	28.53	72.12	37.27
1C2	40.43	30.59	38.75	28.53	97.94	50.67
1S2	38.32	26.54	39.74	31.99	109.52	113.43
1C3	36.39	26.52	39.77	32.15	87.30	45.04
1C4	36.13	26.48	39.76	32.22	94.87	48.94
1S3	36.49	23.64	40.69	34.27	146.38	151.26
1C5	33.92	23.60	40.71	34.52	99.49	51.16
1C6	30.54	23.53	40.72	34.85	72.23	36.91
1S4	28.38	19.23	42.70	37.67	147.17	149.16
1C7	27.47	19.20	42.68	37.79	173.25	87.66
1C8	26.55	19.16	42.65	37.92	106.75	53.94
2S1	38.89	22.92	40.88	34.63	132.97	138.18
2C1	39.00	22.91	40.88	34.64	129.48	67.30
2C2	38.99	22.89	40.87	34.66	134.34	69.84
2S2	27.44	18.08	43.34	38.37	159.11	160.71
2C3	28.94	18.11	43.38	38.19	178.23	90.26
2C4	30.28	18.14	43.41	38.02	218.13	110.73
2S3	27.12	17.66	43.68	38.53	203.53	205.11
2C5	27.49	17.66	43.70	38.48	205.85	103.79
2C6	28.44	17.68	43.72	38.37	217.67	109.94
2S4	29.14	18.43	43.18	38.02	189.16	191.77
2C7	31.96	18.48	43.24	37.69	238.69	121.61
3S1	43.96	21.73	41.34	34.99	208.23	218.40
3C1	46.51	21.74	41.32	34.74	253.62	133.60
3S2	34.24	19.23	42.72	37.19	197.42	202.54
3C2	37.32	19.28	42.76	36.84	258.40	133.27
MEAN	34.15	21.90	41.69	35.36	157.81	109.67

FIGURE 7.20 - COMPARISON OF SEGMENT RESISTANCE PERCENTAGE WITH CARTER'S MATH MODEL PREDICTIONS

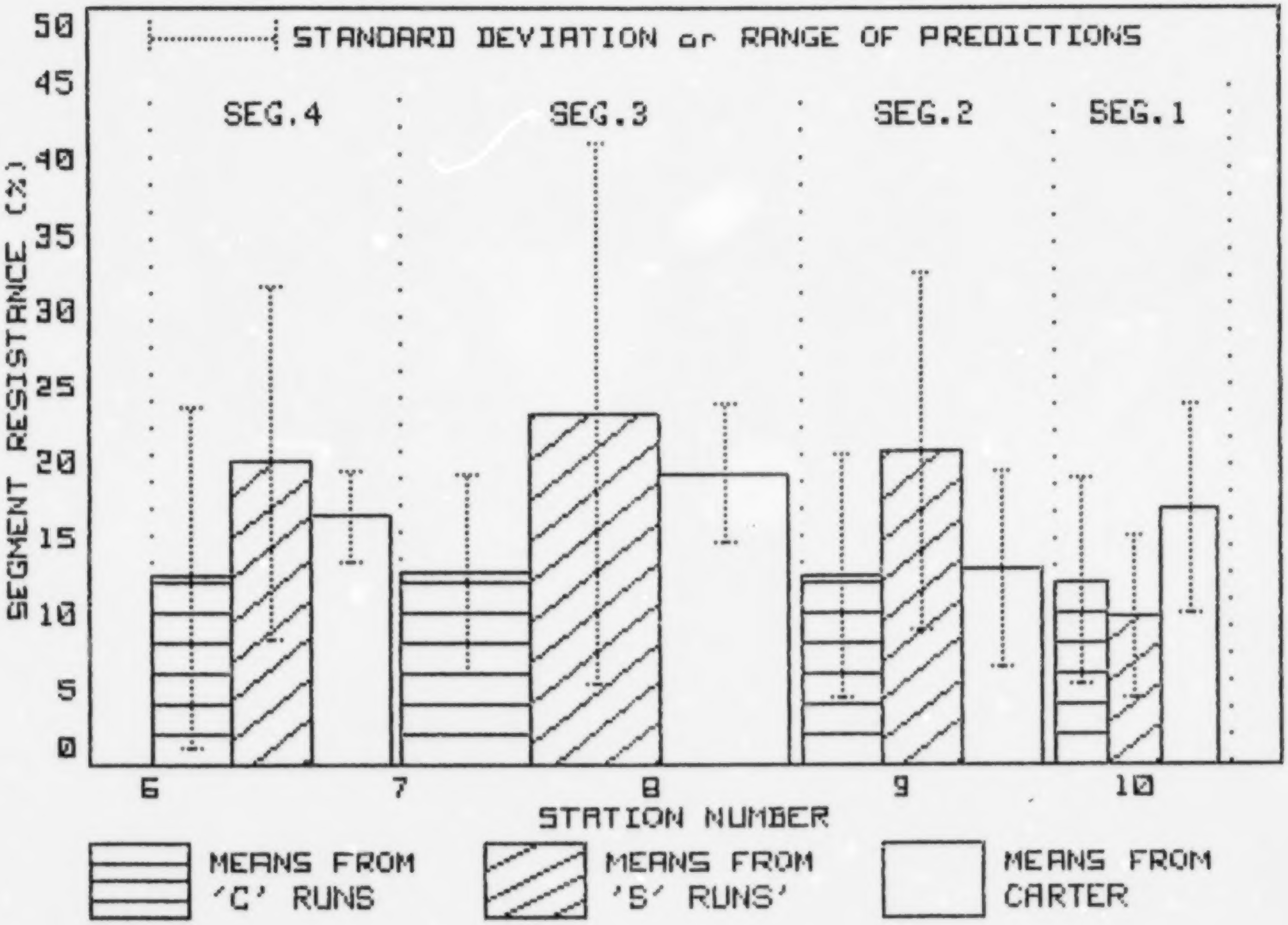

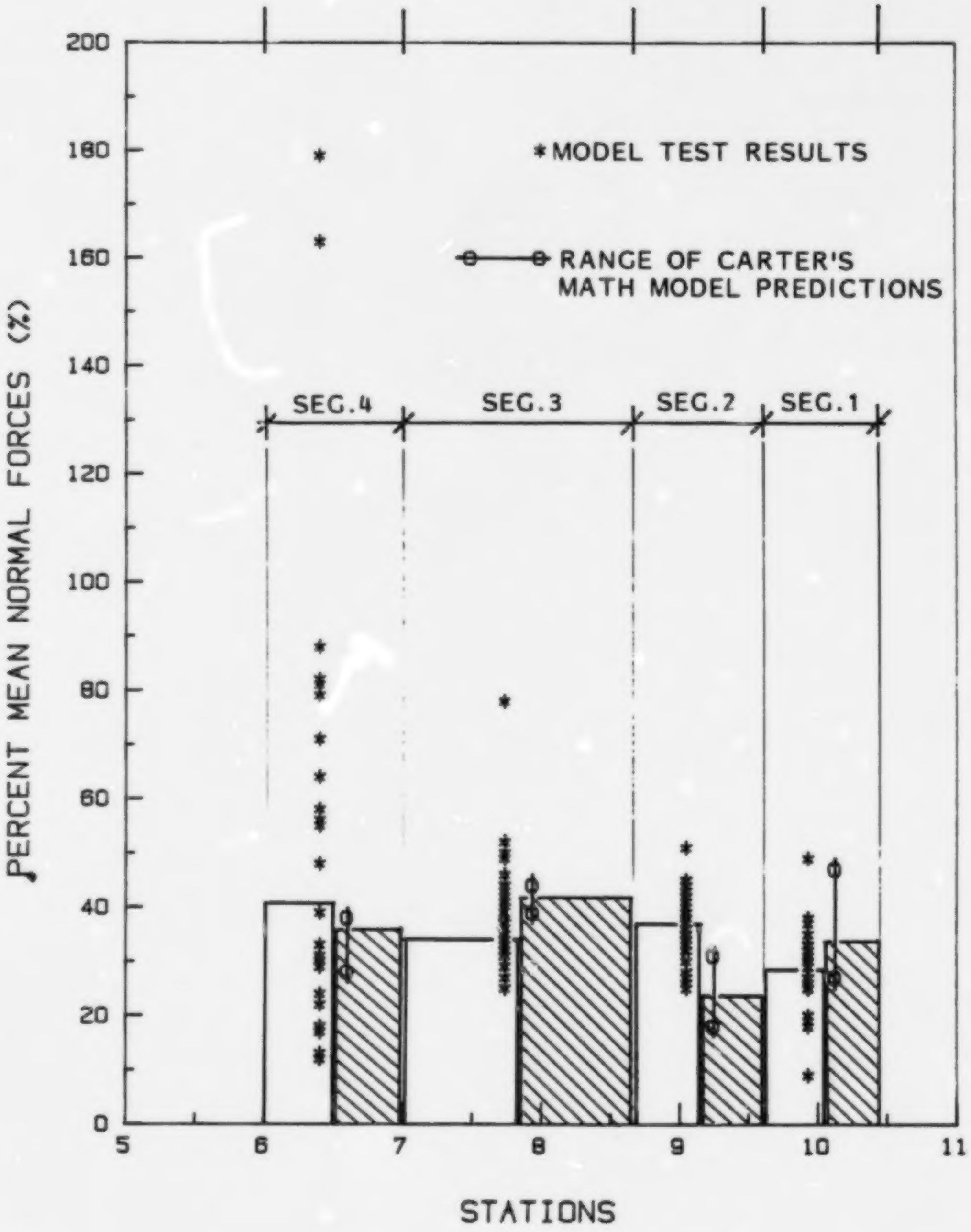

COMPARISON OF PERCENT MEAN NORMAL FORCES SEEN BY SEGMENTS WITH CARTER'S MATH MODEL PREDICTIONS.

☐ MEANS FROM DATA SETS

▨ MEANS FROM CARTER'S PREDICTIONS

FIGURE 7.21

TABLE 7.10 DISTRIBUTION ALONG THE HULL

	PERCENTAGE CONTRIBUTION TO TOTAL FORCE				
SEGMENT RESISTANCE COMPONENT					
	SEG 1	SEG 2	SEG 3	SEG 4	REMAINING
CARTER	16.67%	13.24%	20.63%	16.75%	32.69%
MODEL " S" RUNS	9.17%	16.09%	16.97%	18.19%	39.57%
DIFFERENCE	7.50%	-2.85%	3.66%	-1.44%	-6.88%
MODEL "C" RUNS	6.79%	8.01%	6.66%	11.21%	19.53%
DIFFERENCE	9.88%	5.23%	13.97%	5.54%	13.16%
PERCENTAGE CONTRIBUTION TO MEAN NORMAL FORCE					
	SEG 1	SEG 2	SEG 3	SEG 4	
CARTER	34.15%	21.90%	41.69%	35.36%	
ALL MODEL DATA	29.00%	36.00%	39.00%	40.00%	
DIFFERENCE	5.15%	-14.10%	2.69%	-4.64%	

7.7.4 Assessment of Findings

The foregoing indicates that the Carter model predicts total resistance to be slightly higher than RICE results and generally much higher than the measured model data, and agrees quite well with all available full scale R-Class data. It also indicates that the relative distribution of forces along the hull predicted by the Carter model correlates with the means from data sets reported herein.

In the Carter model, the basic assumption is that the frequency of ice impacts along the hull is a function of the sine of waterline angle. Observations do indicate that the frequency of peak loads is indeed reduced as the loading point moves aft and the waterline angles tend to zero.

It is our assessment that, while the failure process of the model ice may not replicate exactly that of the full scale ice, this phenomenon does exist in full scale, and that the Carter's predictor model accounts for the changing dynamic characteristics of the interaction along the hull, when calculating a mean force.

Icebreaking along a ship hull is a very complex process, in order to simplify the necessary analyses, Carter's formulation contains a number of assumptions. The segmented model has proven an unique means for verifying and validating the force distribution assumptions from a physical point of view.

7.8 Ice Modelling Problems

In carrying out this model test series, it is recognized that the ice modelling material is still not capable of reproducing the precise behaviour of the 'full scale' ice. It is known that refrigerated model ice has deficiencies in crushing/flexural strength ratios, E/σ ratios, secondary cracking/fracture inplane buckling and density. These result in inappropriate energy requirements for ice failure, piece size, flow along the hull.

On the positive side, it is known that initial cusp breaking patterns at model scale reflect those at full scale, and therefore assumptions about what the ice is 'doing' at the different hull locations are considered to be good. Likewise, since the failure process is tied to the characteristic length of the ice, the loading rate and frequency of breaking, etc. is likely to be close to that of full scale.

Due to the ice crushing strength and in-plane strength, individual peak forces occurring prior to failure in bending may be higher at model scale.

Due to density variations and lack of secondary fracture, the movement of broken ice around the hull may not be correct and so loading from this source may not be accurate.

The influence of this on the current test series is such that, while the loading pattern on the segments (e.g. frequency of peaks) is probably valid, the size and density of the ice resulted in significantly more loading on the hull at locations below the segments. This accounts for the fact that only up to 60% of the total loading was accounted for in the resistance of all segments (multiplied by two for both sides).

The influence of the modelling material on these results could be further investigated, using other modelling materials, or by more detailed study of the time series data.

Nevertheless, it has been accepted for a number of years that the total resistance predicted from refrigerated ice model tests, and appropriately scaled with appropriate corrections and friction adjustments gives a reasonable (if generally over predicted) projection of resistance. Errors between full scale and model scale data can be attributed as much to the full scale data as the model. It is only as research moves into investigating local ship-ice interactions (e.g. propeller-ice interaction, hull loads) that the inadequacies of the current model ice become important.

Work is continuing in this area.

8. CONCLUSIONS AND RECOMMENDATIONS

8.1 General

The work reported herein and in previous phases represents a pioneering and ambitious attempt to further understand the ship-ice interaction process as it relates to the ability to produce analytical prediction models. Given the complexity of the model and its measurement system, the constraints on time and money, and current shortfalls in modelling media, it is concluded that it has been a successful program. The analysis of the results has illuminated the potential role which the segmented model can play in defining trends in the ice loads and their relationships to parameters such as model speed, ice thickness and strength, and hull form.

8.2 The Model Test Series

8.2.1 The segmented model program was ambitious in its attempt to distinguish very small force components at different locations along the hull. Given the complexity of the system, the experimental program was executed satisfactorily and the quality of results is as expected.

8.2.2 The desire to perform longer runs, regrettably unable to be accommodated in this program in the end, in order to examine the effect on the results of what is an extremely dynamic and stochastic process, remains.

8.2.3 The technique employed to measure force values and locations was too complex and permitted errors to be introduced through experimental problems such as segment movement and transducer failure, and through data reduction difficulties associated with mathematical manipulation of small numbers (e.g. division by zero).

8.2.4 Currently available ice modelling material has significant shortfalls for examining a local ship-ice interaction phenomena such as the loading on portions of the hull, due to its inability to model all relevant parameters simultaneously. Results must be interpreted acknowledging an understanding of these shortfalls.

8.3 The Results

8.3.1 The results clearly indicate that the cusp breaking pattern results in different loading patterns on each section of the hull. The frequency of loading is high at the fore end and drops off rapidly with movement aft along the hull. These loading patterns exhibit different peak/mean force ratios, and frequency of peak forces. As a result the mean force on the hull does not necessarily increase with increased hull angles (moving aft) while the peak force does, significantly.

8.3.2 While the technique was used to explore friction factor, the results indicate little consistency in the magnitude and direction. The value of μ appears to be higher than expected. The calculated friction vector at the fore end showed a forward direction.

8.3.3 The contribution of the four segments to total resistance is around 60%. Resistance forces from ice pieces that are impinging on the hull below and abaft the segment locations was assumed to be significant, although this may be due to the model ice material and may not be the case in full scale.

8.3.4 The extent and quality of data justifies further investigation.

8.4 Comparison with Math Models

8.4.1 The total resistance predicted by Carter's model was approximately twice that measured on the carriage particularly for the thin ice. Carter's model correlates well with the full scale data for this specific vessel, and there is reason to suppose that the math model predicts well the force distribution along the hull and recognizes the changes in the dynamic load histories. This is underscored by the good correlation between mean values of measured and calculated contributions. The model experimental evidence suggests that there may be high normal loading aft on the bow as is predicted by the Carter Model.

8.4.2 No correlation between the segment resistance and the components of resistance calculated in the program RICE was seen, although the dependency of segment forces in ice-ship parameters was similar to that assumed in RICE. Total resistance on the model compared reasonably with RICE calculations, considering the model was constrained. The proportion of resistance due to 'breaking' that is calculated by RICE is much higher than that apparently measured.

8.4.3 As stated elsewhere, both the above conclusions could be a reflection of the modelling material behaviour, as in the full scale it is possible that more 'breaking' and crushing of overturned floes takes place on the 'shoulders' than was observed.

8.5 Recommendations

8.5.1 Future work directed at examining the components of ice resistance should examine alternative load component modelling techniques in order to eliminate the complexity and shortfalls of the segment system. A continuously instrumented elastic hull model may be a viable alternative.

8.5.2 Notwithstanding the above, consideration should be given to running a limited test series in another testing media, e.g. MODICE, and for a longer run such as is achievable at IMD. However, no further calibrations or changes to the segment system (other than replacement of failed gauges) should be attempted.

8.5.3 A great deal of data was collected during this test series, and it was not possible to examine all the options and possible reduction processes. While there are concerns about the effect of the model ice properties, and the segment instrumentation, it is felt that further examination of the data, both pre and post reduction, would be of value. However, it is proposed that this be pursued in an environment that is more liberal than that afforded by contract research, e.g. in a university environment. A number of specific projects could be identified for on-going examination.

8.5.4 The nature of the loading should be further examined and a method to account for the changing dynamics of the interaction should be introduced into Carter's approach with a view to more closely reflecting the dynamic nature of the ship-ice interaction, and in particular, the changes to it with location on the hull.

9. REFERENCES

[1] Nawwar, A.M., Howard, D., "Segmented Model Testing in Ice - Development of Techniques", TP 5701, June 1984.

[2] Godon, A., and Nawwar, A.M., "Icebreaking Theory Development by Segmented Model Tests: Refinement of Technique", TP 8498C, March 1987.

[3] Nawwar, A.M., Godon, A., Roots, T., Howard, D., and Bayly, I.M.; "Development of a Measuring System for Segmented Ship Models", Proceedings 1987, SEM Spring Conference, Houston, Texas, June 1987.

[4] Carter, D.S., "Ship Resistance to Continuous Motion in Level Ice", TP 3679, March 1983.

[5] Nawwar, A.M., "A Semi-Empirical Ice Resistance Model, Volume III - Principals and Assumptions", Transport Canada, April 1983.

[6] Glen, I.F., "A Semi-Empirical Ice Resistance Model - Summary Report", TP 4377E, August 1982.

[7] Howard, D., Abdelnour, R., "The Testing of the 1:8 Scale Model of the R-Class in Level Ice", TP 8828E, December 1987.

[8] Gary Robertson & Assoc. Inc., "Mensuration of an R-Class Model Icebreaker Using a Photogrammetric Approach", 1988.

[9] Naegle, J.N., "Ice Resistance Prediction and Motion Simulation for Ships Operating in the Continuous Mode of Icebreaking", Ph.D. Thesis, University of Michigan, 1980.

[10] "Segmented Model Tests to Validate Ice Resistance Math Models - Progress Report ", FTL B73108C, June 1988.

APPENDIX A

VALIDATION OF CARTER'S MATH MODEL BY USE OF A SEGMENTED MODEL

FLEET TECHNOLOGY LIMITED
311 Legget Drive,
KANATA, (Ontario), K2K 1Z8

VALIDATION OF CARTER'S MATH MODEL BY USE OF A SEGMENTED MODEL

COMPARISON OF PREDICTIONS WITH EXPERIMENTAL DATA

Report prepared for
FLEET TECHNOLOGY LIMITED

prepared by

Donald Carter,P.Eng.,D.Sc.
DONALD CARTER & ASS.,
CONSULTANTS
1281 Bishop, Ste-Foy,
G1W-3E4
Tel.:(418) 656-0690

15 March 1989

TABLE OF CONTENTS

1.: INTRODUCTION 1
2.: CORRELATION WITH FULL-SCALE DATA 2
3.: ICE FORCE DISTRIBUTION ALONG WATERLINE 12
4.: CONCLUSIONS 20
5.: REFERENCES 20

ANNEX 'A'.: PIERRE RADISSON - TRIAL DATA
ANNEX 'B'.: ICE FORCE DISTRIBUTION

1.: INTRODUCTION

The following report documents the results of a test program with a segmented model developed during the last five years by Fleet Technology Ltd (FTL), formerly Arctec Canada Ltd, (ACL).

The purpose of the testing program was to provide experimental data on the resistance components along different zones of an icebreaking bow to verify the math model developed by Dr. D. Carter. This model can predict the forces in all three directions (X, Y, and Z) acting along the hull/ice interface.

The model tests were conducted at the FTL laboratory in Kanata during January and February 1989. The test results were supplied by FTL to Dr. D. Carter for comparison with the analytical predictions of his math model.

All planned model test runs have been calculated by Carter and submitted to FTL prior to testing for the target test matrix. Once the test program has been completed, the program was rerun to reflect the test matrix as completed. Only slight differences with original predictions were observed.

2.: CORRELATION WITH FULL-SCALE DATA

In order to verify the relative accuracy and reliability of both the Carter's analytical model and the segmented physical model, it is essential that the predicted resistance results be now compared with high quality full-scale data which will act as a benchmark.

Field trials were carried out with the two R-Class icebreakers operated by the Canadian Coast Guard. In February 1979, extensive trials were conducted aboard CCGS Radisson in 0,25 to 1,20 m of winter fresh and saline ice. The trial conditions and the measured ice resistance, reproduced from a report by ACL [1], are listed in ANNEX "A" along with the calculated values by Carter's math model.

In the winter of 1979-80, full-scale trials were also carried out with CCGS Franklin in Lake Melville by Michailidis [2]. His experimental data are also listed in ANNEX "A".

In the model test program, level ice in three thicknesses corresponding to 0,6, 0,9, and 1,2m with properties representative of first-year sea ice were targeted.

Two types of tests were conducted:

a) Standard Level Ice Tests;
b) Channel Widening Tests.

During Channel Widening Tests, the model is towed down the previously broken channel with the bow inside the edge of the sheet, and ice is broken on the segmented side of the model. It was established in earlier tests that results from this type of test are indistinguishable from level ice test. From symmetry considerations, the ice resistance in level ice should be equal to double the ice resistance measured in Channel Widening Tests.

Table 2.1 gives the mean normal forces, Fn1, Fn2, Fn3 and Fn4, acting on each segment. The total normal force acting on all four segments is also given along with the ice resistance, Ri. Table 2.2 reproduces the same information in a non-dimensional form with respect to the average normal force, Fn.

TABLE 2.1

Mean Forces

TEST	Measured Values (n)						Calculated Values (n)					
	Fn1	Fn2	Fn3	Fn4	Fn	Ri	Fn1	Fn2	Fn3	Fn4	Fn	Ri
1S1	16.6	13.2	20.7	6.6	51.9		33.0	24.6	31.1	22.9	80.4	83.3
1C1	11.4	11.8	13.9	6.2	35.9		28.9	22.1	28.0	20.6	72.1	37.3
1C2	18.1	24.1	25.1	20.4	67.2		39.6	30.0	37.9	27.9	97.9	50.7
1S2	10.0	13.2	10.6	9.7	33.8	43.3	42.0	29.1	43.5	35.0	109.5	113.4
1C3	7.7	9.5	9.2	4.4	26.5	24.4	31.8	23.2	34.7	28.1	87.3	45.0
1C4	10.6	19.1	15.1	12.4	42.0	35.6	34.3	25.1	37.7	30.6	94.9	48.9
1S3	22.0	19.8	16.9	22.7	58.6	70.7	53.4	34.6	59.6	50.2	146.4	151.3
1C5	15.3	14.0	17.2	12.8	53.3	34.5	33.7	23.5	40.5	34.3	99.5	51.2
1C6	18.1	16.8	18.0	16.2	55.1	42.8	22.1	17.0	29.4	25.2	72.2	36.9
1S4	10.4	10.7	13.0	28.2	34.9	28.8	41.8	28.3	62.8	55.4	147.2	149.2
1C7	14.4	27.7	21.0	26.2	54.3	26.4	47.6	33.3	73.9	65.5	173.2	87.7
1C8	8.0	9.9	13.5	21.7	30.7	8.4	28.3	20.5	45.5	40.5	106.8	53.9
2S1	6.5	11.7	11.0	46.6	26.1	63.2	51.7	30.5	54.4	46.1	133.0	138.2
2C1	15.1	15.8	10.9	35.3	42.9	39.9	50.5	29.7	52.9	44.9	129.5	67.3
2C2	18.5	20.8	16.5	17.4	52.5	45.8	52.4	30.8	54.9	46.6	134.3	69.8
2S2	11.1	20.2	24.3	32.4	55.9		43.7	28.8	69.0	61.0	159.1	160.7
2C3	17.5	24.1	23.8	38.6	69.6	51.0	51.6	32.3	77.3	68.1	178.2	90.3
2C4	27.9	42.3	27.8	12.1	101.6	73.4	66.1	39.6	94.7	82.9	218.1	110.7
2S3	7.2	29.9	40.9	13.5	78.7	123.9	55.2	35.9	88.9	78.4	203.5	205.1
2C5	25.2	27.6	45.8	12.4	99.7	66.0	56.6	36.4	89.9	79.2	205.8	103.8
2C6	24.6	25.5	46.9	29.4	94.5	61.5	61.9	38.5	95.2	83.5	217.7	109.9
2S4	8.7	20.0	21.5	31.3	49.0	64.7	55.1	34.9	81.7	71.9	189.2	191.8
2C7	15.6	20.5	14.9	8.4	46.6	42.3	63.5	38.1	89.2	78.1	206.5	105.0
2C8	25.4	24.3	25.9	60.3	68.6	51.4	76.3	44.1	103.2	90.0	238.7	121.6
3S1	22.2	17.6	35.2	73.2	45.0	127.7	91.5	45.2	86.1	72.9	208.2	218.4
3C1	31.3	34.4	41.4	22.7	102.0	87.5	118.0	55.1	104.8	88.1	253.6	133.6
3S2	17.9	39.5	45.2	72.8	91.9	80.1	67.6	38.0	84.3	73.4	197.4	202.5
3C2	26.8	34.8	25.7	46.1	82.5	44.1	96.4	49.8	110.5	95.2	258.4	133.3

TABLE 2.2

Mean Forces Normalized with respect to Total Normal Force

TEST	Measured Values (n)						Calculated Values (n)					
	F'n1	F'n2	F'n3	F'n4	F'n	R'i	F'n1	F'n2	F'n3	F'n4	F'n	R'i
1S1	0.32	0.25	0.40	0.13	1.00		0.41	0.31	0.39	0.28	1.00	1.04
1C1	0.32	0.33	0.39	0.17	1.00		0.40	0.31	0.39	0.29	1.00	0.52
1C2	0.27	0.36	0.37	0.30	1.00		0.40	0.31	0.39	0.29	1.00	0.52
1S2	0.30	0.39	0.31	0.29	1.00	1.28	0.38	0.27	0.40	0.32	1.00	1.04
1C3	0.29	0.36	0.35	0.17	1.00	0.92	0.36	0.27	0.40	0.32	1.00	0.52
1C4	0.25	0.45	0.36	0.30	1.00	0.85	0.36	0.26	0.40	0.32	1.00	0.52
1S3	0.38	0.34	0.29	0.39	1.00	1.21	0.36	0.24	0.41	0.34	1.00	1.03
1C5	0.29	0.26	0.32	0.24	1.00	0.65	0.34	0.24	0.41	0.35	1.00	0.51
1C6	0.33	0.30	0.33	0.29	1.00	0.78	0.31	0.24	0.41	0.35	1.00	0.51
1S4	0.30	0.31	0.37	0.81	1.00	0.83	0.28	0.19	0.43	0.38	1.00	1.01
1C7	0.27	0.51	0.39	0.48	1.00	0.49	0.27	0.19	0.43	0.38	1.00	0.51
1C8	0.26	0.32	0.44	0.71	1.00	0.27	0.27	0.19	0.43	0.38	1.00	0.51
2S1	0.25	0.45	0.42	1.79	1.00	2.42	0.39	0.23	0.41	0.35	1.00	1.04
2C1	0.35	0.37	0.25	0.82	1.00	0.93	0.39	0.23	0.41	0.35	1.00	0.52
2C2	0.35	0.40	0.31	0.33	1.00	0.87	0.39	0.23	0.41	0.35	1.00	0.52
2S2	0.20	0.36	0.43	0.58	1.00		0.27	0.18	0.43	0.38	1.00	1.01
2C3	0.25	0.35	0.34	0.55	1.00	0.73	0.29	0.18	0.43	0.38	1.00	0.51
2C4	0.27	0.42	0.27	0.12	1.00	0.72	0.30	0.18	0.43	0.38	1.00	0.51
2S3	0.09	0.38	0.52	0.17	1.00	1.57	0.27	0.18	0.44	0.39	1.00	1.01
2C5	0.25	0.28	0.46	0.12	1.00	0.66	0.27	0.18	0.44	0.38	1.00	0.50
2C6	0.26	0.27	0.50	0.31	1.00	0.65	0.28	0.18	0.44	0.38	1.00	0.51
2S4	0.18	0.41	0.44	0.64	1.00	1.32	0.29	0.18	0.43	0.38	1.00	1.01
2C7	0.33	0.44	0.32	0.18	1.00	0.91	0.31	0.18	0.43	0.38	1.00	0.51
2C8	0.37	0.35	0.38	0.88	1.00	0.75	0.32	0.18	0.43	0.38	1.00	0.51
3S1	0.49	0.39	0.78	1.63	1.00	2.84	0.44	0.22	0.41	0.35	1.00	1.05
3C1	0.31	0.34	0.41	0.22	1.00	0.86	0.47	0.22	0.41	0.35	1.00	0.53
3S2	0.19	0.43	0.49	0.79	1.00	0.87	0.34	0.19	0.43	0.37	1.00	1.03
3C2	0.32	0.42	0.31	0.56	1.00	0.53	0.37	0.19	0.43	0.37	1.00	0.52

Figure 2.1 compares for both the standard level ice tests and the channel widening tests the correlation between the ice resistance Ri and the normal force acting on all four segments, Fn. It is clearly shown that ice resistance measured in channel widening tests represents only half ice resistance in level ice. Therefore, ice resistance measured in channel widening tests will be multiplied by a factor 2 before being compared with full scale data in level ice.

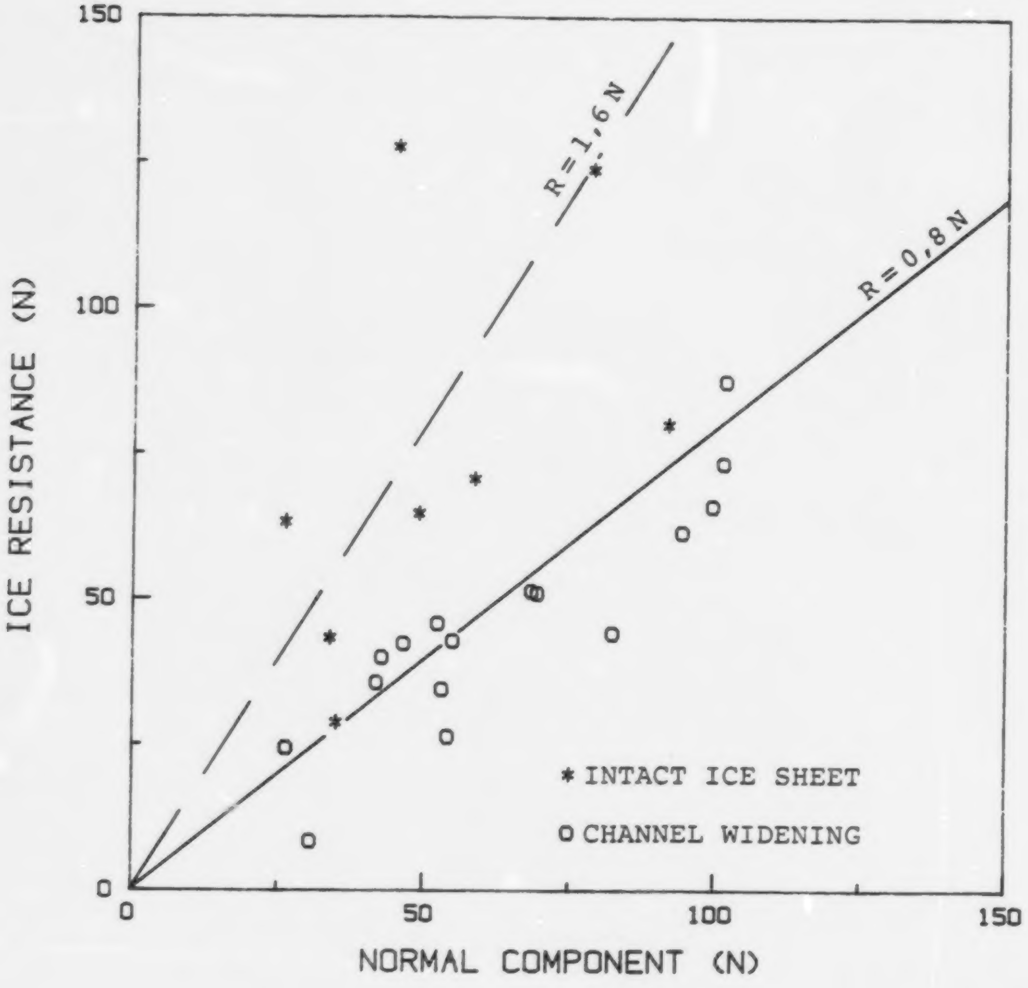

ICE RESISTANCE VERSUS NORMAL COMPONENT

FIGURE 2.1

Figure 2.2 compares full-scale data, model test results, and predictions by Carter's model for ice thicknesses between 0,6 and 0,7 m. An excellent correlation is observed between the math model results and the full-scale data. The model test results exhibit the commonly observed scatter in ice force measurements with a low correlation. The speed dependancy of the model data appears to be too high and, at low speeds, the total resistance is too low.

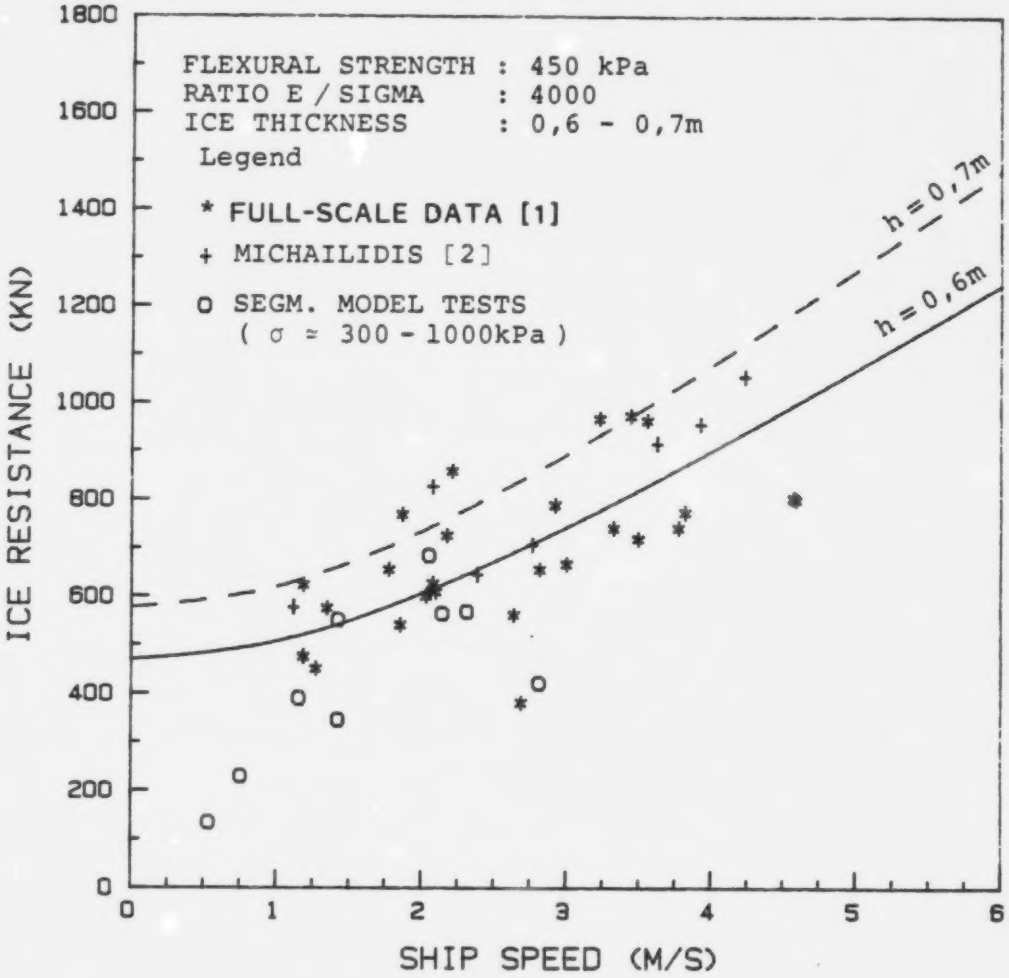

COMPARISON BETWEEN FULL SCALE DATA, MODEL TEST RESULTS AND PREDICTIONS BY CARTER'S MATH MODEL

FIGURE 2.2

Figure 2.3 compares full-scale data, model test results, and predictions by Carter's math model for ice thicknesses between 0,9 and 1,0 m. As previously, a very good correlation is observed between trial data and Carter's predictions. The segmented model results show a large scatter in ice resistance measurements. In general, the model test results over-estimate ice resistance, which may be, in part, explained by the fact that the simulated flexural strength corresponds to 2 to 4 times the actual flexural strength measured during the trials.

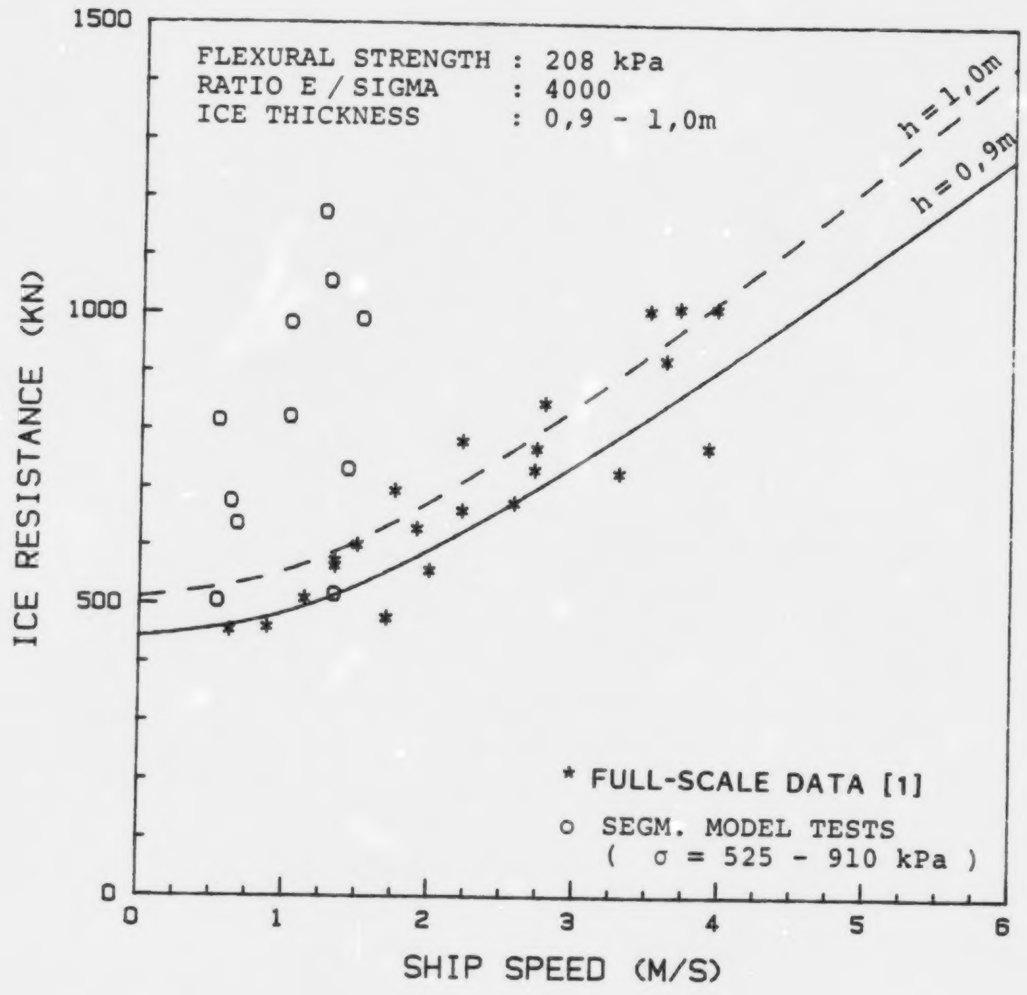

COMPARISON BETWEEN FULL SCALE DATA. MODEL TEST RESULTS AND PREDICTIONS BY CARTER'S MATH MODEL.

FIGURE 2.3

As previously, Figure 2.4 show a good correlation between trial data and Carter's model predictions for ice thicknesses between 1,1 and 1,2 m. The few segmented model results exhibit the usual large scatter in ice resistance measurements which are surevaluated probably due to the high strength of the model ice.

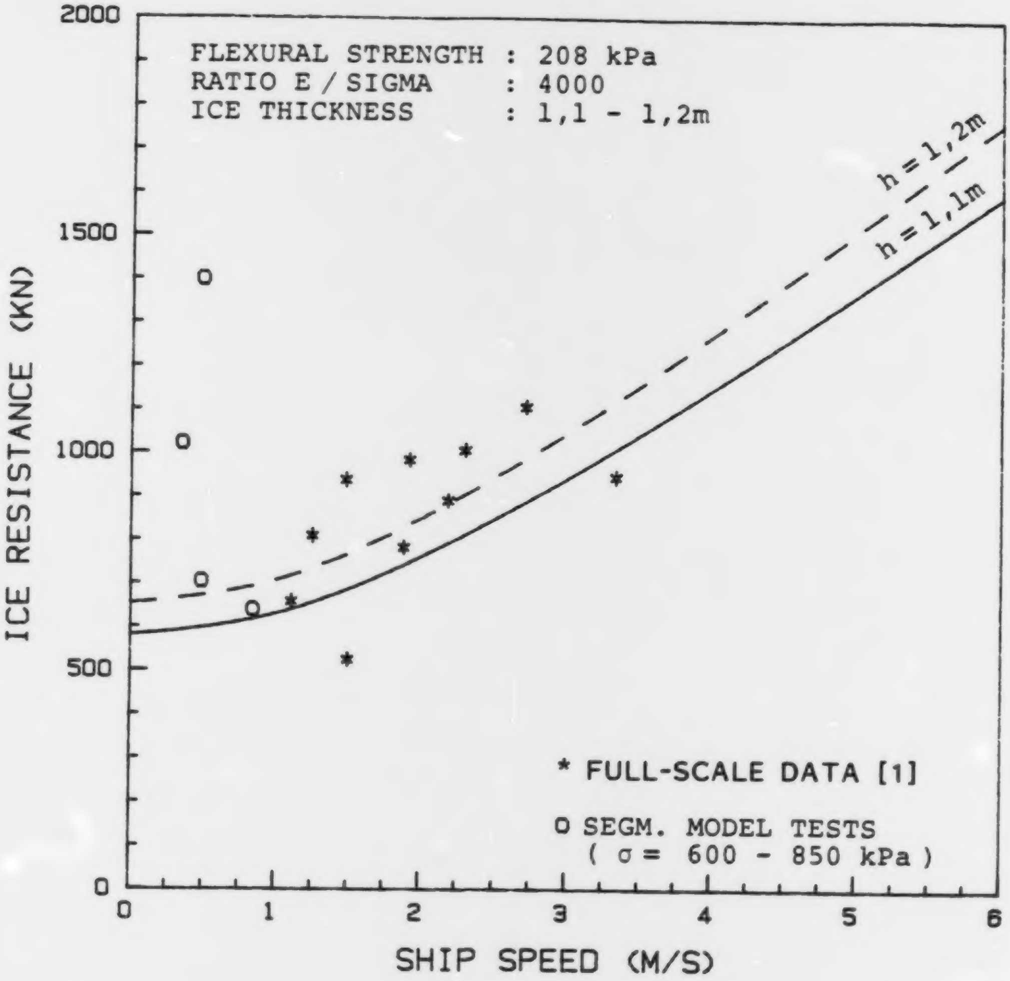

COMPARISON BETWEEN FULL SCALE DATA, MODEL TEST RESULTS AND PREDICTIONS BY CARTER'S MATH. MODEL.

FIGURE 2.4

Figure 2.5 compares the predictions by Carter's model for the test matrix as completed with the ice resistance effectively measured. A general trend is observed: the measured resistance is about 50% the predicted ice resistance.

It is our opinion that the density of model ice being greater than that of natural ice, 0,92 versus 0,82, the broken ice pieces are more readily submerged and pushed under the ice cover. Thus the ice pieces avoid being wedged in between the unbroken ice sheet and the ship hull, thereby reducing significantly the total ice resistance.

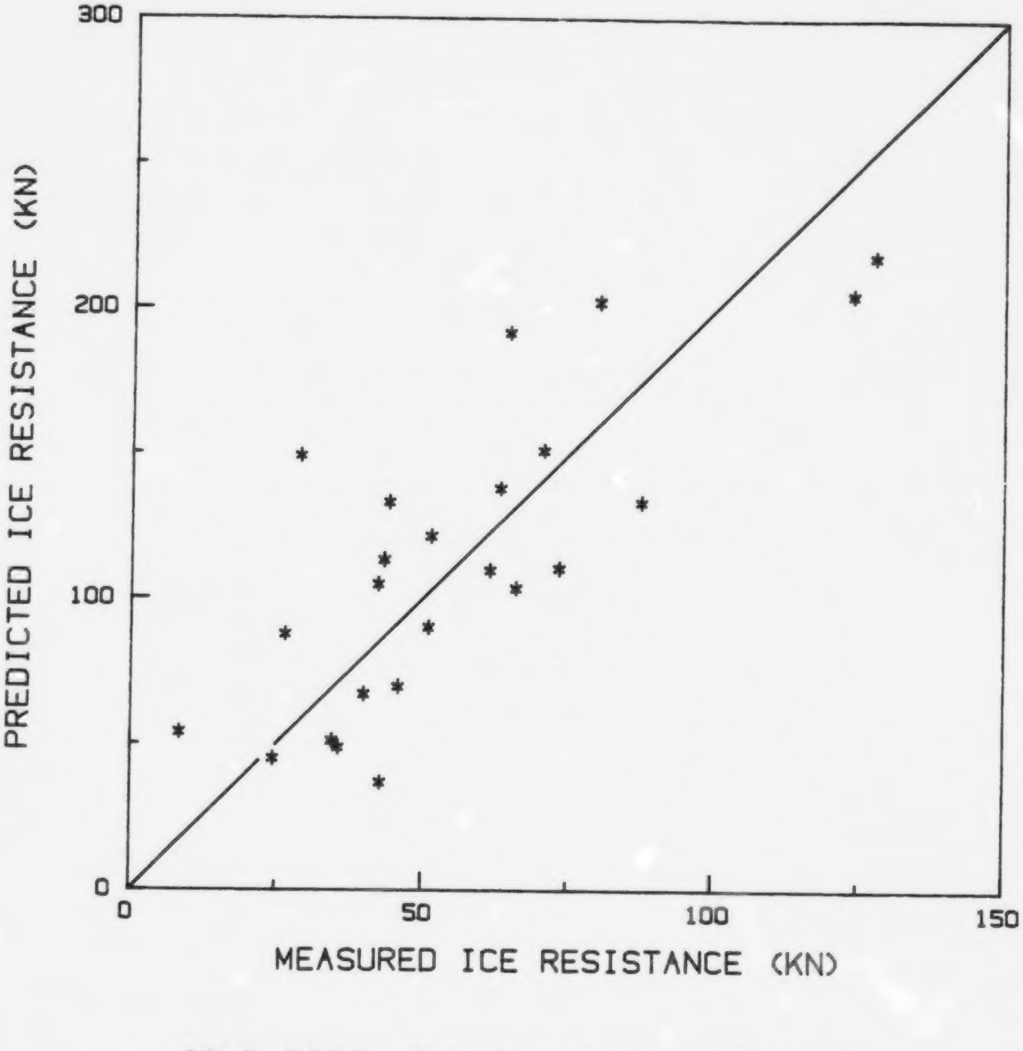

COMPARISON BETWEEN MODEL TEST RESULTS
AND PREDICTIONS BY CARTER'S MATH MODEL

FIGURE 2.5

The technology of testing models is, perhaps, a very powerful tool for determining ice forces on structures and ship hulls, but it is required all similarity relationships to be properly satisfied.

The present state-of-the-art technique does not allow to grow doped model ice that can simulate all natural ice characteristics at model scale. To date, the major drawback with doped ice is its inability to correctly scale the elastic modulus, E. For model ice, the elastic modulus is generally too low by a factor of about 5, which favor the occurence of failure by buckling rather than by crushing as observed under natural conditions for ice covers thicker than 0,3 m.

Furthermore, large variations in mechanical properties exist not only between different ice sheets but also in a single ice sheet, the properties are also very dependent on temperature.

It is our opinion that an acceptable testing medium is still to be developed.

Figure 2.6 and Figure 2.7 compare the regression equation used to represent the model test results with the full-scale data and the predictions from the Carter's model and the RICE model. The model test results are, at low speeds, too low by a factor of at least 2, and the speed dependancy appears too high.

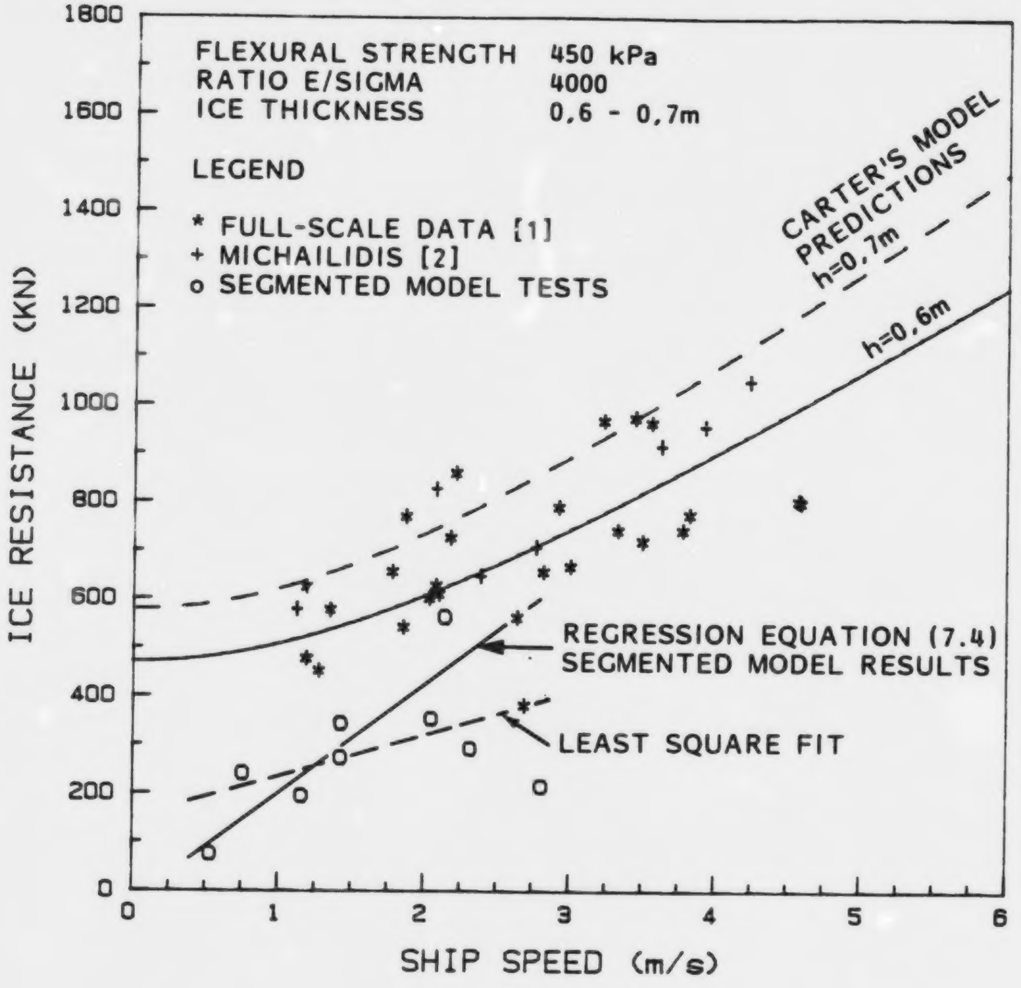

COMPARISON BETWEEN FULL SCALE DATA, MODEL TEST RESULTS AND PREDICTIONS BY CARTER'S MATH MODEL.

FIGURE 2.6

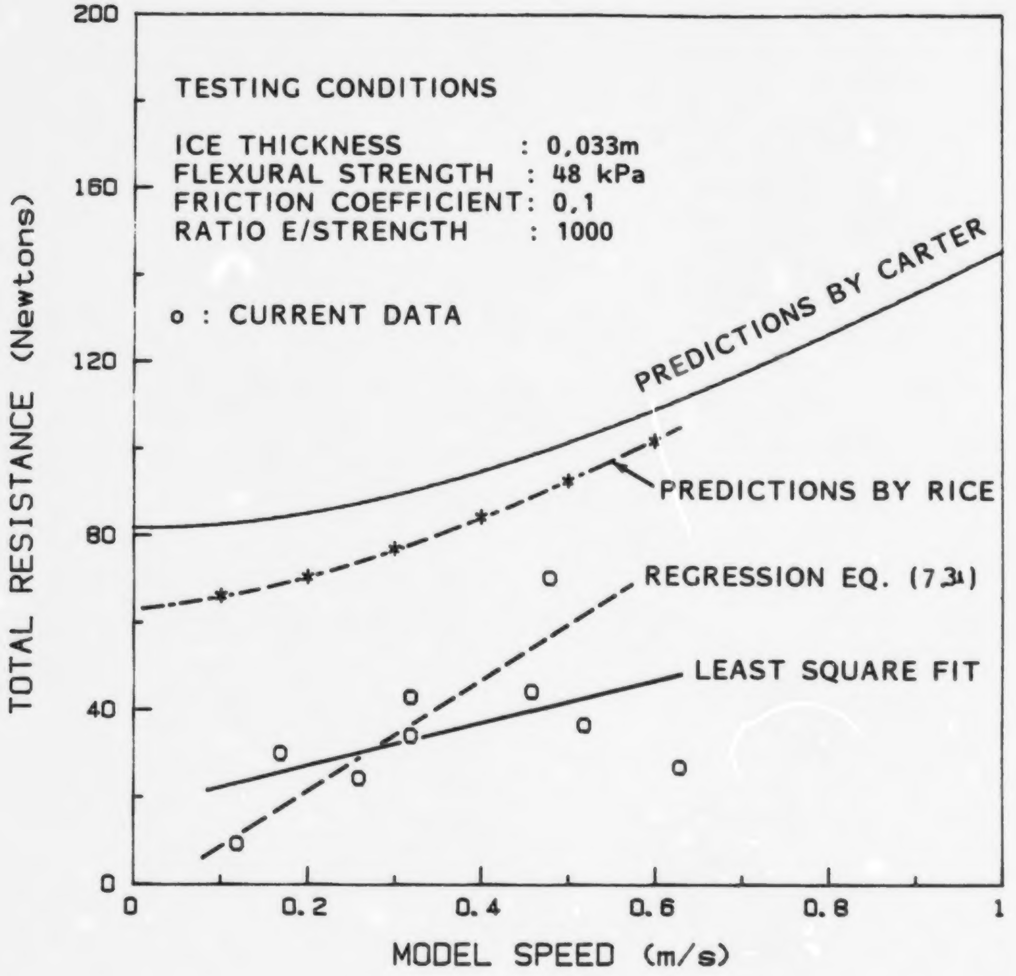

COMPARISON OF TOTAL RESISTANCE

FIGURE 2.7

3.: ICE FORCE DISTRIBUTION ALONG WATERLINE

In this section, it is intended to compare the ice loads measured at various locations on the segmented model with the ice force distribution predicted by Carter's model. This model provides the ice forces in all three directions, X, Y, and Z, along the waterline of an icebreaking bow and is sensitive to the various principal ship and ice parameters and to the operating speed.

Since measured total resistance is, when compared to full-scale data and math model predictions, too low by a factor of two, it is self evident that the examination of the force components on each segment may be made only on a relative basis, i.e. as percentage contribution to total force.

In ANNEX "B", typical ice force distributions are presented for the targeted test matrix with a ratio E/SIGMA of 5000. Figure 3.1 shows the important influence of the elastic modulus, E, on the magnitude of the ice loads.

The total ice forces, corresponding to the particular model test conditions, are presented in TABLE 3.1 and TABLE 3.2, and are summarized in TABLE 3.3. These ice forces acting on each segment were obtained by integrating over the segment length the ice force distribution.

Figure 3.2 and Figure 3.3 compare the calculated and the measured ship resistance and mean normal force. In spite of the large variation in the measured data, a rather good concordance can be observed between the means from experimental data and the predictions by Carter's model, as shown on Figure 3.4.

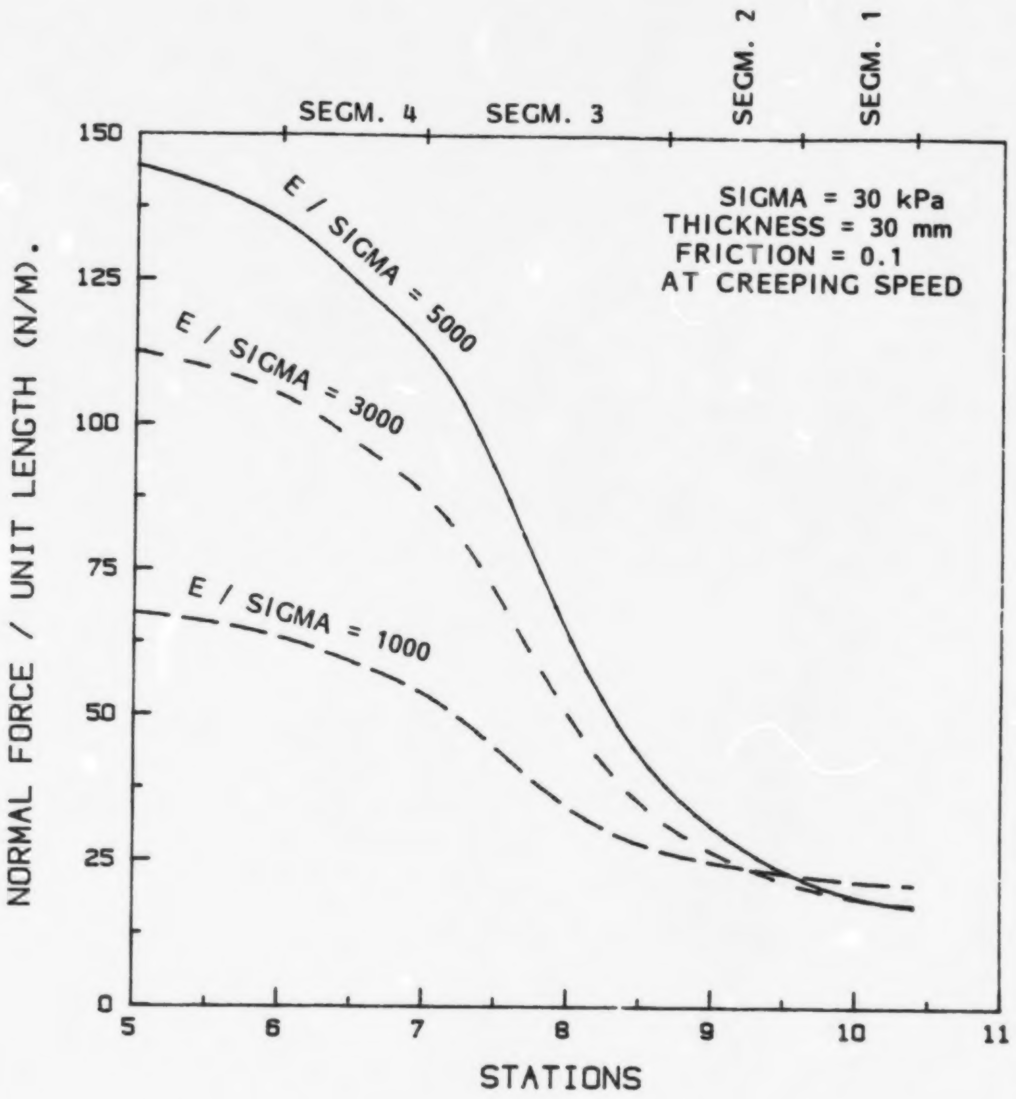

NORMAL FORCE DISTRIBUTION ALONG WATERLINE
FOR THREE DIFFERENT ELASTIC MODULI, E.

FIGURE 3.1

TABLE 3.1

CALCULATED SHIP RESISTANCE AND SEGMENT RESISTANCE

	PERCENT OF TOTAL (%)					
TEST	SEG.1	SEG.2	SEG.3	SEG.4	REMAINING	TOTAL RESIST. (N)
1S1	23.62	19.01	20.17	14.04	23.17	83.27
1C1	23.78	19.37	20.57	14.34	21.94	37.27
1C2	17.39	14.09	14.97	10.44	43.11	50.67
1S2	19.67	15.53	19.29	14.77	30.75	113.43
1C3	19.67	15.94	19.83	15.25	29.30	45.04
1C4	15.93	12.95	16.14	12.44	42.54	48.94
1S3	16.30	12.69	17.93	14.41	38.66	151.26
1C5	17.05	13.79	19.53	15.80	33.83	51.16
1C6	13.70	11.67	16.60	13.56	44.47	36.91
1S4	14.95	12.69	22.61	19.10	30.65	149.16
1C7	10.86	9.38	16.74	14.19	48.83	87.66
1C8	14.59	12.81	22.90	19.51	30.19	53.94
2S1	19.80	14.73	21.49	17.37	26.61	138.18
2C1	19.62	14.57	21.26	17.20	27.34	67.30
2C2	17.97	13.34	19.47	15.76	33.46	69.84
2S2	13.53	11.63	22.17	18.81	33.86	160.71
2C3	14.66	12.24	23.29	19.65	30.15	90.26
2C4	14.15	11.52	21.90	18.38	34.05	110.73
2S3	12.58	10.89	21.32	18.03	37.18	205.11
2C5	13.07	11.23	21.99	18.56	35.15	103.79
2C6	13.75	11.59	22.68	19.08	32.90	109.94
2S4	13.85	11.53	21.53	18.17	34.92	191.77
2C7	15.30	12.36	23.05	19.34	29.95	104.99
2C8	15.20	12.01	22.38	18.69	31.72	121.61
3S1	20.68	14.07	21.72	17.56	25.97	218.40
3C1	21.24	13.97	21.53	17.29	25.97	133.60
3S2	16.35	12.48	22.20	18.51	30.46	202.54
3C2	17.62	12.79	22.69	18.72	28.18	133.27
MEAN	16.67	13.24	20.64	16.75	32.69	109.67

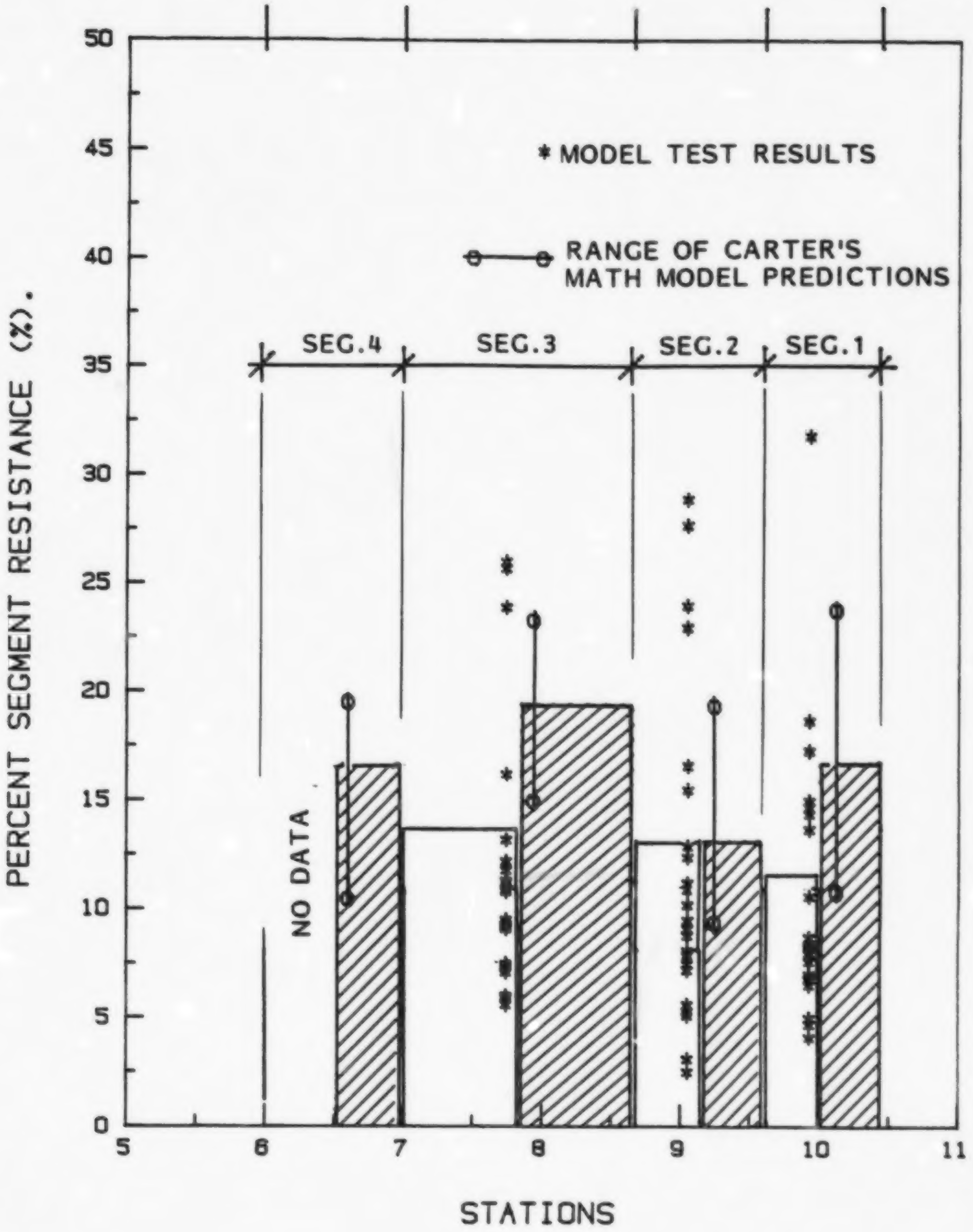

COMPARISON OF PERCENT SEGMENT RESISTANCE WITH CARTER'S MATH MODEL PREDICTIONS.

☐ MEANS FROM DATA SETS

▨ MEANS FROM CARTER'S PREDICTIONS

FIGURE 3.2

TABLE 3.2

CALCULATED MEAN NORMAL FORCE AND SEGMENT NORMAL FORCE

	PERCENT OF TOTAL (%)					
TEST	SEG.1	SEG.2	SEG.3	SEG.4	NORMAL FORCE (N)	TOTAL RESIST. (N)
1S1	41.04	30.61	38.74	28.47	80.40	83.27
1C1	40.04	30.61	38.76	28.53	72.12	37.27
1C2	40.43	30.59	38.75	28.53	97.94	50.67
1S2	38.32	26.54	39.74	31.99	109.52	113.43
1C3	36.39	26.52	39.77	32.15	87.30	45.04
1C4	36.13	26.48	39.76	32.22	94.87	48.94
1S3	36.49	23.64	40.69	34.27	146.38	151.26
1C5	33.92	23.60	40.71	34.52	99.49	51.16
1C6	30.54	23.53	40.72	34.85	72.23	36.91
1S4	28.38	19.23	42.70	37.67	147.17	149.16
1C7	27.47	19.20	42.68	37.79	173.25	87.66
1C8	26.55	19.16	42.65	37.92	106.75	53.94
2S1	38.89	22.92	40.88	34.63	132.97	138.18
2C1	39.00	22.91	40.88	34.64	129.48	67.30
2C2	38.99	22.89	40.87	34.66	134.34	69.84
2S2	27.44	18.08	43.34	38.37	159.11	160.71
2C3	28.94	18.11	43.38	38.19	178.23	90.26
2C4	30.28	18.14	43.41	38.02	218.13	110.73
2S3	27.12	17.66	43.68	38.53	203.53	205.11
2C5	27.49	17.66	43.70	38.48	205.85	103.79
2C6	28.44	17.68	43.72	38.37	217.67	109.94
2S4	29.14	18.43	43.18	38.02	189.16	191.77
2C7	30.77	18.45	43.21	37.83	206.51	104.99
2C8	31.96	18.48	43.24	37.69	238.69	121.61
3S1	43.96	21.73	41.34	34.99	208.23	218.40
3C1	46.51	21.74	41.32	34.74	253.62	133.60
3S2	34.24	19.23	42.72	37.19	197.42	202.54
3C2	37.32	19.28	42.76	36.84	258.40	133.27
MEAN	34.15	21.90	41.69	35.36	157.81	109.67

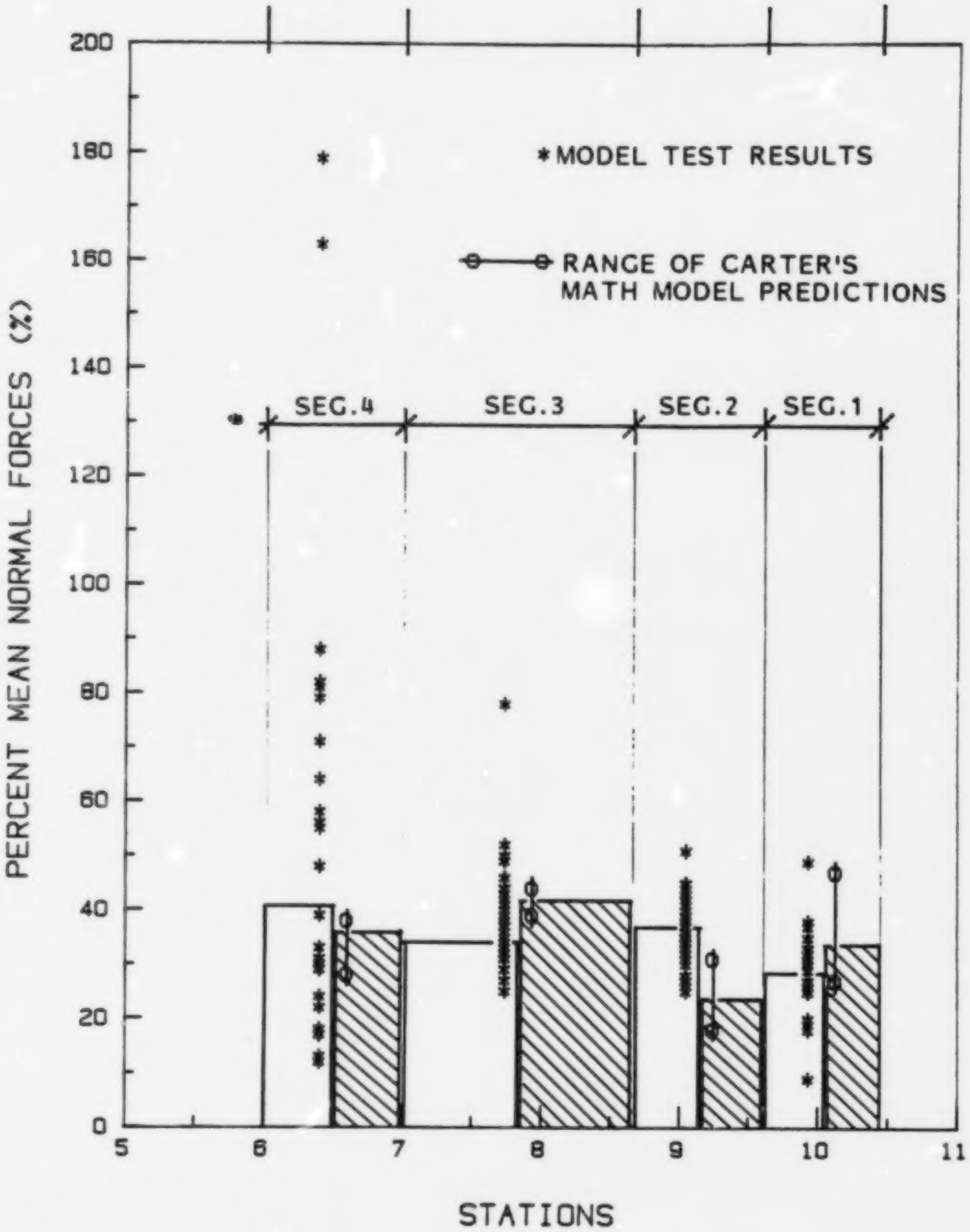

COMPARISON OF PERCENT MEAN NORMAL FORCES SEEN BY SEGMENTS WITH CARTER'S MATH MODEL PREDICTIONS.

☐ MEANS FROM DATA SETS

▨ MEANS FROM CARTER'S PREDICTIONS

FIGURE 3.3

TABLE 3.3

DISTRIBUTION OF FORCE ALONG THE HULL

PERCENTAGE CONTRIBUTION TO TOTAL FORCE

SEGMENT RESISTANCE COMPONENT

	SEG.1	SEG.2	SEG.3	SEG.4	REMAINING
CARTER	16.67%	13.24%	20.63%	16.75%	32.69%
MODEL	11.28%	13.44%	13.79%	61.47%	
DIFFERENCE	5.4%	0.2%	6.8%	12.0%	

PERCENTAGE CONTRIBUTION TO MEAN NORMAL FORCE

	SEG.1	SEG.2	SEG.3	SEG.4
CARTER	34.15%	21.90%	41.69%	35.36%
MODEL	29%	36%	39%	40%
DIFFERENCE	5%	14%	3%	5%

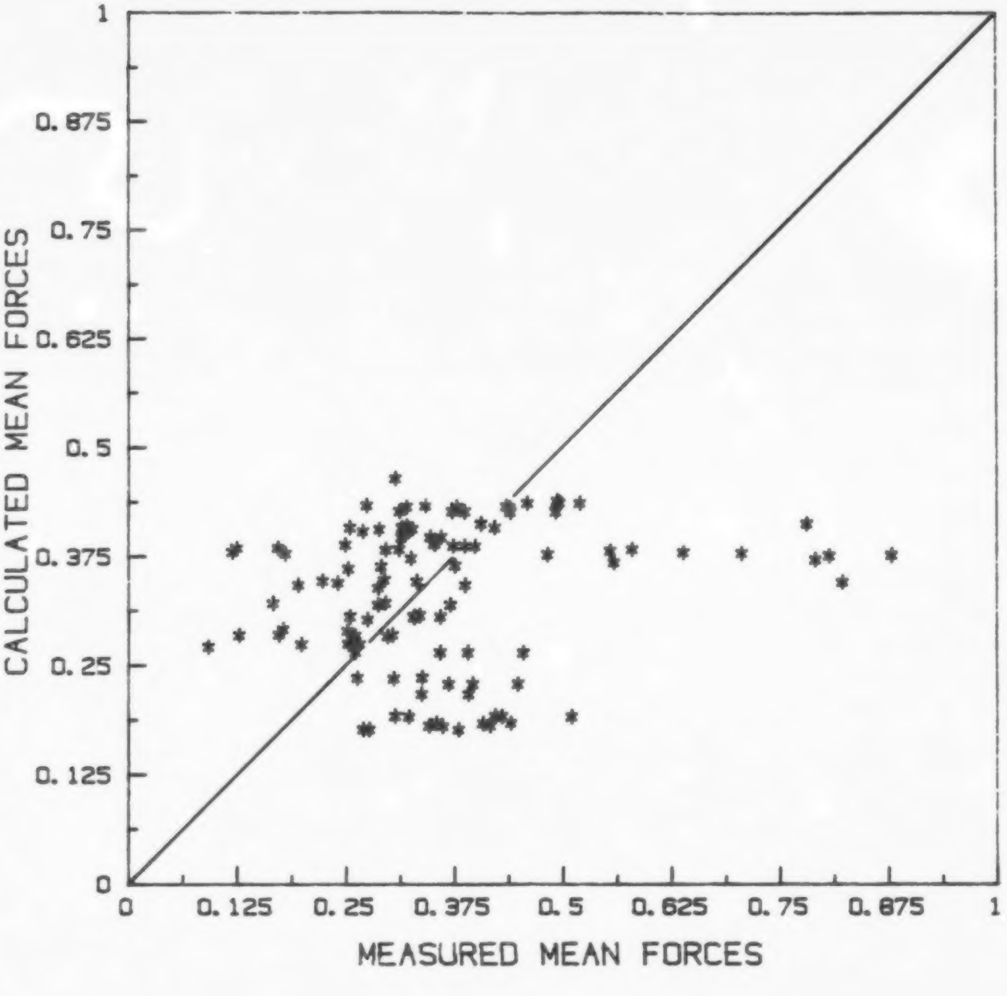

COMPARISON BETWEEN MEASURED AND CALCULATED MEAN FORCES NORMALIZED WITH RESPECT TO TOTAL NORMAL FORCE.

FIGURE 3.4

4.: CONCLUSIONS

The following conclusions may be drawn from the segmented model testing program:

1.: When the model test results are compared to full-scale data, the correlation is far from good, thereby highlighting the deficiencies of doped ice presently used all over the world as a testing medium. We must question the degree of realism in simulating the mechanical behavior of ice with doped ice.

2.: The segmented model has performed relatively well and has demonstrated that the technique could be used successfully to measure the ice force distribution along the different zones of an icebreaking bow or structure. Tests also showed that ice load increases as the point of application moves aft into the shoulder area, with decreasing waterplane and flare angles, exactly as predicted by Carter's math model.

3.: The predictive accuracy and reliability of the Carter's math model has been demonstrated by excellent correlation with full-scale test data. Experimental data on the resistance components along different zones of an icebreaking bow do verify and validate the assumptions and simplifications made in deriving the model developed by D. Carter. Correlation of program results with the existing full-scale field data was shown to be very good over the entire range of ship speeds and ice thicknesses.

5.: REFERENCES

[1] Lewis, J.W., Bulat, V., Glen, I.F., and Kotras, T., 1982 Development of a semi-empirical model for predicting resistance and determining thrust requirements for ships in level ice. Volume II - Appendices. Report prepared for Transportation Development Centre, Montreal, Canada.

[2] Michailidis, M., and Murdey, D.C., 1981, Performance of CCGS FRANKLIN in Lake Melville, 1980. Proc. 6th Ship Technology and Research (STAR) Symposium, SNAME , Ottawa, June 1981.

ANNEX 'A'

TRIAL DATA

PIERRE RADISSON

LISTING OF TRIAL DATA
PIERRE RADISSON

RUN No	ICE THICK (m)	FLEX STRNGT (kPa)	SHIP SPEED (m/s)	MEAS. Ri kN	CALC. Ri kN
1	0.229	408.466	0.823	76	135
2	0.229	408.466	1.852	140	174
3	0.229	408.466	2.726	185	218
4	0.229	408.466	3.807	242	279
5	0.229	408.466	4.990	244	351
6	0.229	408.466	5.813	383	402
7	0.229	408.466	6.997	344	477
8	0.229	408.466	6.997	573	477
9	0.229	408.466	5.813	361	402
10	0.229	408.466	2.932	237	229
11	0.229	408.466	1.955	24	178
12	0.209	408.466	0.720	127	118
13	0.199	408.466	1.749	100	143
14	0.189	408.466	1.183	40	116
15	0.199	408.466	0.668	25	110
16	0.212	408.466	0.617	64	118
17	0.207	408.466	2.315	103	175
18	0.251	408.466	3.138	181	267
19	0.434	408.466	0.617	165	295
20	0.462	408.466	1.440	243	367
21	0.434	408.466	2.160	325	398
22	0.445	408.466	3.133	430	509
23	0.329	408.466	3.827	342	418
24	0.481	408.466	1.749	300	412
25	0.481	408.466	3.755	475	632
26	0.481	408.466	5.762	690	892
27	0.481	408.466	6.276	688	962
28	0.349	408.466	1.111	157	242
29	0.349	408.466	3.133	270	386
30	0.350	408.466	6.822	580	734
31	0.336	408.466	1.291	129	240
32	0.664	477.714	1.183	476	622
33	0.644	477.714	2.099	610	704
34	0.636	477.714	3.328	743	882

LISTING OF TRIAL DATA

PIERRE RADISSON

RUN No	ICE THICK (m)	FLEX STRNGT (kPa)	SHIP SPEED (m/s)	MEAS. Ri kN	CALC. Ri kN
35	0.584	477.714	4.589	801	1004
36	0.641	477.714	3.822	775	976
37	0.651	477.714	2.819	656	822
38	0.687	477.714	1.775	656	717
39	0.663	477.714	2.690	382	819
40	0.677	477.714	2.078	627	746
41	0.554	477.714	3.004	668	704
42	0.577	477.714	3.776	743	857
43	0.605	477.714	4.573	805	1042
44	0.637	477.714	3.498	720	913
45	0.592	477.714	2.639	562	707
46	0.670	477.714	1.852	542	705
47	0.602	477.714	1.270	451	556
48	0.732	477.714	1.867	770	790
49	0.704	477.714	3.231	969	977
50	0.702	477.714	3.560	965	1035
51	0.702	477.714	2.922	790	918
52	0.672	477.714	2.032	602	732
53	0.682	477.714	1.347	576	660
54	0.739	477.714	1.183	624	714
55	0.719	477.714	2.212	859	824
56	0.709	477.714	3.447	975	1025
57	0.709	477.714	2.176	726	804
58	0.829	477.714	1.378	559	854
59	0.829	477.714	0.987	470	809
60	0.692	525.887	4.085	846	1185
61	0.718	525.887	3.833	784	1184
62	0.708	525.887	3.056	641	1011
63	0.715	525.887	2.423	556	908
64	0.723	525.887	1.610	427	796
65	0.697	525.887	1.327	452	726
66	0.692	525.887	1.054	397	692
67	0.717	525.887	3.128	713	1040
68	0.715	525.887	3.786	865	1168

LISTING OF TRIAL DATA

PIERRE RADISSON

RUN No	ICE THICK (m)	FLEX STRNGT (kPa)	SHIP SPEED (m/s)	MEAS. Ri kN	CALC. Ri kN
69	0.719	525.887	3.869	854	1193
70	0.677	525.887	3.622	785	1064
71	1.219	207.745	2.716	1108	1007
72	1.219	207.745	2.186	892	902
73	1.219	207.745	1.919	985	854
74	1.219	207.745	1.497	526	786
75	1.219	207.745	1.883	785	848
76	1.169	207.745	2.299	1008	877
77	1.169	207.745	3.339	947	1087
78	1.169	207.745	1.481	939	743
79	1.169	207.745	1.250	810	713
80	1.169	207.745	1.106	659	696
81	0.989	207.745	1.697	477	627
82	0.959	207.745	3.910	772	963
83	0.979	207.745	3.292	728	873
84	1.029	207.745	2.711	733	820
85	1.069	207.745	1.991	559	736
86	0.999	207.745	3.704	1012	971
87	1.119	207.745	3.961	1012	1164
88	1.049	207.745	2.778	848	851
89	0.929	207.745	2.572	676	703
90	1.159	207.745	1.903	630	799
91	1.029	207.745	1.337	566	614
92	0.949	207.745	0.874	461	511
93	1.019	207.745	3.611	922	975
94	1.019	207.745	2.726	770	813
95	0.929	207.745	2.212	663	650
96	1.039	207.745	1.131	510	599
97	0.979	207.745	0.617	455	515
98	0.879	207.745	1.337	576	502
99	1.119	207.745	1.492	602	704
100	0.799	207.745	1.749	696	487
101	1.149	207.745	2.212	782	843
102	0.979	207.745	3.498	1008	910

ANNEX 'B'

ICE FORCE DISTRIBUTION

TARGETED TEST MATRIX

TABLE 1

AVERAGE NORMAL FORCES (Newtons) ACTING AT DIFFERENT POINTS (X,metres) ALONG THE BOW SIDES (VERY LOW SPEED).

X (metres)	h = 30mm		h = 45mm		h = 60mm	
	$\sigma = 35$	$\sigma = 20$	$\sigma = 35$	$\sigma = 20$	$\sigma = 35$	$\sigma = 20$
0.000	3.936	2.592	6.547	4.310	9.391	6.180
0.048	7.831	5.157	13.023	8.573	18.681	12.295
0.096	7.788	5.129	12.952	8.526	18.579	12.227
0.144	7.743	5.099	12.877	8.477	18.472	12.156
0.191	7.695	5.067	12.797	8.423	18.356	12.080
0.239	7.642	5.032	12.709	8.365	18.230	11.996
0.287	7.584	4.994	12.613	8.302	18.093	11.906
0.335	7.520	4.951	12.507	8.231	17.944	11.806
0.383	7.447	4.902	12.389	8.152	17.777	11.694
0.431	7.365	4.847	12.255	8.062	17.589	11.568
0.478	7.269	4.784	12.099	7.958	17.368	11.421
0.526	7.160	4.712	11.916	7.838	17.107	11.248
0.574	7.037	4.631	11.710	7.703	16.809	11.053
0.622	6.904	4.544	11.484	7.555	16.479	10.837
0.670	6.766	4.453	11.250	7.402	16.137	10.615
0.718	6.633	4.365	11.031	7.256	15.825	10.407
0.765	6.504	4.278	10.830	7.119	15.554	10.221
0.813	6.372	4.187	10.633	6.981	15.304	10.041
0.861	6.228	4.086	10.427	6.834	15.052	9.855
0.909	6.061	3.971	10.188	6.663	14.758	9.639
0.957	5.860	3.833	9.888	6.454	14.374	9.364
1.005	5.621	3.671	9.519	6.201	13.883	9.024
1.052	5.349	3.488	9.090	5.911	13.298	8.625
1.100	5.051	3.290	8.611	5.590	12.634	8.178
1.148	4.735	3.080	8.096	5.247	11.907	7.694
1.196	4.410	2.865	7.557	4.892	11.138	7.186
1.244	4.084	2.651	7.013	4.534	10.354	6.672
1.292	3.766	2.443	6.477	4.185	9.576	6.164
1.340	3.462	2.245	5.962	3.849	8.824	5.676
1.387	3.186	2.065	5.491	3.543	8.132	5.228
1.435	2.936	1.903	5.063	3.267	7.503	4.822
1.483	2.713	1.758	4.680	3.019	6.936	4.457
1.531	2.516	1.630	4.340	2.799	6.431	4.133
1.579	2.343	1.518	4.040	2.606	5.986	3.847
1.627	2.191	1.420	3.776	2.436	5.593	3.595
1.674	2.057	1.333	3.543	2.287	5.245	3.373
1.722	1.938	1.257	3.336	2.154	4.936	3.176
1.770	1.832	1.188	3.151	2.035	4.658	2.998
1.818	1.736	1.127	2.981	1.927	4.402	2.836
1.866	1.648	1.070	2.825	1.828	4.164	2.685
1.914	1.568	1.019	2.680	1.736	3.941	2.545
1.961	1.494	0.972	2.545	1.651	3.732	2.415
2.009	1.426	0.930	2.421	1.574	3.538	2.295
2.057	1.366	0.891	2.308	1.504	3.362	2.186
2.105	1.311	0.857	2.207	1.440	3.203	2.087
2.153	1.261	0.826	2.115	1.383	3.059	1.998
2.201	1.217	0.798	2.033	1.332	2.929	1.918
2.248	1.178	0.773	1.961	1.287	2.817	1.848
2.296	1.145	0.753	1.902	1.250	2.726	1.791
2.344	1.118	0.735	1.854	1.219	2.653	1.745
2.392	0.548	0.360	0.908	0.597	1.299	0.854
2.392	13.037	7.449	29.332	16.761	52.146	29.798

TABLE 2

TOTAL NORMAL FORCES (Newtons) "SEEN" BY THE SEGMENTS (VERY LOW SPEED)

SEGMENTS.	h = 30mm		h = 45mm		h = 60mm	
	$\sigma = 35$	$\sigma = 20$	$\sigma = 35$	$\sigma = 20$	$\sigma = 35$	$\sigma = 20$
SEG. 4A	98.430	64.766	163.853	107.759	235.268	154.669
SEG. 4B	60.873	40.039	101.381	66.647	145.635	95.698
SEG. 3	93.550	61.372	156.772	102.712	226.488	148.221
SEG. 2	15.891	10.317	27.258	17.628	40.209	25.917
SEG. 1	9.143	5.993	15.288	10.012	22.049	14.428

Note Segment 4A runs from Station 5.5 to Station 7.
Segment 4B runs from Station 6.0 to Station 7.

TABLE 3

AVERAGE X-COMPONENTS (Newtons) ACTING AT DIFFERENT POINTS (X,metres) ALONG THE BOW SIDES (VERY LOW SPEED).

X	h = 30mm		h = 45mm		h = 60mm	
(metres)	σ = 35	σ = 20	σ = 35	σ = 20	σ = 35	σ = 20
0.000	1.057	0.696	1.758	1.157	2.522	1.660
0.048	2.103	1.385	3.497	2.302	5.016	3.301
0.096	2.091	1.377	3.478	2.289	4.989	3.283
0.144	2.079	1.369	3.458	2.276	4.960	3.264
0.191	2.066	1.361	3.436	2.262	4.929	3.244
0.239	2.052	1.351	3.412	2.246	4.895	3.221
0.287	2.036	1.341	3.387	2.229	4.858	3.197
0.335	2.019	1.329	3.358	2.210	4.818	3.170
0.383	2.000	1.316	3.327	2.189	4.773	3.140
0.431	1.977	1.302	3.291	2.165	4.723	3.106
0.478	1.952	1.285	3.249	2.137	4.664	3.067
0.526	1.922	1.265	3.200	2.105	4.594	3.020
0.574	1.890	1.243	3.144	2.068	4.513	2.968
0.622	1.854	1.220	3.084	2.029	4.425	2.910
0.670	1.817	1.196	3.021	1.988	4.333	2.850
0.718	1.781	1.172	2.962	1.948	4.249	2.795
0.765	1.746	1.149	2.908	1.912	4.176	2.744
0.813	1.711	1.124	2.855	1.875	4.109	2.696
0.861	1.672	1.097	2.800	1.835	4.042	2.646
0.909	1.627	1.066	2.736	1.789	3.963	2.588
0.957	1.573	1.029	2.655	1.733	3.859	2.514
1.005	1.509	0.986	2.556	1.665	3.728	2.423
1.052	1.436	0.937	2.441	1.587	3.571	2.316
1.100	1.356	0.883	2.312	1.501	3.392	2.196
1.148	1.271	0.827	2.174	1.409	3.197	2.066
1.196	1.184	0.769	2.029	1.313	2.991	1.930
1.244	1.097	0.712	1.883	1.218	2.780	1.791
1.292	1.011	0.656	1.739	1.124	2.571	1.655
1.340	0.930	0.603	1.601	1.034	2.369	1.524
1.387	0.910	0.590	1.568	1.012	2.323	1.493
1.435	0.904	0.586	1.558	1.005	2.308	1.484
1.483	0.893	0.579	1.541	0.994	2.284	1.468
1.531	0.881	0.571	1.519	0.980	2.252	1.447
1.579	0.866	0.561	1.494	0.964	2.214	1.423
1.627	0.850	0.551	1.466	0.946	2.171	1.396
1.674	0.833	0.540	1.435	0.926	2.124	1.366
1.722	0.814	0.528	1.402	0.905	2.074	1.334
1.770	0.794	0.515	1.365	0.882	2.018	1.299
1.818	0.771	0.500	1.323	0.855	1.954	1.259
1.866	0.745	0.484	1.277	0.826	1.882	1.214
1.914	0.717	0.466	1.226	0.794	1.803	1.164
1.961	0.687	0.447	1.170	0.759	1.716	1.110
2.009	0.655	0.427	1.112	0.723	1.625	1.054
2.057	0.623	0.406	1.053	0.686	1.533	0.997
2.105	0.590	0.386	0.994	0.649	1.443	0.940
2.153	0.559	0.366	0.937	0.613	1.356	0.885
2.201	0.529	0.347	0.883	0.578	1.272	0.833
2.248	0.500	0.329	0.833	0.547	1.197	0.785
2.296	0.475	0.312	0.789	0.518	1.130	0.743
2.344	0.452	0.297	0.749	0.493	1.073	0.705
2.392	0.216	0.142	0.357	0.235	0.511	0.336
2.392	6.289	3.594	14.150	8.086	25.156	14.375

TABLE 4

TOTAL X-FORCES (Newtons) "SEEN" BY THE SEGMENTS AT VERY LOW SPEED.

SEGMENTS	h = 30mm		h = 45mm		h = 60mm	
	σ = 35	σ = 20	σ = 35	σ = 20	σ = 35	σ = 20
SEG. 4A	26.430	17.390	43.997	28.935	63.172	41.531
SEG. 4B	16.345	10.751	27.222	17.895	39.105	25.696
SEG. 3	25.119	16.479	42.095	27.579	60.815	39.799
SEG. 2	6.866	4.458	11.775	7.616	17.367	11.195
SEG. 1	7.088	4.381	13.671	8.362	22.093	13.412

Note: Segment 4A runs from Station 5.5 to Station 7;
Segment 4B runs from Station 6.0 to Station 7.

SEGMENTS	h = 30mm		h = 45mm		h = 60mm	
	σ = 35	σ = 20	σ = 35	σ = 20	σ = 35	σ = 20
SEG.1+2+3	39.074	25.319	67.541	43.557	100.275	64.407

TABLE 5

PERCENTAGE (%) OF THE TOTAL RESISTANCE "SEEN" BY THE SEGMENTS

SEGMENTS	h = 30mm		h = 45mm		h = 60mm	
	σ = 35	σ = 20	σ = 35	σ = 20	σ = 35	σ = 20
SEG. 4A	39.559	39.981	38.534	39.065	37.636	38.260
SEG. 4B	24.465	24.717	23.842	24.161	23.298	23.672
SEG. 3	37.598	37.886	36.868	37.236	36.232	36.665
SEG. 2	10.277	10.250	10.313	10.283	10.347	10.314
SEG. 1	10.609	10.073	11.973	11.289	13.163	12.356

Note: Segment 4A runs from Station 5.5 to Station 7;
Segment 4B runs from Station 6.0 to Station 7.

SEGMENTS	h = 30mm		h = 45mm		h = 60mm	
	σ = 35	σ = 20	σ = 35	σ = 20	σ = 35	σ = 20
SEG.1+2+3	58.484	58.209	59.155	58.808	59.741	59.334

TABLE 6

TOTAL RESISTANCE (Newtons) VERSUS MODEL SPEED (m/s).

V	h = 30mm		h = 45mm		h = 60mm	
(m/s)	$\sigma = 35$	$\sigma = 20$	$\sigma = 35$	$\sigma = 20$	$\sigma = 35$	$\sigma = 20$
0.000	133.621	86.993	228.355	148.135	335.699	217.099
0.100	135.400	88.522	230.841	150.265	338.867	219.805
0.200	140.605	92.961	238.145	156.481	348.198	227.731
0.300	148.875	99.920	249.844	166.327	363.217	240.360
0.400	159.736	108.919	265.358	179.204	383.257	257.001
0.500	172.699	119.498	284.062	194.512	407.577	276.931
0.600	187.328	131.274	305.371	211.723	435.461	299.493
0.700	203.265	143.956	328.778	230.413	466.270	324.140
0.800	220.224	157.323	353.868	250.249	499.462	350.431
0.900	237.989	171.215	380.307	270.981	534.595	378.024
1.000	256.391	185.514	407.833	292.417	571.310	406.653

TABLE 7

SPEED AMPLIFICATION FACTOR.

V	h = 30mm		h = 45mm		h = 60mm	
(m/s)	$\sigma = 35$	$\sigma = 20$	$\sigma = 35$	$\sigma = 20$	$\sigma = 35$	$\sigma = 20$
0.000	1.000	1.000	1.000	1.000	1.000	1.000
0.100	1.013	1.018	1.011	1.014	1.009	1.012
0.200	1.052	1.069	1.043	1.056	1.037	1.049
0.300	1.114	1.149	1.094	1.123	1.082	1.107
0.400	1.195	1.252	1.162	1.210	1.142	1.184
0.500	1.292	1.374	1.244	1.313	1.214	1.276
0.600	1.402	1.509	1.337	1.429	1.297	1.380
0.700	1.521	1.655	1.440	1.555	1.389	1.493
0.800	1.648	1.808	1.550	1.689	1.488	1.614
0.900	1.781	1.968	1.665	1.829	1.592	1.741
1.000	1.919	2.133	1.786	1.974	1.702	1.873

Note: Values in Tables 1, 2, 3, and 4 are for very low speed, to take into account the speed effect, the values must be multiplied by the corresponding above factor.

APPENDIX B

STATEMENT OF WORK

VALIDATION OF ICE RESISTANCE MATHEMATICAL MODELS

Translation of par. 5 of the original Work Statement
DSS Contract Serial No. 18200-7-7542/01-SD

5. DETAILED STATEMENT OF WORK

	% Budget Complete	
5.1 Within two weeks of contract commencement date, a work plan shall be submitted to TDC for approval. This plan shall detail the tasks to be accomplished, methods used to execute the tasks, human resources allocated and schedule of tasks accomplishment and cash flow.	.7%	The contract start date was February 12th, 1988. The work plan was reported in a letter of March 8, 1988.
5.2 Evaluation of the mathematical models (CARTER and ARCTEC/NEAGLE) and preparation of a test protocol in accordance with the specific characteristics of each model.	6.9%	The evaluation of the math models and test plan were submitted in a progress report in June 1988.
5.3 Modification of TDC's segmented model through the installation of a fourth segment near the maximum beam of the model.	7.6%	This was completed fully. This took much longer than anticipated and some instrumentation had to be constructed twice.
5.4 Verification of sensors and internal circuits within the model and strengthening as required in order to improve their resistance to the handling inherent in transportation of the model and in its operation in the test tank.	9.7%	Other segments were modified and instrumentation refurbished.
5.5 Modification to the software used for test data processing in order to increase speed of data processing, to make it compatible with the instrumentation of the test tank (IMD) and to facilitate comparison of test results with those of the mathematical models.	4.4%	The data acquisition system was modified as had been proposed earlier.
5.6 Expedition of the segmented model to the ice tank of the Institute of Marine Dynamics (IMD), St-John's, Newfoundland, and verification of the model condition prior to releasing it to the IMD technicians.	12.4%	This was cancelled. The saved transportation funding was used to compensate for overruns in the preparation stage. A contract amendment was prepared.
5.7 Calibration of the segmented model, in collaboration with IMD technicians, in operation over ice-free water and over an ice sheet, provided free of charge by IMD.	7.4%	This calibration took place in the FTL facility. In addition, a contract extension was made to include a photogrammetric check of the hull lines.
5.8 Test of the model in the IMD ice tank, using a maximum of twelve ice sheets. The exact number of ice sheets shall have been justified in task 5.1.	37.4%	The tests took place in the FTL facility using ten ice sheets.
5.9 Analysis of results and of parameters of importance with regard to the mathematical models under review.	9.7%	This was completed as described herein.
5.10 Results of the preceeding tasks shall be presented as reports, prepared as specified in paragraph 9 of this work statement. Monthly reports shall be submitted as specified in paragraph 8. Furthermore, the contractor shall prepare a presentation on this project with audio-visual support.	3.8%	Monthly reports were provided. This document reports the results. Video and 35 mm still photography of the model and tests have been made. A presentation will be made as required.

D1460-194, TDC project 6994.